The Pennsylvania State University

The Graduate School

Eberly College of Science

SURFACE IMMOBILIZED DNA FOR USE IN BIOSENSING

A Dissertation in

Chemistry

by

Sarah Elizabeth Brunker

Submitted in Partial Fulfillment
of the Requirements
for the Degree of

Doctor of Philosophy

December 2010

The dissertation of Sarah Elizabeth Brunker was reviewed and approved* by the following:

Christine Keating
Associate Professor of Chemistry
Dissertation Advisor
Chair of Committee

Philip C. Bevilacqua
Professor of Chemistry

Raymond E. Schaak
Associate Professor of Chemistry

James H. Adair
Professor of Materials Science and Engineering
Director, NSF Particulate Materials Center (PMC)

Barbara J. Garrison
Shapiro Professor of Chemistry
Head of the Department of Chemistry

*Signatures are on file in the Graduate School

ABSTRACT

The overall goal of this work was to understand the factors governing nucleic acid attachment, hybridization, and enzymatic extension in an immobilized format. Surface immobilized DNA is used in biosensing applications to capture an analyte of interest, which is then detected (in this case using fluorescence), as the detection of DNA sequences can be used to diagnose disease. Several encoding strategies are used to correlate the signal generated with the identity of the analyte, including spatial encoding incorporated into planar substrates, where a particular area on the surface corresponds to a particular analyte probe; and anisotropic encoding incorporated into particular substrates, where the particle itself codes for the analyte through its composition, etc. Both planar and particulate surfaces were analyzed in this work; the synthesis, functionalization, nucleic acid attachment and subsequent use as a probe in an assay, and signal transduction of bound analyte were all investigated. Barcoded nanowires serve as the encoded particle in this system, where the immobilized DNA sequence corresponds to the metallic pattern of the wire itself.

Chapters 2 and 3 detail the use of polymerases and ligases, respectively, to perform enzymatic amplification reactions (polymerase chain reaction and ligase chain reaction) when the nucleic acid primer or probe is bound to a barcoded nanowire. Investigations into the reaction mechanism, such as attachment chemistry thermostability measurements and control experiments to determine fluorescence signal origin, were performed and a hypothesis to explain the behavior observed is proposed; these studies are applicable to surface phase amplification between differing systems. Chapter 4 uses microcontact printing, where a polydimethyl siloxane stamp is used to pattern planar substrates with DNA probe sequences. Surface functionalization was studied in order to optimize DNA pattern transfer. These studies pave the way for microcontact insertion printing, which can be used to pattern isolated DNA molecules for use in single

molecule studies. Taken together, these investigations answer fundamental questions about the reactions that occur when DNA is immobilized onto a surface for use in a biological assay.

TABLE OF CONTENTS

LIST OF FIGURES

LIST OF TABLES

LIST OF ABBREVIATIONS

Å	angstrom
AFM	atomic force microscopy
Ag	silver
APTMS	aminopropyltrimethoxysilane
ARNA	armored RNA
Au	gold
BNI	Bernhard Nocht Institute, identified Coronavirus
bp	base pair
BSA	bovine serum albumin
C8-SH	1-octane thiol
cDNA	complementary DNA
cfu	colony forming units
CHES	N-cyclohexyl-2-aminoethanesulfonic acid
Co	cobalt
comp	complementary
conc	concentration
CoVNC	Coronavirus nucleocapsid
cm	centimeter
C_T	threshold cycle
DI	distilled
DIC	differential interference contrast microscopy
DNA	deoxyribonucleic acid

dNTP	deoxynucleotide triphosphate
ds	double stranded
DTT	dithiothereitol
EDC	1-ethyl-3-[3-dimethylaminopropyl]carbodiimide hydrochloride
EDTA	ethylenediaminetetraacetic acid
ELISA	enzyme linked immunosorbent assay
FITC	fluorescein isothiocyanate
g	gram
g	gravitational force unit
GC	percent guanine and cytosine
HAV	hepatitis A virus
HBV	hepatitis B virus
HEPES	4-(2-hydroxyethyl)-1-piperazineethanesulfonic acid
HIV	human immunodeficiency virus
kV	kilovolt
LCR	ligase chain reaction
LDR	ligase detection reaction
OEG	oligo ethylene glycol
Ni	nickel
μCDP	microcontact displacement printing
μCIP	microcontact insertion printing
μCP	microcontact printing
μL	microliter
μm	micron or micrometer

μM	micromolar
M	molar
mA	milliamp
MFI	mean fluorescence intensity
MHDA	mercaptodecanoic acid
mL	milliliter
mm	millimeter
mM	millimolar
MΩ	mega ohm
mp	multiplex
MPa	mega Pascal
MPPTS	2-[methoxy(polyethyleneoxy)propyl] trimethoxysilane
NA	numerical aperture
Na	sodium
NaCl	sodium chloride
no temp	no template
noncomp	noncomplementary
nm	nanometer
nM	nanomolar
ns	not significant
OEG	oligo ethylene glycol
PBS	phosphate buffered saline
PCR	polymerase chain reaction
Pd	paladium

PDMS	polydimethylsiloxane
PEO	polyethelene oxide
PEO silane	N-(triethoxysilylpropyl)-o-polyethyleneoxide urethane
pg	picogram
pM	picomolar
ROC	receiver operator characteristic
Rn	reaction
RNA	ribonucleic acid
RSV	respiratory syncytial virus
RT	reverse transcription
SAM	self assembled monolayer
SARS	severe acute respiratory syndrome
S-C8	1-octane thiol
SEM	scanning electron microscopy
SHA	sandwich hybridization assay
Si	silicon
SiO_2	silica
SNP	single nucleotide polymorphism
soln	solution
SPT-0011	2-(2-(2-(11-mercaptoundecyloxy)ethoxy)ethoxy)ethanol
ss	single stranded
STM	scanning tunneling microscopy
Sulfo-SMCC	sulfosuccinimidyl-4-(*N*-maleimidomethyl)cyclohexane-1-carboxylate
T	thymine

TAE	Tris-acetate EDTA
TAMRA	carboxytetramethylrhodamine
Tcycle	thermocycle
TEM	transmission electron micrograph
TEOS	tetraethoxysilane
T_M	melting temperature
TMR-dCTP	tetramethylrhodamine-deoxycytosinetriphosphate
TRIS	tris(hydroxymethyl)aminomethane
U	enzyme unit
UV	ultra violet / visible
V	volt
W	Watt
WD	working distance
WNV	West Nile virus

ACKNOWLEDGEMENTS

Many different people have had an active presence in my life at certain times over the course of my graduate career. My parents Jean & Dave and my sister Annie have tried to support me throughout graduate school, as have former college friends Eugenides Hermes and Fatma Zahra. I found several good friends at the Unitarian Universalist Fellowship, such as Tina Walther, Laurie Parmele, and Jason Bostron, who were also positive presences in my life. My cat, Bonnie, stuck around even when I got home really late. Mary Shoemaker was both a supervising TA and a friend. Erin Goken, another chemistry graduate student, was a great lunch buddy. Several people within my lab have answered my questions and listened at different times. Ben Smith put a lot of time into helping me format this dissertation, which I really appreciated. Chris Keating is one of the best preceptors there is at Penn State. Deb Grove and Ashley Price at the Nucleic Acids Facility, and Wallace Greene at the Diagnostic Virology Lab at Hershey all answered questions, no matter how odd they sounded at the time, as did my committee members.

Thanks to everyone for all the little things—you know who you are. Peace.

Chapter 1

Introduction

This thesis describes progress made in understanding and controlling the functionalization of surfaces (particulate and planar) with DNA, and using these surfaces as substrates in bioassays for sensing applications. Four projects related to this goal are covered. The first is the use of barcoded nanowires as encoded substrates in the enzymatic amplification reaction Polymerase Chain Reaction (PCR) for detection of sequences of pathogens. The second project is closely related, but uses the exponential amplification method of Ligase Chain Reaction (LCR) in template detection, which provides for a more reproducible, specific assay. The next chapter of this dissertation covers the stamping of patterned DNA sequences onto a planar substrate as the first step in multiplexed (or the detection of more than one analyte simultaneously in the same reaction mixture) target detection based on spatial encoding or further nanoarchitecture generation. Lastly, a general chemistry laboratory exercise in which students synthesized nanoparticles, performed flocculation experiments, and observed slides with multilayers of colloid is discussed.

This introduction explains key concepts related to these projects, including particle background such as: benefits of detecting target molecules on particulate as opposed to planar substrates, how barcoded nanowires are synthesized and analyzed, functionalization of particles, and their use in multiplexed assays for protein or nucleic acid detection. Specifically, methods of detection for use in diagnosing respiratory pathogens will be discussed. Additionally,

background on enzymatic amplification reactions, currently used nucleic acid detection techniques, alternate platforms for nucleic acid functionalization, and nanoarchitecture generation using nucleic acids are also mentioned.

Respiratory Pathogen Detection

Pathogens causing respiratory diseases, where many different ailments cause the same type of symptoms,[1] create difficulty in the identification of the type of pathogen present, or even whether it is bacterial or viral. Respiratory pathogens were therefore focused on in this work. Determination of the pathogen causing the symptoms is important early on in decisions about how to care for patients,[2] as bacterial and viral diseases require differing treatments. Respiratory pathogens such as respiratory syncytial virus and influenza viruses may prove to be fatal in adults, especially those who are immunocompromised or elderly[1], and infect children worldwide.[1, 3] Anti-viral treatment in immunocompromised patients may be lifesaving, and rapid diagnosis limits the amount of hospitalization time as well as antibiotic use.[4, 5] There exists a need for rapid, multiplexable detection of both viral and bacterial pathogens, such as *Haemophilus influenzae*, for clinical diagnoses and public health monitoring.[2]

Current techniques for pathogen diagnosis include culturing of bacteria or viruses, as well as molecular techniques like immunofluorescence and enzyme immuno-assays. Culturing pathogens is necessary when they are present in an amount not directly quantifiable by antigen detection methods, or if a virus is new or unexpected, but it is expensive and very slow, as samples must be sent to facilities capable of culturing pathogens and then grown.[6] Unfortunately, this takes enough time (up to several weeks) that it is not as helpful in determining patient treatment as faster methods.[1] Even the shell vial method, which is a more rapid culturing technique, takes at least 2 days to be a useful diagnostic tool.[5] Molecular techniques that detect

antigens are faster than culturing but can only be used when there are enough antigens present to create a viable signal. Immunofluorescence is rapid, but is heavily dependent on the skill of the technician, as well as the quality of the sample,[4] and is not as sensitive as culturing pathogens.[1] Enzyme linked immunosorbent assay, or ELISA, has greater sensitivity due to the use of an antibody-conjugated enzyme, which in the presence of substrate produces a fluorescent signal, but requires more handling due to rinsing steps and can be unreliable with low-level positives.[4] Some rapid antigen tests, such as those for respiratory syncytial virus, are unreliable for diagnosing adult patients due to the combination of lower amounts of virus present than in child patients, and the quality of samples taken.[7]

PCR presents one solution to the need for a detection scheme that can amplify the pathogen present, even when present in a low titre[1, 3, 6] very quickly, taking only a few hours. Real-time PCR is also precise and has a large dynamic range.[8] Because the pathogen cannot be determined by symptoms alone, multiplexing is necessary, which is possible with PCR in a rapid fashion.[2, 3] To amplify the nucleic acids present in the pathogen, its DNA (or RNA, which initially requires reverse transcription to generate DNA) is first heated to melting from double into single stranded DNA. The reaction mix is cooled and primers, or short sequences complementary to the pathogen sequences, bind to the pathogen DNA, which then acts as a template. A polymerase enzyme is used to covalently add deoxynucleotide triphosphates (or dNTPs) to the 3' end of the primers, in an order complementary to the template, generating an amplicon, or the post-PCR product incorporating both primer sequences and the sequence between them, shown in Figure 1-1. This heating and cooling is repeated in a process called thermocycling and in each cycle there is an exponential increase in the amount of DNA with the pathogen's sequence, as the product of one cycle acts as a substrate in the next cycle. Because this process is so sensitive, the possibility of amplifying contamination sequences introduced when the tube is opened is high.[9] If the template of interest is RNA, a reverse transcriptase

enzyme is first used to convert the RNA into DNA before it is amplified. If a reporter such as a Taqman probe (which fluoresces due to the absence of a quencher after polymerization of the template and subsequent probe digestion) or an intercalating dye (which intercalates primarily into double stranded DNA and fluoresces) is added to the reaction mix, the amplification process can be monitored in real time; this allows for collection of not only amplification plots but also of dissociation curves, as the DNA can be melted post PCR to help determine the identity of the amplicon produced. While Taqman probes are specific to a sequence of interest, a different probe needs to be designed for each template; therefore, intercalating dye was used as the reporter for the presence of double stranded DNA of any sequence.

Ligases can also be used in enzymatic chain reactions that result in exponential template amplification.[10-12] Ligases link together two adjacent DNA sequences, one with a 3' hydroxyl and the other with a 5' phosphate, hybridized to the same template. The oligonucleotide probe captures a template strand, which then hybridizes to a fluorescently tagged oligonucleotide (with a 5' phosphate), creating a sandwich hybridization assay. The ligase covalently attaches the adjacent probe and tag strands. The opposite strands are also present for ligation, as shown in Figure 1-2. Ligase Chain Reaction (LCR) exponentially increases the amount of template DNA present, as the product of one reaction cycle is used as the substrate in the next reaction cycle, much the same as in PCR. Ligase Detection Reaction is also possible, where a linear amplification of template DNA is achieved, as only one side (the sense or antisense strand) is present in a form capable of ligation. Several pathogens and genetic disorders have been detected in clinical samples using ligase chain reaction, such as *Neisseria gonorrhea*[13] and *Chlamydia trachomatis*[14], *Mycobacterium tuberculosis*[15], and sickle cell diseases[10]. LCR has also been used to determine developed drug resistance in Human cytomegalovirus.[16] LCR can be combined with polymerase techniques to create hybrid enzymatic assays for biosensing, screening as well as diagnostic, purposes. PCR and ligation reactions have been combined to detect for sickle cell

diseases in prenatal diagnostics[17], in colorectal nucleic acid cancer marker detection[18], and in point mutations of *Chlamydia trachomatis* using Gap-LCR (where the polymerase fills the gap between two adjacent oligonucleotides so that the ligase can join them together)[19]. Ligation mediated PCR (where only one primer site is known and the other is created by a ligation reaction) has been used in sequencing and methylation analysis of human proteins.[20] Several other biological applications, as well as ways to introduce multiple moieties for capturing and labeling functionalities, etc., have also been discussed.[11, 12]

To analyze several PCR or LCR products, gel electrophoresis is often used, where the amplicons are separated based on size. Unfortunately, this requires the design of the individual primers to create amplicons of different lengths, as well as the added step of opening the reaction tube and running gel electrophoresis on the sequences that can introduce contamination, and limits the number of pathogens detected to approximately 20, correlating to the number of lanes on the gel. When a separate sample is run on each individual lane, samples are not being truly multiplexed, as each analyte is tested for in its own separate reaction volume. Multiplexed real-time PCR is possible, although limited due to the use of fluorophores for the identification of the sequences amplified. Because of the bandwidth of the fluorophores' spectra, only four fluorophores can be used in a single experiment without causing spectral overlap.[9] One benefit, however, is that the reaction tube does not need to be opened for amplicon identification, thereby reducing the risk of contamination. In this thesis, encoded nanowires are used as a multiplexing platform, and methods for on-wire amplification are investigated. A long-term goal of this work is to provide rapid (in only a few hours) multiplexing for respiratory pathogen detection, which has relevance for other pathogens' detection and other surface based amplification platforms.

Particle-Based Detection & Suspension Arrays

Some of the most exciting recent progress in nanoscience and nanotechnology has been in the area of particle-based biodetection.[21, 22] Advances have included dramatic improvements in sensitivity and increased selectivity, in some cases coupled with the ability to detect multiple targets simultaneously (i.e., multiplexing).[23, 24-32]

Suspension arrays are collections of encoded particles that serve as a platform for multiplexed detection, analogous to planar arrays.[33] Planar microarrays have become accepted tools in biology, enabling massive multiplexing for simultaneous testing of genomics (e.g., every gene in an organism's genome).[34, 35] In planar arrays, the identities of probe DNA sequences are known based on their placement in the array. Encoded particles offer an alternative approach, in which probe identity is encoded by the properties of the particle to which it is attached. Encoding strategies range from embedded fluorescent dyes to overall shape or particle composition.[36-45] For medical-diagnostic applications, in which genome-level multiplexing is not required, suspension arrays consisting of probe-functionalized encoded particles are an attractive option. Advantages over planar arrays, which are prepared by robot spotters or photolithography, include greater flexibility and ease of preparation.[22, 33] Changes to array composition (i.e., the addition of new probes as new biomarkers are identified, changes in relative quantities of different probe types) are made simply by adding the desired particles to the tube containing the array. Because encoded particles are prepared in suspensions with 10^7–10^9 particles of a given code per milliliter, biomolecule-coupling chemistries can be optimized independently for different probes as needed and each batch of encoded particles can contribute to many suspension arrays.[22, 33] Additionally, suspension arrays enable radial diffusion and thus faster assay times in unmixed solutions and are amenable to mixing even in small sample volumes.[22, 33]

Fluorescence is used commonly to encode particle identity for suspension arrays, either as a ratio of fluorescence intensities at different wavelengths or as a spatial pattern of emission. For example, the commercial Luminex-bead technology[38, 46] uses intensity ratios of microsphere-embedded dyes to differentiate particles, with a separate dye for assay quantification. A dedicated flow cytometry-style instrument is used for readout and up to 500 particle codes are available commercially. Modifications of this basic strategy will permit high levels of multiplexing.[47, 48] Barcoded nanowires are encoded compositionally with different metals along their length; this pattern is read out using reflectance optical microscopy, using instrumentation already common in clinics.[36, 49-51] Barcoded Ag/Au nanowires and several other encoded nanowires that have been or could be used for multiplexed biosensing are pictured in Figure 1-3.[36, 40, 52-54] Because no fluorescence is used for encoding, fluorophore selection for bioassay quantification is not constrained, such that any dye or dye combination can be used. This is in contrast to encoded bead technologies, which use intensity ratios of different fluorescent dyes to identify the particle code. The high density of metallic nanowires makes them easy to separate from suspension and the versatility of their synthesis enables facile incorporation of multiple striping patterns and multiple metals, including magnetic Ni or Co. Readout of bioassays performed on metallic barcode suspension arrays is accomplished using a conventional fluorescence optical microscope, instrumentation already common in clinical diagnostic laboratories.

Barcoded nanowires are discussed in Chapters 2 and 3 as substrates in multiplexed pathogen sequence detection utilizing PCR and LCR, respectively. Fluorescence signal from intercalating dye was evaluated as a strategy to enable closed tube readout and is discussed in Chapter 2; florescent DNA tags employed are discussed in Chapters 3 & 4. Synthesis and use of colloidal nanoparticles are covered in the Appendix.

Synthesis & Optical Readout of Metallic Barcodes

Barcoded metallic nanowires are made by electrodepositing metal into the pores of alumina template membranes; this templated electrodeposition approach to single-component particles was pioneered by the groups of Martin and Moskovits (Figure 1-4).[55-57] The metal composition along the length of the nanowire is encoded by changing the metal-plating solution to generate a desired barcode pattern.[58] The approach is general: segments of various metals, semiconductors and even conducting polymers can be deposited.[36, 50, 55, 59] Nanowire diameter and the length of each segment are controlled by pore size and plating times, respectively. Pore densities in these alumina membranes are high, such that approximately one billion nanowires are produced from a single one-inch template. After synthesis, the membrane is dissolved in base to release the metallic barcodes.[36, 50, 60] For optical barcoding, commercial-filter membrane templates with nominal pore size of 200 nm are generally used, yielding nanowires of approximately 300 nm in diameter. Nanowire lengths are generally in the order of 6 μm. Owing to the relatively large size of the particles and the high density of gold and silver metals, these particles sediment rather than staying suspended by Brownian motion. They can be resuspended readily by agitation.

Figure 1-5A shows a cross-section of the template membrane, after deposition of Au–Ag–Au nanowires in the pores. Suspensions of the released nanowires are opaque, appearing brownish-orange for Au wires and grey for magnetic Ni or Co wires (Figure 1-5B). The metal striping pattern encoded during synthesis is visualized by brightfield optical reflectance microscopy. Although the striping pattern can be seen in a white light color image of the wires (Figure 1-5C), improved contrast and resolution are achieved by illuminating with blue light (~430 nm). The reflectivities of Au and Ag segments vary substantially at short wavelengths

(Figure 1-6).[36, 49] Many other metals have intermediate reflectivities between that of Ag and Au and can be incorporated in the barcoded nanowires as a third component.

Figure 1-7 shows a reflectance image of a mixture of several metallic-barcode particles, along with line-scans illustrating how the nanowire patterns are distinguished from one another. The number of barcode patterns possible for metallic nanowires is determined by: (1) synthetic control over the electroplating, (2) optical diffraction limits, and (3) the number of different optically distinguishable metals. For a standard 6 μm length, the number of patterns possible for 2 metals (i.e., Au and Ag) and eight 0.75 μm segments is 2^8 or 256. Because the wires are dispersed randomly, their two ends are indistinguishable, reducing the number of patterns in practice to 136 (e.g., pattern 10000000, where 1 = Ag and 0 = Au cannot be distinguished from pattern 00000001). If a third metal (e.g., Pd) is added, the number of patterns for an eight-striped particle library is more than 3000.[36, 60] Nanowires with 13 distinguishable segments have been reported;[50] for just two metals, 13 segments yield 4160 and, for three metals, more than 1×10^5 possible patterns. Larger numbers of metals are synthesized easily but would require more than one illumination wavelength to assign unambiguously. Practical limits to the degree of multiplexing lie in controlling the monodispersity of nanowires within a single batch/pattern and in collecting data from many copies of each nanowire pattern in a small number of total images. Freeman and coworkers have reported a 100-member library of eight-segment Au/Ag barcoded nanowires, of which 74 were identified in software with more than 90% accuracy and 85 with more than 80% accuracy.[51] This approaches the 100-member Luminex library, which relies on fluorescence ratios for encoding. For most applications in medical diagnostics, more than 100 patterns will not be necessary.

Surface Functionalization

The metallic surface of the nanowires can be coated with biological-probe molecules for use in bioassays. This can be accomplished by direct adsorption, for example, of NeutrAvidin or an antibody, or using more elaborate methods, such as those based on ω-functionalized alkanethiol self-assembled monolayers (SAMs) or organosilanes bound to SiO_2 thin films on the particle surface.[36, 49, 54, 60-62] Nanowire bioconjugates can be prepared before use and survive storage for at least 2 months.[63] Many copies of the probe chemistry are present on each metallic-barcode particle. The surface area of a single 300-nm diameter, 6 micron-long particle is 5.8×10^{-8} cm^2. At a density of 1×10^{12} thiolated oligonucleotide probes/cm^2, this single particle will harbor 3×10^5 probes. Attachment of biotinylated oligonucleotides to NeutrAvidin on the particle surface yields lower densities. Au and Ag have similar surface chemistries, thus we anticipate steric and electrostatic repulsions between adjacent probes to be dominant over differences in binding affinities for probes to the metal surface.[49, 60] Surface densities of thiolated oligonucleotide probes on Au and Ag nanowires are the same within our measurement error.[60] Variations in biomolecule density on Au versus Ni, however, are expected based on their different surface chemistries and are suggested by fluorescence ratios.[49, 64]

Surface functionalization has also been reported where metallic wires were coated first in glass and then biomolecules. Glass coatings of metallic nanowires were prepared by exposing the nanowires to a silica precursor in the presence of water and a catalyst, in this case tetraethoxysilane (TEOS) and ammonium hydroxide, respectively, and agitating them in solution for a given period of time. The precursor underwent a hydrolysis reaction, generating a silica shell around the metallic nanowire. Recently, Sioss *et al*. demonstrated increased signal intensity for metallic barcodes that had a silica shell.[65] The silica coating also resulted in reduced oxidation rates for the Ag segments and more robust probe attachment chemistry, able to

withstand thermocycling conditions.[65] The attachment chemistry used by Sioss *et al.* of aminopropyltrimethoxysilane to aminate the glass shell and Sulfosuccinimidyl-4-(*N*-maleimidomethyl)cyclohexane-1-carboxylate to crosslink the surface amine with the thiolated DNA was also predominantly used in this work. Dean, *et al.* coated metallic wires in several different glass compositions, which allows for tailoring functionalities to particle applications, and then coated the particles in biomolecules.[66] Barcoded nanowires used in this work were functionalized with silica and subsequently nucleic acid sequences; optimizing this attachment chemistry and the use of the coated particles in enzymatic assays is discussed in Chapters 2 and 3.

Multiplexed Immunoassays

In an early proof-of-principle experiment, Au–Ag–Au nanowires were functionalized with anti-human immunoglobulin and Au–Ni–Au nanowires with anti-rabbit immunoglobulin, after which the two nanowire patterns were mixed together. Subsequent exposure to both antigens and fluorescently tagged secondary antibodies, which had differing fluorophores – FITC for human and Texas Red for rabbit antibodies – resulted in green and red fluorescence on the Au–Ag–Au and Au–Ni–Au nanowires, respectively (Figure 1-8).[36] The two separate bioassays were readily distinguishable based on the nanowire-reflectance patterns. There was little nonspecific binding in this bioassay, that is, not much green fluorescence on the Au–Ni–Au nanowires nor red on the Au–Ag–Au nanowires. These data suggested that nanowire pattern alone could be used for analyte identification and, thus, a single fluorophore should be sufficient for multiplexed assays.

When magnetic metals, such as Ni or Co, are incorporated along the length of the nanowires, magnetic manipulation[67] and bioseparations[68] become possible. Mirkin and coworkers took advantage of the affinity of histidine-tagged proteins for Ni surfaces to separate

hexahistidine-labeled from unlabeled proteins using magnetic Au–Ni–Au-patterned nanowires.[68] After magnetic separation, the hexahistidine-labeled proteins were removed from the nanowires, with more than half of the initial protein recovered.

Tok and colleagues have demonstrated the feasibility of a tetraplex biodetection assay using barcoded wires.[62] Three biothreat-agent simulants, including *Bacillus globigii* spore (simulating *Bacillus anthracis*), RNA MS2 bacteriophage (simulating the smallpox virus *Variola*) and ovalbumin protein (simulating protein toxins), were used in this multiplexed assay, along with bovine-serum albumin, which acted as a negative control. Each target was assigned its own nanowire-barcode pattern, which enabled identification of each analyte. Titration curves were performed in a multiplexed format, with reported limits of detection of 1×10^5 colony-forming units (cfu)/ml for *B. globigii*, 1×10^5 plaque-forming units (pfu)/ml for MS2 bacteriophage and 5 ng/ml for ovalbumin protein. Tok *et al*. report a higher sensitivity of 10 pg/ml for the cytokine fibroblast growth factor (FGF)4 when they limited the number of nanowires available for target binding to 1×10^4; a 100-fold increase in the number of nanowires led to a 100-fold loss in sensitivity to a detection limit of 1000 pg/ml. Using less nanowires increased the difficulty of the assay, however, owing to wire loss during multiple wash steps. These authors also explored using barcoded nanowires with 50 nm Ni tips in multiplexed detection, with the ultimate goal of incorporating this assay onto a portable microfluidic chip for biothreat detection. These very short Ni segments were sufficient for separations and were selected over larger Ni segments to minimize nanowire clumping, which interferes with barcode readout.

Multiplexed Nucleic Acid Detection

Nucleic acid detection can also provide information on disease states. Nucleic acids can be easier to detect than proteins because (1) cross-reactivity can limit the degree of multiplexing

possible for immunoassays and (2) nucleic acids can be amplified by PCR or other enzymatic chain reactions before detection. Thus, nucleic acid probes offer the potential for detecting larger numbers of different targets simultaneously, from smaller initial target concentrations.

Nicewarner-Peña *et al*. demonstrated a triplexed DNA-sandwich hybridization assay using barcoded nanowires in which various combinations of three different target oligonucleotides were identified.[49] Probe DNA oligonucleotides were attached by 5' biotin to NeutrAvidin on the nanowire surface; each of three different probe sequences was attached to nanowires having a different barcode pattern. As illustrated in Figure 7, the barcoded nanowires were then mixed together, exposed to one or more target DNA sequences and finally exposed to a mixture of three different fluorescently tagged detection sequences (one for each target DNA).[49] It was possible to determine from fluorescence microscopy which particles had bound target strands and, by the corresponding fluorescence images, which barcode pattern and therefore which target strand was bound. Wires exposed to noncomplementary oligonucleotide targets were much less fluorescent, indicating the specificity of this assay.

As many as 30 separate bioassays have been performed simultaneously using barcoded nanowires. Penn and coworkers from Nanoplex Technologies used oligonucleotides ligation (linking) assays to test each allele of 15 different single nucleotide polymorphisms (SNPs) in the cytochrome P450 gene family.[69] Each of 30 different nanowire patterns was functionalized with one of the 30 probe DNA sequences (each complementary to one of two alleles possible for each SNP position). Figure 1-10 illustrates how this assay works.[69] The probe:nanowire conjugate is exposed to single-stranded PCR product of the region of genomic DNA where the SNP might be present. If the sequences are complementary, after the third, fluorescently tagged sequence also hybridizes, enzymatic ligation between the probe and the tag strand occurs, resulting in fluorescently labeled barcoded nanowires for allele discrimination. Also shown in Figure 1-10 are the reflectance and fluorescence images for a two-plex version of this assay, illustrating the

ability to discriminate between wild-type and mutant alleles, and the corresponding quantitative data.[69] These authors then tested 20 human genomic DNA samples for eight different SNPs, thus determining 160 genotypes, demonstrating both the barcoded nanowire multiplexing capability and applicability to clinically relevant samples. As compared with other multiplexed SNP assays, the amount of genomic DNA that was required here was rather large (6 pg per SNP), making the multiplexed PCR amplification step limiting. The use of clinical samples as templates in on-wire enzymatic amplification reactions is discussed in the Future Directions chapter of this thesis. Optimization of the multiplexed PCR sample preparation will improve the practicality of the barcoded nanowire approach to SNP detection.

Barcoded nanowires have also been used to detect viral pathogens in a multiplexed format. A critical concern in pathogen detection is avoiding sample cross-contamination. Reducing the number of wash steps and ideally performing the entire assay in a sealed container is therefore desirable. Penn, Keating and coworkers[70] introduced a molecular beacon-based approach for pathogen detection on barcoded nanowires. Au/Ag-striped wires were coated with 5' thiolated, 3' dye-labeled molecular beacon-style hairpin probes. These probe nucleic acids had a 5 base-pair region of self-complementarity at the 3' and 5' ends, such that, on folding, the 3' fluorescent-dye molecule was held close to the metal surface, where its emission was quenched. The remaining portion of the probe sequence (the 'loop') was complementary to a virus-specific target strand, such that, on hybridization to the target, the 3' end was drawn away from the surface and fluorescence could occur. Figure 1-11 diagrams the multiplexed pathogen detection with molecular beacons coupled to nanowires.[70] Here, the target strands are PCR products of five pathogenic viral RNA sequences: Severe Acute Respiratory Syndrome (SARS), West Nile Virus (WNV), Hepatitis A (HAV), Hepatitis C (HCV) and HIV. Because these are RNA viruses, multiplexed reverse transcription (RT) PCR, which converts the pathogenic RNA to DNA before amplification, was performed. Single-stranded PCR products were generated by using

phosphorylated 5' primers to enable exonuclease digestion of the 5' strands after amplification; this gave better sensitivity as compared with double-stranded target. Figure 9 shows quantitative results obtained for multiple permutations of this assay, in which different targets were added.[70] Comparison of the RT-PCR targets to synthetic oligonucleotide targets was particularly encouraging because little degradation of assay performance was observed. This suggests that, despite steric hindrance at the nanowire surface for these hairpin probes, which could not be spaced further from the metal to provide more solution-like environment owing to the need for fluorescence quenching, hybridization to the long target strands produced by RT-PCR was reasonably efficient.

This combination of barcoded nanowires and molecular-beacon probes made it possible to perform multiplexed nucleic acid detection in a sealed chamber. Stoermer *et al.* demonstrated this in a triplex assay for HIV, HCV and SARS. Figure 1-12 shows representative microscope images and fluorescence quantification for different permutations of target addition.[71] Target oligonucleotide solutions were added directly to the barcoded nanowire suspension on a microscope slide, which was then sealed for hybridization and imaged without breaking this seal. Assay performance was essentially the same in the sealed chamber as when performed in eppendorf tubes with a wash step after target hybridization. Background signal in these on-wire molecular beacon assays arises primarily from incomplete quenching of the probe fluorophores by the metal surface and is relatively insensitive to noncomplementary oligonucleotides. Probe structure and hybridization reaction conditions have been investigated to identify initial design rules for surface beacon assays.[61, 70] The multiplexed, closed-tube capability of the nanowire beacon assay, paired with a detection limit of 100 pM as determined by a binding curve (Figure 1-13), has the potential for use in a clinical setting.[70] Although further optimization of this detection scheme will need to be made to account for genomic samples, molecular beacons conjugated to barcoded-metal nanowires hold great promise for future clinical biosensing

applications. In order to increase the sensitivity, which would be beneficial in analyzing clinical samples, while retaining multiplexing capability, nucleic acid amplification reactions such as PCR and LCR were investigated in this thesis using primers and probes attached to the nanowire surface.

Enzymatic Amplification of Surface-Immobilized Nucleic Acids

Using encoded particles to identify different amplicon sequences has potential for multiplexed PCR without the need for differing amplicon lengths or the use of fluorophores for identification,[24] thereby increasing the number of possible sequences detectable in one assay. There has been limited literature published on the use of enzymes for exponential amplification of nucleic acids when primer or probe sequences were immobilized to a surface. Most literature, while stating that it is a surface phase reaction, instead captures the post enzymatic amplification product on a surface, but does not perform the amplification on bound nucleic acids.[72-77] While there have been some reported surface bound amplification reactions, such as with emulsion PCR,[78-80] Chrisey and coworkers PCR on beads,[81] or Alivisatos and coworkers LCR on colloidal particles (the only mention of LCR for surface immobilized exponential amplification),[82] only a small handful have truly performed multiplexed amplification[78] When multiplexing is claimed, most often the reaction is performed serially in segregated reaction chambers, as is the case with emulsion PCR.[79, 80] One example of multiplexing within the same reaction volume[78] performed PCR in an emulsion and then performed allele-specific labeling of the beads; additionally, only the top 20th percentile of fluorescence intensity was compared, claiming the rest of the signal as background.

Oligonucleotides have been enzymatically extended off colloidal nanoparticles using Klenow polymerase[83], and in one instance, Chrisey et al. used primers bound to glass beads for

the purpose of reusable substrates for transcription reactions, but did not use an encoded particle, multiplex, or detect any pathogens.[81] PCR has been combined with a ligation reaction for the detection of Single Nucleotide Polymorphisms (SNPs) using barcoded nanowires as surface substrates,[84] however, the enzymatic chain reaction was not performed on the nanowires, which introduces the possibility of cross contamination. Mathies and coworkers performed on-bead PCR for use in sequencing DNA using capillary electrophoresis and flow cytometry.[80] While this method is useful for sequencing, it has several drawbacks, such as instrumentation demands that are not necessary when using barcoded nanowires, and is not multiplexed, but rather high throughput singleplexed analysis.

Most often the attachment chemistry used in literature studies is that of EDC,[81, 85-89] which, as is shown in Chapter 2, is not thermostable and allows for release of surface bound oligonucleotides into solution. This continued loss of nucleic acid into solution would allow for solution phase amplification, skewing the results of the amplification reaction. Additionally, the absolute number of oligonucleotides bound and the subsequent absolute number of amplicons generated is often transduced by the fluorescence signal of tagged sequences bound to the amplicons in a post-amplification step.[85, 89] While we have used fluorescence to quantify relative amounts of amplification within our systems, using fluorophores bound to a surface to calculate the absolute number of nucleic acid particles on a surface is nonideal, as they may interact with each other to produce incorrect results.[85]

In spite of the technical challenges of the assay, if each nanowire pattern were functionalized with primers of a different sequence, multiplexed PCR could be possible (see Figure 1-14) using an optical microscope, a great benefit in the world of clinical diagnostics, as this is an instrument most clinical labs already possess. Metallic nanowires can be coated in glass to provide additional functional groups for thermostable attachment methods.[65] The functionalization of the 5' end of the reverse primer sequence and the reaction of hydroxyl groups

on the glass surface to introduce other moieties generates a number of possible covalent chemistries. By fluorescently tagging the DNA (using an intercalating dye) and using the data processing program NBSee, the amount of fluorescence on each nanowire can be quantified. When the primers are immobilized to barcoded nanowires the ability to rinse out any contaminating sequences is presented, and post-amplification sample manipulation is limited to imaging processes, greatly reducing possible contamination. While PCR performed on the surface of a particle would have advantages over solution phase PCR, such as ease of multiplexing and sequence identification, it also would have certain disadvantages, such as increased steric hindrance of DNA hybridization and enzyme association due to the proximity of the particle surface. Methods attempting to overcome these sterics and increase on-wire amplification during PCR are discussed in Chapter 2.

Both on-wire LDR and LCR are also promising; instead of covalently attaching a primer to the barcoded nanowire, an oligonucleotide probe is used. This oligonucleotide probe could capture a template strand, which would then hybridize to a fluorescently tagged oligonucleotide (with a 5' phosphate), creating a sandwich hybridization assay. The ligase could then attach the probe and tag strands, therefore covalently attaching a fluorescent probe to the barcoded nanowire only in the presence of sequence-specific template. As the opposite strand is present for ligation in solution, there is the possibility for an exponential increase in fluorescently labeled barcoded nanowires specific for the pathogen sequence of interest (see Figure 1-15). On-wire LCR would have the same benefits as on-wire PCR in multiplexing and sequence identification, but has the added benefit that where the polymerase has to perform an enzymatic reaction for the addition of each base, the ligase has to perform only one enzymatic reaction to link the entire tag to the probe sequence. This decreases the overall number of required enzymatic reactions per nanowire and increases the specificity of the reaction, as three strands need to hybridize before ligase association and activity, as opposed to only two strands needed to hybridize before polymerase

activity. On-wire LCR faced the same steric hindrance challenge that on-wire PCR faces, and optimization to overcome this limitation is discussed in Chapter 3.

Work done towards the goal of detecting sequences for pathogens of interest in a rapid fashion without the need for additional equipment aside from a thermocycler and microscope, which are already present in most clinical laboratories, by performing on-wire PCR or LCR is discussed in Chapters 2 and 3, respectively. Parameter optimization and the multiplexed detection of template strands are also discussed in detail in Chapters 2 and 3.

Alternate Platforms and Nanoarchitecture

Chapter 4 covers work done on optimizing surface interactions on planar surfaces instead of particulate surfaces, specifically that of the polydimethylsiloxane (PDMS) used to stamp DNA and the gold surface the DNA is stamped onto. Instead of using encoded particles for multiplexing capability, stamped DNA sequences were spatially encoded. Gold surfaces patterned with DNA strands have applications in both biological detection strategies as well as in the generation of nanoarchitectures.

The development of a spatially encoded substrate similar to a microarray, but that circumvents the need for robotics or photolithography, was also investigated. One possible way of making DNA patterns on a substrate is by performing microcontact printing, where molecules of interest, such as DNA, are inked onto a PDMS stamp, the stamp is brought into contact with the substrate, and a SAM is then generated on the unpatterned surface, creating a pattern of molecules of interest, see Figure 1-16. This method may result in the diffusion of the probes across the surface, or the disruption of the probe pattern by the generation of a SAM.[90] Microcontact insertion printing, which is much the same as microcontact printing, except the ink is printed into a preexisting SAM and therefore stamped molecules remain isolated from one

another, overcomes these issues and has the potential for generating substrates to be used in single molecule studies.[90, 91] Both these methods are also less expensive than lithographic techniques and can pattern a larger area.[92]

Creating stamped patterns of individual DNA strands could be beneficial in single molecule studies, but also for other purposes. DNA is a biologically relevant molecule with built in specificity for its complementary strand; this functionality makes it ideal for use in tethering particles or other biomolecules. DNA thus has capabilities for acting as a scaffold and creating ordered structures, such as those used in circuits.[93] Some possible functions for these ordered scaffolds include, but are not limited to, increasing efficiency of catalysis by placing certain moieties near each other, biosensing applications such as microfluidic devices or microarrays, and nanomaterial design, where nanoparticles or other functional moieties can be oriented in a certain way.[94] Sensing applications may also include the detection of biothreat agents.[91] Patterned SAMS can also be used in lithography resists and in altering film properties.[95] By stamping individual DNA molecules into a predetermined pattern, several possible functionalization methods and applications become possible, such as sensing, catalysis, developing nanoarchitectures, and altering film properties.

Both the work done on particle and the work done on planar substrates could be harnessed for use in assembling ordered nano-scale features, in addition to sensing purposes. Several papers have discussed the generation of multi-nanoparticle structures, as well as the tethering of biomolecules to surfaces in specific orientations. Structural architecture design is possible using several enzyme functionalities and nanotechnology methods. Nanotemplates have been generated using Rolling Circle Amplification, a technique utilizing a polymerase for copying circular nucleic acid sequences.[96] Restriction enzymes, those that cut nucleic acid sequences, have been used to catalyze nanostructure generation when followed by the use of a ligase,[97] as well as disassemble the nanoarchitectures[98]. Additionally, restriction enzymes are

proposed for use in programmed biomolecule release into solution and deprotection of nanoarchitectures for further modification.[98] Ligation reactions have been used to generate polycatenated scaffolds for subsequent functionalization,[94] to asymmetrically functionalize nanoparticles,[99] and to create multinanoparticle structures.[82] DNA attached to planar surfaces has been used as a scaffold to attach particles and proteins in a specified arrangement;[94] and small molecules have been inserted into a self assembled monolayer (SAM), covalently attached to planar surfaces, and used as capture probes, such as with serotonin and the corresponding antibody.[100, 101] Optimization of stamping DNA from PDMS stamps to gold substrates is discussed in Chapter 4.

Summary and Objectives

Chapter 2 discusses an on-wire PCR assay that was developed and investigated to determine if pairing PCR with a suspension array in which each bound DNA sequence is identified by a barcoded nanowire and quantified using fluorescence would then make multiplexed PCR possible. Investigations into the surface interactions between the glass, crosslinker molecules, DNA, fluorophores, enzyme, etc. are covered. Efforts at increasing sensitivity, specificity, and reproducibility, as well as reducing background are also addressed. Chapter 3 details the use of LCR for on-wire multiplexed pathogen-encoding sequence detection. This technique allowed for rapid, sensitive detection of multiple sequences without the need for spectrally differentiable fluorophores for identification. LCR parameter optimization and multiplexed detection are discussed. Chapter 4 details the progress towards microcontact printing of DNA molecules onto gold substrates. This includes confirmation of the DNA inking the stamp, the DNA transferring from the stamp to the substrate, and the visualization of the DNA pattern on the substrate. The Appendix covers an undergraduate laboratory exercise to introduce

students to nanotechnology. Students synthesized and functionalized nanoparticles, and observed differences between bulk and nano-scale materials. These projects all focus on understanding and controlling the functionalization of surfaces, and using these surfaces in subsequent experimentation.

References

1. Liolios, L.; Jenney, A.; Spelman, D.; Kotsimbos, T.; Catton, M.; Wesselingh, S. Comparison of a Multiplex Reverse Transcription-PCR-Enzyme Hybridization Assay with Conventional Viral Culture and Immunofluorescence Techniques for the Detection of Seven Viral Respiratory Pathogens. *J. Clin. Microbiol.* **2001**, *39 (8)*, 2779-2783.

2. Puppe, W.; Weighl, J. A. I.; Aron, G.; Gröndahl, B.; Schmitte, H.-J.; Niesters, H. G. M.; Groen, J. Evaluation of a multiplex reverse transcriptase PCR ELISA for the detection of nine respiratory tract pathogens. *J. Clin. Virol.* **2004**, *30*, 165-174.

3. Kuypers, J.; Wright, N.; Morrow, R. Evaluation of quantitative and type-specific real-time RT-PCR assays for detection of respiratory syncytial virus in respiratory specimens from children. *J. Clin. Virol.* **2004**, *31*, 123-129.

4. Madeley, C. R.; Peiris, J. S. M. Methods in virus diagnosis: immunofluorescence revisited. *J. Clin. Virol.* **2002**, *25*, 121-134.

5. Weinberg, A.; Brewster, L.; Clark, J.; Simoes, E. Evaluation of R-Mix shell vials for the diagnosis of viral respiratory tract infections. *J. Clin. Virol.* **2004**, *30*, 100-105.

6. Ogilvie, M. Molecular techniques should not now replace cell culture in diagnostic virology laboratories. *Rev. Med. Virol.* **2001**, *11*, 351-354.

7. Casiano-Colón, A. E.; Hulbert, B. B.; Mayer, T. K.; Walsh, E. E.; Falsey, A. R. Lack of sensitivity of rapid antigen tests for the diagnosis of respiratory syncytial virus infection in adults. *J. Clin. Virol.* **2003**, *28*, 169-174.

8. Klein, D. Quantification using real-time PCR technology: applications and limitations. *Trends Mol. Med.* **2002**, *8*, 257-260.

9. Mackay, I. M.; Arden, K. E.; Nitsche, A. Real Time PCR in Virology. *Nucleic Acids Res.* **2002**, *30 (6)*, 1292-1305.

10. Barany, F. Genetic disease detection and DNA amplification using cloned thermostable ligase. *Proc. Natl. Acad. Sci. USA.* **1991**, *88*, 189-193.

11. Barany, F. The ligase chain reaction in a PCR world. *Genome Res.* **1991**, *1*, 5-16.

12. Wiedmann, M.; Wilson, W. J.; Czajka, J.; Luo, J.; Barany, F.; Batt, C. A. Ligase Chain Reaction (LCR)—Overview and Applications. *PCR Methods. Appl.* Cold Spring Harbor Laboratory Press. **1994**, *3S*, 51-64.

13. Poulakkainen, M.; Hiltunen-Back, E.; Reunala, T.; Suhonen, S.; Lähteenmäki, P.; Lehtinen, M.; Paavonen, J. Comparison of performances of two commercially available tests, a

PCR assay and a Ligase Chain Reaction test, in detection of urogenital *Chlamydia trachomatis* infection. *J. Clin. Microbiol.* **1998**, *36 (6)*, 1489-1493.

14. Locksmith, G. J. New diagnostic tests for Gonorrhea and Chlamydia. *Prim. Care Update Ob/Gyn*. **1997**, *4 (5)*, 161-167.

15. Tortoli, E.; Lavinia, F.; Simonetti, M. T. Evaluation of a commercial Ligase Chain Reaction kit (Abbott LCx) for direct detection of *Mycobacterium tuberculosis* in pulmonary and extrapulmonary specimens. *J. Clin. Microbiol.* **1997**, *35 (9)*, 2424-2426.

16. Bourgeois, C.; Sixt, N.; Bour, J. B.; Pothier, P. Value of a ligase chain reaction assay for detection of ganciclovir resistance-related mutation 594 in UL97 gene of human cytomegalovirus. *J. Virological Methods.* **1997**, *67*, 167-175.

17. Day, N. S.; Tadin, M.; Christiano, A. M.; Lanzano, P.; Piomelli, S.; Brown, S. Rapid prenatal diagnosis of sickle cell diseases using oligonucleotide ligation assay coupled with laser-induced capillary fluorescence detection. *Prenat. Diagn.* **2002**, *22*, 686-691.

18. Dong, S. M.; Traverso, G.; Johnson, C.; Geng, L.; Favis, R.; Boynton, K.; Hibi, K.; Goodman, S. N.; D'Allessio, M.; Paty, P.; Hamilton, S. R.; Sidransky, D.; Barany, F.; Levin, B.; Shuber, A.; Kinzler, K. W.; Vogelstein, B.; Jen, J. Detecting colorectal cancer in stool with the use of multiple genetic targets. *J. National Cancer Institute.* **2001**, *93 (11)*, 858-865.

19. Abravaya, K.; Carrino, J. J.; Muldoon, S.; Lee, H. H. Detection of point mutations with a modified ligase chain reaction (Gap-LCR). *Nucleic Acids Res.* **1995**, *23 (4)*, 675-682.

20. Pfeifer, G. P.; Steigerwald, S. D.; Mueller, P. R.; Wold, B.; Riggs, A. D. Genomic sequencing and methylation analysis by ligation mediated PCR. *Science*. **1989**, *246 (4931)*, 810-813.

21. Rosi, N. L.; Mirkin, C. A. Nanostructures in biodiagnostics. *Chem. Rev.* **2005**, *105* (4), 1547-1562.

22. Patolsky, F.; Zheng, G.; Lieber, C. M. Nanowire sensors for medicine and the life sciences. *Nanomed.* **2006**, *1* (1), 51-65.

23. Zheng, G.; Patolsky, F.; Cui, Y.; Wang, W. U.; Lieber, C. M. Multiplexed electrical detection of cancer markers with nanowire sensor arrays. *Nat. Biotechnol.* **2005**, *23* (10), 1294-1301.

24. Penn, S. G.; He, L.; Natan, M. J. Nanoparticles for bioanalysis. *Curr. Opin. Chem. Biol.* **2003**, *7* (5), 609-615.

25. Nam, J.-M.; Thaxton, C. S.; Mirkin, C. A. Nanoparticle-based bio-bar codes for the ultrasensitive detection of proteins. *Science* **2003**, *301* (5641), 1884-1886.

26. Cui, Y.; Wei, Q.; Park, H.; Lieber, C. M. Nanowire nanosensors for highly sensitive and selective detection of biological and chemical species. *Science* **2001**, *293* (5533), 1289-1292.

27. Gao, X.; Cui, Y.; Levenson, R. M.; Chung, L. W. K.; Nie, S. *In vivo* cancer targeting and imaging with semiconductor quantum dots. *Nat. Biotechnol.* **2004**, *22* (8), 969-976.

28. Wu, X.; Liu, H.; Liu, J.; Haley, K. N.; Treadway, J. A.; Larson, J. P.; Ge, N.; Peale, F.; Bruchez, M. P. Immunofluorescent labeling of cancer marker Her2 and other cellular targets with semiconductor quantum dots. *Nat. Biotechnol.* **2003**, *21* (1), 41-46.

29. Fritz, J.; Baller, M. K.; Lang, H. P.; Rothuizen, H.; Vettiger, P.; Meyer, E.; Güntherodt, H.-J. Gerber, Ch.; Gimzewski, J. K. Translating biomolecular recognition into nanomechanics. *Science* **2000**, *288* (5464), 316-318.

30. Zhang, X.; Shah, N. C.; Van Duyne, R. P. Sensitive and selective chem/bio sensing based on surface-enhanced Raman spectroscopy (SERS). *Vib. Spectrosc.* **2006**, *42* (1), 2-8.

31. Zhao, J.; Zhang, X.; Yonzon, C. R.; Haes, A. J.; Van Duyne, R. P. Localized surface plasmon resonance biosensors. *Nanomed.* **2006**, *1* (2), 219-228.

32. Ilic, Y.; Yang, Y.; Aubin, K.; Reichenbach, R.; Krylov, S.; Craighead, H. G. Enumeration of DNA molecules bound to a nanomechanical oscillator. *Nano Lett.* **2005**, *5* (5), 925-929.

33. Nolan, J. P.; Sklar, L. A. Suspension array technology: evolution of the flat-array paradigm. *Trends Biotechnol.* **2002**, *20* (1), 9-12.

34. *DNA Microarrays A Practical Approach.* Schena, M., Ed.; Oxford University Press Inc.: New York, 1999.

35. *Microarray Biochip Technology.* Schena, M., Ed.; A Biotechniques Books Publication Eaton Publishing: Natick, MA, 2000.

36. Nicewarner-Peña, S. R.; Freeman, R. G.; Reiss, B. D.; He, L.; Peña, D. J.; Walton, I. D.; Cromer, R.; Keating, C. D.; Natan, M. J. Submicrometer metallic barcodes. *Science* **2001**, *294* (5540), 137-141.

37. Pregibon, D. C.; Toner, M.; Doyle, P. S. Multifunctional encoded particles for high-throughput biomolecule analysis. *Science* **2007**, *315* (5817), 1393-1396.

38. Kellar, K. L.; Iannone, M. A. Multiplexed microsphere-based flow cytometric assays. *Exp. Hematol.* **2002**, *30* (11), 1227-1237.

39. Dejneka, M. J.; Streltsov, A.; Pal, S.; Frutos, A. G.; Powell, C. L.; Yost, K.; Yuen, P. K.; Müller, U.; Lahiri, J. Rare earth-doped glass microbarcodes. *Proc. Natl. Acad. Sci. U.S.A.* **2003**, *100* (2), 389-393.

40. He, B.; Son, S. J.; Lee, S. B. Shape-coded silica nanotubes for biosensing. *Langmuir* **2006**, *22* (20), 8263-8265.

41. Hernandez, C. J.; Mason, T. G. Colloidal alphabet soup: monodisperse dispersions of shape-designed LithoParticles. *J. Phys. Chem. C* **2007**, *111* (12), 4477-4480.

42. Battersby, B. J.; Bryant, D.; Meutermans, W.; Matthews, D.; Smythe, M. L.; Trau, M. Toward larger chemical libraries: encoding with fluorescent colloids in combinatorial chemistry. *J. Am. Chem. Soc*. **2000**, *122* (9), 2138-2139.

43. Han, M.; Gao, X.; Su, J. Z.; Nie, S. Quantum-dot-tagged microbeads for multiplexed optical coding of biomolecules. *Nat. Biotechnol.* **2001**, *19* (7), 631-635.

44. Braeckmans, K.; De Smedt, S. C.; Roelant, C.; Leblans, M.; Pauwels, R.; Demeester, J. Encoding microcarriers by spatial selective photobleaching. *Nat. Mater*. **2003**, *2* (3), 169-173.

45. Zhi, Z.; Morita, Y.; Hasan, Q.; Tamiya, E. Micromachining microcarrier-based biomolecular encoding for miniaturized and multiplexed immunoassay. *Anal. Chem.* **2003**, *75* (16), 4125-4131

46. Luminex Corporation. http://www.luminexcorp.com. Accessed 10 July 2007.

47. Eastman, P. S.; Ruan, W.; Doctolero, M.; Nuttall, R.; de Feo, G.; Park, J. S.; Chu, J. S. F.; Cooke, P.; Gray, J. W.; Li, S.; Chen, F. F. Qdot nanobarcodes for multiplexed gene expression analysis. *Nano Lett.* **2006**, *6* (5), 1059-1064.

48. Han, M.; Gao, X.; Su, J. Z.; Nie, S. Quantum-dot-tagged microbeads for multiplexed optical coding of biomolecules. *Nat. Biotechnol.* **2001**, *19* (7), 631-635.

49. Nicewarner-Peña, S. R.; Carado, A. J.; Shale, K. E.; Keating, C. D. Barcoded metal nanowires: optical reflectivity and patterned fluorescence. *J. Phys. Chem. B* **2003**, *107* (30), 7360-7367.

50. Reiss, B. D.; Freeman, R. G.; Walton, I. D.; Norton, S. M.; Smith, P. C.; Stonas, W. G.; Keating, C. D.; Natan, M. J. Electrochemical synthesis and optical readout of striped metal rods with submicron features. *J. Electroanal. Chem.* **2002**, *522* (1), 95-103.

51. Walton, I. D.; Norton, S. M.; Balasingham, A.; He, L.; Oviso, D. F., Jr.; Gupta, D.; Raju, P. A.; Natan, M. J.; Freeman, R. G. Particles for multiplexed analysis in solution: detection and identification of striped metallic particles using optical microscopy. *Anal. Chem.* **2002**, *74* (10), 2240-2247.

52. True, R. J.; Taylor, M. K.; Chakarova, G. S.; Walton, I. D. Microfabricated templates for the electrodeposition of metallic barcodes for use in multiplexed bioassays. Proceedings of the 26th Annual Conference of the IEEE EMBS. San Francisco, USA, 2004.

53. Matthias, S.; Schilling, J.; Nielsch, K.; Müller, F.; Wehrspohn, R. B.; Gösele, U. Monodisperse diameter-modulated gold microwires. *Adv. Mater*. **2002**, *14* (22), 1618-1621.

54. Sioss, J. A.; Keating, C. D. Batch preparation of linear Au and Ag nanoparticle chains via wet chemistry. *Nano Lett.* **2005**, *5* (9), 1779-1783.

55. Martin, C.R. Membrane-based synthesis of nanomaterials. *Chem. Mater*. **1996**, *8* (8), 1739-1746.

56. Martin, C. R. Nanomaterials: a membrane-based synthetic approach. *Science* **1994**, *266* (5193), 1961-1966.

57. Al-Mawalawi, D.; Liu, C. Z.; Moskovits, J. Nanowires formed in anodic oxide nanotemplates. *J. Mater. Res.* **1994**, *9* (4), 1014-1018.

58. Martin, B. R.; Dermody, D. J.; Reiss, B. D.; Fang, M.; Lyon, A.; Natan, M. J.; Mallouk, T. E. Orthogonal self-assembly on colloidal gold-platinum nanorods. *Adv. Mater.* **1999**, *11* (12), 1021-1025.

59. Kline, T. R.; Tian, M.; Wang, J.; Sen, A.; Chan, M. W. H.; Mallouk, T. E. Template-grown metal nanowires. *Inorg. Chem.* **2006**, *45* (19), 7555-7565.

60. Keating, C. D.; Natan, M. J. Striped metal nanowires as building blocks and optical tags. *Adv. Mater.* **2003**, *15* (5), 451-454.

61. Stoermer, R. L.; Keating, C. D. Distance-dependent emission from dye-labeled oligonucleotides on striped Au/Ag nanowires: effect of secondary structure and hybridization efficiency. *J. Am. Chem. Soc.* **2006**, *128* (40), 13243-13254.

62. Tok, J. B. H.; Chuang, F. Y. S.; Kao, M. C.; Rose, K. A.; Pannu, S. S.; Sha, M. Y.; Chakarova, G.; Penn, S. G.; Dougherty, G. M. Metallic striped nanowires as multiplexed immunoassay platforms for pathogen detection. *Angew. Chem., Int. Ed. Engl.* **2006**, *45* (41), 6900-6904.

63. Stoermer, R. L.; Sioss, J. A.; Keating, C. D. Stabilization of silver metal in citrate buffer: barcoded nanowires and their bioconjugates. *Chem. Mater.* **2005**, *17* (9), 4356-4361.

64. Wildt, B.; Mali, P.; Searson, P. C. Electrochemical template synthesis of multisegment nanowires: fabrication and protein functionalization. *Langmuir* **2006**, *22* (25), 10528-10534.

65. Sioss, J. A.; Stoermer, R.L.; Sha, M.Y.; Keating, C.D. Silica coated, Au/Ag striped nanowires for bioanalysis. *Langmuir* **2007**, *23* (22), 11334-11341.

66. Dean, S. L.; Stapleton, J. J.; Keating, C. D. Organically modified silicas on metal nanowires. *Langmuir* **2010**, *in press*. doi: 10.1021/la102070c

67. Tanase, M.; Bauer, L.A.; Hultgren, A.; Silevitch, D. M.; Sun, L.; Reich, D. H.; Searson, P. C.; Meyer G. J. Magnetic alignment of fluorescent nanowires. *Nano Lett.* **2001**, *1* (3), 155-158.

68. Lee, K.-B.; Park, S.; Mirkin, C. A. Multicomponent magnetic nanorods for biomolecular separations. *Angew. Chem. Int. Ed. Engl.* **2004**, *43* (23), 3048-3050.

69. Sha, M. Y.; Walton, I. D.; Norton, S. M.; Taylor, M.; Yamanaka, M.; Natan, M. J.; Xu, C.; Drmanac, S.; Huang, S.; Dorcherding, A.; Drmanac, R.; Penn, S. G. Multiplexed SNP genotyping using nanobarcode particle technology. *Anal. Bioanal. Chem.* **2006**, *384* (3), 658-666.

70. Sha, M. Y.; Yamanaka, M.; Walton, I. D.; Norton, S. M.; Stoermer, R. L.; Keating, C. D.; Natan, M. J.; Penn, S. G. Encoded metal nanoparticle-based molecular beacons for multiplexed detection of DNA. *Nanobiotechnol.* **2005**, *1* (4), 327-336.

71. Stoermer, R. L.; Cederquist, K. B.; McFarland, S. K.; Sha, M. Y.; Penn, S. G.; Keating, C. D. Coupling molecular beacons to barcoded metal nanowires for multiplexed, sealed chamber DNA bioassays. *J. Am. Chem. Soc.* **2006**, *128* (51), 16892-16903.

72. Song, L.; Ahn, S.; Walt, D. R. Fiber-optic microsphere-based arrays for multiplexed biological warfare agent detection. *Anal. Chem.* **2006**, *78* (4), 1023-1033.

73. Piersimoni, C.; Callegaro, A.; Scarparo, C.; Penati, V.; Nista, D.; Bornigia, S.; Lacchini, C.; Scagnelli, M.; Santini, G.; De Sio, G. Comparative evaluation of the new gen-probe *Mycobacterium tuberculosis* amplified direct test and the semiautomated Abbott LCx *Mycobacterium tuberculosis* assay for direct detection of *Mycobacterium tuberculosis* complex in respiratory and extrapulmonary specimens. *J. Clin. Microbiol.* **1998**, *36* (12), 3601-3604.

74. Dean, D.; Ferrero, D.; McCarthy, M. Comparison of performance and cost-effectiveness of direct fluorescent-antibody, ligase chain reaction, and PCR assays for verification of chlamydial enzyme immunoassay results for populations with a low to moderate prevalence of *Chlamydia trachomatis* infection. *J. Clin. Microbiol.* **1998**, *36* (1), 94-99.

75. Moore, D. F.; Curry, J. I. Detection and identification of *Mycobacterium tuberculosis* directly from sputum sediments by ligase chain reaction. *J. Clin. Microbiol.* **1998**, *36* (4), 1028-1031.

76. Wilson, W. J.; Erler, A. M.; Nasarabadi, S. L.; Skowronski, E. W.; Imbro, P. M. A multiplexed PCR-coupled liquid bead array for the simultaneous detection of four biothreat agents. *Mol. Cell. Probes* **2005**, *19* (2), 137-144.

77. Guo, Z.; Guilfoyle, R. A.; Thiel, A. J.; Wang, R.; Smith, L. M. Direct fluorescence analysis of genetic polymorphisms by hybridization with oligonucleotide arrays on glass supports. *Nucleic Acids Res.* **1994**, *22* (24), 5456-5465.

78. Tiemann-Boege, I.; Curtis, C.; Shinde, D. N.; Goodman, D. B.; Tavaré, S.; Arnheim, N. Product length, dye choice, and detection chemistry in the bead-emulsion amplification of millions of single DNA molecules in parallel. *Anal. Chem.* **2009**, *81* (14), 5770-5776.

79. Shendure, J.; Porreca, G. J.; Reppas, N. B.; Lin, X.; McCutcheon, J. P.; Rosenbaum, A. M.; Wang, M. D.; Zhang, K.; Mitra, R. D.; Church, G. M. Accurate multiplex polony sequencing of an evolved bacterial genome. *Science* **2005**, *309* (5741), 1728-1732.

80. Kumaresan, P.; Yang, C. J.; Cronier, S. A.; Blazej, R. G.; Mathies, R. A. High-throughput single copy DNA amplification and cell analysis in engineering nanoliter droplets. *Anal. Chem.* **2008**, *80*, 3522-3529.

81. Andreadis, J.D.; Chrisey, L. A. Use of immobilized PCR primers to generate covalently immobilized DNAs for *in vitro* transcription/translation reactions. *Nucleic Acids Res.* **2000**, *28* (2), e5.

82. Claridge, S. A.; Mastroianni, A. J.; Au, Y. B.; Liang, H. W.; Micheel, C. M.; Fréchet, J. M. J.; Alivisatos, A. P. Enzymatic ligation creates discrete multinanoparticle building blocks for self-assembly. *J. Am. Chem. Soc.* **2008**, *130 (29)*, 9598-9605.

83. Nicewarner-Peña, S. R.; Raina, S.; Goodrich, G. P.; Fedoroff, N. V.; Keating, C. D. Hybridization and enzymatic extension of Au nanoparticle-bound oligonucleotides. *J. Am. Chem. Soc.* ***2002***, *124* (24), 7314-7323.

84. Sha, M. Y.; Walton, I. D.; Norton, S. M.; Taylor, M.; Yamanaka, M.; Natan, M. J.; Xu, C.; Drmanac, S.; Huang, S.; Borcherding, A.; Drmanac, R.; Penn, S. G. Multiplexed SNP genotyping using nanobarcode particle technology. *Anal. Bioanal. Chem.* 2**006**, *384*, 658-666.

85. Carmon, A.; Vision, T. J.; Mitchell, S. E.; Thannhauser, T. W.; Müller, U.; Kresovich, S. Solid-phase PCR in microwells: Effects of linker length and composition on tethering, hybridization, and extension. *Biotechniques* **2002**, *32* (2), 410-420.

86. von Nickish-Rosenegk, M.; Marschan, X.; Andresen, D.; Abraham, A.; Heise, C.; Bier, F. F. On-chip PCR amplification of very long templates using immobilized primers on glassy surfaces. *Biosens. Bioelectron.* **2005**, *20* (8), 1491-1498.

87. Adessi C.; Matton, G.; Ayala, G.; Turcatti, G.; Mermod, J.-J.; Mayer, P.; Kawashima, E. Solid phase DNA amplification: Characterisation of primer attachment and amplification mechanisms. *Nucleic Acids Res.* **2000**, *28* (20), e87.

88. von Nickisch-Rosenegk, M.; Marschan, X.; Andresen, D.; Bier, F. F. Reverse transcription-polymerase chain reaction on a microarray: The integrating concept of 'active arrays.' *Anal. Bioanal. Chem.* **2008**, *391* (5), 1671-1678.

89. Palanisamy, R.; Connolly, A. R.; Trau, M. Considerations of solid-phase DNA amplification. *Bioconjugate Chem.* **2010**, *21* (4), 690-695.

90. Saavedra, H. M.; Mullen, T. J.; Zhang, P.; Dewey, D. C.; Claridge, S. A.; Weiss, P. S. Hybrid strategies in nanolithography. *Rep. Prog. Phys.* **2010**, *73* (3), 036501.

91. T. J. Mullen, Ph. D. Thesis, The Pennsylvania State University, 2008.

92. Mullen, T. J.; Srinivasan, C.; Hohman, J. N.; Gillmor, S. D.; Shuster, M. J.; Horn, M. W.; Andrews, A. M.; Weiss, P. S. Microcontact Insertion Printing. *Appl. Phys. Lett.* **2007**, *90*, 063114.

93. Lin, C.; Liu, Y.; Rinker, S.; Yan, H. DNA Tile Based Self-Assembly: Building Complex Nanoarchitectures. *Chem. Phys. Chem.* **2006**, *7*, 1641-1647.

94. Weizmann, Y.; Braunschweig, A. B.; Wilner, O. I.; Cheglakov, Z.; Willner, I. A polycatenated DNA scaffold for the one-step assembly of hierarchical nanostructures. *PNAS.* **2008**, *105 (14)*, 5289-5294.

95. Smith, R. K.; Lewis, P. A.; Weiss, P. S. Patterned Self-Assembled Monolayers. *Prog. Surf. Sci.* **2004**, *75*, 1-68.

96. Beyer, S.; Nickels, P.; Simmel, F. C. Periodic DNA nanotemplates synthesized by Rolling Circle Amplification. *Nano Lett* **2005**, *5 (4)*, 719-722.

97. Kanaras, A. G.; Wang, Z.; Hussain, I.; Brust, M.; Cosstick, R.; Bates, A. D. Site-specific ligation of DNA-mediated gold nanoparticles activation by the restriction enzyme *Sty*1. *Small* **2007**, *3 (1)*, 67-70.

98. Kanaras, A. G.; Wang, Z.; Brust, M.; Cosstick, R.; Bates, A. D. Enzymatic disassembly of DNA-gold nanostructures. *Small* **2007**, *3 (4)*, 590-594.

99. Xu, X.; Rosi, N. L.; Wang, Y.; Huo, F.; Mirkin, C. A. Asymmetric functionalization of gold nanoparticles with oligonucleotides. *J. Am. Chem. Soc.* **2006**, *128 (9)*, 9286-9287.

100. Shuster, M. J.; Vaish, A.; Szapacs, M. E.; Anderson, M. E.; Weiss, P. S.; Andrews, A. M. Biospecific recognition of tethered small molecules diluted in self-assembled monolayers. *Adv. Mater*. **2008**, *20* (1), 164-167.

101. Mullen, T. J.; Dameron, A. A.; Andrews, A. M.; Weiss, P. S. Selecting and driving monolayer structures through tailored intermolecular interactions. *Aldrichimica Acta* **2007**, *40* (1), 21-31.

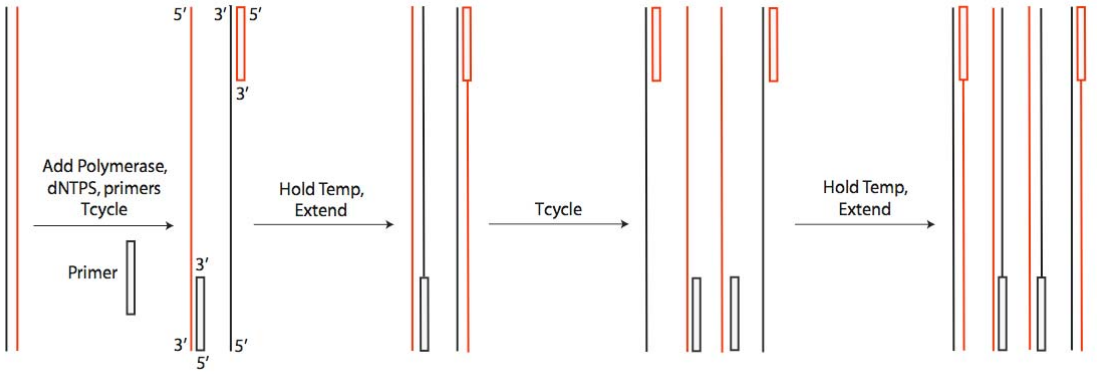

Figure 1-1. Representation of solution phase PCR, an exponential amplification method for DNA, where the red and black lines indicate complementary sense and antisense strands.

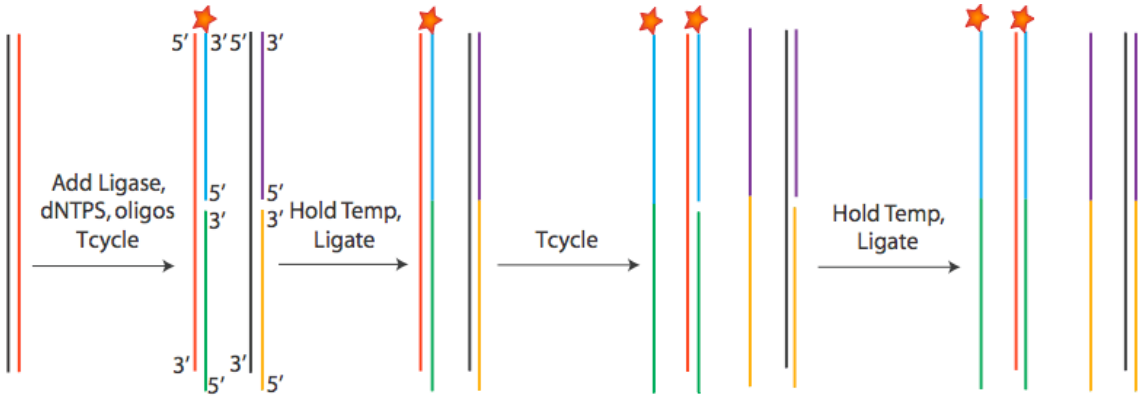

Figure 1-2. Representation of solution phase ligase chain reaction (LCR). The red and black lines represent the sense and antisense strands of the template, the green and yellow lines represent probe strands, and the blue and purple lines represent tag strands that have 5' phosphate groups.

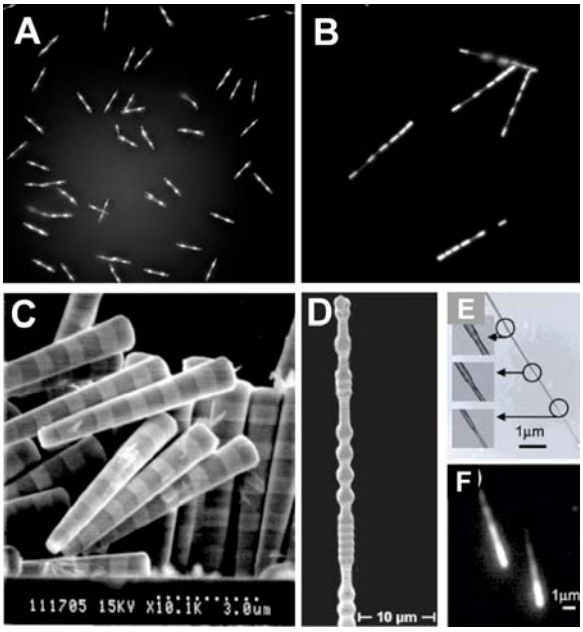

Figure 1-3. Encoded nanowires prepared in alumina or silica templates. (A) Reflectance image of 6 µm Au–Ag–Au–Au–Ag–Au barcoded nanowires; (B) reflectance image of 8 µm glass shells containing Au segments left behind after etching sacrificial Ag stripes from barcoded nanowires; (C) conical metallic barcoded wires prepared in lithographic templates (reprinted in part with permission from reference 52, © 2004); (D) diameter-modulated gold wires prepared in silica templates (reproduced with permission from reference 53, © Wiley-VCH Verlag GmbH & Co. KGaA); (E) TEM and (F) reflectance images of shape-coded silica nanotubes (reprinted in part with permission from reference 40, © 2006 American Chemical Society).

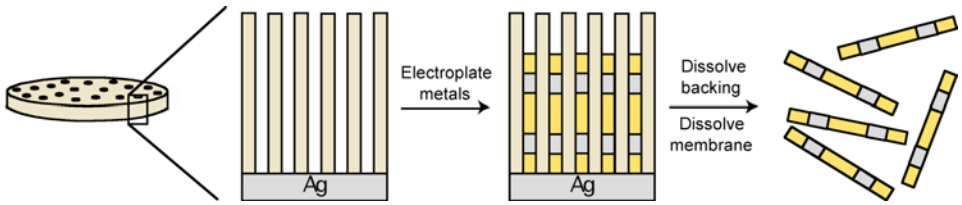

Figure 1-4. Barcoded metal nanowire synthesis by templated electrodeposition. Barcoded nanowires are grown in alumina membranes, which have been given a silver coating on one side to serve as the working electrode. Metal is electrodeposited into the pores; by alternating metal solutions, the barcode pattern is achieved. The silver backing and the membrane are dissolved with nitric acid and sodium hydroxide, respectively, releasing the wires into suspension.

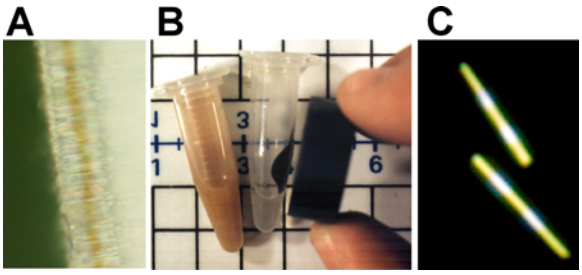

Figure 1-5. Metallic barcoded particles. (A) Microscopic cross-section of Ag–Au–Ag wires before release from the membrane. (B) Au (left) and Co (right) nanowires in ethanol suspension. Co particles can be manipulated magnetically. (C) White-light reflectance microscope image of barcoded nanowires of pattern Au–Ag–Au–Ag–Au.

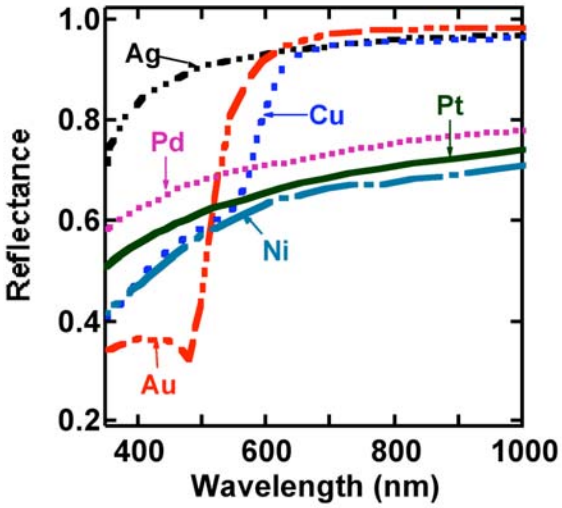

Figure 1-6. Bulk reflectance of several metals as a function of the wavelength of light. Because the reflectivities for segments of barcoded wires match reasonably well with the reflectivities of the bulk metals shown here, it is possible to use these bulk reflectance values to select wavelengths for distinguishing different metals. Reprinted with permission from *Science* [http://www.aaas.org], Ref. 36. © 2001 American Association for the Advancement of Science.

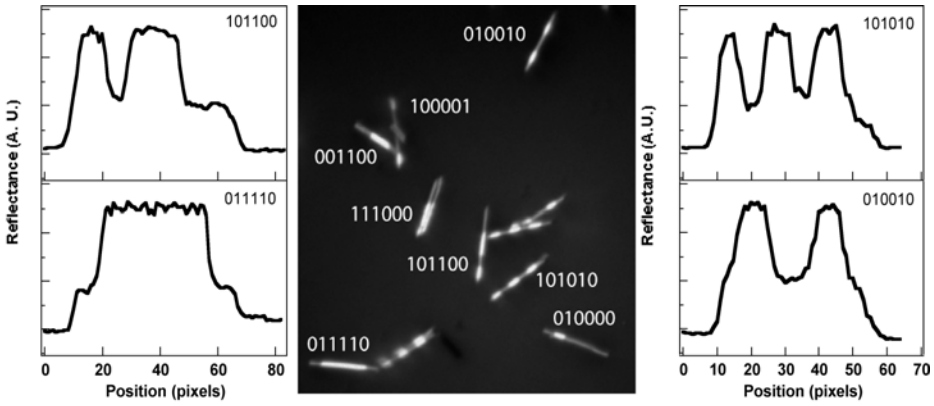

Figure 1-7. Decoding the metal striping pattern. The reflectance image under blue illumination (center) is acquired using optical-reflectance microscopy. Line-scans corresponding to four out of the eight wire patterns shown are on either side of the reflectance image and demonstrate how wire barcodes are distinguished from one another. Particle patterns are represented with 0 = Au and 1 = Ag for a single metal segment.

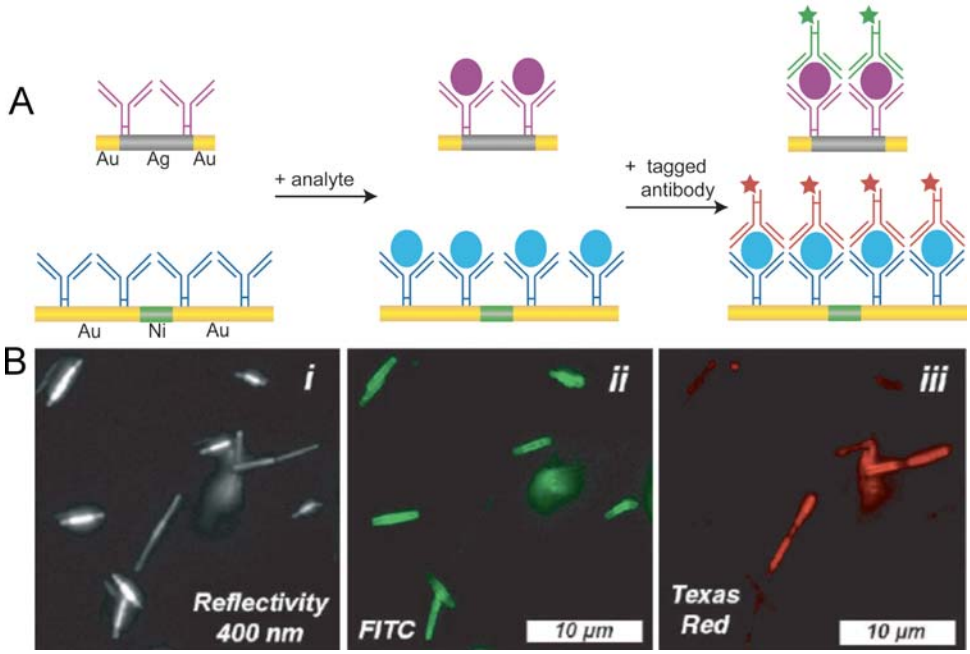

Figure 1-8. Two simultaneous immunoassays on barcoded nanowires. (A) Illustration of the experiment. Each batch of wires is functionalized with a single type of capture antibody (the shorter gold and silver wires to human immunoglobulin and the longer nickel and gold wires to rabbit immunoglobulin). They are then mixed together and exposed to both types of antigens and the corresponding antigen binds. Fluorescently labeled antibodies are then added, which bind to and label the present antigens for which they are specific (in this case green for human and red for rabbit antigens). (B) Reflectance and fluorescence microscope images show nanowire identity and target presence, respectively. Reprinted with permission from *Science* [http://www.aaas.org], Ref. 36. © 2001 American Association for the Advancement of Science.

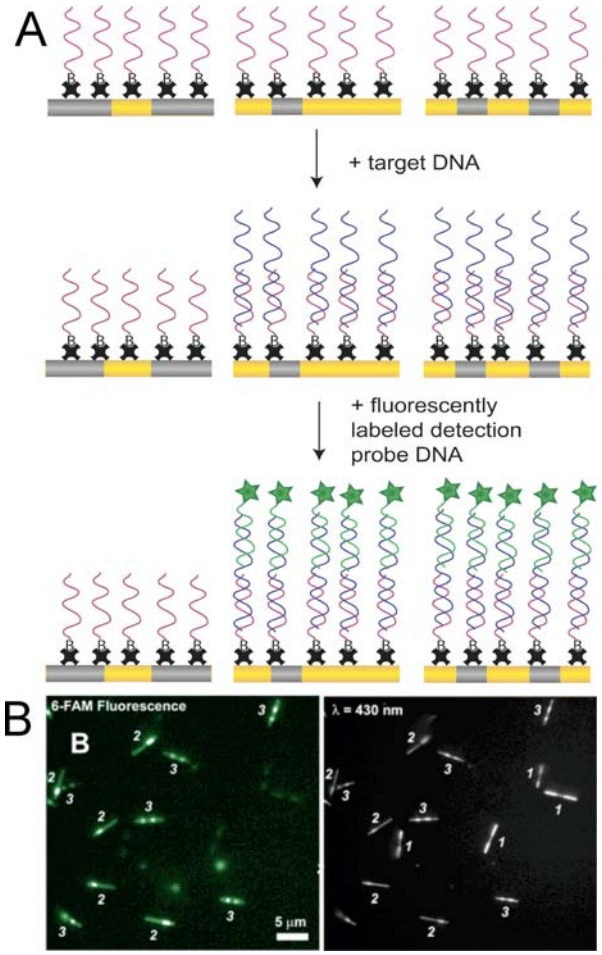

Figure 1-9. Multiplexed DNA hybridization assay on barcoded nanowires. (A) Representation of triplexed sandwich hybridization assay on barcoded nanowires. In this illustration, wires patterned 11011 (left), 01000 (middle) and 01010 (right) are coated with different probe sequences. Complementary target oligonucleotides have been added for the probes on 01000 and 01010 particles. (B) The reflectance image at right shows the barcode pattern of each wire. The selective hybridization is shown in the fluorescence image at the left. Image pairs such as these are used for identification and quantification of target analytes in simultaneous assays. Reprinted in part with permission from Ref. 49. © 2003 American Chemical Society.

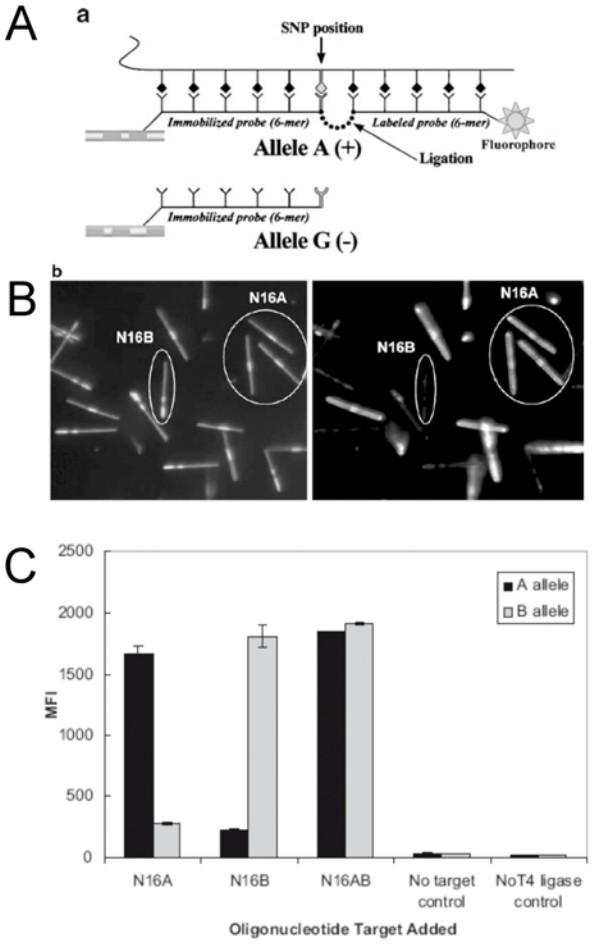

Figure 1-10. Genotype determination using oligonucleotide ligation strategy on barcoded nanowires. (A) Representation of the ligation strategy performed on barcoded nanowires for genotype discrimination, in which a short fluorescently tagged sequence is attached enzymatically to a surface-immobilized probe sequence in the presence of the fully complementary target. (B) Reflectance (left) and fluorescence (right) images representative for the 2-plex ligation assay. (C) Quantification of this 2-plex assay is shown. Reprinted in part with permission from Ref. 69 (figures 1 and 2) and with kind permission of Springer Science and Business Media. © 2006 Springer Science and Business Media.

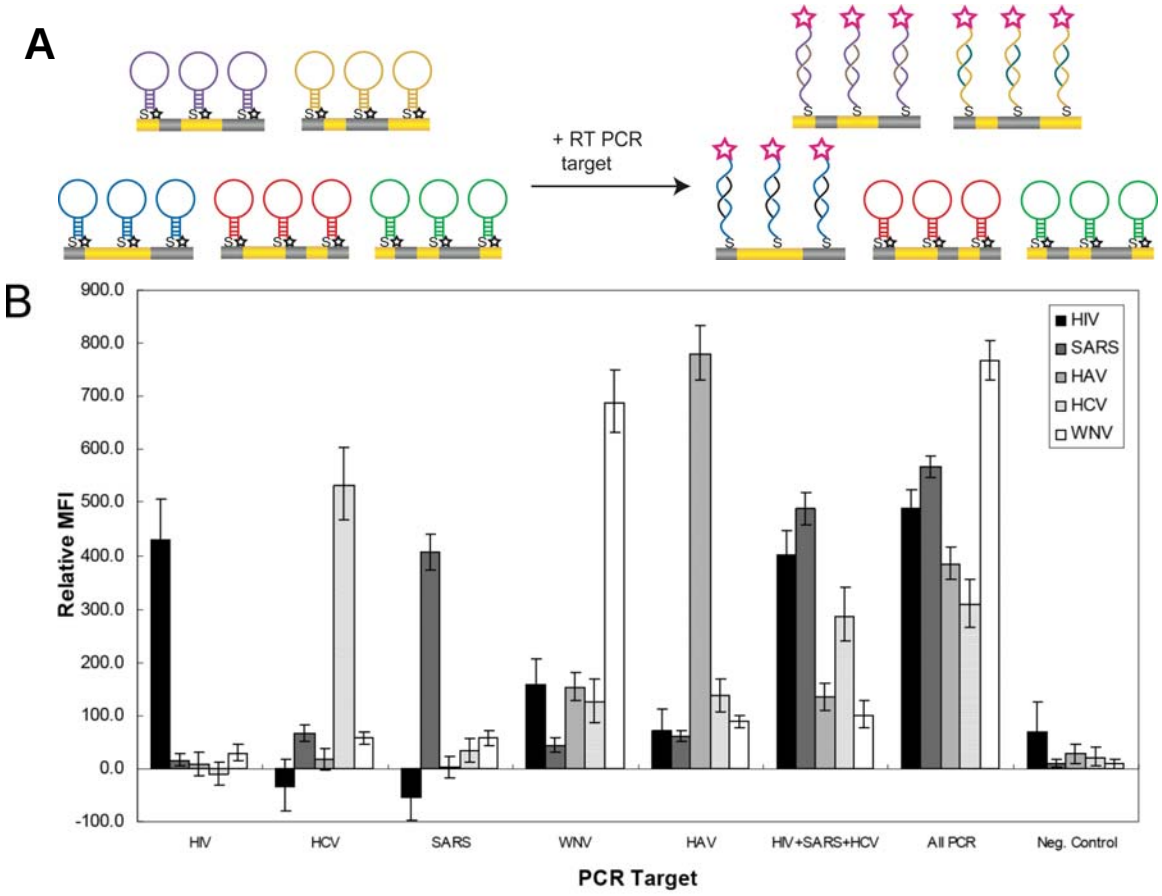

Figure 1-11. Multiplexed detection of PCR-product DNA using nanowire-bound molecular beacons. (A) Representation of multiplexed detection of nucleic acids by nanowire-bound hairpin probes. Nanowires of one type of wire pattern are functionalized with a single sequence of DNA (a molecular beacon) and then mixed with wires of other patterns. They are then exposed to target sequences. Those beacons that are complementary to the targets hybridize and unfold, moving the fluorophore away from the quenching metal surface and resulting in fluorescence. In this assay, the metal surface of the barcoded wires takes the place of a molecular quencher that is usually required in molecular beacon probes. (B) Quantification of several permutations of a multiplexed assay testing for five different PCR products of viral pathogens. Figure reprinted with permission from Ref. 70. © original publisher BioMed Central.

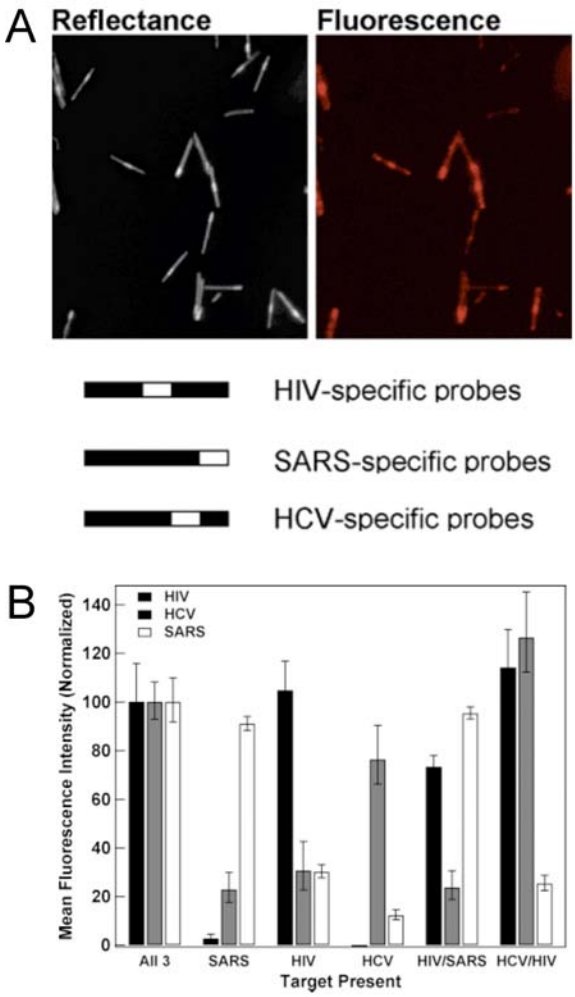

Figure 1-12. Sealed-chamber multiplexed detection of viral DNA using molecular beacons on barcoded nanowires. (A) The reflectance image (left) shows the barcode pattern (with corresponding viral sequences labeled below) and the fluorescence image (right) shows which pathogenic oligonucleotide sequences are present; in this case SARS and HIV. (B) Quantification for this sealed chamber assay with serial target combinations. Reprinted in part with permission from Ref. 71. © 2006 American Chemical Society.

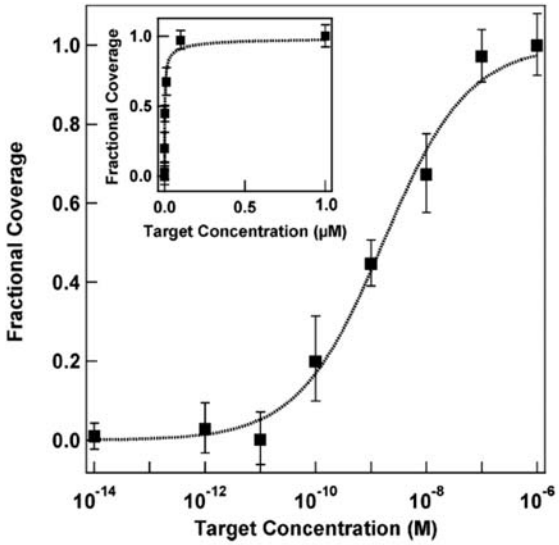

Figure 1-13. Binding isotherm for molecular beacon probes on barcoded nanowires. The binding curve illustrates that the detection limit of the multiplexed nanowire-bound molecular beacon assay is 100 pM when using the HCV beacon to capture its oligonucleotide target. Reprinted in part with permission from Ref. 71. © 2006 American Chemical Society.

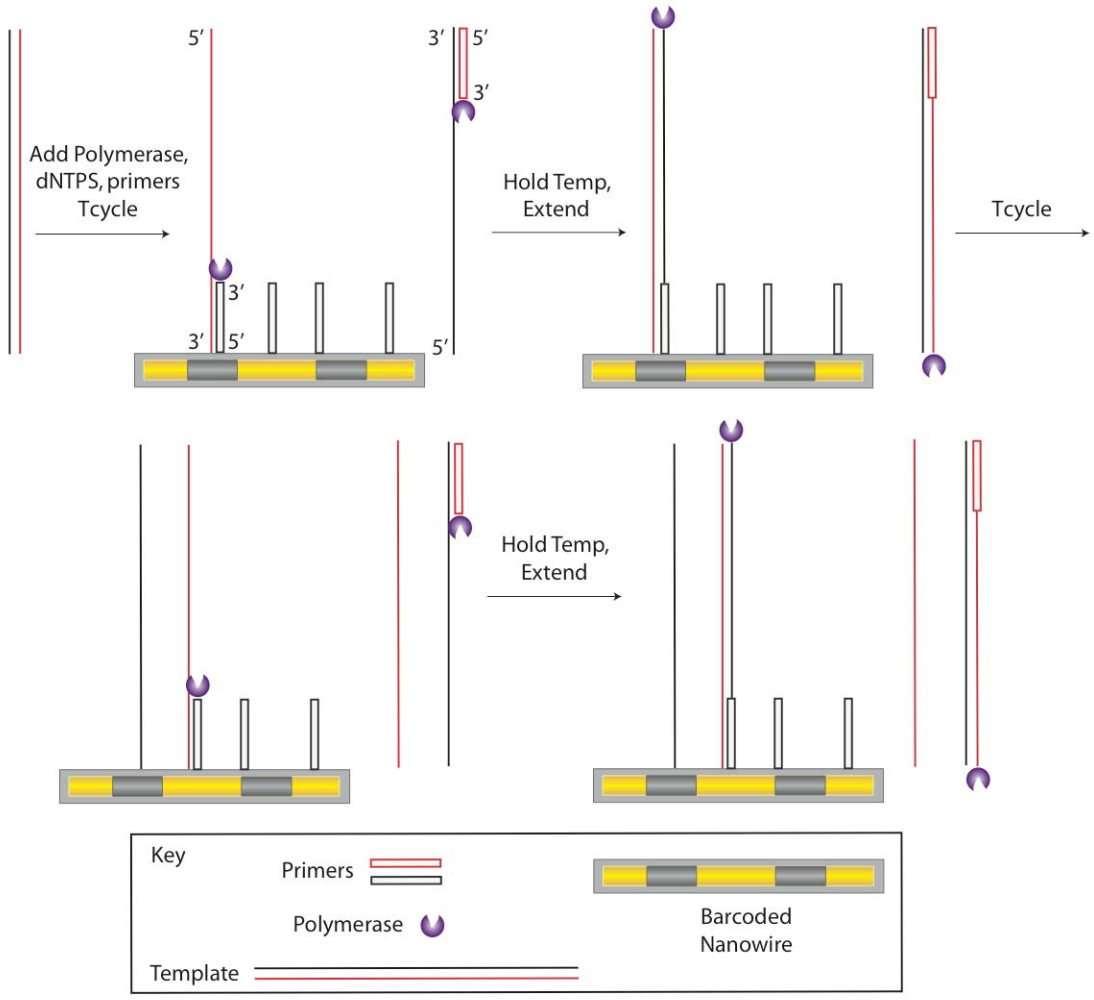

Figure 1-14. On-wire PCR, where each barcode pattern is paired with a primer of a pathogen-specific sequence. Post-PCR the only double stranded (ds) DNA in solution is the negligible amount of initial template DNA, all other ds DNA is bound to the nanowire, allowing for the use of an intercalating dye for DNA quantification.

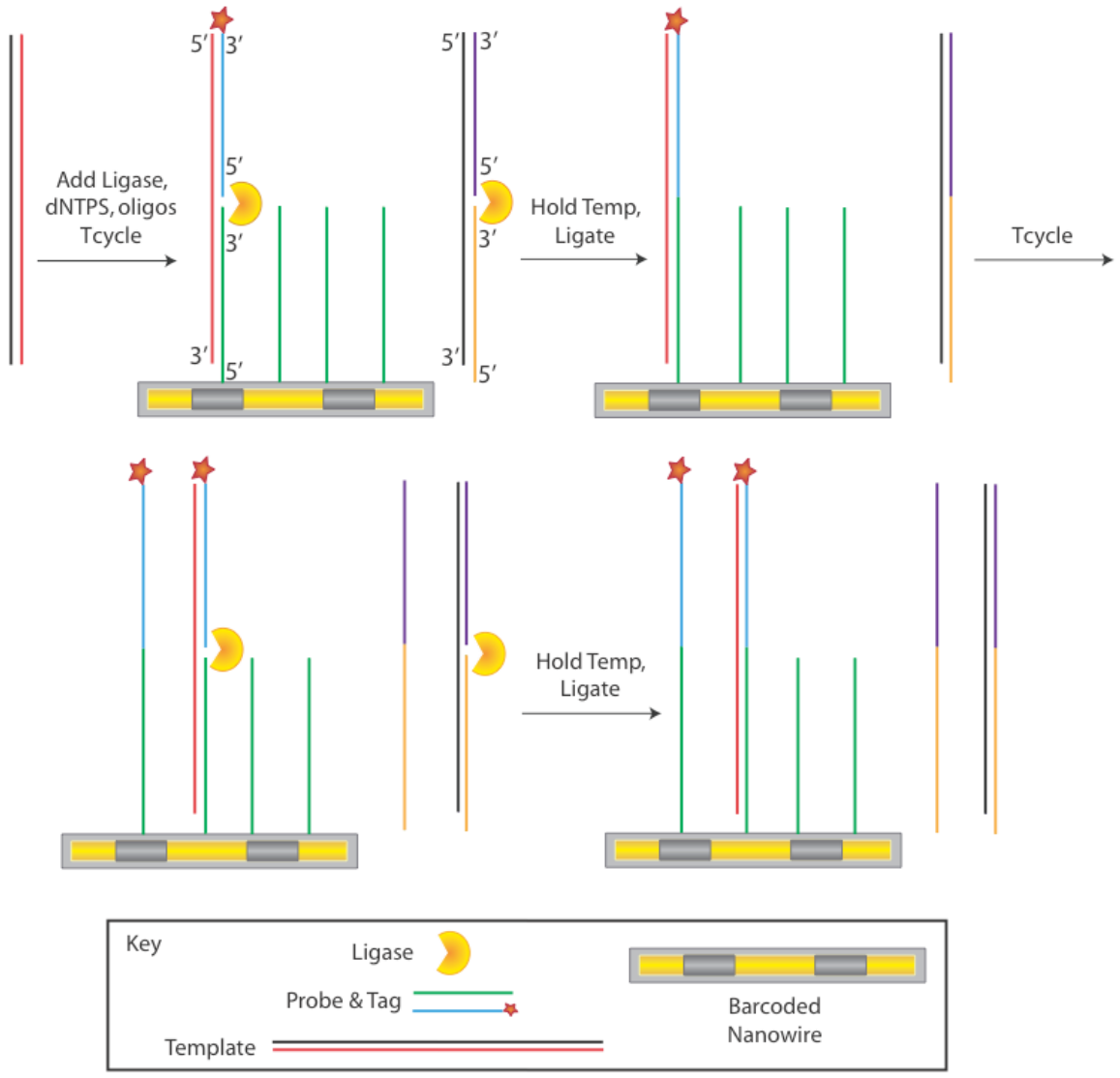

Figure 1-15. On-wire Ligase Chain Reaction, where each barcode pattern is paired with a probe oligonucleotide of a pathogen-specific sequence.

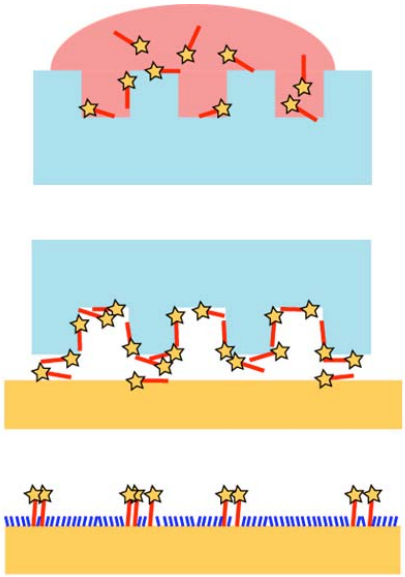

Figure 1-16. Scheme of stamping method to create spatially encoded surfaces with DNA probes, where the stamp is first inked with DNA, then brought into contact with the substrate, and finally a self assembled monolayer is generated in the unpatterned regions.

Chapter 2

Polymerase Chain Reaction Performed on Barcoded Nanowire Surfaces for Pathogen Sequence Detection

Additional attachment chemistry studies were performed by James Sioss and Bo He. Mfold assistance and ROC curve generation were provided by Kristin Cederquist. Jihye Kim worked in parallel performing complementary experiments and extension reactions. Glass coated wires used in one control experiment were provided by Stacey Dean, and Transmission Electron Micrograph images were taken by myself, Jihye Kim, Stacey Dean, Ben Smith, or David Kirby. Gel electrophoresis was performed with Melissa Mullen.

Abstract

The development of polymerase chain reaction (PCR) amplification of oligonucleotides immobilized onto the surface of encoded particles is reported. Barcoded nanowires serve as the encoded particles, and are used for identification of nucleic acid sequences of interest. This method was investigated to determine if pairing PCR with a suspension array in which each DNA sequence is identified by a barcoded nanowire and quantified using fluorescence, would allow for multiplexed detection of template strands, including oligonucleotide, ultramer (synthetic DNA up to 200 bases long), bacteriophage lambda DNA (several thousand base long double stranded DNA), or Armored RNA (several hundred base long double stranded RNA expressed in a protective protein coat) templates. Amplification plots, dissociation curves, and quantified on-wire fluorescence intensities were all used to analyze enzymatic products. On-wire PCR was optimized in order to increase reproducibility and specificity, and decrease background fluorescence. Attachment chemistry, factors impacting steric hindrance, and nucleic acid concentration and sequence were all optimized, and several controls investigating the surface chemistry were performed. 1-Ethyl-3-[3-dimethylaminopropyl]carbodiimide Hydrochloride (EDC) chemistry was found to be insufficiently thermostable for use in a PCR reaction. Primer

sequence was found to be the main contributor to background fluorescence. Gel electrophoresis of enzymatic products was performed, and suggests the formation of a mat of DNA present on the nanowire surface. The lack of thermostability when using EDC attachment chemistry and generation of a mat of DNA on the nanowire surface helps explain the difficulties encountered in performing multiplexed PCR using immobilized primers, both in the research discussed below as well as in the literature.

Introduction

When pathogens cannot be diagnosed by symptoms alone, as is the case with many respiratory pathogens,[1] clinical samples are often analyzed using culturing of bacteria or viruses, as well as molecular techniques such as immunofluorescence and enzyme immuno-assays. While culturing is sensitive, it often takes days to weeks to complete,[1-3] and molecular techniques are often not as sensitive[1] or require more handling steps.[4] Polymerase chain reaction is capable of amplifying several nucleic acid sequences of interest quickly over a large dynamic range, and is quite sensitive.[1, 3, 5] If the pathogen being detected is an RNA virus, which many respiratory pathogens are, the RNA is first reverse transcribed into DNA. After the subsequent hybridization of a complementary primer strand, the DNA is copied base-by-base by the addition of deoxynucleotide triphosphates (or dNTPs) to the 3' end of the primer using a polymerase enzyme. During PCR, the reaction is thermocycled, repeatedly generating amplicon (post-PCR product incorporating both primer sequences and the sequence between them), melting it apart, and hybridizing it to a new strand, so that the product of one reaction is the substrate in the next, exponentially amplifying the sequence that has been primed. Modified multiplexed PCR for the detection of respiratory pathogen sequences was thus focused on in this work. Because this

process is so sensitive, the possibility of cross contamination when the tube is opened is high,[6] which care must be taken to avoid.

Current methods for multiplexing PCR often use fluorescence as a means of sequence identification, but due to the bandwidth of their excitation and emission spectra, flourophores are usually limited to four per reaction mixture.[6] One benefit, however, is that the reaction tube does not need to be opened for amplicon identification, thereby reducing the risk of contamination. Gel electrophoresis is often used to analyze PCR product, but because separate samples are often run in their own reaction mixture and then loaded into individual lanes, this may not be considered multiplexing, which is usually used to describe assays that detect for more than one analyte in the same reaction volume. Additionally, gel electrophoresis requires the design of primers that generate amplicons of different lengths and that the sample be opened post-PCR, introducing possible contamination. Biological multiplexing is already possible with microarrays (used for monitoring gene expression), but the suspension arrays (typically used for detection—but not amplification—of biomolecules) of nanowires proposed here are more flexible and less difficult to prepare.[7, 8] The planar microarrays also have limited dynamic range and necessitate a large amount of starting material.[9] Unlike planar arrays, where robotics or photolithography is necessary, these suspension array elements are prepared in bulk, thus reducing preparation difficulty and allowing for more replicate measurements to be made in each experiment. The suspension array is also more flexible; if additional pathogens are suspected, the particle functionalized with a primer for this pathogen is easily included in the preexisting array, unlike with planar arrays.[7, 8]

Encoded particles provide for an increased amount of multiplexing over detection methodologies such as using fluorescence for identification; metallic barcoded nanowires serve as the encoded particle in this system (see Figure 2-1) and can be functionalized with glass to provide for thermostable attachment chemistries.[10] The glass is coupled via a crosslinking

molecule to a moiety at the 5' end of sequence specific primers for use in on-wire PCR; these sequence specific primers are paired with a particular barcode for multiplexed sequence identification. Amplified DNA is detected using an intercalating dye, the fluorescence of which greatly increases in the presence of double stranded DNA. Coupling sequence detection using an intercalating dye with sequence identification using a barcoded nanowire introduces the possibility of performing a closed tube assay, greatly reducing possible contamination. While PCR performed on the surface of a particle has advantages over solution phase PCR, such as ease of multiplexing and sequence identification, it also has certain disadvantages, such as increased steric hindrance of DNA hybridization and enzyme association due to the proximity of the particle surface.

Most literature that reports surface phase enzymatic amplification instead captures the post enzymatic amplification product on a surface.[11-13] Surface bound reactions include: emulsion PCR,[14] Chrisey and coworkers PCR on beads,[15] and Alivisatos and coworkers Ligase Chain Reaction (LCR) on colloidal particles,[16] but only a small handful have performed truly multiplexed amplification.[17] When multiplexing is claimed, most often the reaction is performed serially in segregated reaction chambers, as is the case with emulsion PCR.[14, 18] One example of multiplexing within the same reaction volume[17] performed PCR in an emulsion and then performed allele-specific labeling of the beads. Additionally, only the top 20th percentile of fluorescence intensity was compared, claiming the rest of the signal as background; while some beads would be dark due to the lack of template present within the emulsion droplet, florescence intensity that was present but was not within the top 20th percentile was also discarded.[17] One elegant use of immobilized PCR was performed by Mitra and Church, where primers were immobilized to the surface of a gel and the amplification reaction was performed within the gel; this system has been successfully used for sequencing[19] and genetic mutation identification,[20] but

like a microarray uses fluorescent and spatial encoding, which can be limit the ease of multiplexing.

There have been a handful of reactions similar to on-wire PCR reported in the literature; oligonucleotides have been enzymatically extended off colloidal nanoparticles in a one step reaction held at a constant lower temperature with Klenow polymerase,[21] using a thiol attachment chemistry not suitable for PCR as it cannot withstand the thermocycling protocol.[10] In one instance, Chrisey et al. used primers bound to glass beads through the thermally unstable EDC chemistry for the purpose of reusable substrates for transcription reactions, but did not use an encoded particle, multiplex, or detect any pathogens.[15] PCR has been combined with a ligation reaction for the detection of Single Nucleotide Polymorphisms (SNPs) using barcoded nanowires as surface substrates,[22] however, the enzymatic chain reaction was not performed on the nanowires, which introduces the possibility of cross contamination. Mathies and coworkers performed on-bead PCR for use in sequencing DNA using capillary electrophoresis and flow cytometry.[14] While this method is useful for sequencing, it has several drawbacks, such as instrumentation demands that are not necessary when using barcoded nanowires, and is not multiplexed, but rather high throughput singleplexed analysis.

Most often the attachment chemistry used in literature studies is that of EDC,[15, 23-27] which, as is shown in this chapter, is not thermostable and allows for release of approximately 50 % of surface bound oligonucleotides into solution.[15, 24] This continued loss of nucleic acid into solution would allow for solution phase amplification, which could be misconstrued as an increased occurrence of the surface-bound amplification reaction. Because of the steric hindrance present in PCR performed on surface-bound primers, the solution phase reaction would be expected to proceed at substantially greater rate. The sterics and attachment chemistry of nanowire-immobilized primer amplification introduced challenging optimization steps that will be discussed in this work. Additionally, the absolute number of oligonucleotides bound and the

subsequent absolute number of bound amplicons generated is often transduced by the fluorescence signal of a sequence hybridized to the amplicon post amplification, the efficiency of which would not scale with coverage.[23, 27, 28] While we have used fluorescence to quantify relative amounts of amplification within our systems, using fluorophores bound to a surface to calculate the absolute number of nucleic acid particles on a surface is nonideal, as they may interact with each other to produce incorrect results.[23] Most likely due to the differing systems of each study, many different factors have been identified as the key issue in obtaining quality surface bound amplification. These range from reagent concentration to thermocycling protocol to volume of reaction chamber.[23, 27, 29] In order to maintain applicability to other systems in which surface bound amplification reactions are performed, several control experiments were run in this work, which are discussed in the following sections.

Reported here is the development of the enzymatic chain reaction amplification of oligonucleotides immobilized onto encoded particles, here barcoded nanowires, which are used for identification of nucleic acid sequences of interest. This method was investigated to determine if pairing PCR with a suspension array in which each DNA sequence is identified by a barcoded nanowire (instead of fluorescence—increasing the multiplexing capability and leaving the spectral window open for detecting amplification products), multiplexed PCR would be possible. Wires were glass coated to provide multiple options for thermostable attachment chemistries necessary for thermocycling, and the intercalating dye Sybr Green was chosen as the reporter dye, as it would permit the assay to remain closed after the amplification step, preventing possible contamination. This technique would allow for rapid, sensitive detection of multiple sequences without the need for spectrally differentiable fluorophores for identification. On-wire PCR shows promise for detecting pathogenic sequences in a rapid, multiplexed fashion without the need for additional equipment aside from a thermocycler and microscope, which are already present in most clinical laboratories.

Materials and Methods

Materials

Nanowires were either purchased from Oxonica Inc. (Mountain View, CA) or made in house as previously described.[30-37] All nanowire volumes reported correspond to batch concentration, where one membrane is dissolved, releasing approximately one billion wires into solution, which are suspended in 1 mL total volume. Tetraethoxysilane (TEOS) and N-(triethoxysilylpropyl)-o-polyethyleneoxide urethane (polyethelene oxide or PEO-containing silane) were purchased from Gelest Inc. Aminopropyltrimethoxysilane (APTMS) was purchased from either Gelest Inc. or TCI. Water was purified to 18.2 MΩ using a Barnstead nanopure system and all water and buffer solutions were autoclaved prior to used. Dithiothereitol (DTT), ethylenediaminetetraacetic acid (EDTA), and buffer salts for phosphate buffered saline (PBS), N-Cyclohexyl-2-aminoethanesulfonic acid (CHES), 4-(2-hydroxyethyl)-1-piperazineethane sulfonic acid (HEPES), and sodium citrate were purchased from Sigma Aldrich. Bovine Serum Albumin (BSA) was purchased from Sigma Aldrich, which when made up to a 1 L solution contained 0.01 M PBS (0.138 M NaCl and 0.0027 M KCl) with 1 % w/v BSA, pH 7.4. Sulfosuccinimidyl-4-(N-maleimidomethyl)cyclohexane-1-carboxylate (Sulfo-SMCC), 1-Ethyl-3-[3-dimethylaminopropyl]carbodiimide Hydrochloride (EDC), and NeutrAvidin were purchased from Pierce Protein Research Products (Thermo Scientific). Sodium Chloride was purchased from VWR. The thiolated OEG backfill molecule used was 2-(2-(2-(11-mercaptoundecyloxy)ethoxy)ethoxy)ethanol (SPT-0011) purchased from Sensopath Technologies Inc. All DNA sequences were analyzed using Mfold software[38, 39] and synthesized by Integrated DNA Technologies Inc., except Taqman probes, which were purchased from Biosearch Technologies. The unlabeled dNTP set was purchased from New England Biolabs and the

fluorescently tagged dNTP (TMR-dCTP) was purchased from Perkin Elmer. All Armored RNA (ARNA) solutions were purchased from Asuragen Inc.; suggested primer sets were provided for each template sequence. *Dra I* restriction endonuclease and Phusion polymerase were purchased from New England Biolabs and Klenow was purchased from Invitrogen. GeneAmp 10× PCR Gold Buffer and bacteriophage Lambda genomic DNA were provided in the GeneAmp Gold PCR Reagent Kit, purchased from Applied Biosystems. Power Sybr Green PCR Master Mix intercalating dye and the High Capacity Reverse Transcription Universal kit were also purchased from Applied Biosystems.

Cleaving Thiolated DNA

A CentriSpin 10 column (Princeton Scientific) was vortexed for 15 seconds to remove air bubbles and left to sit for 30 minutes after the addition of 650 μL H_2O. A 100 mM DTT solution was made and 50 μL of this was added to 50 μL of a 100 μM thiolated DNA solution. The mix was left to sit for at least 30 minutes. The spin column (with caps removed) was placed in a flat bottom wash tube and centrifuged at 750 *g* for 2 minutes. The bottom wash tube with the water was thrown away and the spin column was placed in a centrifuge tube. The DNA/DTT solution was placed on the column and the column was spun at 750 *g* for 2 minutes. The cleaved DNA was in the centrifuge tube and its concentration was determined by measuring its absorbance at 260 nm using a Hewlett-Packard 8453 diode-array UV Visible spectrophotometer.

Nanowire Coatings

Glass To glass coat nanowires, 300 μL nanowires were mixed with 160 μL water, 10 μL ammonium hydroxide (EMD), and 490 μL 200 proof ethanol (Pharmo-Aaper).[10] Nanowires

were sonicated to mix, then 40 μL Tetraethoxysilane was added and the solution was immediately sonicated (with water cooling) for one hour. Nanowires were rinsed once at 300 *g* for 30 seconds in ethanol, and then three times with 300 μL ethanol, spinning for 1 minute at 7700 *g*. Nanowires were imaged using a Transmission Electron Microscope to ensure good glass coating. A JEOL JEM 1200 EXII TEM instrument was used with a high resolution Tietz F224 digital camera at an accelerating voltage of 80 kV. Nanowires used in samples shown in Figures 2-4, 2-6, and 2-9 were glass coated twice;[10] increased primer concentrations were used during attachment to account for increased surface area.

DNA with EDC attachment Glass-coated nanowires, 50 μL, were mixed with 60 μL APTMS and 550 μL ethanol and vortexed for one hour. They were rinsed three times with ethanol and 2 times with HEPES 10 mM pH 7.0 buffer (600 μL). Two mg EDC dissolved in 600 μL HEPES buffer was added to the tube. Phosphorylated DNA was added to bring the final concentration to 1.5 μM. The tube was tumbled overnight at 50 ^{o}C and then vortexed at room temperature for one day. It was rinsed 2 times in 50 mM Sodium Phosphate buffer (600 μL), one time in water and resuspended in its original 50 μL volume. This procedure was scaled up or down to accommodate the number of samples generated. EDC attachment chemistry was used in samples shown in Figures 2-4, 2-6, and 2-9; Sulfo-SMCC attachment chemistry was used in all other experiments shown. To determine EDC thermostability, 12.5 μL nanowires coated in fluorescent DNA were suspended in 30 μL water; 60 μL water and 10 μL GeneAmp 10× PCR Gold Buffer were added to solution, and the solution was run through two thermocycling protocols of 25 cycles of 94 ^{o}C for 30 seconds and 68 ^{o}C for one minute. Aliquots of DNA-coated nanowires were imaged before and after each thermocycling run. The supernatant was also tested using a Horiba Jobin Yvon Fluorolog 3-21 fluorimeter (equipped with a 450 W lamp, and double grating excitation and single grating emission spectrometer) using 2 nm excitation and

emission slits, before and after each thermocycling run (nanowires were rinsed after supernatant samples were removed). Thermocycling was proven to not detriment the fluorophore itself by running tagged DNA samples through all thermostability tests.

DNA with Sulfo-SMCC attachment To attach DNA to nanowires, 13.3 μL nanowires of one glass-coated barcode pattern were mixed with 26.6 μL ethanol and 4.4 μL APTMS, and vortexed for 30 minutes. They were rinsed 3 times with 44.4 μL ethanol and 3 times with CHES buffer (10 mM, pH 9.0). A solution of 1 mg Sulfo-SMCC in 400 μL CHES buffer was made. The nanowires were resuspended in 8.8 μL of CHES buffer and 8.8 μL Sulfo-SMCC solution was added; they were then vortexed for one hour. The nanowires were rinsed in 13.3 μL CHES buffer 3 times and PBS buffer (0.3 M NaCl, 10 mM phosphate, pH 7.0) 3 times. Thiolated, cleaved DNA was added to a final concentration of 1 μM, and the total volume was brought to 33.3 μL with PBS buffer; the nanowires were vortexed for 2 hours. The nanowires were then rinsed 3 times in 33.3 μL PBS buffer and transferred to a new PCR tube. They were placed in a thermocycler and heated to 95^{o}C for 10 minutes and then 25^{o}C for 10 minutes, and then rinsed in 33.3 μL H_2O. The nanowires were resuspended in 13.3 μL H_2O, transferred to a new PCR tube, and stored at 4^{o}C until the following morning. If required, these procedures were scaled up to accommodate more samples per experiment. Sulfo-SMCC thermostability determined by James Sioss is reported elsewhere.[10]

Lysing and Reverse Transcription of Armored RNA

Armored RNA, 5 μL, was placed in a PCR tube and heated at 75^{o}C for 15 minutes to lyse the protein coat. Two solutions were usually lysed, one complementary and one noncomplementary sample. The solution was then quick spun. A High Capacity cDNA Reverse

Transcription Kit from Applied Biosystems was used. Reverse Transcription (RT) master mix was made by mixing in a dead air box: 9.3 μL 10× RT buffer, 3.7 μL 25× dNTP Mix, 19.6 μL H_2O, and 4.6 μL RT Enzyme. In a PCR hood, 9.3 μL 10× Random Primers were added and the solution was split into three tubes, 14.6 μL in each. To the first tube, 3.6 μL complementary lysed ARNA and 11 μL water were added, to the second 3.6 μL noncomplementary ARNA and 11 μL water were added, and to the last only 14.6 μL water was added for a no template control. These solutions were mixed with a pipetter and placed in a Perkin Elmer Gene Amp PCR System 2400 thermocycler at 37^{o}C for 2 hours for the reverse transcription reaction to take place. When an ultramer or bacteriophage Lambda genomic DNA (Applied Biosystems Kit part number 4312778) was used as the template, the lysing and reverse transcription steps were skipped.

Polymerase Chain Reaction

DNA sequences used are in Table 2-1. A 50 μL solution was made up, 25 μL of which was the Sybr Green PCR Master Mix, and 10 μL of which was the template from the RT reaction, generating a template concentration of 1 pM. One μL of 20 μM forward primer and 1 μL 20 μM reverse primer were added in solution phase controls, and in on-wire samples, 3.2 μL nanowire:primer conjugates were added instead of the reverse primer solution. In multiplexed samples, 0.5 μL each primer sequence and 1.6 μL each nanowire:primer conjugate was added to each sample. The reaction volume was brought to 50 μL with water. If samples did not have primers in solution, 1 μL water was added in each primer's place, and if samples were spiked, an additional 1 μL of 0.2 μM spiking DNA solution was added to the reaction mix. When ultramer template was used, 0.38 μL of 20 nM template was added. When used as the template, 4 μL bacteriophage Lambda genomic DNA was added to the solution (Figures D & H); 1.1 μL 20 μM

forward primer and 1.8 μL nanowire:reverse primer are also used. Each tube was quick spun, mixed with a pipetter, and two 19 μL aliquots of each sample were placed into wells of a 96 well tray. This procedure may be scaled down to 40 μL total. The well plate was thermocycled on an Applied Biosystems 7300 Real Time thermocycler using an extended procedure: 95^{o}C for 10 minutes, 45 cycles of 95^{o}C for 15 seconds and 60^{o}C for 2 minutes, and then held at 95^{o}C for 15 seconds. The dissociation curve was generated by heating from 60^{o}C to 95^{o}C over 30 minutes, and holding at the end for 15 seconds. Nanowires were not rinsed before imaging.

Several parameters were altered in order not only to increase the reproducibility of the reaction, but also to increase the specificity and sensitivity, and decrease the background fluorescence. Use of dedicated workstations and pre-mixed hot start enzyme kits, minimizing the number of pipetting steps, and autoclaving tips and buffers, were all instituted. Rinsing out the intercalating dye post PCR and changing the buffer in which the primers were attached was also done, but were not found to be reproducibly beneficial. In order to reduce contamination and misidentification, plates were restricted to single use, nanowire:primer conjugates were used for PCR assays within 24 hours of being made, and nanowire patterns were chosen for optimal discrimination. To confirm that the settling of the nanowires during the thermocycling was not the cause of the lack of reproducibility, Jihye Kim thermocycled and shook nanowires by hand between each temperature change; this did not result in increased reaction specificity.

The time taken to lyse the protein coat (protecting the Armored RNA) and the time taken to convert the RNA to DNA in the reverse transcription reaction was increased to 15 minutes and 2 hours, respectively, to ensure reaction completion. The Armored RNA protein coat was lysed using a thermocycler. Several different reverse transcription kits were also explored; the one giving the fastest amplification of the correct complementary sample (shown by the melting temperature) and the slowest amplification of the no template sample (the High Capacity RT Universal kit) was chosen for future work. For the reverse transcription reaction, both random

hexamers and gene-specific primers were examined. The use of gene-specific primers did not speed up the reaction and so were not used in subsequent reactions. Increasing the enzyme concentration in order to counteract the steric hindrance was also done by Jihye Kim, but this did not result in a specific increase in on-wire amplification. The template sequence was diluted, and in multiplexed samples the concentrations of both templates were made equal, to avoid overwhelming the system or driving noncomplementary reactions, but it did not increase the specificity of the on-wire reaction.

Enzymatic Extension of Bound Oligonucleotides

This work modified a previously published procedure for use with gold nanoparticles.[21] Nanowires (364.6 μL) suspended in water, 36.5 μL of 68.5 μM thiolated oligonucleotide, and 117.8 μL water were added to solution and placed into a 37 ^{o}C water bath for eight hours. The solution was brought to 0.1 M NaCl/10 mM phosphate over 90 minutes with the addition of a total of 250 μL 0.3 M NaCl/10 Na phosphate pH 7 and placed in a water bath at 37 ^{o}C for at least 16 hours. The samples were rinsed twice with 0.1 M NaCl, 10 mM Na phosphate and resuspended in 750 μL. Twenty four μL of this solution was added to 7.2 μL of 30 μM template and brought to a final volume of 50 μL using 0.3 M NaCl, 10 mM Na phosphate. The samples were heated to 65 ^{o}C for 5 minutes and then kept at room temperature in a water bath for 30 minutes; the samples were again heated to 65 ^{o}C for 5 minutes and kept at room temperature in a water bath for 2 hours. The reactions were brought to a total volume of 75 μL with the addition of 7.5 μL 10× React 2 Buffer, 16.1 μL nuclease free water, 0.3 μL 6 U/mL Klenow polymerase, and 0.6 μL Klenow Dilution Buffer, and placed in a water bath at 37 ^{o}C for 2 hours. Four μL 0.5 M EDTA pH 8.0 solution was added and the samples rinsed with water once and three times with 0.3 M NaCl, 10 mM Na phosphate.

Background Fluorescence Controls

Nanowires were coated in TEOS/PEO glass using the following mixture: 300 μL wires were rinsed one time into acetonitrile, the supernatant was removed, and 790 μL acetonitrile, 160 μL water, 30 μL TEOS, 24.7 μL PEO-containing silane, and 10 μL ammonium hydroxide were added, and the reaction was sonicated for one hour. The nanowires were rinsed three times and the coating & rinsing process was repeated an additional two times. Glass coated nanowires (TEOS or TEOS/PEO glass), 3.2 μL, were mixed with 25 μL Sybr Green PCR Master Mix and 21.7 μL water, and thermocycled using the PCR temperature profile above. The nanowires were not rinsed before imaging. To do step by step controls, the nanowire functionalization procedure above was followed, with a 3.5 μL aliquot removed at each step and the total volume adjusted accordingly. Nanowires, 3.2 μL, were mixed with 25 μL Sybr Green PCR Master Mix, and brought to 50 μL total with water. If samples contained DNA, 1 μL of 20 μM DNA was added. The samples were thermocycled using the PCR procedure outlined above.

Imaging Parameters

Nanowire samples were imaged on a Nikon inverted TE 300 microscope equipped with a Lambda LS Xenon 300 Watt light source coupled to a liquid light guide. A plan apo 60 × oil immersion objective (NA 1.4) was used. A reflectance cube with a half-silvered mirror paired with a 430/60 nm long pass filter was used to take reflectance images; a Lambda 10-2 optical filter changer (Sutter Instruments) controlled filter and shutter movement. A FITC fluorescence cube (Chroma set number 31001) with excitation filter D480/30 nm, emission filter D535/40 nm, and dichroic 505 nm long pass, was used to take fluorescence images. Images were acquired using ImagePro 7.0 and captured on an HQ Coolsnap digital camera from Photometrics. Samples

were prepared by first sonicating and mixing samples with a pipetter, then dropping 10 μL onto a cover slip, onto which a glass slide was placed. The software program NBSee was used to take linescans of nanowires and compile average fluorescence intensities for each nanowire pattern.

Gel Electrophoresis

A 3 % Agarose gel was made by mixing 1.8 g "NuSieve GTG" Agarose and 40 mL 1 × TAE (0.04 M Tris-acetate, 0.001 M EDTA). After microwaving to melt the agarose, 2.5 μL of 10 mg/mL Ethidium Bromide was added. The solution was poured into a gel mold and two 15 well combs were used. The loading buffer was 10 × Agarose Loading Buffer (1 % Xylene Cyanol, 0.25 % Bromo Phenol Blue, 15 % Ficol and 0.1 × TAE). The running buffer was 1 × TAE. The gel was run in a BioRad MiniSub Cell GT at 90 V, ~ 80 mA. The gel was visualized by scanning on a Phosphorimager; the wavelength range used was 595-625 nm.

Results and Discussion

Multiple types of experiments were performed to analyze the on-wire Polymerase Chain Reaction efficiency, specificity, reproducibility, and substrate interactions. On-wire PCR can be visualized in a number of ways when using the intercalating dye Sybr Green as a reporter dye. Because the dye fluoresces significantly more intensely in the presence of double stranded DNA versus single stranded DNA, real time measurements at the end of every thermocycle can be obtained. This fluorescence in the presence of double stranded DNA negates the need for a sequence specific fluorescently tagged strand, as well as the need to open the sample chamber after amplification in order to introduce this tagged strand and subsequently rinse, which is a common method of detection,[23, 27] but introduces the possibility of contamination between

samples. A scheme of the on-wire PCR reaction is shown in Figure 2-2. Many different parameters in on-wire PCR can be altered, including the molecules used in the attachment chemistry and the nucleic acid sequences involved in the enzymatic reaction. Several different types of templates were also investigated for use in on-wire PCR, and are discussed below. These include bacteriophage Lambda genomic DNA, ultramer DNA (synthetic DNA under 200 bases long), and several different sequences of commercially available Armored RNA, which are several hundred base long RNA strands encapsulated in a protective protein coat. Armored RNAs of the viral sequences SARS, Norwalk Virus, West Nile Virus, and Enterovirus were all studied. The Armored RNA was heat lysed to expose the RNA, and reverse transcribed to generate DNA from the RNA before being added to the PCR solution (shown in Figure 2-3). The use of these different templates allowed for analysis of the effects of differing template length. A number of characteristics, such as attachment chemistry, primer concentrations, dye interactions, etc. were investigated in this work. This chapter is divided into sections covering the investigation of different surface parameters: primer efficiency, the chemistry of DNA attachment, steric hindrance, template and primer identities and concentrations. The end of this chapter focuses on single- and multi-plexed on-wire PCR data, and background fluorescence controls, which aided in the generation of a hypothesis to describe the challenges of on-wire PCR.

Primer Efficiency

On-wire PCR was performed at different template concentrations to determine primer efficiency. Primer efficiency reports the percentage of primers available for enzymatic extension that are acted upon by the polymerase and converted into amplicon; when immobilizing primers onto the surface of nanowires, it is expected that the primer efficiency would be greatly reduced from the more common surface phase efficiency of 100 %.[40] By plotting the log of the

fluorescence intensity against the number of cycles, reaction progression can be monitored (typically observed as a sigmoidal reaction curve). A threshold cycle (C_T—or the cycle number where the baseline fluorescence is several standard deviations away from the fluorescence due to amplification),[41] was determined for each reaction curve. Because of the exponential amplification in PCR, a dilution of one order of magnitude in template concentration should result in a decrease in C_T value by 3.3 cycles. Plotting the C_T vs. the Log (copy number) generates a slope M used to calculate the efficiency of the primers (when all is held constant aside from template concentration), based on the equation:

$$E = e^{\ln 10/-m} - 1 \qquad \text{(EQN 1)}^{40}$$

When the slope of the line in this standard curve is -3.3, the primer efficiency is 100 %. An amplification plot showing the real time measurements of on-wire PCR performed in the presence of serially diluted template is shown in Figure 2-4, as is the accompanying standard curve. Using the approximate concentrations listed in the caption of Figure 2-4, the approximate primer efficiency on-wire was found to be 60 %, lower than the more common 100 % of the solution phase reaction, but still conspicuously high for bound primers, as Trau and coworkers measured a primer efficiency of 9 % on the surface of microbeads, and Carmon et al. measured an efficiency of 20 %.[23, 27] Because of reports of primer loss into solution,[15, 24] the 1-ethyl-3-(3-dimethylaminopropyl) carbodiimide (EDC) attachment chemistry (see Figure 2-5) was investigated.

Attachment Chemistry

Several attachment chemistries were investigated for thermostability between the glass and the probe DNA. EDC chemistry was initially investigated, as it had been selected by Chrisey for PCR performed on glass beads.[15] Microscopy images were taken before samples were run

through a thermocycling protocol, and after each of the two thermocycling protocols that followed; the fluorescence present was then quantified, as shown in Figure 2-6. Also after each step, the fluorescence intensity of the supernatant (indicating how much DNA had been lost to solution) was measured. Many of the fluorescent probes attached with EDC chemistry were lost into solution after 25 thermocycles (illustrated by the decrease in fluorescence intensity on the surface of the nanowire by 68 % and the continued presence of fluorescent DNA in solution), indicating that if used in on-wire PCR experiments primers would be available in solution, a great detriment to the on-wire primer extension as it already was hindered sterically. EDC attachment chemistry continued to release 46 % of the existing fluorescent probes into solution after an additional 25 thermocycles, showing that a heating pretreatment step is not enough to make the EDC attachment chemistry useful for on-wire PCR. The presence of fluorescently labeled DNA in solution before thermocycling was performed may have been due to inadequate rinsing after DNA attachment to the nanowire, but is more likely to have been due to release of DNA from the surface of the nanowire over time, even without heating. The fluorescence images and quantification (generated using microscopy and fluorimetry) show that EDC chemistry lacks thermostability. EDC chemistry may have promoted nonspecific adsorption (in addition to covalent linkage) of the DNA onto the nanowire surface (EDC chemistry has been hypothesized to promote DNA attachment through points other than the 5' end)[24] and subsequent release of these nucleic acids strands over time, which heating simply drove to a faster rate. This possible continued release of DNA into solution from the surface may have also affected studies using EDC chemistry in the literature, such as work by Chrisey and coworkers.[15] One study done by Adessi et al. showed that approximately 50 % of the primers were driven from the surface during thermocycling, but claimed that these solution phase primers did not affect the surface phase amplification.[24] They determined this by rinsing off the supernatant and replacing it with fresh PCR reagents at the end of each cycle, but this sample did not include template, and did not

account for the continued loss of primers over the course of thermocycling. Amplicon detection was also performed at the end of the thermocycling protocol after rinsing the surface and exposing it to another labeled DNA strand, which would have removed any solution phase amplification, and so was not indicative of the reactions occurring during the assay.

Several members of our group have looked into multiple DNA attachment chemistries for use in on-wire assays. Dr. Bo He investigated several different attachment chemistries discussed in the literature[42, 43] for their thermostability: 1) EDC crosslinker with phosphorylated DNA and aminated glass, 2) Sulfo-SMCC crosslinker with thiolated DNA and aminated glass, 3) aminated DNA with aldehyde-functionalized glass, 4) and aminated DNA with an epoxy-functionalized glass chemistry, shown in Figure 2-5. Each attachment chemistry was evaluated for thermostability by exposing nanowires coupled using the chemistry of interest with fluorescently tagged DNA to thermocycling conditions, and comparing the fluorescence intensity before and after heating. Both the aldehyde and epoxy functionalities gave very low initial probe coverage, as shown in Figure 2-7, which may be due to inherent instabilities of the silanes, or the susceptibility of the participating functional group (*i.e.*, moisture can be detrimental to epoxy chemistry).[24, 44] While the Sulfo-SMCC attachment gave a lower initial fluorescence of bound probe DNA than did the EDC chemistry, it did not lose as much DNA to solution as the EDC chemistry after thermocycling. Sulfo-SMCC attachment thermostability was also investigated, and compared to that of DNA attachment between a thiol moiety and the bare gold of uncoated nanowires, by Dr. James Sioss.[10] The thermostability of both these attachment mechanisms was investigated using the same method described above. There was a significantly smaller dropoff in fluorescence (and amount of conjugated DNA) when using Sulfo-SMCC, indicating its improved thermostability over gold-thiol bonds. Biotinylated DNA coupled with NeutrAvidin-coated nanowires was also investigated by Jihye Kim as an alternative attachment method. The post-PCR microscopy revealed a completely nonspecific on-wire amplification, most likely due

to the loss of primers from the nanowire. This was confirmed in the amplification plot and temperature stability studies of this attachment method (not shown). In light of these studies, Sulfo-SMCC attachment chemistry was chosen for all future on-wire enzymatic assays.

Two different backfilling molecules were used in an attempt to block possible nonspecific adsorption to the nanowire surface. After the DNA primers were attached to the nanowire, a thiolated-OEG (oligo ethylene glycol) molecule or the protein BSA (Bovine Serum Albumin) was coated onto the nanowires. While the on-wire amplification could be seen and looked specific in the amplification plots, there was no decrease in the on-wire background fluorescence observed in either sample.

Steric Hindrance

The exact primer coverage on the surface of the nanowires is difficult to determine as the typical method employed, that of removing the DNA from the surface and quantifying in solution,[45-47] is not as accurate when using attachment chemistry employing glass. However, using the size of the molecules involved, an approximate maximum DNA coverage can be calculated to be around 10^{13} molecules/cm^2, which is comparable with the maximum coverage found in studies of nanowire-bound DNA probes performed previously.[21] At this high a density of primers (such as 10^{13} molecules/cm^2) on the surface of the nanowires, the hybridization of the template DNA (and the subsequent association of the enzyme)[21, 23] would be hindered; similar work has shown that increasing the probe density on the surface of the nanowire decreases the efficiency to which they can bind their target.[28] Spacers, or a multi-base region incorporated between the linking moiety and the hybridization region, have been proposed to decrease the inaccessibility of the primers to the enzyme.[27] A similar interaction utilizing enzymatic extension of DNA on the surface of colloidal particles was performed successfully.[21] (In that case the

curvature of the particle was much more—with a diameter of 12 nm compared to that of the nanowire at approximately 320 nm; increased curvature has been shown to make surface-bound DNA more accessible to the surrounding solution[48, 49]). In order to alleviate the sterics in on-wire PCR arising from the proximity of bound DNA molecules and both the DNA and the enzymes associating to the surface-bound DNA, a spacer was incorporated into the DNA primer sequence. The addition of this typically 10 base (or 7 base) spacer would increase the distance from the surface approximately 3.4 nm. The binding of the primer to the template occupies the subsequent approximate 6.0 to 6.5 nm distance from the surface; enzyme association thus occurs 9.4 to 9.9 nm from the wire surface.

To increase the probability of extension for on-wire primers, several parameters were investigated. The primer coverage on the nanowire was decreased to alleviate the steric hindrance of the enzyme binding to the primers immobilized on the nanowire surface. Using diluent molecules to alter the coverage of bound oligonucleotides has been shown to affect the hybridization efficiency of target molecules.[50] The primer was mixed with a thiolated 10-T sequence to decrease the primer coverage to 50 %. This had no visible effect on the amplification efficiency, as seen by comparing open versus closed markers in the amplification plot in Figure 2-8. One DNA parameter that did increase overall amplification was the concentration of nanowire-bound primers (and thus the number of nanowires per reaction), as shown in Figure 2-8. (Other aspects of the graphs shown in Figure 2-8 are analyzed in the following section.) Increasing the nanowire:primer conjugate concentration from the 1 × to the 2 × amount (square versus triangle markers in Figure 2-8) did increase the amount of overall amplification, but does not appear to scale directly and did not necessarily increase the amount of amplification per individual nanowire. The manipulation of fluorescence intensity per particle caused by changing the overall number of particles has been investigated in other systems that do not have an enzymatic amplification step;[51, 52] this is one parameter that may be investigated in the future.

Additionally, because the polymerization reaction was happening in close proximity to the nanowire surface, the reaction needed to be as efficient as possible, maximizing the enzyme activity when it was in the presence of its substrate. In order to accomplish this, the number of thermocycles and the length of the extension step in each thermocycle were altered. It is not uncommon for polymerase reactions performed on surfaces to have extended thermocycling protocols.[24, 27] The number of cycles was increased to from 40 to 45 to allow for more chances for the enzyme to extend the nanowire-bound primer. The extension time was increased from 1 to 2 minutes to provide the enzyme with more time to perform the on-wire extension without causing the enzyme to denature. The amplification plots are shown for PCR reactions where 40 cycles were used with a one-minute extension time, and 45 cycles were used with a two-minute extension time. The number of minutes the extension step was performed for dramatically increased the amplification (represented by the lower C_T and the higher intensity plateau phase) from one plot to the next, as shown in Figure 2-9. The melting temperature of the amplicon was the same between the samples subjected to different thermocycling protocols, indicating that this change did not alter the amplification product generated. While the melting temperature was also the same between the in solution and on-wire samples, indicating the length and thus the identity of the amplicon was consistently correct, (exemplified in Figure 2-9), and the amplification plots did not show significant extension in the noncomplementary samples, there was often fluorescence present on the nanowires in the noncomplementary and no template microscopy samples. Stopping the reaction at an earlier number of thermocycles (keeping the two minute extension time consistent) did not decrease the background fluorescence on-wire, which is shown in the amplification plots and quantified on-wire fluorescence in Figure 2-10. The signal generated from the sample containing complementary template was significantly different than that of the sample containing no template (p value < 0.001), but was not significantly different than that of the sample containing noncomplementary template (p value < 0.1). This indicates

that parameters other than decreasing the number of thermocycles influences the specificity of the reaction.

Template and Primer Identity and Concentration

Template, Primer, & Amplicon Sequences It was tested whether the decrease in template length from tens of thousands of bases for bacteriophage Lambda genomic DNA to several hundred bases for Armored RNA to around one hundred bases for ultramers would decrease the hindering sterics of the nanowire-immobilized PCR reaction. The single-plex on-wire PCR assay was performed using an ultramer template; the resulting microscopy showed no increase in specificity as compared to using an Armored RNA template, as the fluorescence intensities were approximately 600 and 540 for the wires exposed to complementary or no template, respectively, therefore other nucleic acid properties were investigated. Additionally, there seems to be no correlation between the location of the primed region within the template and the on-wire amplification efficiency, which can be seen in Table 2-1.

For each template amplified with on-wire PCR, several primer sets were examined; primers to be used in noncomplementary samples in on-wire PCR were first checked for a lack of complementarity to sequences of interest in solution phase PCR. By altering the primer set, the amplicon length (not the template length) was also altered. An example solution phase amplification plot and dissociation curve for three different Armored RNA templates and 4 different primer sets is shown in Figure 2-11. Two of the primer sets amplified different regions of the SARS virus, the first being the nucleocapsid (CoVNC)[53] and the second being a region discovered at the Bernhard Nocht Institute (BNI)[54], which are referred to as SARS-1 and SARS-2, respectively. The other two primer sets amplified different parts of the same region in the West Nile Virus (WNV) sequence, those used by Lanciotti and coworkers, and Lipkin and

coworkers, which are referred to as WNV-1 and WNV-2, respectively.[55] (While the primers were not the same length, they all had melting temperatures between 55 and 60 ^{o}C.) The C_T of the reaction increased with increasing amplicon length, the differing lengths being: SARS-1 67 bp, WNV (amplified by either primer set 1 or 2) 70 bp, and SARS-2 109 bp. SARS-1 and SARS-2 primer sets prime different template strands of the same viral sequence, while WNV-1 and WNV-2 primer sets prime different regions of the same template strand. The dissociation curves showed no significant alternate extension, even when templates were in the presence of noncomplementary primer sets. As these primer sets performed well in solution phase PCR, they were further investigated in on-wire PCR.

To determine if amplicon length would affect the specificity of the on-wire reaction, on-wire PCR was performed with the template and primer pairs listed above. The SARS-1 and WNV-2 primer sets amplified the best both in solution and on-wire (Figure 2-12); the other two primer sets led to no detectable product in on-wire real time PCR experiments. Imaging results, shown in Figure 2-12B, are consistent, with statistically different (p value < 0.01) fluorescent signal between complementary and noncomplementary samples only for SARS-1 and WNV-2. The SARS-1 and WNV-2 primer sets generated significantly shorter amplicons than the SARS-2 primer set and had significantly more on-wire amplification, suggesting improved on-wire extension with decreasing amplicon length. The nanowires used in this work were coated in silica, APTMS, and Sulfo-SMCC as a large batch and then split into separate reaction volumes in order to conjugate known primer sequences to a known nanowire subset; because of this, there was little to no variation between nanowires coated in different primer sequences. Although the WNV-1 and WNV-2 primer sets primed amplicons that are the same size, and use the same template sequence, the background (and hence specificity) was quite different between the two. Thus, the background intensity was determined almost wholly by the sequence of the primers, and is most likely not due to double stranded amplicons forming in solution and then adsorbing to

the wire surface, as the double stranded amplicons are forming almost exclusively for the SARS-1 and WNV-2 samples.

The parameters of these primers were compared to each other in order to elucidate why some gave specific signal and others did not. The immobilized primer sequence was examined to try to identify a pattern in on-wire successful priming. Melting temperature and secondary structure were analyzed (see Table 2-2 and Figure 2-13). A higher melting temperature and lack of secondary structure increased amplification amount and specificity. This aligns with the theory that the hybridization of the template to the on-wire sequence is so disfavored because of the presence of the nanowire that any other factors that contribute to the decrease in stability of the on-wire primer:template hybridization severely inhibit the amplification amount and specificity. This discrepancy is especially enhanced when other DNA strands are available in solution (primer dimers—or the product of a polymerization reaction between two primers, etc.) to be amplified by the enzyme, as even if they are not traditionally favorable reactions, they may still be more favorable than the on-wire amplification.

Primer Concentrations The concentrations of the solution primers involved in the reaction were varied in order to increase the specificity and decrease the background fluorescence signal in the on-wire samples; this was done to test if the one side of the exponential amplification reaction that was happening in solution could be manipulated to increase correct amplification on the surface of the nanowire in the other side of the exponential reaction (see Figure 2-1 for clarification). The concentration of the solution phase primer (the forward primer free in solution) was increased in order to generate more solution phase amplicons that could act as on-wire templates, driving the on-wire reaction. While increased solution primer did result in more amplification, the resulting dissociation curves showed that the amplicons did not have the same melting temperature, and thus the same length or identity, as when lower primer concentrations were used, this can be seen in Figure 2-8 (previously mentioned). This indicated

that the incorrect sequence was preferentially amplified; it is likely that amplification occurred more often, but was nonspecific and in solution when using increased solution phase primer concentration. Increased solution phase primer concentrations were avoided in future experiments. Having little to no DNA present in solution, or having an addition of the reverse primer (the immobilized primer sequence) as well as the forward primer (already free in solution) both in solution, were tested to determine if they would help increase the amount of correct amplification on-wire by driving the reaction. There was minimal difference between the complementary and no template on-wire fluorescence intensities in only the sample containing both the free and the immobilized primer present in solution at a lower concentration (not shown), but this was not an improvement over previous results. In light of these studies, manipulation of the interactions of the DNA on the surface of the nanowires impacted the outcome of the reaction more than manipulation of the DNA in solution. By evaluating the individual experiments described above investigating the attachment chemistry, thermocycling protocol, and primer conditions, etc., the parameter set most favorable for the on-wire amplification reaction was decided upon, and used in subsequent on-wire PCR assays, discussed below.

Single- and Multi-plexed PCR

Real time amplification plots for SARS-1 and Norwalk Armored RNA single-plexed on-wire complementary samples are shown in Figure 2-14. The solution phase plot shows good amplification, with a C_T of around 11 cycles, indicating that the template concentration was in a linearly detectable range and providing enough cycles to calculate the background fluorescence intensity. While the amplification was slower on-wire, indicated by a higher C_T, and there was less overall amplicon produced (indicated by the lower plateau phase) there was an appreciable amplification observed in samples where the primers were bound to the nanowire surface. An

image set from the Norwalk samples, where the reflectance images were used to identify the barcode pattern and thus the DNA sequence, is shown in Figure 2-15. The resulting average fluorescence intensities for the single-plex SARS-1 and Norwalk samples are shown in Figure 2-16. Signal from complementary samples for both SARS-1 and Norwalk templates were significantly different when compared to signal from either noncomplementary or no template samples (p value < 0.001). This data illustrates a differentiable fluorescence signal between complementary and noncomplementary single-plex samples; the SARS-1 and Norwalk Armored RNA sequences have generated the best on-wire PCR results.

Multiplexed PCR was also performed, where both SARS-1 and Norwalk primer-coated nanowires were present in solution. The microscopy results for this reaction (including the background subtracted, normalized data, where the signal from the sample without template is subtracted out and the fluorescence values are normalized to the complementary intensity) are shown in Figure 2-17. The multiplexed samples are most likely dimmer than the single-plex samples due to the decrease in complementary nanowire:primers available, as the total DNA in solution was kept constant. The on-wire PCR signal specificity decreased when performed in a multiplexed fashion, perhaps due to nonideal on-wire amplification products (which was investigated and is discussed in the next section). The complementary sample was extremely significant (p value < 0.001) when using SARS-1 template, and significant when using Norwalk template (p value < 0.02), when compared to the noncomplementary template sample. In this instance, the on-wire PCR assay was able to distinguish between two different templates in a statistically significant way. Unfortunately, repeating this level of significant discrimination has proven challenging; the lack of sufficient amplification produced in surface phase PCR has been reported previously,[23, 27] but most systems that have been analyzed have generated conclusions that are not necessarily directly applicable to other systems. In order to determine the cause of

the lack of reproducibility, which may also be applicable to other systems, several control experiments were performed that are discussed below.

Background Fluorescence Controls and Hypothesis

Intercalating dye was used as the amplification reporter in our system, as it is directly applicable to the clinical setting, where avoiding opening sample chambers post amplification is important to avoid cross contamination. Instead of intercalating dye, fluorescently tagged strands are often hybridized to the enzymatic product post amplification;[23, 27] because of the sequence specific detection scheme, it is possible that other investigations have not been able to visualize all of the amplification products shown using intercalating dye. To confirm that the background fluorescence was not due to the intercalating dye binding to the porous glass coating, nanowires coated with the previously used tetraethoxy silane (TEOS—see Figure 2-5) glass and nanowires coated with Polyethylene oxide containing silane and TEOS (PEO-TEOS mixed glass) were incubated with the PCR reagents (aside from the DNA sequences) and thermocycled. Neither sample had appreciable fluorescence, as can be seen in Figure 2-18, indicating that the fluorescence background was not originating from the intercalating dye fluorescing on the glass coating. In a separate control experiment, glass coated nanowires were added to the solution phase PCR reaction, which was then monitored in real time; the addition of the coated nanowires did not poison the solution phase enzymatic reaction. Additionally, on-wire PCR with different fluorescent tags was performed by Jihye Kim using Taqman probes (DNA featuring a fluorophore and quencher, that when digested by a polymerase fluoresces) for real time measurements and the incorporation of fluorescently labeled deoxynucleotidetriphosphates (dNTPs or single bases available for enzymatic incorporation) for on-wire fluorescence measurements (using the same Sulfo-SMCC attachment chemistry); this dye change did not

reduce the amount of background fluorescence present in the microscopy images. This indicates that the fluorescent background seen on the nanowires is not intercalating dye specific, but could still be due to the visualization of additional amplification products not seen when using a sequence specific reporter, as any amplified DNA would be fluorescent. Further controls were performed to determine to what the background was attributed.

In order to elucidate at what step the background fluorescence predominantly increased, controls were also performed by removing an aliquot of nanowires at each functionalization step, incubating them with the intercalating dye mix, and thermocycling them. Fluorescence intensity increased after DNA was introduced into the system; this indicates that the Sybr Green was reacting with the DNA more than with other possible side reactions. It is possible that the DNA oligonucleotides are forming a mat on the surface of the nanowire, which the Sybr Green is intercalating into and creating a large background signal. Possible side reactions that may occur during on-wire PCR, which may contribute to mat formation, are shown in Scheme 5; these include primer dimers generated on-wire as well as the products of amplifying these nonspecific sequences in subsequent thermocycles. The exponential amplification would increase the amount of nonspecific amplicon with each thermocycle.

An interwoven network of DNA on particles has been discussed in relation to ligation reactions performed on gold colloidal nanoparticles, where particles linked by sandwich hybridizations are available for more enzymatic activity (subsequent restriction enzyme reactions) than those linked by direct hybridizations (such as in PCR).[56, 57] This is due to the increased number of linkages in the two-strand system as opposed to the three-strand system (because the stoichiometry of the reaction is not controllable by the linking target concentration), and the resulting interwoven DNA and conjoined nanoparticles create too much steric hindrance for the enzyme to act on the bound DNA.[57] Other literature cites that as the surface immobilized polymerase chain reaction amplification occurs, the reaction becomes inhibited by the product

generation.[24, 27] It was proposed in these reports that this inhibition is generated by the increased interaction of bound nucleic acid strands with each other as the amplification progresses. The interaction of primers bound to a surface was also discussed as producing surface amplification products, where the oligonucleotides are primed by already bound DNA strands.[24, 27] An interwoven set of DNA would provide both a competing enzymatic substrate and an environment for the intercalating dye (and the fluorescently labeled dNTPs) to fluoresce, see Figure 2-19.

To test the hypothesis that a mat of DNA was generated on-wire during thermocycling, PCR was performed in solution and on-wire, and one duplicate of each sample was digested with the restriction endonuclease *Dra I*. Products of these enzymatic reactions were analyzed using gel electrophoresis, and are shown in Figure 2-20. *Dra I* should have cut at only one recognition sequence within the template, and so lanes with samples that were digested should have shown at most 3 bands: the digested halves of amplicon (approximately 50 and 80 bases long), and (in the case of solution phase PCR) unreacted (or semi-reacted) primers (17 bases long), which cannot be rinsed out. These three bands could be seen in the lane containing digested solution phase PCR product, where the first two bands are very strong and the third band is faint. Only one band could be seen in the lane containing undigested solution phase PCR product, corresponding to the correct amplicon length (approximately 130 bases). There is also a band present in solution phase samples exposed to noncomplementary template, which is most likely due to generation of amplicons when solution phase samples are run through the longer thermocycling protocol optimized for on-wire amplification. The lane with the digested on-wire PCR product showed a smear of bands from the correct amplicon length down to below the lowest ladder marker at 25 bases. This smear showed a variety of different enzymatic product lengths, indicating the recognition site for the restriction endonuclease was present in DNA strands of varying lengths, while only one length should be present (50 bases) as it is the half of the strand released into solution upon digestion. The smear on the gel may have been generated by the products depicted

in Figure 2-19, where a length distribution resulted from the amplification (and digestion) of incorrect amplicon sequences and the disassociation of the enzyme from the template strand before complete amplicon generation. This interwoven mat of amplification products would contain recognition sequences at different sites, releasing a variety of digestion products into solution. The undigested on-wire sample produced one faint band around the correct length of the amplicon (this band is difficult to clearly identify as it is near the dye loaded into the samples). Both the digested and undigested noncomplementary samples also produced faint bands around the size of the amplicon, but there is no corresponding digest band. This is most likely due to nonspecific amplicons generated reactions between bound noncomplementary primers, which do not contain the restriction endonuclease site and therefore are not digested.

The generation of a mat of interwoven DNA on-wire when immobilized primers are run through the PCR reaction was further supported by the improvement in on-wire specificity when only one extension step was performed. On-wire extension has been performed previously on gold colloid surfaces,[21] when performed on gold nanowire surfaces the specificity is better than that of on-wire PCR, as shown in the data generated by Jihye Kim in Figure 2-21. Subsequent thermocycling reactions seem to decrease the specificity of the on-wire PCR reaction, perhaps due to the enzymes' generation of and activity with a mat of increasingly incorrect DNA sequences.

In order to bypass the generation of a mat of DNA on the nanowire surface, Ligase Chain Reaction (LCR), which uses a ligase in place of a polymerase, was investigated and will be discussed further in the next chapter. One way to directly compare the capability of two assays in distinguishing true from false positive results is to generate a Receiving Operating Characteristic (ROC) curve.[58-60] The diagram shown in Figure 2-22 illustrates examples of three different levels of discrimination between signal generated in the presence vs. absence of the target, where the first case of complete discrimination is represented by the green line in the ROC curve, the

moderate level of discrimination the blue line, and the lack of discrimination the red line. A ROC curve showing complete discrimination between correct and false results will be composed of two straight lines, the first vertical along the y axis and the second horizontal along the value of 1 on the x axis, indicating a perfectly specific assay and a complete lack of overlap between signal in the presence vs. signal in the absence of the target. A ROC curve was generated using the on-wire fluorescence intensities of the single- and multiplexed samples shown in Figure 2-16. The percentage of the area under the curve can be used to quantitatively compare the accuracy of differing assays. For singleplexed PCR samples, SARS wire:probes generated an area of 90 %, while Norwalk virus wire:probes generated an area of 93 %. For multiplexed PCR samples, the area under the curve when exposing nanowire:probes to SARS template was 89 %, while the area under the curve when exposing nanowire:probes to Norwalk virus template was 64 %. For singleplexed LCR samples, SARS wire:probes generated an area of 100 %, while Swine Flu H1N1 wire:probes generated an area of 98 %. For multiplexed LCR samples, the area under the curve when exposing nanowire:probes to SARS template was 94 %, while the area under the curve when exposing nanowire:probes to Swine Flu H1N1 template was 91 %. This indicates a small decrease in accuracy for the on-wire LCR assay when moving from single- to multi-plexed assays, but this is a substantial improvement over the accuracy for on-wire PCR.

Conclusions and Future Directions

On-wire multiplexed PCR has been performed, but has not been easily reproduced. One reason for this lack of reproducibility is that the intercalating dye and the fluorescently labeled dNTPs reported all double stranded amplification product, as opposed to detecting only amplicons of a specific sequence using a secondary hybridization step with a tagged oligonucleotide. While a separate labeling step is possible, and can be attempted in the future, it

was not initially implemented as it negates the possibility of performing a closed tube assay where the sample chamber is not opened post-amplification, reducing the risk of contamination between samples. Several parameters were investigated and adjusted in order to increase the reproducibility of specific on-wire PCR reactions. Sulfo-SMCC used with thiolated DNA and an aminated glass surface was shown to be the most thermostable attachment chemistry. Other, more widely used, attachment chemistries were investigated and were found to lack necessary thermostability. These investigations demonstrate that previous literature showing solid phase polymerase chain reaction may have been incorrectly stating amplification exclusively occurs on the surface, as primers were most likely continuously released into solution where they were amplified over time, without the investigators' knowledge.

Increasing the number of cycles and the time for the extension step, and increasing the number of nanowire:primer conjugates present in the solution both increase the overall on-wire amplification. One parameter of on-wire PCR that may also increase the amount of amplification per nanowire is the number of nanowires in the given reaction volume. The manipulation of fluorescence intensity per particle caused by changing the overall number of particles has been investigated in other systems that do not have an enzymatic amplification step;[51, 52] this is one parameter that may be investigated in the future. Control experiments indicated that the background fluorescence was generated from the interaction of the intercalating dye with the DNA, and was specifically dependent on the sequence of the primers. The findings of these experiments may be applied to other enzymatic amplification reactions performed on primers bound to surfaces, as appropriate controls were carried out.

The lack of reproducibility and specificity in the on-wire PCR is most likely due to the generation of a mat of DNA on the nanowire, which would provide both a competing enzymatic substrate and an environment for the intercalating dye to fluoresce. When on-wire amplicon was digested post-PCR and then run on a gel, a smear of bands resulted, indicating a variety of lengths

of PCR products generated during thermocycling. This distribution may be due to the generation of a mat of non-specific amplification products on the nanowire surface. One-step extension reactions increased the specificity of the on-wire reaction, further supporting the theory of DNA mat generation, as extension reactions do not undergo thermocycling and amplification, they therefore eliminate the step causing the amplification of incorrect bound sequences. On-wire PCR will be further investigated by Jihye Kim.

On-wire LCR was investigated as an alternative to on-wire PCR (instead of adding bases complementary to a template one at a time, the ligase links together two larger pieces of DNA complementary to the template), and will be discussed in the next chapter. In short, LCR was shown to reproducibly amplify the DNA present without generating high background. This increase in reproducibility of the ligase may have been due to the need for only one enzymatic linkage reaction per amplicon, as opposed to polymerases, which need to perform an enzymatic linkage for every base added and have the opportunity to incorporate incorrect sequences at every reaction step. The increase in specificity of the reaction may be due to the need for three strands of DNA to hybridize, as opposed to only two strands in PCR, to generate an amplicon, which coincides with the findings from Kanaras *et al.*, discussed previously.[57] Enzymatic amplification reactions utilizing immobilized primer or probe sequences can be optimized in the future for use in pathogen detection; on-wire LCR shows great promise for this application.

References

1. Liolios, L.; Jenney, A.; Spelman, D.; Kotsimbos, T.; Catton, M.; Wesselingh, S. Comparison of a multiplex reverse transcription-PCR-enzyme hybridization assay with conventional viral culture and immunofluorescence techniques for the detection of seven viral respiratory pathogens. *J. Clin. Microbiol.* **2001**, *39 (8)*, 2779-2783.

2. Weinberg, A.; Brewster, L.; Clark, J.; Simoes, E. Evaluation of R-Mix shell vials for the diagnosis of viral respiratory tract infections. *J. Clin. Virol.* **2004**, *30*, 100-105.

3. Ogilvie, M. Molecular techniques should not now replace cell culture in diagnostic virology laboratories. *Rev. Med. Virol.* **2001**, *11*, 351-354.

4. Madeley, C. R.; Peiris, J. S. M. Methods in virus diagnosis: immunofluorescence revisited. *J. Clin. Virol.* **2002**, *25*, 121-134.

5. a.) Puppe, W.; Weighl, J. A. I.; Aron, G.; Gröndahl, B.; Schmitte, H.-J.; Niesters, H. G. M.; Groen, J. Evaluation of a multiplex reverse transcriptase PCR ELISA for the detection of nine respiratory tract pathogens. *J. Clin. Virol.* **2004**, *30*, 165-174. b.) Kuypers, J.; Wright, N.; Morrow, R. Evaluation of quantitative and type-specific real-time RT-PCR assays for detection of respiratory syncytial virus in respiratory specimens from children. *J. Clin. Virol.* **2004**, *31*, 123-129.

6. Mackay, I. M.; Arden, K. E.; Nitsche, A. Real time PCR in virology. *Nucleic Acids Res.* **2002**, *30 (6)*, 1292-1305.

7. Penn, S. G.; He, L.; Natan, M. J. Nanoparticles for bioanalysis. *Curr. Opin. Chem. Biol.* **2003**, *7*, 609-615.

8. Nolan, J. P.; Sklar, L. A. Suspension array technology: evolution of the flat-array paradigm. *Trends Biotechnol.* **2002**, *20 (1)*, 9-12.

9. Klein, D. Quantification using real-time PCR technology: applications and limitations. *Trends Mol. Med.* **2002**, *8*, 257-260.

10. Sioss, J. A.; Stoermer, R. L.; Sha, M. Y.; Keating, C. D. Silica-coated, Au/Ag striped nanowires for bioanalysis. *Langmuir* **2007**, *23*, 11334-11341.

11. Song, L.; Ahn, S.; Walt, D. R. Fiber-optic microsphere-based arrays for multiplexed biological warfare agent detection. *Anal. Chem.* **2006**, *78* (4), 1023-1033.

12. Wilson, W. J.; Erler, A. M.; Nasarabadi, S. L.; Skowronski, E. W.; Imbro, P. M. A multiplexed PCR-coupled liquid bead array for the simultaneous detection of four biothreat agents. *Mol. Cell. Probes* **2005**, *19* (2), 137-144.

13. Guo, Z.; Guilfoyle, R. A.; Thiel, A. J.; Wang, R.; Smith, L. M. Direct fluorescence analysis of genetic polymorphisms by hybridization with oligonucleotide arrays on glass supports. *Nucleic Acids Res.* **1994**, *22* (24), 5456-5465.

14. Kumaresan, P.; Yang, C. J.; Cronier, S. A.; Blazej, R. G.; Mathies, R. A. High-throughput single copy DNA amplification and cell analysis in engineering nanoliter droplets. *Anal. Chem.* **2008**, *80*, 3522-3529.

15. Andreadis, J. D.; Chrisey, L. A. Use of immobilized PCR primers to generate covalently immobilized DNAs for *in vitro* transcription/translation reactions. *Nucleic Acids Res.* **2000**, *28 (2)*, i-viii.

16. Claridge, S. A.; Mastroianni, A. J.; Au, Y. B.; Liang, H. W.; Micheel, C. M.; Fréchet, J. M. J.; Alivisatos, A. P. Enzymatic ligation creates discrete multinanoparticle building blocks for self-assembly. *J. Am. Chem. Soc.* **2008**, *130 (29)*, 9598-9605.

17. Tiemann-Boege, I.; Curtis, C.; Shinde, D. N.; Goodman, D. B.; Tavaré, S.; Arnheim, N. Product length, dye choice, and detection chemistry in the bead-emulsion amplification of millions of single DNA molecules in parallel. *Anal. Chem.* **2009**, *81* (14), 5770-5776.

18. Shendure, J.; Porreca, G. J.; Reppas, N. B.; Lin, X.; McCutcheon, J. P.; Rosenbaum, A. M.; Wang, M. D.; Zhang, K.; Mitra, R. D.; Church, G. M. Accurate multiplex polony sequencing of an evolved bacterial genome. *Science* **2005**, *309* (5741), 1728-1732.

19. Nardi, V.; Raz, T.; Cao, X.; Wu, C. J.; Stone, R. M.; Cortes, J.; Deininger, M. W. N.; Church, G.; Zhu, J.; Daley, G. Q. Quantitative monitoring by polymerase colony assay of known mutations resistant to ABL kinase inhibitors. *Oncogene* **2007**, *27* (6), 775-782.

20. Mitra, R. D.; Church, G. M. *In situ* localized amplification and contact replication of many individual DNA molecules. *Nucleic Acids Res.* **1999**, *27* (24), e34.

21. Nicewarner-Peña, S.; Raina, S.; Goodrich, G. P.; Fedoroff, N. V.; Keating, C. D. Hybridization and enzymatic extension of Au nanoparticle-bound oligonucleotides. *J. Am. Chem. Soc.* **2002**, *124 (25)*, 7314-7323.

22. Sha, M. Y.; Walton, I. D.; Norton, S. M.; Taylor, M.; Yamanaka, M.; Natan, M. J.; Xu, C.; Drmanac, S.; Huang, S.; Borcherding, A.; Drmanac, R.; Penn, S. G. Multiplexed SNP genotyping using nanobarcode particle technology. *Anal. Bioanal. Chem.* **2006**, *384*, 658-666.

23. Carmon, A.; Vision, T. J.; Mitchell, S. E.; Thannhauser, T. W.; Müller, U.; Kresovich, S. Solid-phase PCR in microwells: Effects of linker length and composition on Tethering, Hybridization, and Extension. *Biotechniques* **2002**, *32* (2), 410-420.

24. Adessi C.; Matton, G.; Ayala, G.; Turcatti, G.; Mermod, J.-J.; Mayer, P.; Kawashima, E. Solid phase DNA amplification: Characterisation of primer attachment and amplification mechanisms. *Nucleic Acids Res.* **2000**, *28* (20), e87.

25. von Nickisch-Rosenegk, M.; Marschan, X.; Andresen, D.; Bier, F. F. Reverse transcription-polymerase chain reaction on a microarray: The integrating concept of 'active arrays.' *Anal. Bioanal. Chem.* **2008**, *391* (5), 1671-1678.

26. von Nickish-Rosenegk, M.; Marschan, X.; Andresen, D.; Abraham, A.; Heise, C.; Bier, F. F. On-chip PCR amplification of very long templates using immobilized primers on glassy surfaces. *Biosens. Bioelectron.* **2005**, *20* (8), 1491-1498.

27. Palanisamy, R.; Connolly, A. R.; Trau, M. Considerations of solid-phase DNA amplification. *Bioconjugate Chem.* **2010**, *21* (4), 690-695.

28. Peterson, A. W.; Heaton, R. J.; Georgiadis, R. M. The effect of surface probe density on DNA hybridization. *Nucleic Acids Res.* **2001**, *29* (24), 5163-5168.

29. Drobyshev, A. L.; Nasedkina, T. V.; Zakharova, N. V. The role of DNA diffusion in solid phase polymerase chain reaction with gel-immobilized primers in planar and capillary microarray format. *Biomicrofluidics* **2009**, *3* (4), 0441122.

30. Martin, C.R. Membrane-based synthesis of nanomaterials. *Chem. Mater*. **1996**, *8* (8), 1739-1746.

31. Martin, C.R. Nanomaterials: a membrane-based synthetic approach. *Science **1994**, 266* (5193), 1961-1966.

32. Al-Mawalawi, D.; Liu, C. Z.; Moskovits, M. Nanowires formed in anodic oxide nanotemplates. *J. Mater. Res.* **1994**, *9* (4), 1014-1018.

33. True, R. J.; Taylor, M. K.; Chakarova, G. S.; Walton, I. D. Microfabricated templates for the electrodeposition of metallic barcodes for use in multiplexed bioassays. Proceedings of the 26th Annual Conference of the IEEE EMBS. San Francisco, USA, 2004.

34. Nicewarner-Peña, S. R.; Freeman, R. G.; Reiss, B. D.; He, L.; Peña D. J.; Walton, I. D.; Cromer, R.; Keating, C. D.; Natan, M. J. Submicrometer metallic barcodes. *Science* **2001**, *294* (5540), 137-141.

35. Keating, C. D.; Natan, M. J. Striped metal nanowires as building blocks and optical tags. *Adv. Mater*. **2003**, *15* (5), 451-454.

36. Walton, I. D.; Norton, S. M.; Balasingham, A.; He, L.; Oviso, D. F., Jr.; Gupta, D.; Raju, P. A.; Natan, M. J.; Freeman, R. G. Particles for multiplexed analysis in solution: detection and identification of striped metallic particles using optical microscopy. *Anal. Chem.* **2002**, *74* (10), 2240-2247.

37. Reiss, B. D.; Freeman, R. G.; Walton, I. D.; Norton, S. M.; Smith, P. C.; Stonas, W. G.; Keating, C. D.; Natan, M. J. Electrochemical synthesis and optical readout of striped metal rods with submicron features. *J. Electroanal. Chem.* **2002**, *522* (1), 95-103.

38. Zuker, M. Mfold web server for nucleic acid folding and hybridization prediction. *Nucleic Acids Res.* **2003**, *31* (13), 3406-3415.

39. Markham, N. R.; Zuker, M. DINAMelt web server for nucleic acid melting prediction. *Nucleic Acids Res.* **2005**, *33* (web server issue), w577-w581.

40. Dieffenbach, C. W.; Dveksler, G. S., Eds. *PCR Primer: A laboratory manual*, 2nd ed.; Cold Spring Harbor Laboratory Press: Cold Spring Harbor, NY, 2003.

41. Templeton, K. E.; Claas, E. C. J. "Comparison of Four Real-time PCR Detection Systems: Bio-Rad I-Cycler, ABI 7700, Roche LightCycler, and the Cepheid Smartcycler." In *PCR Primer A Laboratory Manual*, Second Edition; Dieffenbach, C. W.; Dveksler, G. S.; Cold Spring Harbor Laboratory Press: Cold Spring Harbor, NY, 2003; 194.

42. Zammatteo, N.; Jeanmart, L.; Hamels, S. Courtois, S.; Louette, P.; Hevesi, L.; Remacle, J. Comparison between different strategies of covalent attachment of DNA to glass surfaces to build DNA microarrays. *Anal. Biochem.* **2000**, *280*, 143-150.

43. Chrisey, L. A.; Lee, G. U.; O'Ferrall, C. E. Covalent attachment of synthetic DNA to self-assembled monolayer films. *Nucleic Acids Res.* 1996, 24 (15), 3031-3039.

44. Brinker, C. J.; Scherer, G. W. *Hydrolysis and Condensation II: Silicates*. In *Sol-Gel Science: The Physics and Chemistry of Sol-Gel Processing*; Academic Press, Inc.: Boston, 1990; 97-234.

45. Demers, L. H.; Mirkin, C. A.; Mucic, R. C.; Reynolds, R. A. III.; Letsinger, R. L.; Elghanian, R.; Viswanadham, G. A fluorescence-based method for determining the surface coverage and hybridization efficiency of thiol-capped oligonucleotides bound to gold thin films and nanoparticles. *Anal. Chem.* **2000**, *72* (22), 5535–5541.

46. Stoermer, R. L.; Cederquist, K. B.; McFarland, S. K.; Sha, M. Y.; Penn, S. G.; Keating, C. D. Coupling molecular beacons to barcoded metal nanowires for multiplexed, sealed chamber DNA bioassays. *J. Am. Chem. Soc.* **2006**, *128* (51), 16892–16903.

47. Cederquist, K. B.; Golightly, R. S.; Keating, C. D. Molecular beacon-metal nanowire interface: Effect of probe sequence and surface coverage on sensor performance. *Langmuir* **2008**, *24* (16), 9162-9171.

48. Cederquist, K. B.; Keating, C. D. Curvature effects in DNA:Au nanoparticle conjugates. *ACS Nano* **2009**, *3* (2), 256-260.

49. Hill, H. D.; Millstone, J. E.; Banholzer, M. J.; Mirkin, C. A. The role radius of curvature plays in thiolated oligonucleotide loading on gold nanoparticles. *ACS Nano* **2009**, *3* (2), 418–424.

50. Herne, T. M.; Tarlov, M. J. Characterization of DNA probes immobilized on gold surfaces. *J. Am. Chem. Soc.* **1997**, *119* (38), 8916-8920.

51. He, B.; Son, S. J.; Lee, S. B. Suspension array with shape-coded silica nanotubes for multiplexed immunoassays. *Anal. Chem.* **2007**, *79*, 5257-5263.

52. Tok, J. B.-H.; Chuang, F. Y. S.; Kao, M. C.; Rose, K. A.; Pannu, S. S., Sha, M. Y.; Chakarova, G.; Penn, S. G.; Dougherty, G. M. Metallic striped nanowires as multiplexed immunoassay platforms for pathogen detection. *Angew. Chem. Int. Ed.* **2006**, *45*, 6900-6904.

53. Emery, S. L.; Erdman, D. D.; Meyer, R. F.; Bowen, M. D.; Tong, S.; Cook, B.; Holloway, B. P.; McCaustland, K. A.; Rota, P. A.; Bankamp, B.; Lowe, L. E.; Ksiazek, T. G.; Bellini, W.; Anderson, L. J. Real-time RT-PCR Assay for the SARS-Associated Coronavirus *Emerging Infectious Diseases* **2004**, *10* (2), 311-316.

54. Drosten, C.; Günther, S.; Preiser, W.; Van der Werf, S.; Brodt, H. R.; Becker, S.; Rabenau, H.; Panning, M.; Kolesnikova, L.; Fouchier, R.; Berger, A.; Burguière, A. M.; Cinatl, J.; Eickmann, M.; Escriou, N.; Grywna, K.; Kramme, S.; Manuguerra, J. C.; Müller, S.; Rickerts, V.; Stürmer, M.; Vieth, S.; Klenk, H. D.; Osterhaus, A.; Schmitz, H.; Doerr, H. W. Identification of a novel Coronavirus in patients with Severe Acute Respiratory Syndrome. *N Engl J Med*. **2003**, *348***,** 1967-1976.

55. a.) Lanciotti, R. S.; Kerst, A. J.; Nasci, R. S.; Godsey, M. S.; Mitchell, C. J.; Savage, H. M.; Komar, N.; Panella, N. A.; Allen, B. C.; Volpe, K. E.; Davis, B. S.; Roehrig, J. T. Rapid detection of West Nile Virus from human clinical specimens, field-collected mosquitoes, and avian samples by a TaqMan Reverse Transcriptase-PCR Assay. *J. Clin. Microbiol*. **2000**, *38*, 4066–4071. b.) Briese, T.; Glass, W. G.; Lipkin, W. I. Detection of West Nile Virus sequences in cerebrospinal fluid. *Lancet*. **2000**, *355* (9215), 1614-1615.

56. Kanaras, A. G.; Wang, Z.; Hussain, I.; Brust, M.; Cosstick, R.; Bates, A. D. "Site-specific ligation of DNA-mediated gold nanoparticles activation by the restriction enzyme *Sty*1." *Small* **2007**, *3 (1)*, 67-70.

57. Kanaras, A. G.; Wang, Z.; Brust, M.; Cosstick, R.; Bates, A. D. Enzymatic disassembly of DNA-gold nanostructures. *Small* **2007**, *3 (4)*, 590-594.

58. Zweig, M. H.; Campbell, G. Receiver-operating characteristic (ROC) plots: A fundamental evaluation tool in clinical medicine. *Clin. Chem.* **1993**, *39* (4), 561-577.

59. Greiner, M.; Pfeiffer, D.; Smith, R. D. Principles and practical application of the receiver-operating characteristic analysis for diagnostic tests. *Prev. Vet. Med.* **2000**, *45* (1-2), 23-41.

60. Chemical and Biological Sensor Standards Study, Defense Advanced Research Projects Agency, LTC John Carrano, Study Chair.

61. Ando, T.; Monroe, S. S.; Gentsch, J. R.; Jin, Q.; Lewis, D. C.; Glass, R. I. Detection and differentiation of antigenically distinct small round-structured viruses (Norwalk-like viruses) by reverse transcription-PCR and Southern hybridization. *J. Clin. Microbiol*. **1995**, *33***,** 64-71.

62. Gunson, R. N.; Collins, T. C.; Carman, W. F. Real-time RT-PCR detection of 12 respiratory viral infections in four triplex reactions. *J. Clin. Virology* **2005**, *33* (4), 341-344.

63. *CDC protocol of real time RTPCR for swine influenza A(H1N1)*; CDC Reference #I-007-05; WHO Collaborating Center: Atlanta, GA, October 6, 2009; 1-8.

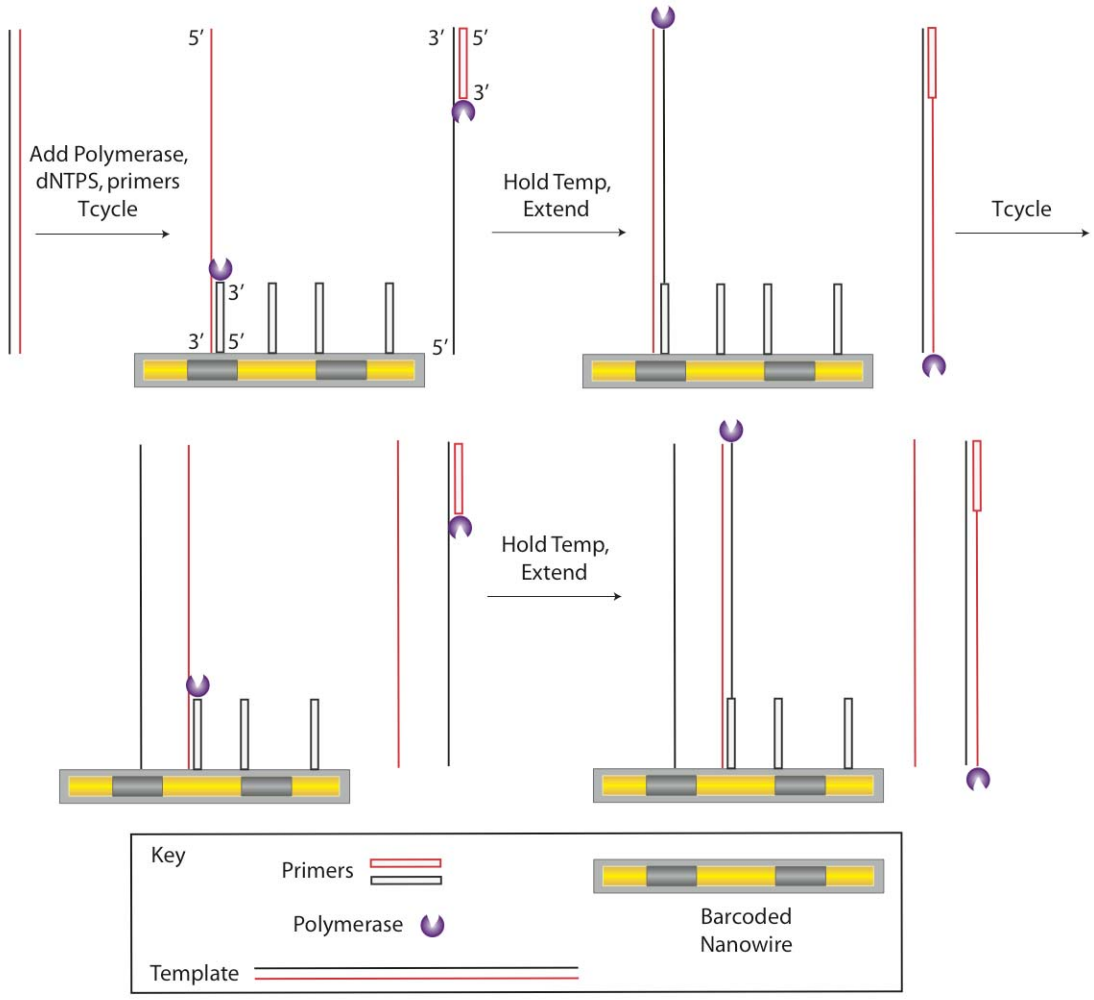

Figure 2-1. On-wire PCR, where each barcode pattern is paired with a primer of a pathogen-specific sequence. Post-PCR the only ds DNA in solution should be the negligible amount of initial template DNA, all other ds DNA is bound to the wire, allowing for the use of an intercalating dye for DNA quantification.

Table 2-1: DNA Sequences used in PCR Investigations[A]

Name	Sequence (5′ to 3′)	Comments
Lambda phage DNA Free Primer	ATG AAC TGA TTG CCC GTC TCC	Forward, base number 82[B]
Lambda phage DNA Immobilized Primer	Phos – ttt ttt ttt tCG CTG ATC CCA CCT CAT TTT	Reverse, base number 282
SARS-1 (CoVNC) Free Primer	GGA GCC TTG AAT ACA CCC AAA G	Forward[53]
SARS-1 (CoVNC) Immobilized Primer	Thiol –ttt ttt ttt tGC ACG GTG GCA GCA TTG	Reverse
SARS-1 (CoVNC) Armored RNA Template	CCG AAG AGC TAC CCG ACG AGT TCG TGG TGG TGA CGG CAA AAT GAA AGA GCT CAG CCC CAG ATG GTA CTT CTA TTA CCT AGG AAC TGG CCC AGA AGC TTC ACT TCC CTA CGG CGC TAA CAA AGA AGG CAT CGT ATG GGT TGC AAC TGA G*GG AGC CTT GAA TAC ACC CAA AG*A CCA CAT TGG CAC CCG CAA TCC TAA TAA *CAA TGC TGC CAC CGT GC*T ACA ACT TCC TCA AGG AAC AAC ATT GCC AAA AGG CTT CTA CGC AGA GGG AAG CAG AGG CGG CAG TCA AGC CTC TTC TCG CTC CTC ATC ACG TAG TCG CGG TAA TTC AAG AAA TTC AAC TCC TGG CAG CAG TAG GGG AAA TTC TCC TGC TCG AAT GGC TAG CGG AGG TGG TGA AAC TGC CCT CGC GCT ATT GCT GCT AGA CAG ATT GAA CCA GCT TGA GAG CAA AGT TTC TGG TAA AGG CCA ACA ACA ACA AGG CCA AAC TGT CAC TAA GAA ATC TGC TGC TGA GGC ATC TAA AAA GCC TCG CCA AAA ACG TAC TGC CAC AAA ACA GTA CAA CGT CAC TCA AGC ATT TGG GAG ACG TGG TCC AGA ACA AAC CCA AGG AAA TTT CGG GGA CCA AGA CCT AAT CAG ACA AGG AAC TGA TTA CAA ACA TTG GCC GCA AAT TGC ACA ATT TGC TCC AAG TGC CTC TGC ATT CTT TGG AAT GTC ACG CAT TG	

[A] Lower case letters indicate bases used as spacers, which are not part of the hybridized sequence. Phos abbreviation symbolizes phosphate functionality. Lambda phage kit Applied Biosystems part number 4312778. Italics symbolizes primer binding sites.
[B] Template 48 kbp.

Table 2-1: DNA Sequences used in PCR Investigations, cont.[A]

Name	Sequence (5′ to 3′)	Comments
SARS-2 (BNI) Free Primer	GAAGCTATTCGT CACGTTCG	Forward[54]
SARS-2 (BNI) Immobilized Primer	Thiol – ttt ttt ttt tCT GTA GAA AAT CCT AGC TGG AG	Reverse
SARS-2 (BNI) Armored RNA Template	*ATG AAT TAC CAA GTC AAT GGT TAC* CCT AAT ATG TTT ATC ACC CGC *GAA GAA GCT ATT CGT CAC GTT CG*T GCG TGG ATT GGC TTT GAT GTA GAG GGC TGT CAT GCA ACT AGA GAT GCT GTG GGT ACT AAC CTA CCT CTC CAG CTA GGA TTT TCT ACA GGT GTT AAC TTA GTA GCT GTA CCG ACT GGT TAT G	
Norwalk Free Primer	TGG AAT TCC ATC GCC CAC TGG	Forward[61]
Norwalk Immobilized Primer	Thiol – ttt ttt ttt tAC TGA CAA TTT CAT CAT CAC C	Reverse
Norwalk Armored RNA Template	CCA GAT AGT TGC AGA AGA CCT TCT ATC TCC TAG TGT GAT GGA TGT GGG TGA CTT CAA AAT ATC AAT CAA TGA GGG CCT TCC CTC TGG TGT GCC CTG CAC CTC TCA A*TG GAA TTC CAT CGC CCA CTG G*CT CCT CAC TCT CTG TGC ACT CTC TGA AGT TAC AAA CCT GTC CCC TGA CAT CAT ACA GGC TAA TTC CCT CTT TTC CTT CTA T*GG TGA TGA TGA AAT TGT CAG T*AC AGA TAT AAA CTT AAA CCC AGC CCG CCT CAC TCA AAT TCT CAA GGA ATAT G	

[A] Lower case letters indicate bases used as spacers, which are not part of the hybridized sequence. Phos abbreviation symbolizes phosphate functionality. Italics symbolizes primer binding sites.

Table 2-1: DNA Sequences used in PCR Investigations, cont.[A]

Name	Sequence (5′ to 3′)	Comments
WNV-1 (Lanciotti) Free Primer	TCA GCG ATC TCT CCA CCA AAG	Forward[55A]
WNV-1 (Lanciotti) Immobilized Primer	Thiol – ttt ttt ttt tGG GTC AGC ACG TTT GTC ATT G	Reverse
WNV-2 (Lipkin) Free Primer	GCT CCG CTG TCC CTG TGA	Forward[55B]
WNV-2 (Lipkin) Immobilized Primer	Thiol – ttt ttt ttt tCA CTC TCC TCC TGC ATG GAT G	Reverse
WNV Armored RNA Template	GCA GTT ATT GCT ATT TGG CTA CCG *TCA GCG ATC TCT CCA CCA AAG* CTG CGT GCC CGA CCA TGG GAG AAG CTC A*CA ATG ACA AAC GTG CTG ACC C*AG CTT TTG TGT GCA GAC AAG GGT ACT TCC ACA GAA GAG ACC TGC GGC TCA TGG CCA ACG CCA TTT *GCT CCG CTG TCC CTG TGA* ATT GGG TCC CTA CCG GAA GAA CCA CGT GGT C*CA TCC ATG CAG GAG GAG AGT G*GA GGA CAA CAG AGG ACA TGT TGG CCA CAT GTT GTA ACT TCA AAG CCC AAT GTC AGA CCA CGC TAC GGC GTG CTA CTC TGC GGA GAG TGC AGT CTG CGA TAG TGC CCC AGG AGG ACT GGG TTA ACA AAG GCA AAC CAA CGC CCC ACG CGG CCC TAG CCC CGG TAA TGG TGT TAA CCA GGG CGA AAG GAC TAG AGG TTA G	Used for both WNV-1 and WNV-2 primer sets.
RSV A Forward Primer	AGA TCA ACT TCT GTC ATC CAG CAA	
RSV A Reverse Primer	Phos - TTC TGC ACA TCA TAA TTA GGA	Digested after solution phase PCR of clinical isolate[62]
RSV B Forward Primer	AAG ATG CAA ATC ATA AAT TCA CAG GAT TAA TAG GTA	
RSV B Reverse Primer	Phos - TGA TAT CCA GCA TCT TTA AGT A	Digested after solution phase PCR of clinical isolate[62]

[A] Lower case letters indicate bases used as spacers, which are not part of the hybridized sequence. Phos abbreviation symbolizes phosphate functionality. Italics symbolizes primer binding sites.

Table 2-1: DNA Sequences used in PCR Investigations, cont.[A]

Name	Sequence (5′ to 3′)	Comments
Swine Flu H1N1 Free Primer	GTG CTA TAA ACA CCA GCC TCC CA	Forward[63]
Swine Flu H1N1 Immobilized Primer	Thiol – ttt ttt ttt tCG GGA TAT TCC TTA ATC CTG TGG C	Reverse, (phosphorylated analogue digested after solution phase PCR)
Swine Flu H1N1 Positive Control Ultramer	ATT TAG GTG ACA CTA TAG AA*G TGC TAT AAA CAC CAG CCT CCC A*TT CAG AAT ATA CAT CCA GTC ACA ATT GGA AAA TAG AGT TTA AAC AGA T*GC CAC AGG ATT AAG GAA TAT CCC G*CC CTA TAG TGA GTC GTA TTA	Template in PCR digested by restriction endonuclease
SSF	Moiety – ttt ttt ttt tCC ATC AAT GAG GAA GCT GCA – Alexa 647	Used for all surface coverage studies, moiety = thiol, phos, or amine[10]
Comp C6N7P12	TAA CAT TCG CAT TCA GGA T	Comp primer used in extension
Noncomp N18	CGA TAA CGG TCG GTA CGG	Noncomp primer used in extension
Template T88	TAC GAG TTG AGA ACA CAG ACG TAC TAT CAT TGA CGC ATC AGA CAA CGT GCG TCA AAA ATT ACG TGC GGA AGG AGT TAT CCT GAA TGC G	Template for extension[21]

[A] Lower case letters indicate bases used as spacers, which are not part of the hybridized sequence. Phos abbreviation symbolizes phosphate functionality. Italics symbolizes primer binding sites.

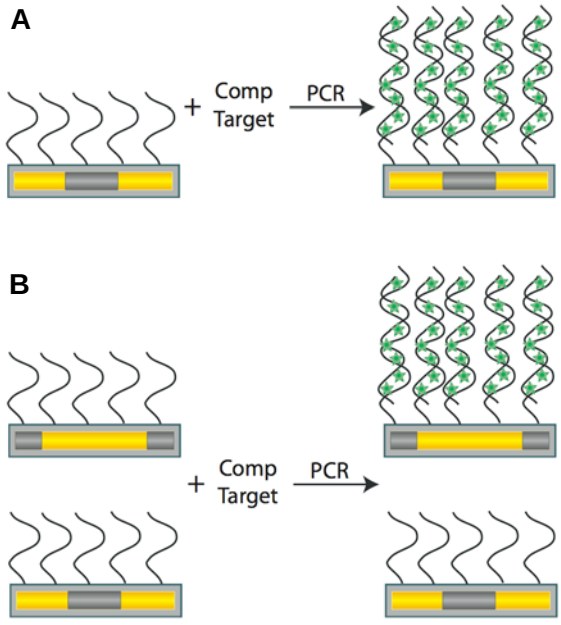

Figure 2-2. Schemes representing single-plex (A) and multiplexed (B) on-wire PCR assays before and after addition of the complementary template and PCR reagents, and subsequent thermocycling. Images show activity happening in individual reaction volumes; multiplexed samples contain noncomplementary controls within each reaction volume as multiple primer sequences are present, each on a nanowire with a corresponding barcode, while single-plexed samples contain noncomplementary controls in a separate reaction volume as only one primer sequence and the corresponding barcoded nanowire are present.

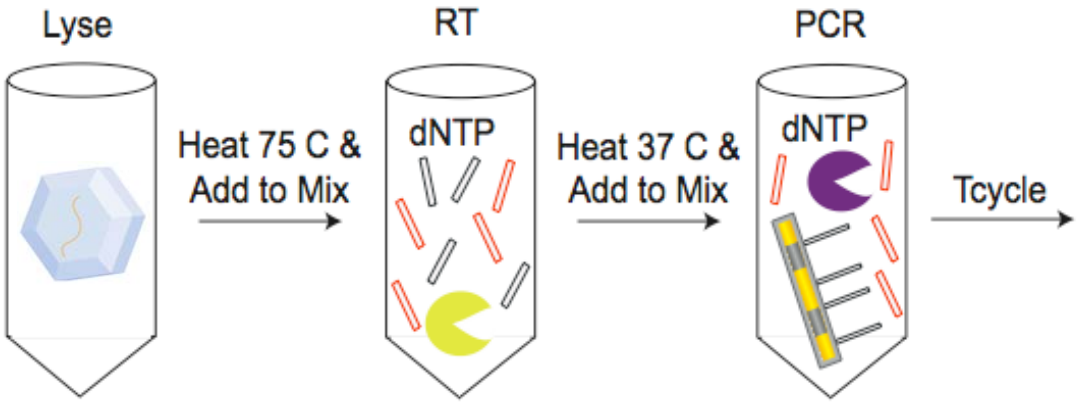

Figure 2-3. Scheme showing the processing steps for on-wire PCR using Armored RNA. The protein coat surrounding the RNA is first heat lysed and is then added to a reverse transcription reaction containing primers (boxes), dNTP's, and reverse transcriptase. The DNA generated during this reaction is placed into the PCR reaction tube, along with dNTP's, polymerase, solution phase forward primers, and immobilized primers. The mixture is thermocycled and imaged.

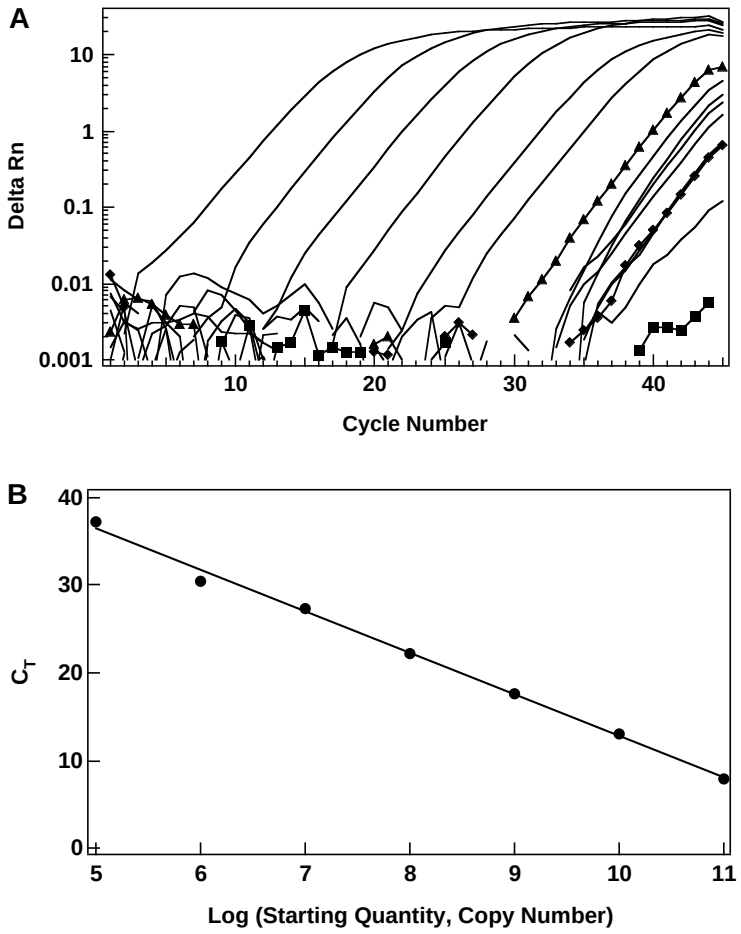

Figure 2-4. Primer linearity determination for on-wire PCR using lambda phage DNA as the template. The highest template concentration was 1 x 10^{11} copies (48 kb in length), shown in the amplification plot (A) with the lowest C_T. Each subsequent amplification plot represents a sample with a decrease in template concentration by one order of magnitude, present in 25 μL reaction volume. The linear primer response deteriorates at 1 x 10^4 copies. The noncomplementary template sample is indicated by filled triangles, the no template sample by filled diamonds, and the noncomplementary primer sample by filled squares. (B) shows the standard curve generated using the data from (A). A primer efficiency of approximately 60 per cent was determined.

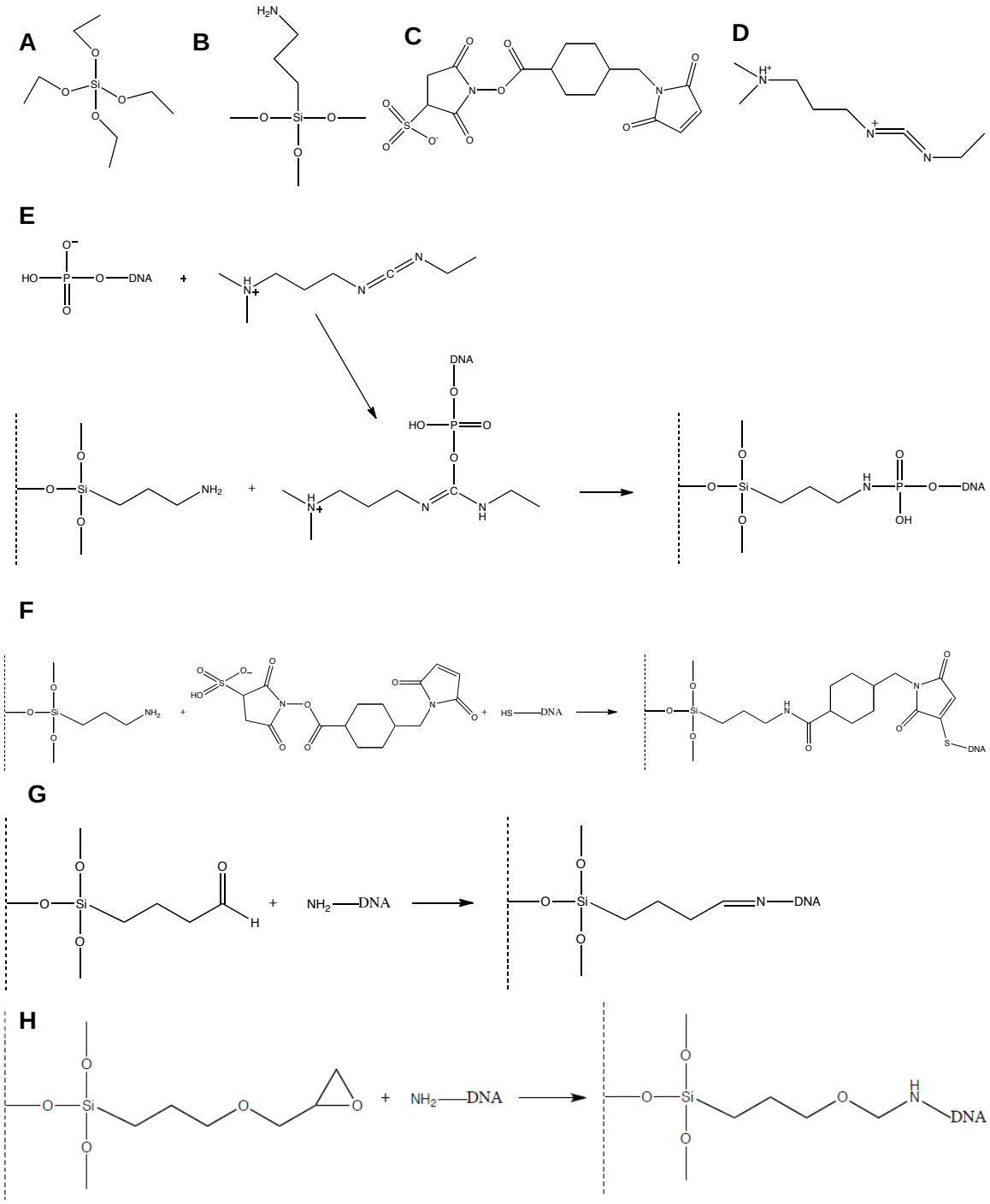

Figure 2-5. Molecules used during attachment chemistry between glass-coated wires and DNA: (A) TEOS, (B) APTMS, (C) Sulfo-SMCC, and (D) EDC. Step-by-step attachment of DNA is shown using (E) EDC, (F) Sulfo-SMCC, (G) triethoxsilylbutyraldehyde, and (H) 3-glycidoxypropyl-trimethoxysilane. Stacey Dean assisted with figure drawing.

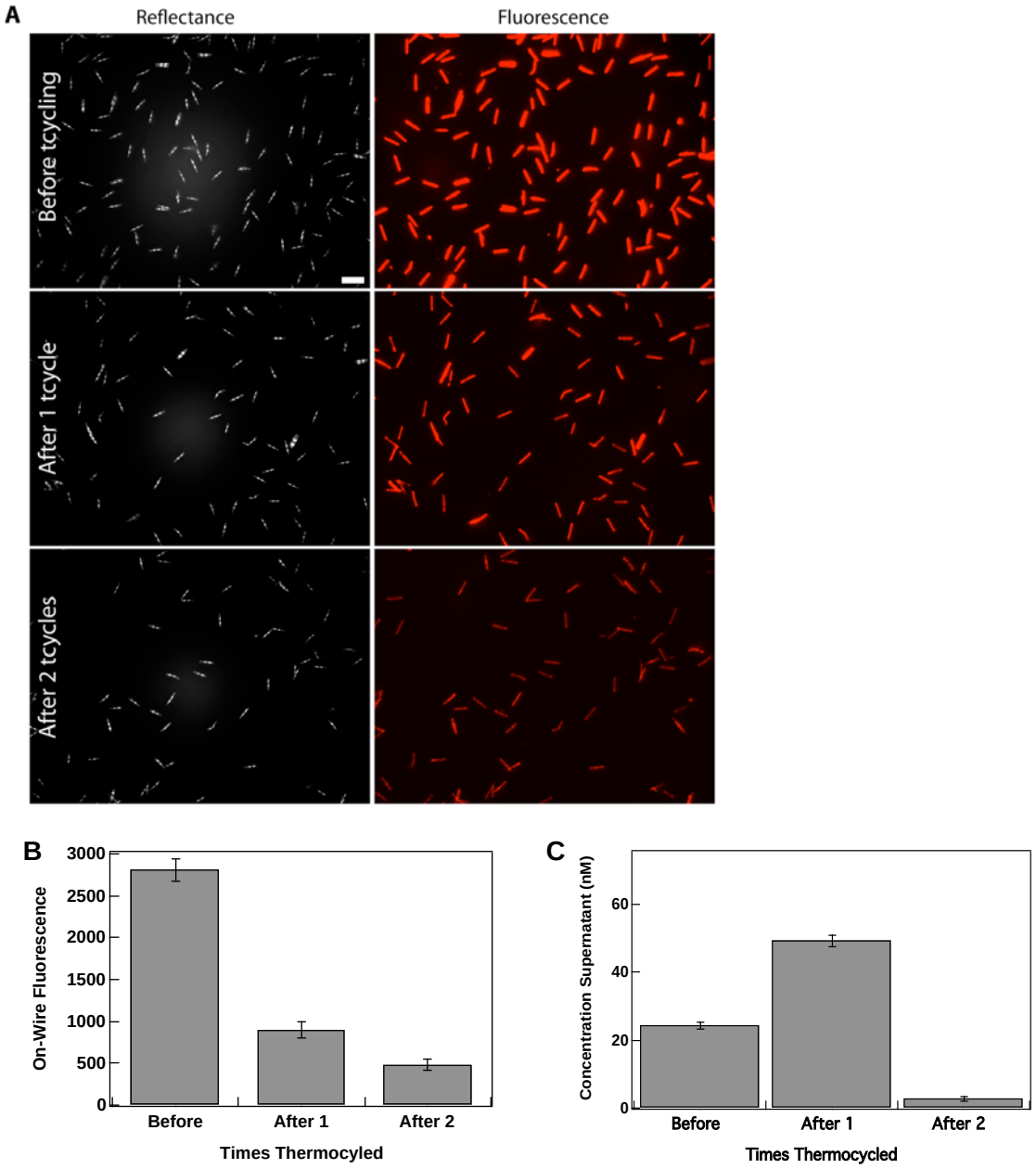

Figure 2-6. (A) On-wire reflectance and fluorescence images of fluorescently tagged DNA bound to nanowires using EDC attachment chemistry before and after being run through two thermocycling protocols, scale bar represents 10 μm. On-wire fluorescence (B) was quantified and in solution fluorescence of the supernatant (C) was also quantified before and after the samples were run through two thermocycling protocols. The concentration shown reflects a ten fold dilution of the supernatant when analyzed on the fluorimeter. At least 30 nanowires were used to generate the mean shown for each sample in bar graphs, and error bars represented the 95th percent confidence interval. Error bars on fluorimetry data represent the standard deviation of five replicate measurements and subsequent conversion to concentration using a calibration curve. The data indicate that the EDC attachment chemistry is not thermostable enough to withstand thermocycling conditions.

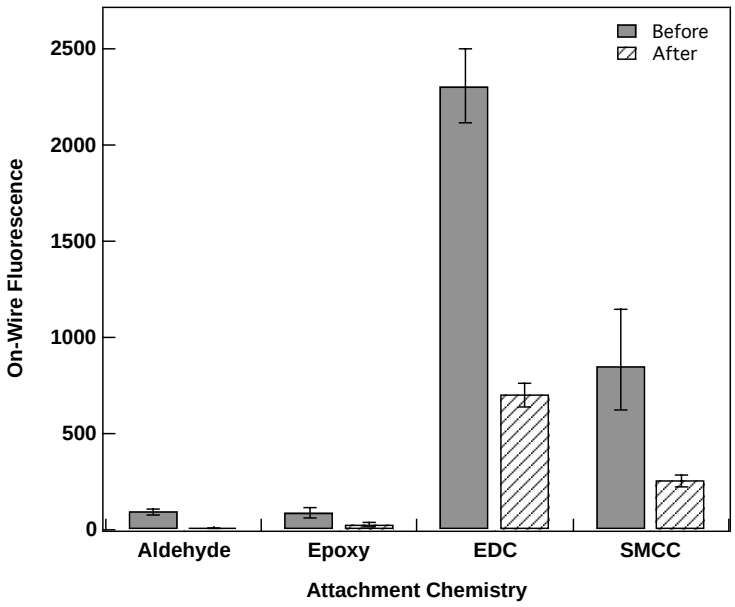

Figure 2-7. Quantified on-wire fluorescence intensity of fluorescently tagged DNA bound to nanowires through the attachment chemistries listed before and after being thermocycled. Attachment chemistries are shown in Scheme 3. EDC was added in the presence of imidazole. All attachment chemistries were analyzed using silicon nanowires from the same batch. To attach DNA using aldehyde and epoxy chemistries, 75 μL wires were first coated in 10 % of the appropriate silane and brought up to 500 μL total. 10 μL fluorescently tagged DNA were added to 100 μL nanowires and were reacted overnight. Data was collected by Bo He.

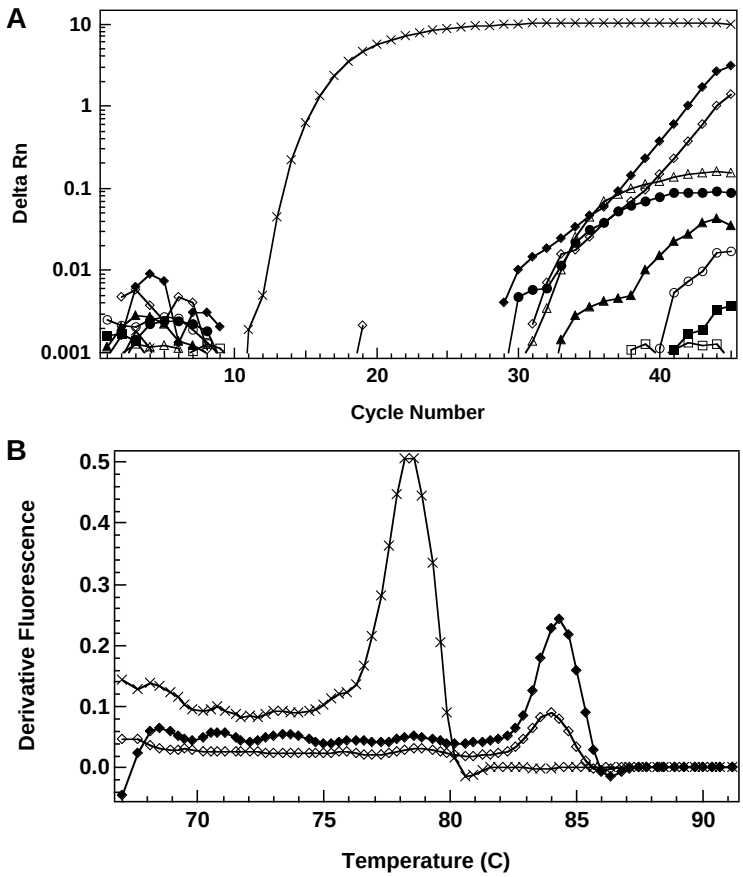

Figure 2-8. Amplification plot (A) showing solution phase and wire-bound extension during PCR. All traces represent samples exposed to complementary template, where the open markers show wires at 100 percent primer coverage, and closed markers show wires at 50 percent primer coverage. Square makers represent a solution containing 1× solution primer and 1× wire concentrations, triangle markers represent 1× solution primer and 2× wire concentrations, circle markers represent 2× solution primer and 1× wire concentrations, and diamond markers represent 10× solution primer and 1× wire concentrations. The decreased surface coverage of immobilized primer on-wire was accomplished by attaching to the wire a diluted immobilized primer solution, 50 percent of which was a thiolated 10 T spacer. Wires with ten times the normal primer concentration exhibited the largest amount of extension the fastest, but the dissociation curve (B) shows that the T_M between the on-wire samples and the solution phase samples is not the same.

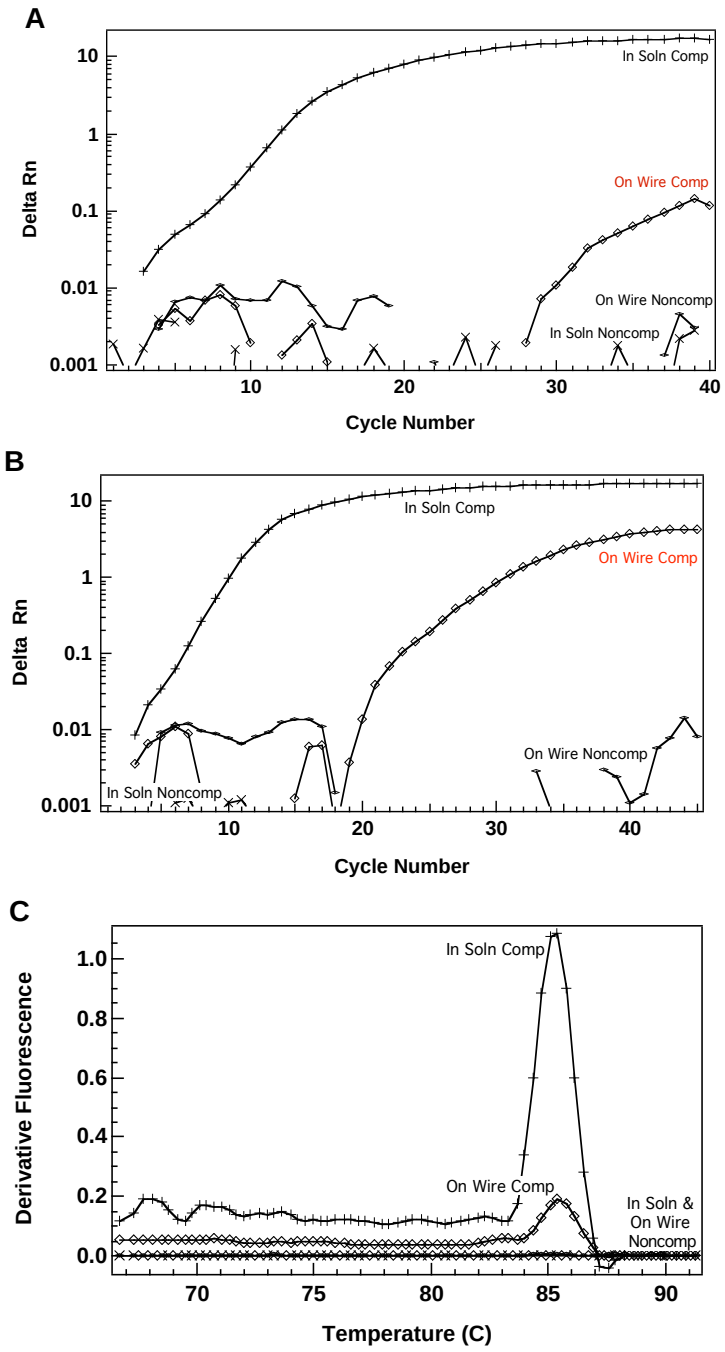

Figure 2-9. Amplification plots showing the increase in on-wire amplification produced when increasing the number of thermocycles from 40 (A) to 45 (B) and increasing the extension time during each cycle from one to two minutes, respectively. The post-PCR dissociation curve (C) when using two minutes per extension step shows the T_M of the amplicon on-wire is the quite similar to that in solution (minor differences in T_M are due to slight variations, e.g., salt concentration, from well-to-well, similar to variations from lane-to-lane in a gel), and that there are no other amplicon lengths produced, indicating the fidelity of the reaction.

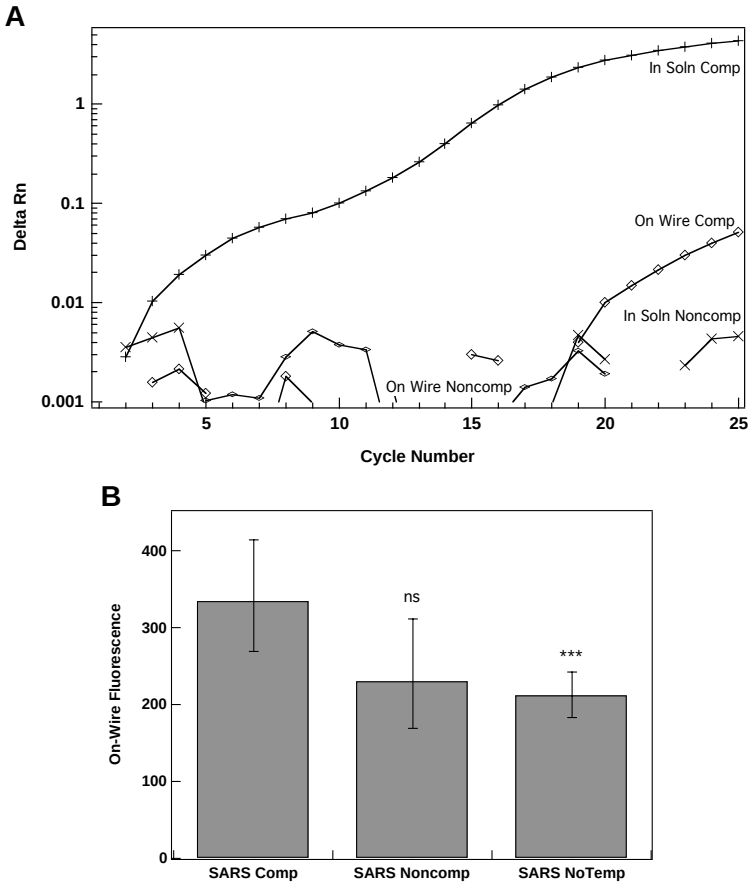

Figure 2-10. Amplification plot (A) and quantified on-wire PCR sample microscopy images (B) showing that decreasing the number of thermocycles performed does not increase the specificity of the microscopy data (the background is not being generated by running the reaction for too long). *** p value < 0.001 versus signal generated from complementary template, ns indicates that the p value was not significant.

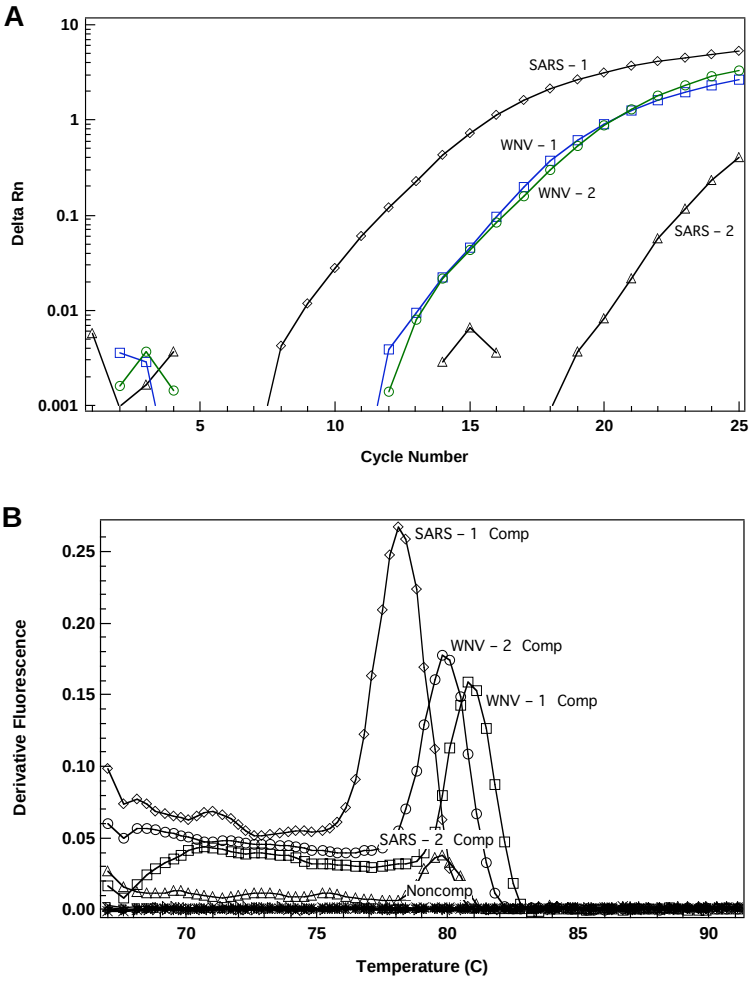

Figure 2-11. Amplification plot (A) and dissociation curve (B) showing the amplification of solution phase Armored RNA samples primed by different primer sets. These were generated using a shorter thermocycling protocol for solution phase amplification. The C_T increases with increasing amplicon length; SARS-1 (diamonds) and SARS-2 (triangles) templates and primer sets differ, and have amplicons of 67 and 109 bases long, respectively. West Nile Virus template is used for multiple primer sets (1—blue squares and 2—green circles) that prime different regions, but generate amplicons that are both 70 bases long. Noncomplementary samples include WNV-1 or WNV-2 primers paired with SARS-1 or SARS-2 template, and either SARS-1 or SARS-2 primers used with the other SARS template, or West Nile Virus template.

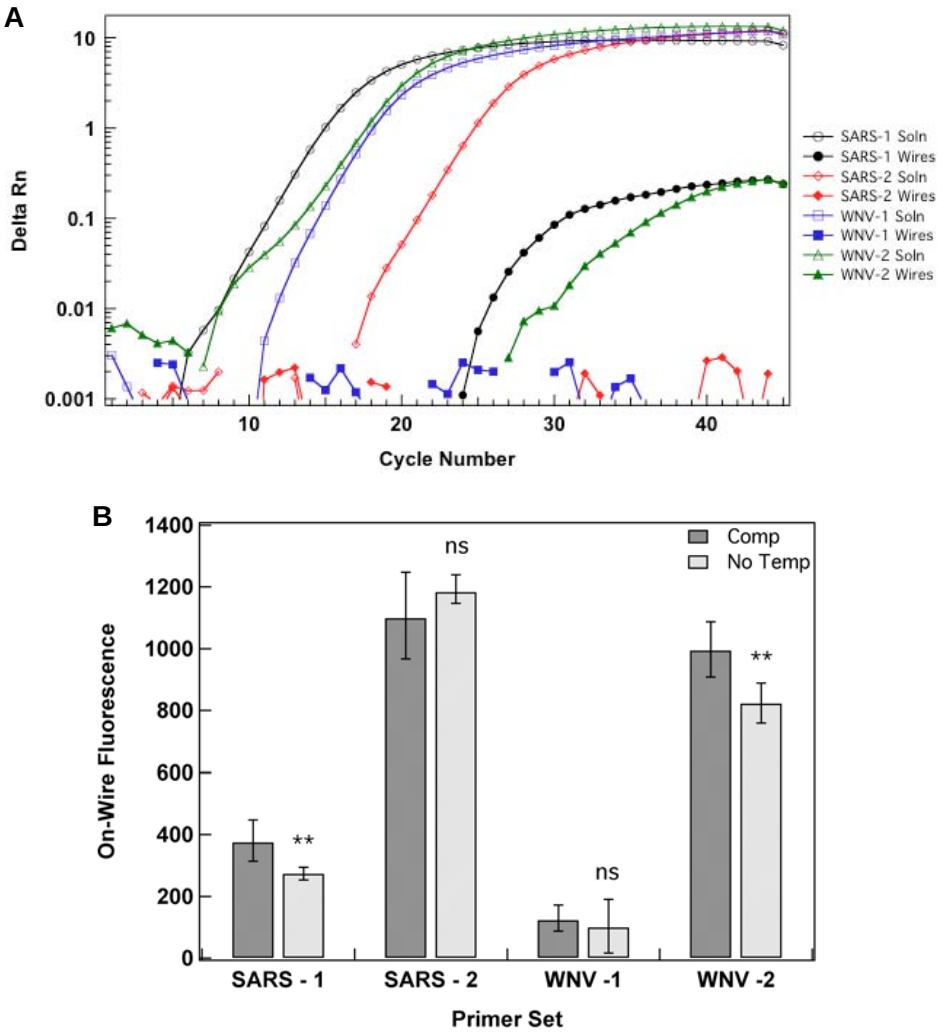

Figure 2-12. Amplification plot (A) for on-wire Armored RNA PCR samples; only samples using SARS-1 and WNV-2 primer sets show on-wire extension. Quantification of on-wire microscopy images is also shown (B), where the background signal (that of the sample lacking template) corresponds to the primer set used. The best specificity is observed in the SARS-1 and WNV-2 samples, which showed on-wire extension in the amplification plot. ** p value < 0.01 when compared to signal from complementary template; ns indicates p value is not significant.

Table 2-2. Properties of immobilized primers used to amplify Armored RNA template sequences during PCR

Immobilized Primer	T_M	Length	GC
SARS-1	*60.1*	27	40.7
WNV-1	59.4	31	35.4
WNV-2	*59.5*	31	38.7
SARS-2	56.3	32	31.2

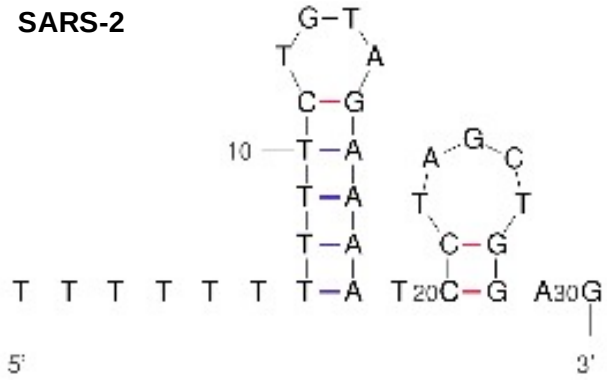

Figure 2-13. Secondary structure of immobilized primer used to amplify SARS-2 template (which resulted in nonspecific amplification) with a ΔG of -5.4, analyzed with the following parameters: 25 ^{o}C, sodium concentration of 50 mM and magnesium concentration of 2.5 mM. Other immobilized primers did not show significant secondary structure (none showed complementarity with primers of the same sequence). Mfold assistance from Kristin Cederquist.

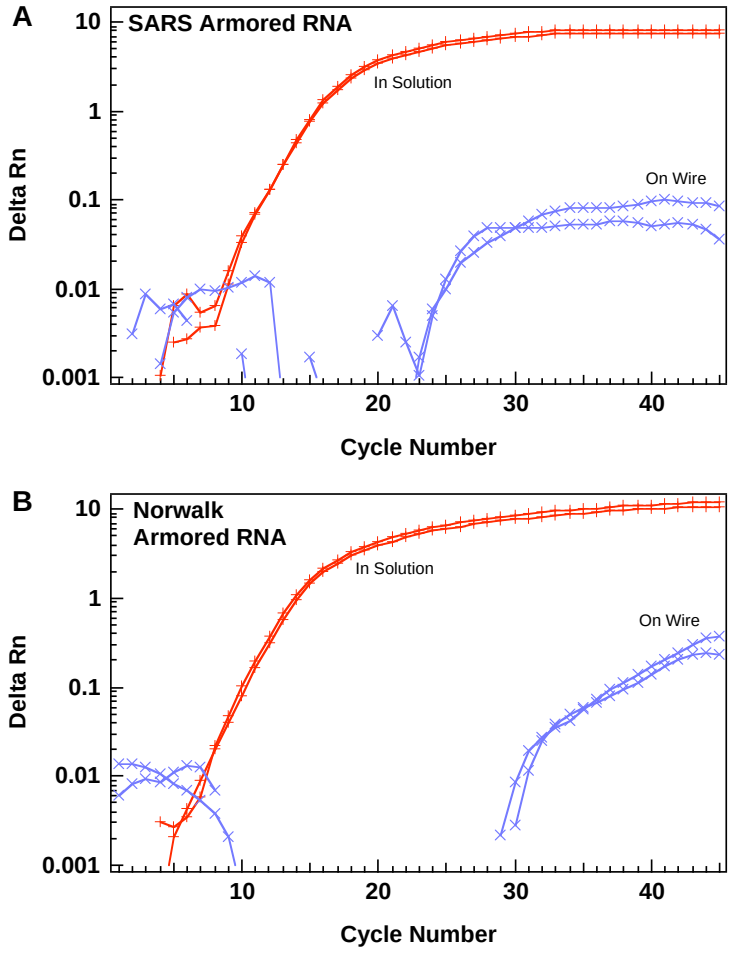

Figure 2-14. Amplification plots for single-plex PCR in solution and on-wire for SARS (A) and Norwalk (B) Armored RNA samples. On-wire amplification is slower than solution phase amplification, indicated by the higher C_T, and generates less amplicons, as shown by the lower plateau phase. A threshold level of 0.1 Delta Rn (background subtracted fluorescence intensity data shown in all amplification plots) was chosen to eliminate any contribution from the remaining background signal (visible here due to performing the log function on the slight fluorescent intensities still present).

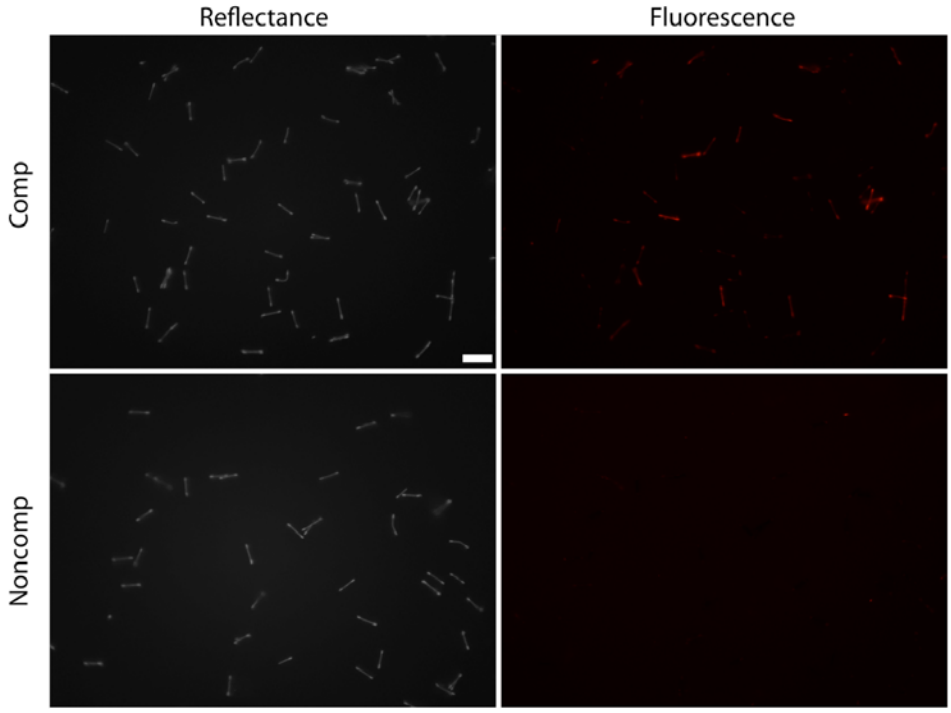

Figure 2-15. Images shown are of single-plexed on-wire PCR of Norwalk Armored RNA samples, where the reflectance images are used to identify the barcode pattern and thus the DNA sequence, and the fluorescence images are used to quantify wire-bound fluorescence due to amplification. Scale bar is 10 μm.

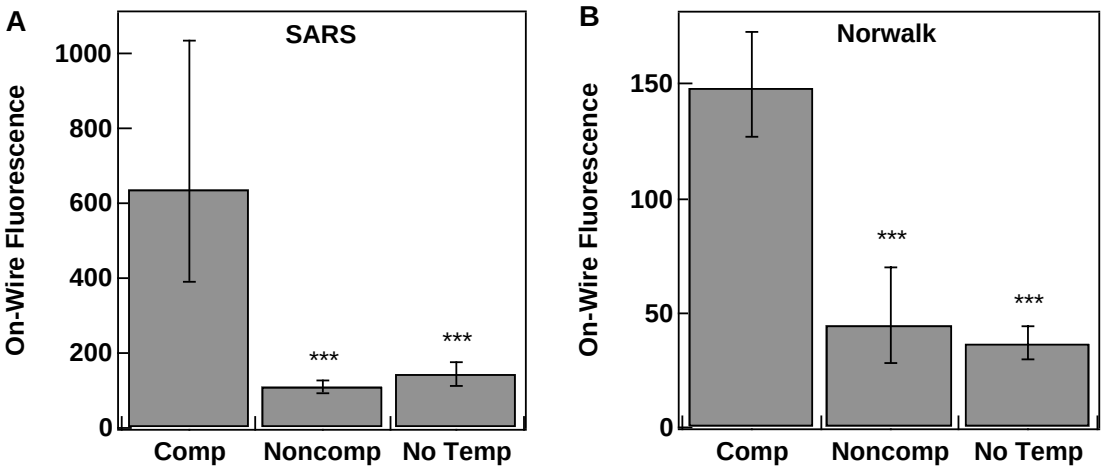

Figure 2-16. Bar graphs showing the on-wire fluorescence for single-plexed on-wire PCR samples quantified using the software NBSee for the complementary, noncomplementary, and no template samples for both SARS (A) and Norwalk (B) Armored RNA samples. *** p value < 0.001 verses fluorescence signal of complementary sample.

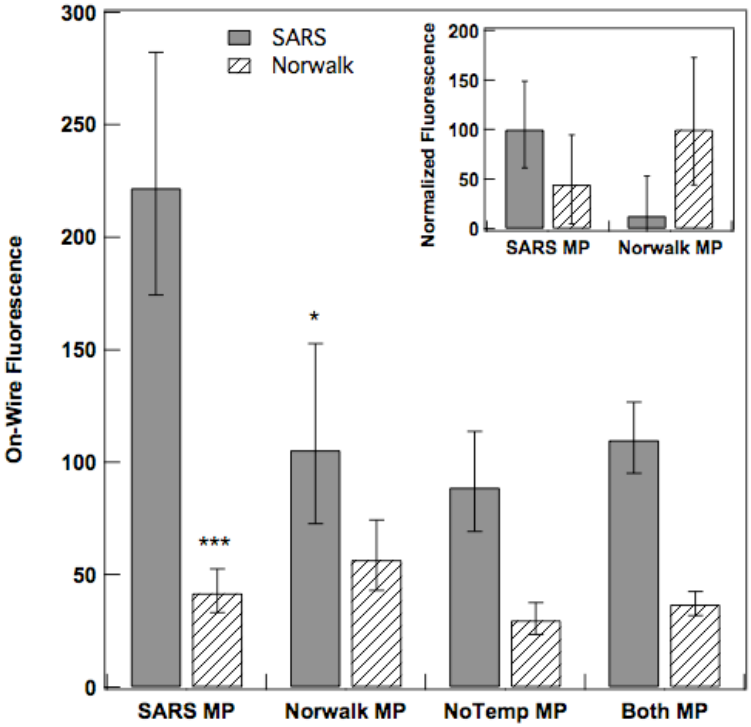

Figure 2-17. Quantified on-wire fluorescence data for multiplexed on-wire PCR using SARS and Norwalk Armored RNA. Inset shows background subtracted, normalized data. *** p value < 0.001, and * p value < 0.05, between signals generated from complementary and noncomplementary wire:probes within the same multiplexed sample.

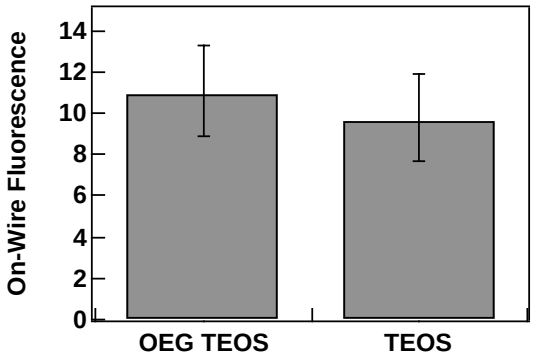

Figure 2-18. Background fluorescence signal generated when glass-coated wires were thermocycled in the presence of PCR Master Mix containing Sybr Green intercalating dye. Both the TEOS glass normally used and TEOS-OEG hybrid glass were tested; the fluorescence was similar between the two and did not account for the large background signal observed in on-wire PCR microscopy images. Glass-coated wires prepared by Stacey Dean.

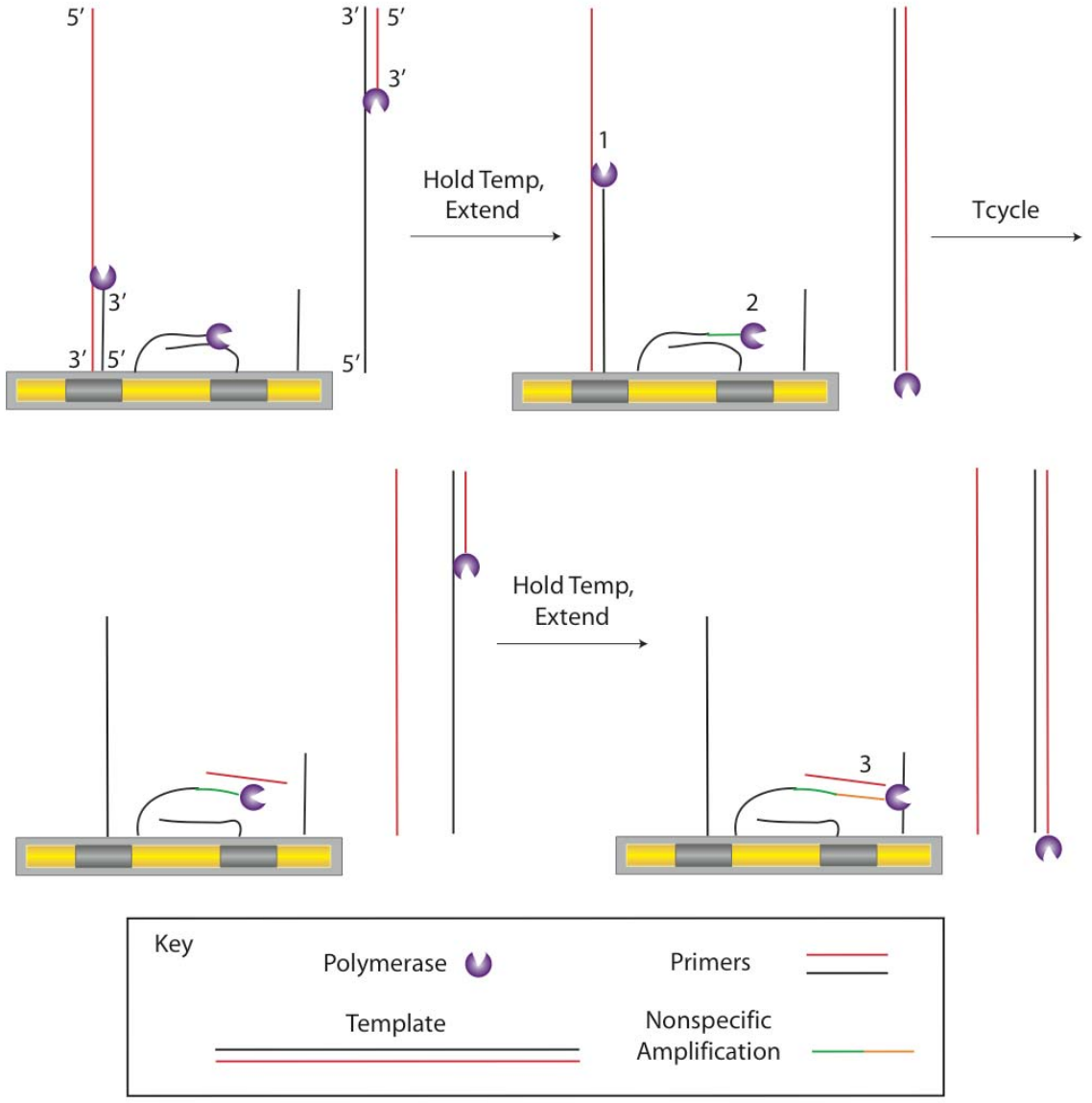

Figure 2-19. Scheme of possible non-ideal on-wire amplification morphologies, which may lead to the formation of a mat of nonspecific amplification products. Three possible undesired enzymatic products are shown here: 1) short amplicon generated by the enzyme dissociating from the hybridized DNA before reaching the end of the template, 2) primer dimer generated by the interaction of wire-bound primers, 3) subsequent amplicon that is not the same sequence of the original template generated by serial nonspecific hybridization events. The exponential amplification would increase the amount of nonspecific amplicon with each thermocycle.

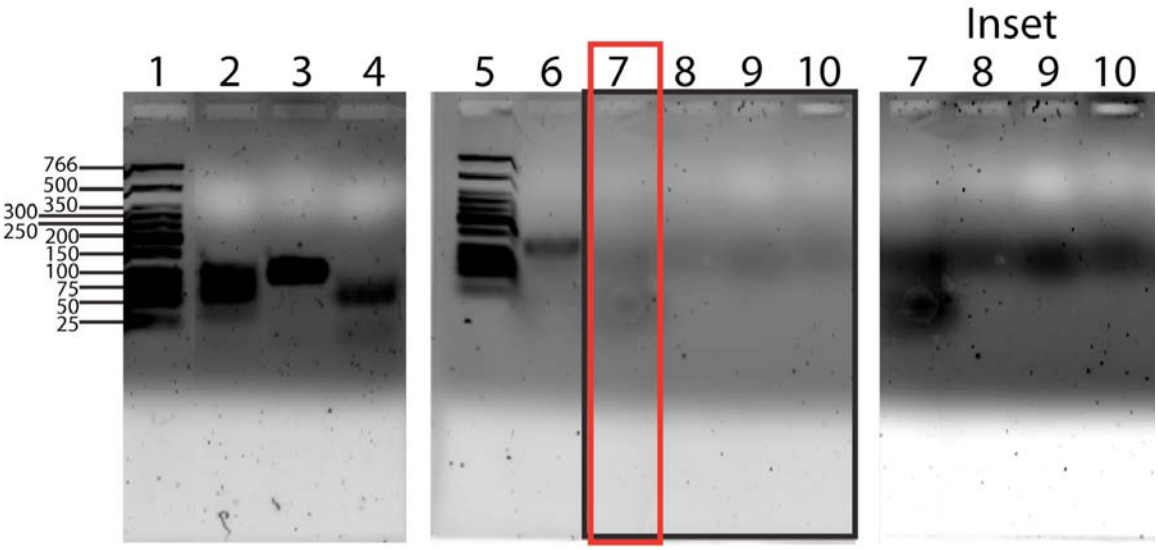

Figure 2-20. Photo of agarose gels taken with a phosphorimager. PCR product (both in solution and on-wire) were digested with the restriction enzyme *Dra I*. Gel electrophoresis was used to separate the enzymatic products in both the digested and undigested samples. The lanes contain these samples: 1) low molecular weight DNA ladder, 2) solution phase digested complementary PCR product, 3) solution phase undigested complementary PCR product, 4) solution phase digested noncomplementary PCR product, 5) low molecular weight DNA ladder, 6) solution phase undigested noncomplementary product, 7) on-wire digested complementary PCR product, and 8) on-wire undigested complementary PCR product, 9) on-wire digested noncomplementary PCR product (highlighted), 10) on-wire undigested noncomplementary product. Inset shows contrast enhanced bands for on-wire PCR samples lanes 7 through 10. Ladder bands (from the top) are: 766, 500, 350, 300, 250, 200, 150, 100, 75, 50, and 25 base pairs long. Digested halves of the amplicon are approximately 50 and 80 bases (end bound to wire) long, the amplicon is approximately 130 bases long, and primers are 17 bases long. Gel run with the assistance of Melissa Mullen.

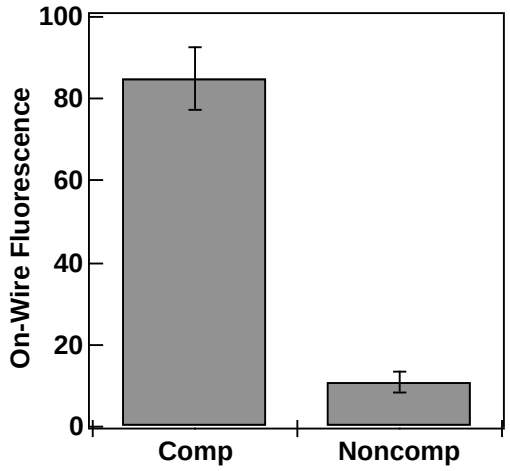

Figure 2-21. Enzymatic extension of thiolated oligonucleotides bound to metallic nanowires via gold thiol bonds. No thermocycling was performed, as this was a single step extension at 37 ^{o}C, which may be the cause for the increased specificity of the reaction. Data from Jihye Kim.

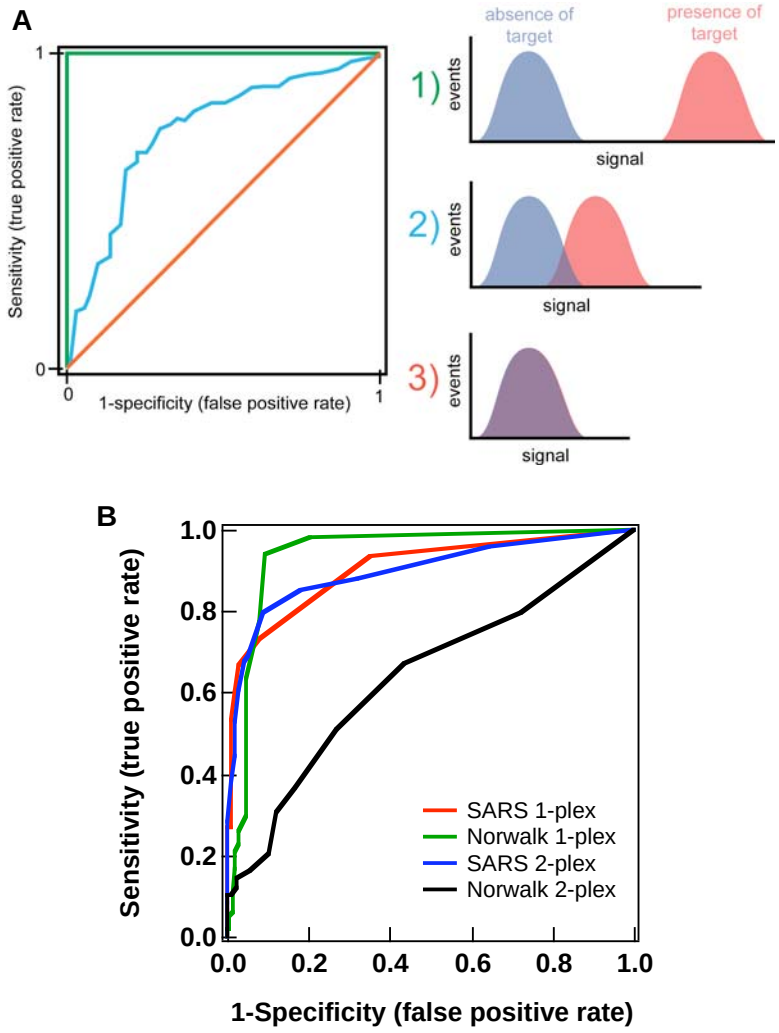

Figure 2-22. (A) Diagram of a Receiving Operating Characteristic curve illustrating examples of three different levels of discrimination between signal generated in the presence vs. absence of the target, where the first case of complete discrimination is represented by the green line in the ROC curve, the moderate level of discrimination the blue line, and the lack of discrimination the red line. A ROC curve showing complete discrimination between correct and false results will be composed of two straight lines, the first vertical along the y axis and the second horizontal along the value of 1 on the x axis, indicating a perfectly specific assay. (B) A ROC curve for the single- and multiplexed on-wire PCR fluorescence data shown previously in Figure B. The ROC curve shown here demonstrates the moderate specificity of the on-wire PCR assay. Figures plotted by Kristin Cederquist.

Chapter 3

Ligase Chain Reaction Performed on Barcoded Nanowire Surfaces for Pathogen Sequence Detection

Abstract

Ligase Chain Reaction (LCR) has been performed on nucleic acids bound to the surface of a barcoded nanowire for multiplexed pathogen sequence detection. The barcode pattern of the nanowire provides for template sequence identification and the exponential addition of fluorescently tagged sequences to nanowire-bound probes in the presence of a complementary template allows for quantifiable detection of template sequences. Several parameters, such as the ligase used and the enzyme concentration, were optimized to achieve improved amplification and reaction specificity. Probe strands designed for detection of four different respiratory virus sequences were attached to nanowires having a different striping pattern. One- and four-plexed on-wire LCR data using double stranded short oligonucleotide or longer (up to 200 bases long) templates is shown. Selectivity for 3 of the 4 sequences was very good, with a detection limit for the Swine Flu H1N1 sequence of 0.1 nM. The detection of longer templates resulted in decreased on-wire fluorescence, indicating less surface bound amplification.

Introduction

Ligase Chain Reaction (LCR) is an enzymatic chain reaction capable of amplifying the nucleic acids of pathogens present in a rapid fashion. LCR, when detecting for sickle cell anemia or human papillomavirus, has achieved routine detection at approximately the attomoles (~10^6

molecules) range, and achieved a limit of detection at approximately a few hundred molecules.[1] Ligases link together two adjacent DNA sequences, one with a 3' hydroxyl and the other with a 5' phosphate, hybridized to the same template, shown in Figure 3-1. Ligase Chain Reaction (LCR) exponentially increases the amount of template DNA present, as the product of one reaction cycle is used as the substrate in the next reaction cycle, much the same as in Polymerase Chain Reaction (PCR). Ligase *Detection* Reaction is also possible, where a linear amplification of template DNA is achieved, as only one side (the sense or antisense strand) is present in a form capable of ligation. Because respiratory pathogens are difficult to diagnose by symptoms alone, sequences of respiratory pathogens were used as templates in these studies, illustrating on-wire LCR's applicability in a clinical setting.

In a study performed by Winn-Deen et al., direct fluorescence measurements of LCR products that were captured post amplification on a microtitre plate were not sufficiently sensitive due to the detection limit of the plate reader (10 nM), and so enzyme immunoassays that were chromogenic, fluorogenic, or luminogenic were investigated to boost the detectable signal produced post LCR; this method also suffered from signal variations due to the plate properties.[2] Solution phase LCR products are most often directly detected by running radiolabeled DNA through gel electrophoresis,[3-5] or indirectly (after capturing the ligation product on a particle) by performing a sandwich immunoassay, which uses a secondary enzyme subsequently linked to the ligation product to generate its own detectable fluorescent product.[5-10] Fluorescence measurements have been recorded using a laser scanning sequencer, but this requires that the ligation products first be run through a sequencing gel;[2, 11] Southern blotting[12] and dedicated instrumentation such as capillary electrophoresis[13] have also been utilized for detection, but all three of these methods are time consuming and labor intensive.

There have been few publications on the use of enzymes for exponential amplification of nucleic acids when primer or probe sequences were immobilized to a surface. Most literature,

while stating that it is a surface phase reaction, instead captures the post enzymatic amplification product on a surface, but does not perform the amplification on bound nucleic acids, as is the case with the Abbott LCx system, where post LCR product is captured on the surface of a bead.[5-9, 14, 15] Most reported ligation reactions that are performed on a surface, whether it is a bead,[16-18] a quartz crystal microbalance,[19] an electrode,[20] or an array,[21-23] do not perform amplification reactions as there is no thermocycling involved. When thermocycling was incorporated, ligase detection reaction (LDR) was performed, generating a linear DNA amplification.[24] Alivisatos and coworkers performed LCR on nucleic acids bound to colloidal particles, but to our knowledge this has been the only mention of LCR on a surface performing exponential amplification, which was used for nanoarchitecture design and not detection purposes.[25] PCR has been combined with a ligation reaction for the detection of Single Nucleotide Polymorphisms (SNPs) using barcoded nanowires as surface substrates[26], however, the enzymatic chain reaction was not performed on the nanowires, which introduces the possibility of cross contamination.

The use of barcoded nanowires for sequence identification precludes the need for radiolabeled or differing fluorescently tagged sequences, differing amplicon (post amplification product) lengths, or the use of indirect quantification, as the nanowire pattern is used for identification, which increases the number of possible sequences detectable in one assay. When each nanowire pattern is functionalized with probes of a different sequence, multiplexing LCR is feasible (see Figure 3-2). To image the LCR product an optical microscope is all that is required, enabling clinical facilities that already possess microscopes, but do not possess to other instrumentation such as a fluorimeter or a capillary electrophoresis system to perform this assay.

Figure 3-2 shows the sandwich hybridization assay created when the oligonucleotide probe captures a template strand, and the template strand also captures a fluorescently tagged oligonucleotide (with a 5' phosphate). The adjacent probe and tag strands are covalently bound by the ligase, which results in the fluorescent tagging of the associated barcoded nanowire only in

the presence of sequence-specific template. As the opposite strand is present for ligation in solution, there is an exponential increase in fluorescently labeled barcoded nanowires specific for the pathogen sequence of interest. On-wire LCR has the same advantages of multiplexing and sequence identification as on-wire PCR, but has the added benefit that where the polymerase has to perform an enzymatic reaction for the addition of each base, the ligase has to perform only one enzymatic reaction to link the entire tag to the probe sequence. This decreases the overall number of required enzymatic reactions per nanowire and increases the specificity of the reaction, as three strands need to hybridize before ligase association and activity, as opposed to only two strands needed to hybridize before polymerase activity. On-wire LCR faces the same difficulty of increased steric hindrance over solution phase amplification that on-wire PCR faces, and optimization to overcome this issue is discussed, however, no evidence for the generation of a mat of DNA on the surface of the nanowire was seen when using ligases in place of polymerases.

We report here the use of on-wire LCR for the rapid, multiplexed detection of pathogens utilizing the enzymatic chain reaction amplification of oligonucleotides immobilized onto encoded particles, here barcoded nanowires, which are used for identification of nucleic acid sequences of interest.

Materials and Methods

Materials

Nanowires were either purchased from Oxonica Inc. or made in house as previously described.[27-34] Tetraethoxysilane (TEOS) was purchased from Gelest Inc. Aminopropyltrimethoxysilane (APTMS) was purchased from either Gelest Inc. or TCI. Water was purified to 18.2 MΩ using a Barnstead nanopure system and all water and buffer solutions

were autoclaved prior to used. Dithiothereitol (DTT) and buffer salts for phosphate buffered saline (PBS) and N-Cyclohexyl-2-aminoethanesulfonic acid (CHES) were purchased from Sigma Aldrich, and ammonium hydroxide was purchased from EMD. Sodium Chloride was purchased from VWR. Sulfosuccinimidyl-4-(N-maleimidomethyl)cyclohexane-1-carboxylate (Sulfo-SMCC) was purchased from Pierce Protein Research Products (Thermo Scientific). All DNA sequences were analyzed using Mfold software[35, 36] with the assistance of Kristin Cederquist and synthesized by Integrated DNA Technologies Inc. Ligases were purchased from New England Biolabs Inc. DNA sequences used in this work are listed in Tables 3-1 through 3-5.

Cleaving Thiolated DNA

A CentriSpin 10 column (Princeton Scientific) was vortexed for 15 seconds to remove air bubbles, then left to sit for 30 minutes after the addition of 650 μL H_2O. A 100 mM DTT solution was made and 50 μL of this was added to 50 μL of a 100 μM thiolated DNA solution. The mix was left to sit for at least 30 minutes. The spin column (with caps removed) was placed in a flat bottom wash tube and centrifuged for 2 minutes at 750 g. The bottom wash tube with the water was thrown away and the spin column was placed in a centrifuge tube. The DNA/DTT solution was placed on the column and the column was spun at 750 g for 2 minutes. The cleaved DNA was in the centrifuge tube and its concentration was determined by measuring its absorbance at 260 nm using a Hewlett-Packard 8453 diode-array UV Visible spectrophotometer.

Nanowire Coating

To glass coat nanowires, 300 μL nanowires were mixed with 160 μL water, 10 μL ammonium hydroxide, and 490 μL 200 proof ethanol (Pharmo-Aaper).[37] Nanowires were

sonicated to mix, then 40 μL Tetraethoxysilane was added and the solution was immediately sonicated (with water cooling) for one hour. Nanowires were rinsed once at 300 g for 30 seconds in ethanol, and then three times with 300 μL ethanol, spinning for 1 minute 7700 g. Nanowires were imaged using a Transmission Electron Microscopy (by myself, Jiyhe Kim, Stacey Dean, Ben Smith, or David Kirby) to ensure good glass coating. A JEOL JEM 1200 EXII TEM instrument was used with a high resolution Tietz F224 digital camera at an accelerating voltage of 80 kV.

To attach DNA to nanowires, 13.3 μL nanowires of one glass-coated barcode pattern were mixed with 26.6 μL ethanol and 4.4 μL APTMS, and vortexed for 30 minutes. They were rinsed 3 times with 44.4 μL ethanol and 3 times with CHES buffer (10 mM, pH 9.0). A solution of 1 mg Sulfo-SMCC in 400 μL CHES buffer was made. The nanowires were resuspended in 8.8 μL of CHES buffer and 8.8 μL Sulfo-SMCC solution was added; they were then vortexed for one hour. The nanowires were rinsed in 13.3 μL CHES buffer 3 times and PBS buffer (0.3 M NaCl, 10 mM phosphate, pH 7.0) 3 times. Thiolated, cleaved DNA was added to a final concentration of 1 μM, and the total volume was brought to 33.3 μL with PBS buffer; the nanowires were vortexed for 2 hours. The nanowires were then rinsed 3 times in 33.3 μL PBS buffer and transferred to a new PCR tube. They were placed in a Perkin Elmer Gene Amp PCR System 2400 thermocycler and heated to 95^{o}C for 10 minutes and then 25^{o}C for 10 minutes, and then rinsed in 33.3 μL H_2O. The nanowires were resuspended in 13.3 μL H_2O, transferred to a new PCR tube, and stored at 4^{o}C until the following morning. If required, these procedures were scaled up to accommodate more samples per experiment.

Ligase Detection and Chain Reaction

After coating nanowires with the oligonucleotide probe, 3.28 μL nanowire were mixed with 1 μL of 0.05 μM of each side of the complementary or noncomplementary oligonucleotide template (or water in no template samples). They were also mixed with 2.5 μL of 20 μM of the solution phase probe, and both the nanowire-bound (phosphorylated and fluorescently tagged) and solution phase (phosphorylated) tag oligonucleotides. When adding in the solution phase tags and probes in samples shown in Figures 3-3, 3-4, and 3-5, 2.5 μL of 0.2 μM solution phase oligonucleotides were used; when adding in solution phase tags to the samples shown in Figures 3-6, 3-7, 3-8, and 3-9 (performed after optimization), 2.5 μL of 0.002 μM were used. Ligase was added, 0.37 μL 9^{o}N. The solution was brought up to 50 μL with the Enzyme Reaction Buffer in Figures 3-3, 3-4, and 3-5; samples shown in Figures 3-6, 3-7, 3-8, and 3-9 had 5 μL Enzyme Reaction Buffer added and were brought to 50 μL with water. In LDR reactions, the solution phase probe, template, and tag were not added. The tubes were quick spun and then mixed with a pipetter; two 19 μL aliquots of each sample were placed in wells of a 96 well plate. All thermocycling of ligase samples was done on a Applied Biosystems 7300 Real Time thermocycler. The plate was thermocycled with an extended procedure of 30 cycles of 94^{o}C for 1 minute and 65^{o}C for 4 minutes. The samples shown in Figure 3-7 contained twice as much Swine wire tag as SARS wire tag, and were thermocycled for 30 cycles of 94 ^{o}C for 1 minute and 65 ^{o}C for 6 minutes. Nanowires were transferred to PCR tubes and rinsed once or twice with PBS before imaging. When increasing concentrations of certain parameters in order to increase fluorescence intensity, 10× enzyme or wire tag were used, and 2× nanowire:oligonucleotides were used.

Imaging Parameters

Nanowire samples were imaged on a Nikon inverted TE 300 microscope equipped with a Lambda LS Xenon 300 Watt light source coupled to a liquid light guide. A plan apo 60 × oil immersion objective (NA 1.4) was used. A reflectance cube with a half-silvered mirror paired with a 430/60 nm long pass filter was used to take reflectance images; a Lambda 10-2 optical filter changer (Sutter Instruments) controlled filter and shutter movement. A Cy 5 fluorescence cube (Chroma set number 41008) with excitation filter HQ620/60 nm, emission filter HQ700/75 nm, and dichroic 660 nm long pass, was used to take fluorescence images. Images were acquired with a 1500 ms exposure time using ImagePro 7.0 and captured on an HQ Coolsnap digital camera from Photometrics. Samples were prepared by first sonicating and mixing samples with a pipetter, then dropping 10 μL onto a cover slip, onto which a glass slide was placed. The software program NBSee was used to take linescans of nanowires and compile average fluorescence intensities for each nanowire pattern.

Results and Discussion

Several factors were important in the optimization of the on-wire LCR assay that are discussed below. These factors include: which ligase was used and its concentration, other reagent concentrations such as the fluorescently labeled tag DNA and the nanowire:probe conjugates, the ratio between the different DNA strands present in the reaction mixture, the thermocycling protocol, and the length of the template. After parameter optimization, both single-plexed and multiplexed on-wire LCR was performed, the data for which is analyzed below.

On-Wire Ligase Chain Reaction and Optimization

Initial reaction parameters were based on ligase reaction guidelines recommended by the manufacturer and modified in order to optimize them for use in on-wire ligase chain reaction, *i.e.* to overcome the detrimental steric hindrance without reducing the fidelity of the system. On-wire Ligase Chain Reaction (LCR) was performed using one of two enzymes: Taq or 9^{o} N ligase, as they are very thermostable and were recommended for use in thermocycling. While neither enzyme generated extremely specific amplification, the 9^{o} N ligase performed better on-wire, generating more fluorescence signal, which was interpreted as increased surface-bound amplification product in the presence of the complementary template, as shown in Figure 3-3. This may be due to the fact that Taq enzyme requires a higher salt concentration than the 9^{o} N ligase, which is not as ideal in the on-wire system. Fluorescence intensity was found to be statistically significant (* p value < 0.05) for the on-wire fluorescence signal in the presence of the complementary template versus the signal in the presence of the noncomplementary or the lack of template samples when either Taq or 9^{o} N was used; because of the increased amplification produced with 9^{o} N than Taq, this ligase was chosen for all future LCR optimization experiments.

On-wire LCR was optimized by altering the concentrations of several reagents in the reaction. In on-wire LCR the nanowire-bound probe is ligated to the fluorescent tag when the complementary template hybridizes, bringing the probe and tag in close proximity for ligase activity. Complementary sequences are also present in solution, where a probe and (nonfluorescent) tag are present in solution and are ligated after template hybridization and enzymatic activity. The resulting ligated sequence can act as a template in the on-wire ligation, creating an exponential amplification, but may also act as a competing enzymatic substrate as it is more sterically favorable than the nanowire-bound substrate. The ratio between the nanowire-

bound sequences and the solution phase sequences is one aspect of the on-wire LCR that was optimized in order to balance conditions that were favorable for the enzyme as well as the surface-bound nucleic acids.

Figure 3-4 shows the result of adding into solution 1 μM (a common concentration used in solution phase LCR) of either: the solution phase probe sequence, or both the solution phase and the nanowire-immobilized probe sequences for SARS. The graph shows on-wire fluorescence when solution phase probes and tags (complementary to nanowire-bound probes and tags—the green and blue strands in Figure 3-2) were added to LCR reactions; the resulting ligated strand acted as a template in the on-wire LCR, providing for exponential amplification. The graph also shows on-wire fluorescence when strands both complementary to, and the same sequence as (the orange and purple strands in Figure 3-2), the nanowire probes and tags were added into solution; the solution phase strands compete with nanowire-bound strands for enzymatic activity, decreasing the overall complementary on-wire ligation. The samples with only the solution phase probe sequence in solution maximized on-wire enzymatic amplification and showed vastly better specificity in on-wire microscopy. A range of concentrations of the solution phase SARS probe and tag oligonucleotides was also investigated in the LCR assay (data not shown). A final solution phase probe and tag concentration of 0.1 nM was gave the most overall amplification and the best discrimination between samples containing complementary or no templates (and performed better than LDR), and was used in future experiments.

In addition to altering the solution phase probe concentration, the nanowire:probe conjugate, the fluorescently labeled wire tag oligonucleotide, and the enzyme concentrations were also altered in the LCR assay detecting SARS template. Figure 3-3 shows the use of a 2× nanowire:probe concentration, and 10× wire tag and enzyme concentrations (in comparison with 1× concentrations of all three reagents, shown in Figure 3-4). The 2× wire:probe conjugate

concentration provided the opportunity for more overall ligation reactions without allocating so large a percentage of the volume available to particles that they would create a large pellet. A 10× enzyme concentration was chosen in order to increase the amount of enzyme available to ligate the nanowire-bound oligonucleotide (and therefore the occurrence of ligation), but not to increase it to the point of generating nonspecific amplification. The amount of wire tag available was also increased to drive the ligation reaction but not so much that it would drive incorrect reactions. Increasing the concentration of nanowire:probes and wire tag both decreased the specificity of the assay. The increase of the enzyme concentration resulted in an increase in specificity from 27 (Figure 3-4) to 32 times more fluorescence for complementary than for no template samples. Due to these findings, a range of enzyme concentrations was investigated, the results of which are shown in Figure 3-6. The 1× enzyme concentration represents the concentration recommended by the manufacturer for solution phase LCR assays. The 10× enzyme concentration gave the most specific microscopy results for the detection of SARS (and performed better than a Sandwich Hybridization Assay—SHA) and was used for all future experiments.

Thermocycling parameters were also examined to ensure ample time for enzymatic activity on-wire without allowing for nonspecific activity. The extension time was increased to as much as 8 minutes per cycle, the number of cycles ranged from 15 to 30, and the extension temperatures of 45 and 65 ^{o}C were tested. An optimal thermocycling protocol of 20 cycles of 94 ^{o}C for 1 minute and 65 ^{o}C for 6 minutes (a total thermocycling protocol time of approximately 3 hours) was found to yield the most ligation and the most specific ligation on-wire, as indicated by on-wire microscopy results after rinsing (where imaging each sample took approximately 15 minutes). The on-wire fluorescence results for an LCR assay utilizing this thermocycling protocol are shown in Figures 3-7, 3-8, and 3-9.

Single- and Multi-plexed LCR On-Wire

Microscopy images from single-plexed on-wire LCR samples generated using synthetic oligonucleotide templates of SARS and Swine Flu H1N1 are shown in Figure 3-7. In the single-plex samples, nanowire:probes were exposed to complementary, noncomplementary, and no template, each in an individual sample tube. In the corresponding multiplexed samples, multiple nanowire:probes conjugates—each with their own barcode pattern and bound nucleic acid sequence (SARS—0011111111, and Swine Flu H1N1—0000001010, where 0 is gold and 1 is silver), were exposed to template sequence(s) complementary to one, none, or both of the probes bound to the wires in solution. The graphs in Figure 3-8 represent fluorescence intensity measured on-wire, which for multiplexed samples was background subtracted and normalized (where the signal from the sample without template is subtracted out and the fluorescence values are normalized to the complementary intensity). Significant discrimination between complementary and noncomplementary samples is seen (*** p values < 0.001) for both single- and multi-plexed samples. This is a general improvement over the multiplexed on-wire PCR, indicating that on-wire LCR is more specific.

A Receiving Operating Characteristic (ROC) curve can be used to discriminate actual positive and negative results from false positive and negative results determined by an assay.[38, 39] The diagram shown in Figure 3-9 illustrates examples of three different levels of discrimination between signal generated in the presence vs. absence of the target, where the first case of complete discrimination is represented by the green line in the ROC curve, the moderate level of discrimination the blue line, and the lack of discrimination the red line. A ROC curve showing complete discrimination between correct and false results will be composed of two straight lines, the first vertical along the y axis and the second horizontal along the value of 1 on the x axis, indicating a perfectly specific assay and a complete lack of overlap between signal in the

presence vs. signal in the absence of the target. A ROC curve was generated using the on-wire fluorescence intensities of the single- and multiplexed samples shown in Figure 3-8. The curve shown in Figure 3-9 is very close to the model of complete discrimination between true and false positives and negatives, confirming the specificity of the on-wire LCR assay. The percentage of the area under the curve can be used to quantitatively compare the accuracy of differing assays. For single-plexed LCR samples, SARS wire:probes generated an area of 100 %, while Swine Flu H1N1 wire:probes generated an area of 98 %. For multiplexed LCR samples, the area under the curve when exposing nanowire:probes to SARS template was 94 %, while the area under the curve when exposing nanowire:probes to Swine Flu H1N1 template was 91 %. This indicates a small decrease in accuracy for the on-wire LCR assay when moving from single- to multi-plexed assays, but this is an improvement over the accuracy for on-wire PCR, where single-plexed samples generated areas of 90 % and 93 %, and where multiplexed samples generated areas of 89 % and 64 % for SARS and Norwalk Virus, respectively. This is most likely due to the need for 3 strands to hybridize before enzymatic association and activity in LCR (as opposed to only 2 in PCR), as well as the need for only one enzymatic reaction per bound oligonucleotide, reducing the likelihood of nucleic acid mat formation on the nanowire surface when using a ligase.

Single- and multi-plexed LCR was also performed with ultramer templates, synthetic sequences of up to 200 bases in length. While the steric hindrance was increased when using ultramer templates, as opposed to oligonucleotide templates, specific amplification was still seen in both single- and multi-plexed LCR samples, as shown in the fluorescence quantification in Figure 3-10, and the images and their quantification in Figures 3-11 and 3-12, respectively. Single-plexed samples comparing LCR performed with complementary versus noncomplementary templates for sequences of SARS, Swine Flu H1N1, RSV A, and RSV B were found to be statistically significant (*** p values < 0.001). Multiplexed samples were also tested using all of the sequences listed. Analyzing the raw data resulted in p values < 0.001 for

all four sequences permutations of all three combinations of signal comparisons. These include comparing nanowire:probes exposed to complementary template, to signal from either other nanowire:probes exposed to the same template within the same sample or the same nanowire:probes exposed to different templates in other multiplexed samples, as well as the same nanowire:probes exposed to no template in a separate multiplexed sample. The only exception was a less significant p value of < 0.05 generated when comparing the complementary RSV A signal to the noncomplementary Swine Flu H1N1 signal in the same multiplexed sample. This may be due to undesirable association of the Swine Flu H1N1 wire tag sequence with the RSV A template sequence hybridized to the nanowire-bound RSV A probe strand, which could be reduced in the future by optimizing the design of the Swine Flu H1N1 wire probe to reduce interactions with the noncomplementary RSV A template. Background subtracted, normalized signals for the multiplexed samples are also shown in Figure 3-12, and more clearly show the difference between complementary and noncomplementary samples. LCR has been shown here to specifically detect oligonucleotides and ultramers of pathogen sequences in a multiplexed format and shows promise for future assays.

Serial dilutions of the Swine Flu H1N1 ultramer template were tested in a multiplexed LCR assay also containing nanowire:probes for SARS (for generation of a noncomplementary signal), shown in Figure 3-13. The p values for samples with template concentrations of 1 nM and 0.1 nM were both < 0.001. The confidence levels that the signals were statistically different drop off relatively quickly after those samples, however, to non-significant values. This is most likely due to the sterics of the enzyme association to the sandwich hybridization occurring between the DNA strands on the surface of the nanowire inhibiting ligation of template strands present in low concentrations.[40] The sensitivity of the reaction was therefore 0.1 nM, which is significantly less sensitive than solution phase LCR that has a routine detection limit at the attomolar range,[1] however, the sensitivity of other bead or array based ligation assays ranges from

nanomolar to attomolar detection,[16, 18, 19, 21] most likely due to the use of pre- or post-ligation amplification steps to achieve lower limits of detection. There is room for future optimization of the on-wire LCR system in order to increase the sensitivity of the LCR reaction, perhaps by increasing the probability of ligase association to nanowire-bound oligonucleotides, which may be accomplished by altering parameters such as probe surface coverage, or use of an oligo ethylene glycol linker instead of DNA bases between the thiolated end of the probe and the segment of sequence that hybridizes to the template.[40] The detection limit when using oligonucleotides as opposed to longer synthetic sequences will most likely improve, as the steric hindrance is reduced. While altering parameters such as these did not assist in on-wire amplification performed by polymerases, this may be due to the enzyme-specific interaction with the bound oligonucleotides in the generation of a mat of DNA on the surface, which can be circumvented with the use of ligases for DNA amplification.

Conclusions and Future Directions

On-wire multiplexed LCR using oligonucleotide or ultramer templates has been reproducibly performed and found to be specific. The increase of ligation enzyme concentration and the addition of the solution phase probe and tag strands increased the fluorescence intensity generated on-wire and the specificity of the amplification. An optimal concentration of the solution phase probe and tag was found to be 0.1 nM, and the optimal concentration of the ligase was found to be 10 ×. 9^{o} N was determined to be the best ligase for on-wire LCR and optimized thermocycling conditions for this system were determined. ROC curves were generated, which confirmed the specificity of the on-wire LCR in single and multiplexed environments. Up to four templates were analyzed simultaneously in multiplexed experiments and serial dilutions of the template in multiplexed experiments were performed. There has been very limited use of Ligase

Chain Reaction coupled with any surface;[5-9, 14, 25] this demonstrates the first known use of multiplexed LCR performed with a surface bound oligonucleotide probe. In the future, analysis of clinical samples may be performed; this will be discussed in the future directions section at the end of the dissertation. In short, successfully performing an enzymatic amplification reaction such as LCR on oligonucleotides bound to the surface of an encoded particle has great promise in the detection of multiple different types of pathogens at concentrations lower than currently can be detected without labor intensive and lengthy processing.

References

1. Barany, F. The ligase chain reaction in a PCR world. *Genome Res.* **1991**, *1*, 5-16.

2. Winn-Deen, E. S.; Batt, C. A.; Wiedmann, M. Non-radioactive detection of *Mycobacterium tuberculosis* LCR products in a microtitre plate format. *Mol. Cell. Probes* **1993**, *7* (3), 179-186.

3. Barany, F. Genetic disease detection and DNA amplification using cloned thermostable ligase. *Proc. Natl. Acad. Sci. USA.* **1991**, *88*, 189-193.

4. Dong, S. M.; Traverso, G.; Johnson, C.; Geng, L.; Favis, R.; Boynton, K.; Hibi, K.; Goodman, S. N.; D'Allessio, M.; Paty, P.; Hamilton, S. R.; Sidransky, D.; Barany, F.; Levin, B.; Shuber, A.; Kinzler, K. W.; Vogelstein, B.; Jen, J. Detecting colorectal cancer in stool with the use of multiple genetic targets. *J. National Cancer Institute.* **2001**, *93 (11)*, 858-865.

5. Abravaya, K.; Carrino, J. J.; Muldoon, S.; Lee, H. H. Detection of point mutations with a modified ligase chain reaction (Gap-LCR). *Nucleic Acids Res.* **1995**, *23 (4)*, 675-682.

6. Piersimoni, C.; Callegaro, A.; Scarparo, C.; Penati, V.; Nista, D.; Bornigia, S.; Lacchini, C.; Scagnelli, M.; Santini, G.; De Sio, G. Comparative evaluation of the new gen-probe *Mycobacterium tuberculosis* amplified direct test and the semiautomated Abbott LCx *Mycobacterium tuberculosis* assay for direct detection of *Mycobacterium tuberculosis* complex in respiratory and extrapulmonary specimens. *J. Clin. Microbiol.* **1998**, *36* (12), 3601-3604.

7. Tortoli, E.; Lavinia, F.; Simonetti, M. T. Evaluation of a commercial Ligase Chain Reaction kit (Abbott LCx) for direct detection of *Mycobacterium tuberculosis* in pulmonary and extrapulmonary specimens. *J. Clin. Microbiol.* **1997**, *35 (9)*, 2424-2426.

8. Puolakkainen, M.; Hiltunen-Back, E.; Reunala, T.; Suhonen, S.; Lähteenmaki, P.; Lehtinen, M.; Paavonen, J. Comparison of performances of two commercially available tests, a PCR assay and a ligase chain reaction test, in detection of urogenital *Chlamydia trachomatis* infection. *J. Clin. Microbiol.* **1998**, *36* (6), 1489-1493.

9. Moore, D. F.; Curry, J. I. Detection and identification of *Mycobacterium tuberculosis* directly from sputum sediments by ligase chain reaction. *J. Clin. Microbiol.* **1998**, *36* (4), 1028-1031.

10. Fiore, M; Mitchell, J.; Doan, T.; Nelson, R.; Winter, G.; Grandone, C.; Zeng, K.; Haraden, R.; Smith, J.; Harris, K.; Leszczynski, J.; Berry, D.; Safford, S.; Barnes, G.; Schoinick, A.; Ludington, K. The Abbott IMx™ automated benchtop immunochemistry analyzer system. *Clin. Chem.* **1988**, *34* (9), 1726-1732.

11. Landegren, U.; Kaiser, R.; Sanders, J.; Hood, L. A ligase-mediated gene detection technique. *Science* **1988**, *241* (4869), 1077-1080.

12. Kälin, I.; Shephard, S.; Candrian, U. Evaluation of the ligase chain reaction (LCR) for the detection of point mutations. *Mut. Res. Lett.* **1992**, *283* (2), 119-123.

13. Cheng, J.; Shoffner, M. A.; Mitchelson, K. R.; Kricka, L. J.; Wilding, P. Analysis of ligase chain reaction products amplified in a silicon-glass chip using capillary electrophoresis. *J. Chromatogr. A* **1996**, *732* (1), 151-158.

14. Dean, D.; Ferrero, D.; McCarthy, M. Comparison of performance and cost-effectiveness of direct fluorescent-antibody, ligase chain reaction, and PCR assays for verification of chlamydial enzyme immunoassay results for populations with a low to moderate prevalence of *Chlamydia trachomatis* infection. *J. Clin. Microbiol.* **1998**, *36* (1), 94-99.

15. Wang, H.; Li, J.; Wang, Y.; Jin, J.; Yang, R.; Wang, K.; Tan, W. Combination of DNA ligase reaction and gold nanoparticle-quenched fluorescent oligonucleotides: A simple and efficient approach for fluorescent assaying of single-nucleotide polymorphisms. *Anal. Chem.*, in press. DOI: 10.1021/ac101503t

16. Skobeltsyna, L. M.; Pyshnyi, D. V.; Shishkina, I. G.; Tabatadze, D. R.; Dymshits, G. M.; Zarytova, V. F.; Ivanova, E. M. Development of a colorimetric test system for detection of point mutations via ligation of a tandem of short oligonucleotides on methacrylate beads. *Molecular Biology* **2000**, *34* (3), 321-327.

17. Pyshnyi, D. V.; Skobeltsyna, L. M.; Gushchina, E. N.; Pyshnaya, I. A.; Shishkina, I. G.; Dymshits, G. M.; Zarytova, V. F.; Ivanova, E. M. Detection of single-base substitutions in amplified fragments via ligation of a tandem of short oligonucleotides in solution and on a solid carrier. *Molecular Biology* **2000**, *34* (6), 840-851.

18. Li, J.; Zhong, W. Typing of multiple single-nucleotide polymorphisms by a microsphere-based rolling circle amplification assay. *Anal. Chem.* **2007**, *79* (23), 9030-9038.

19. Pang, L.; Li, J.; Jiang, J.; Shen, G.; Yu, R. DNA point mutation detection based on DNA ligase reaction and nano-Au amplification: A piezoelectric approach. *Anal. Biochem.* **2006**, *358* (1), 99-103.

20. Wan, Y.; Lao, R.; Liu, G.; Song, S.; Wang, L.; Li, D.; Fan, C. Multiplexed electrochemical DNA sensor for single-nucleotide polymorphism typing by using oligonucleotide-incorporated nonfouling surfaces. *J. Phys. Chem. B* **2010**, *114* (19), 6703-6706.

21. Zhong, X.-B.; Reynolds, R.; Kidd, J. R.; Kidd, K. K.; Jenison, R.; Marlar, R. A.; Ward, D. C. Single-nucleotide polymorphism genotyping on optical thin-film biosensor chips. *Proc. Natl. Acad. Soc. USA* **2003**, *100* (20), 11559-11564.

22. Deng, J.-Y.; Zhang, X.-E.; Mang, Y.; Zhang, Z.-P.; Zhou, Y.-F.; Liu, Q.; Lu, H.-B.; Fu, Z.-J. Oligonucleotide ligation assay-based DNA chip for multiplex detection of single nucleotide polymorphism. *Biosen. Bioelectron.* **2004**, *19* (10), 1277-1283.

23. Kashkin, K. N.; Strizhkov, B. N.; Gryadunov, D. A.; Surzhikov, S. A.; Grechishnikova, I. V.; Kreindlin, E. Ya.; Chupeeva, V. V.; Evseev, K. B.; Turygin, A. Yu.; Mirzabekov, A. D.

Detection of single-nucleotide polymorphisms in the p53 gene by LDR/RCA in hydrogel microarrays. *Molecular Biology* **2005**, *39* (1), 30-39.

24. Mikhailovich, V.; Lapa, S.; Gryadunov, D.; Sobolev, A.; Strizhkov, B.; Chernyh, N.; Skotnikova, O.; Irtuganova, O.; Moroz, A.; Litvinov, V.; Vladimirskii, M.; Perelman, M.; Chernousova, L.; Erokhin, V.; Zasedatelev, A.; Mirzabekov, A. Identification of Rifampin-resistant *Mycobacterium tuberculosis* strains by hybridization, PCR, and ligase detection reaction on oligonucleotide microchips. *J. Clin. Microbiol.* **2001**, *39* (7), 2531-2540.

25. Claridge, S. A.; Mastroianni, A. J.; Au, Y. B.; Liang, H. W.; Micheel, C. M.; Fréchet, J. M. J.; Alivisatos, A. P. Enzymatic ligation creates discrete multinanoparticle building blocks for self-assembly. *J. Am. Chem. Soc.* **2008**, *130 (29)*, 9598-9605.

26. Sha, M. Y.; Walton, I. D.; Norton, S. M.; Taylor, M.; Yamanaka, M.; Natan, M. J.; Xu, C.; Drmanac, S.; Huang, S.; Borcherding, A.; Drmanac, R.; Penn, S. G. Multiplexed SNP genotyping using nanobarcode particle technology. *Anal. Bioanal. Chem.* **2006**, *384*, 658-666.

27. Martin, C.R. Membrane-based synthesis of nanomaterials. *Chem. Mater.* **1996**, *8* (8), 1739-1746.

28. Martin, C.R. Nanomaterials: a membrane-based synthetic approach. *Science **1994**, 266* (5193), 1961-1966.

29. Al-Mawalawi, D.; Liu, C. Z.; Moskovits, M. Nanowires formed in anodic oxide nanotemplates. *J. Mater. Res.* **1994**, *9* (4), 1014-1018.

30. True, R. J.; Taylor, M. K.; Chakarova, G. S.; Walton, I. D. Microfabricated templates for the electrodeposition of metallic barcodes for use in multiplexed bioassays. Proceedings of the 26th Annual Conference of the IEEE EMBS. San Francisco, USA, 2004.

31. Nicewarner-Peña, S. R.; Freeman, R. G.; Reiss, B. D.; He, L.; Peña D. J.; Walton, I. D.; Cromer, R.; Keating, C. D.; Natan, M. J. Submicrometer metallic barcodes. *Science* **2001**, *294* (5540), 137-141.

32. Keating, C. D.; Natan, M. J. Striped metal nanowires as building blocks and optical tags. *Adv. Mater.* **2003**, *15* (5), 451-454.

33. Walton, I. D.; Norton, S. M.; Balasingham, A.; He, L.; Oviso, D. F., Jr.; Gupta, D.; Raju, P. A.; Natan, M. J.; Freeman, R. G. Particles for multiplexed analysis in solution: detection and identification of striped metallic particles using optical microscopy. *Anal. Chem.* **2002**, *74* (10), 2240-2247.

34. Reiss, B. D.; Freeman, R. G.; Walton, I. D.; Norton, S. M.; Smith, P. C.; Stonas, W. G.; Keating, C. D.; Natan, M. J. Electrochemical synthesis and optical readout of striped metal rods with submicron features. *J. Electroanal. Chem.* **2002**, *522* (1), 95-103.

35. Zuker, M. Mfold web server for nucleic acid folding and hybridization prediction. *Nucleic Acids Res.* **2003**, *31* (13), 3406-3415.

36. Markham, N. R.; Zuker, M. DINAMelt web server for nucleic acid melting prediction. *Nucleic Acids Res.* **2005**, *33* (web server issue), w577-w581.

37. Sioss, J. A.; Stoermer, R.L.; Sha, M.Y.; Keating, C.D. Silica coated, Au/Ag striped nanowires for bioanalysis. *Langmuir* **2007**, *23* (22), 11334-11341.

38. Zweig, M. H.; Campbell, G. Receiver-operating characteristic (ROC) plots: A fundamental evaluation tool in clinical medicine. *Clin. Chem.* **1993**, *39* (4), 561-577.

39. Greiner, M.; Pfeiffer, D.; Smith, R. D. Principles and practical application of the receiver-operating characteristic analysis for diagnostic tests. *Prev. Vet. Med.* **2000**, *45* (1-2), 23-41.

40. Carmon, A.; Vision, T. J.; Mitchell, S. E.; Thannhauser, T. W.; Müller, U.; Kresovich, S. Solid-phase PCR in microwells: Effects of linker length and composition on tethering, hybridization, and extension. *Biotechniques* **2002**, *32* (2), 410-420.

41. Gunson, R. N.; Collins, T. C.; Carman, W. F. Real-time RT-PCR detection of 12 respiratory viral infections in four triplex reactions. *J. Clin. Virology* **2005**, *33* (4), 341-344.

42. *CDC protocol of real time RTPCR for swine influenza A(H1N1)*; CDC Reference #I-007-05; WHO Collaborating Center: Atlanta, GA, October 6, 2009; 1-8.

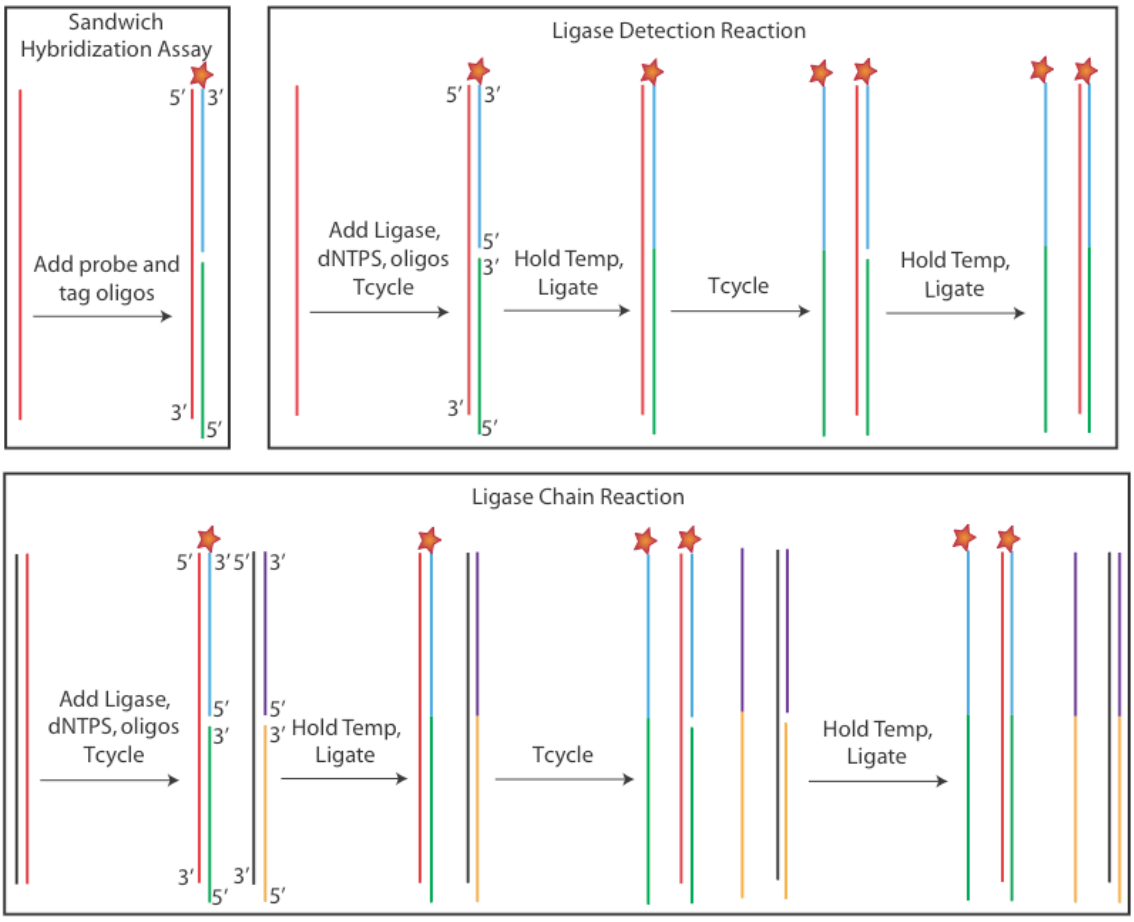

Figure 3-1. Representation of solution phase sandwich hybridization assay, ligase detection reaction, and ligase chain reaction. The red and black lines represent the sense and antisense strands of the template, the green and orange lines represent probe strands, and the blue and purple lines represent tag strands that have 5' phosphate groups. Ligase detection reaction amplification is linear, and ligase chain reaction amplification is exponential.

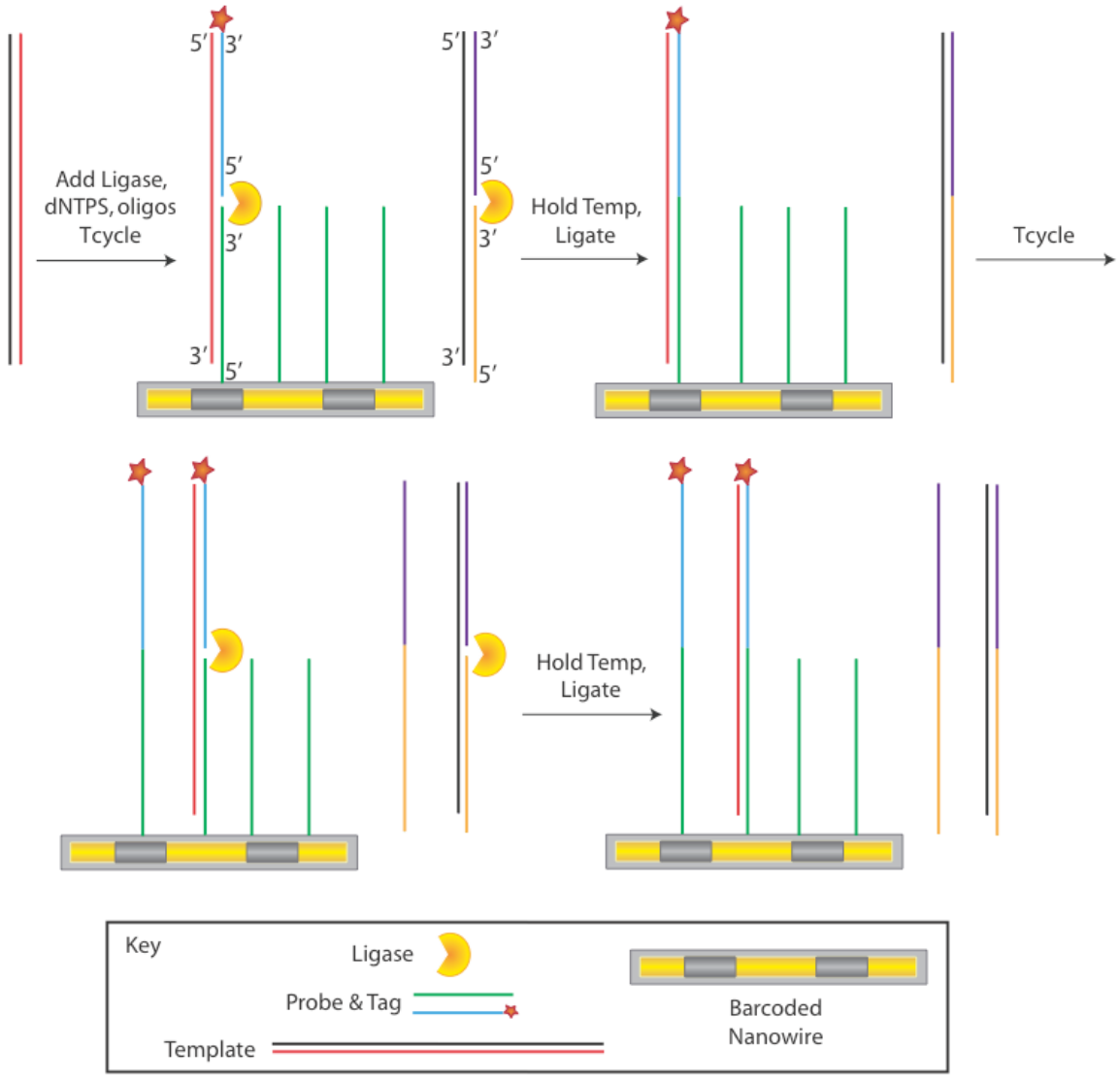

Figure 3-2. On-wire Ligase Chain Reaction, where each barcode pattern is paired with a probe oligonucleotide of a pathogen-specific sequence. The green and blue lines represent the wire bound strands and the orange and purple lines represent the strands in the solution of the reaction mix.

Table 3-1: RSV A Sequences used in LCR[A]

Name	Sequence (5′ to 3′)	Comments
RSVA Soln Tag	Phos – GAT AGT ATT GAT ACT CCT AAT TAT GAT GTG CAG AA	Ligated to soln probe
RSVA Soln Probe	CAT CCA ACG GAG CAC AGG A	
RSVA Wire Tag	Phos – TCC TGT GCT CCG TTG GAT G – Alexa 647	Ligated to wire probe
RSVA Wire Probe	Thiol – taa cat tTT CTG CAC ATC ATA ATT AGG AGT ATC AAT ACT ATC	Bound to wire
RSVA Oligonucleotide Template	CAT CCA ACG GAG CAC AGG AGA TAG TAT TGA TAC TCC TAA TTA TGA TGT GCA GAA	Comp to wire probe and tag
RSVA Oligonucleotide Complement Template	TTC TGC ACA TCA TAA TTA GGA GTA TCA ATA CTA TCT CCT GTG CTC CGT TGG ATG	Comp to soln probe and tag
RSVA Ultramer Template	*AGA TCA ACT TCT GTC ATC CAG CAA* ATA CAC CAT CCA ACG GAG CAC AGG AGA TAG TAT TGA TAC *TCC TAA TTA TGA TGT GCA GAA*	Comp to wire probe and tag
RSVA Ultramer Complement Template	*TTC TGC ACA TCA TAA TTA GGA G*TA TCA ATA CTA TCT CCT GTG CTC CGT TGG ATG GTG TAT *TTG CTG GAT GAC AGA AGT TGA TCT*	Comp to soln probe and tag

[A] RSV A sequences code for respiratory syncytial virus A, Accession number X00001.1, adapted from reference 41. Lower case letters indicate bases used as spacers, which are not part of the hybridized sequence. Italicized letters indicate primer binding regions. Complementarity between probe & tag strands and the corresponding oligonucleotide or ultramer template are indicated by the same font color. Phos abbreviation symbolizes phosphate functionality, thiol abbreviation symbolizes thiol functionality. Alexa 647 symbolizes fluorescently tagged strand.

Table 3-2: RSV B Sequences used in LCR[A]

Name	Sequence (5′ to 3′)	Comments
RSVB Soln Tag	Phos – AGA CAC TAT AAA GAT ACT TAA AGA TGC TGG ATA TCA	Ligated to soln probe
RSVB Soln Probe	GCT ATG TCC AGG TTA GGA AGG GA	
RSVB Wire Tag	Phos – TCC CTT CCT AAC CTG GAC ATA GC– Alexa 647	Ligated to wire probe
RSVB Wire Probe	Thiol – taa cat tTG ATA TCC AGC ATC TTT AAG TAT CTT TAT AGT GTC T	Bound to wire
RSVB Oligonucleotide Template	GCT ATG TCC AGG TTA GGA AGG GAA GAC ACT ATA AAG ATA CTT AAA GAT GCT GGA TAT CA	Comp to wire probe and tag
RSVB Oligonucleotide Complement Template	TGA TAT CCA GCA TCT TTA AGT ATC TTT ATA GTG TCT TCC CTT CCT AAC CTG GAC ATA GC	Comp to soln probe and tag
RSVB Ultramer Template	*AAG ATG CAA ATC ATA AAT TCA CAG GAT TAA TAG GTA* TGT TAT ATG CTA TGT CCA GGT TAG GAA GGG AAG ACA CTA TAA AGA *TAC TTA AAG ATG CTG GAT ATC A*	Comp to wire probe and tag
RSVB Ultramer Complement Template	*TGA TAT CCA GCA TCT TTA AGT A*TC TTT ATA GTG TCT TCC CTT CCT AAC CTG GAC ATA GCA TAT AAC A*TA CCT ATT AAT CCT GTG AAT TTA TGA TTT GCA TCT T*	Comp to soln probe and tag

[A] RSV B sequences code for respiratory syncytial virus B, Accession number DQ780569.1, adapted from reference 41. Lower case letters indicate bases used as spacers, which are not part of the hybridized sequence. Italicized letters indicate primer binding regions. Complementarity between probe & tag strands and the corresponding oligonucleotide or ultramer template are indicated by the same font color. Phos abbreviation symbolizes phosphate functionality, thiol abbreviation symbolizes thiol functionality. Alexa 647 symbolizes fluorescently tagged strand.

Table 3-3: SARS CoVNC Sequences used in LCR[A]

Name	Sequence (5′ to 3′)	Comments
SARS COVNC Soln Tag	Phos – AAT GTG GTC TTT GGG TGT ATT CAA GGC TCC	Ligated to soln probe
SARS COVNC Soln Probe	GCA GCA TTG TTA TTA GGA TTG CGG GTG CC	
SARS COVNC Wire Tag	Phos – GGC ACC CGC AAT CCT AAT AAC AAT GCT GC – Alexa 647	Ligated to wire probe
SARS COVNC Wire Probe	Thiol – taa cat tGG AGC CTT GAA TAC ACC CAA AGA CCA CAT T	Bound to wire
SARS COVNC Oligonucleotide Template	GCA GCA TTG TTA TTA GGA TTG CGG GTG CCA ATG TGG TCT TTG GGT GTA TTC AAG GCT CC	Comp to wire probe and tag
SARS COVNC Oligonucleotide Complement Template	GGA GCC TTG AAT ACA CCC AAA GAC CAC ATT GGC ACC CGC AAT CCT AAT AAC AAT GCT GC	Comp to soln probe and tag
SARS COVNC Ultramer Template	TTG TA*G CAC GGT GGC AGC ATT G*TT ATT AGG ATT GCG GGT GCC AAT GTG G*TC TTT GGG TGT ATT CAA GGC TCC CTC* AGT TGC AAC CCA TAC GAT GCC TTC T	Comp to wire probe and tag
SARS COVNC Ultramer Complement Template	AGA AGG CAT CGT ATG GGT TGC AAC TGA G*GG AGC CTT GAA TAC ACC CAA AGA* CCA CAT TGG CAC CCG CAA TCC TAA TAA *CAA TGC TGC CAC CGT GC*T ACA A	Comp to soln probe and tag

[A] SARS CoVNC sequences code for severe acute respiratory syndrome nucleocapsid. Primer sequence were recommended by the Armored RNA manufacturer, Asuragen. Lower case letters indicate bases used as spacers, which are not part of the hybridized sequence. Italicized letters indicate primer binding regions. Complementarity between probe & tag strands and the corresponding oligonucleotide or ultramer template are indicated by the same font color. Phos abbreviation symbolizes phosphate functionality, thiol abbreviation symbolizes thiol functionality. Alexa 647 symbolizes fluorescently tagged strand.

Table 3-4: SWH1 Control Sequences used in LCR[A]

Name	Sequence (5′ to 3′)	Comments
SWH1 Soln Tag	Phos – GCC ACA GGATTA AGG AAT ATC CCG	Ligated to soln probe
SWH1 Soln Probe	CCA GTC ACA ATT GGA AAA TAG AGT TTA AAC AGA T	
SWH1 Wire Tag	Phos – ATC TGT TTA AACTCT ATT TTC CAATTG TGA CTG G – Alexa 647	Ligated to wire probe
SWH1 Wire Probe & Reverse Primer Thiolated	Thiol – ttt ttt ttt tCG GGA TAT TCC TTA ATC CTG TGG C	Bound to wire
SWH1 Wire Oligonucleotide	CCA GTC ACA ATT GGA AAA TAG AGT TTA AAC AGA TGC CAC AGG ATT AAG GAA TAT CCC G	Comp to wire probe and tag
SWH1 Soln Oligonucleotide (Complement)	CGG GAT ATT CCT TAA TCC TGT GGC ATC TGT TTA AAC TCT ATT TTC CAA TTG TGA CTG G	Comp to soln probe and tag
SWH1 Positive Control Ultramer	ATT TAG GTG ACA CTA TAG AA*G TGC TAT AAA CAC CAG CCT CCC A*TT CAG AAT ATA CAT CCA GTC ACA ATT GGA AAA TAG AGT TTA AAC AGA *TGC CAC AGG ATT AAG GAA TAT CCC G*CC CTA TAG TGA GTC GTA TTA	Comp to wire probe and tag
SWH1 Positive Control Ultramer Complement	TAA TAC GAC TCA CTA TAG GG*C GGG ATA TTC CTT AAT CCT GTG GC*A TCT GTT TAA ACT CTA TTT TCC AAT TGT GAC TGG ATG TAT ATT CTG AAT *GGG AGG CTG GTG TTT ATA GCA C*TT CTA TAG TGT CAC CTA AAT	Comp to soln probe and tag

[A] SWH1 Control sequences code for Swine Flu H1N1 using the sequences indicated by the CDC.[42] Lower case letters indicate bases used as spacers, which are not part of the hybridized sequence. Italicized letters indicate primer binding regions. Complementarity between probe & tag strands and the corresponding oligonucleotide or ultramer template are indicated by the same font color. Phos abbreviation symbolizes phosphate functionality, thiol abbreviation symbolizes thiol functionality. Alexa 647 symbolizes fluorescently tagged strand.

Table 3-5: Swine H1 Sequences used in LCR[A]

Name	Sequence (5′ to 3′)	Comments
Swine H1 Soln Tag	Phos – CAT ATT TTG GAC ATT CTC CAA TTG TGA CTG GAT GTA TAT T	Ligated to soln probe
Swine H1 Soln Probe	CCT TAATCC TGT GGC CAT TCT CAGTTT AGT ACT TTT TA	
Swine H1 Wire Tag	Phos – TAA AAA GTA CTA AAC TGA GAA TGG CCA CAG GAT TAA GG – Alexa 647	Ligated to wire probe
Swine H1 Wire Probe	Thiol – taa cat tAA TAT ACATCC AGT CAC AATTGG AGA ATG TCC AAA ATATG	Bound to wire
RSVA Oligonucleotide Template	CCT TAA TCC TGT GGC CAT TCT CAG TTT AGT ACT TTT TAC ATA TTT TGG ACA TTC TCC AAT TGT GAC TGG ATG TAT ATT	Comp to wire probe and tag
RSVA Oligonucleotide Complement Template	AAT ATA CAT CCA GTC ACA ATT GGA GAA TGT CCA AAA TAT GTA AAA AGT ACT AAA CTG AGA ATG GCC ACA GGA TTA AGG	Comp to soln probe and tag

[A] Swine H1 sequences code for a highly virulent form of swine flu, Accession number GQ484355.1. Lower case letters indicate bases used as spacers, which are not part of the hybridized sequence. Italicized letters indicate primer binding regions. Complementarity between probe & tag strands and the corresponding oligonucleotide or ultramer template are indicated by the same font color. Phos abbreviation symbolizes phosphate functionality, thiol abbreviation symbolizes thiol functionality. Alexa 647 symbolizes fluorescently tagged strand.

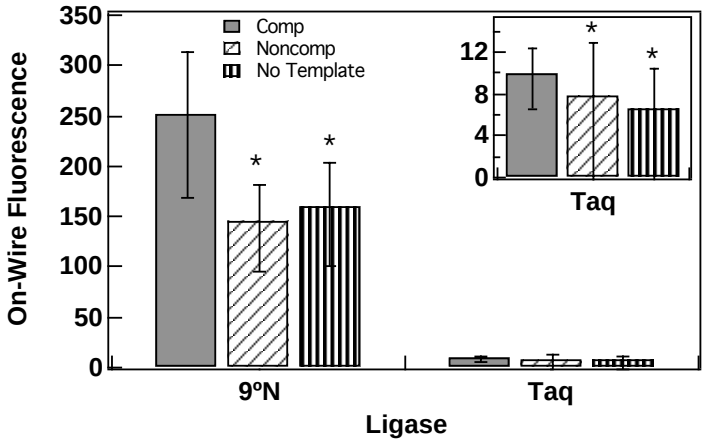

Figure 3-3. Quantification of on-wire fluorescence after on-wire LCR performed with one of two enzymes: 9°N or Taq. Inset shows enlarged view of signal generated from Taq ligase. * p value of < 0.05 versus signal from complementary template. At least 30 nanowires are used per fluorescence measurement to generate the mean intensity and error bars represent the 95 per cent confidence interval (in all on-wire fluorescence graphs).

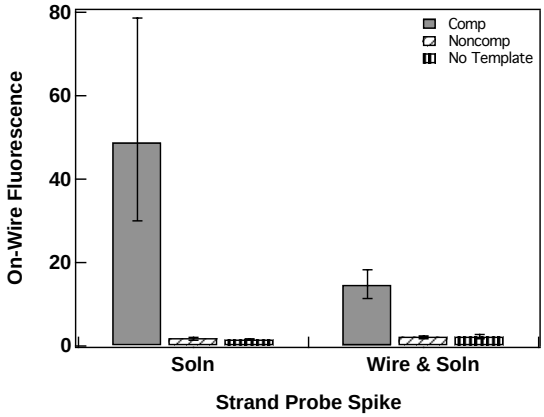

Figure 3-4. Quantification of microscope images for on-wire LCR performed with SARS sequence oligonucleotide template. The graph shows on-wire fluorescence when solution phase probes and tags (complementary to wire-bound probes and tags) were added to LCR reactions and when strands both complementary to and the same sequence as the wire probes and tags were added into solution.

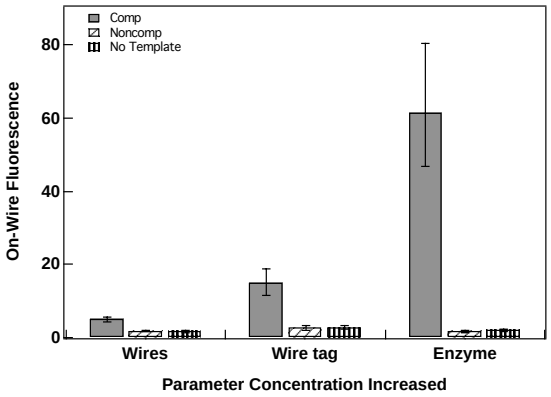

Figure 3-5. Quantification of microscopy images taken of on-wire LCR performed with variations in three parameters: 2× wire:probe conjugate, 2× wire tag, and 10× enzyme concentration. For comparison, 1× concentrations of all variables are shown in Figure A. Increasing the wire:probe and wire tag concentrations both decreased the specificity of the reaction, but an increase in specificity was observed with increased enzyme concentration, which was further investigated (shown in Figure D).

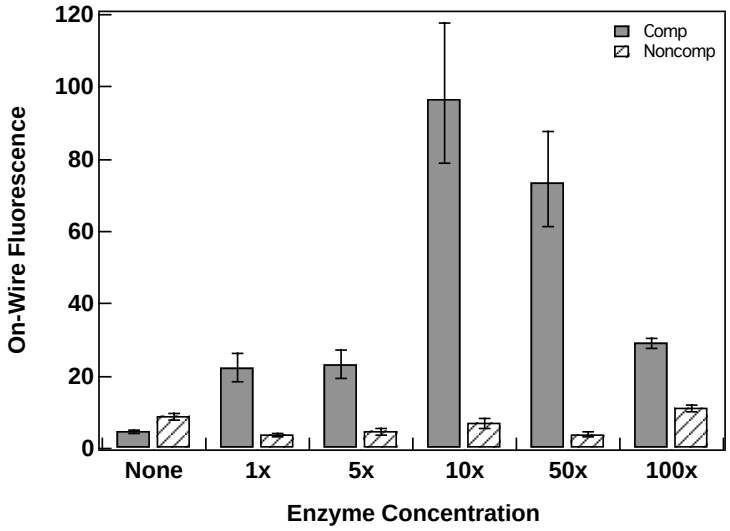

Figure 3-6. On-wire LCR performed over a range of enzyme concentrations. A concentration of 10× enzyme was chosen for future experiments as it gave the most amplification and also retained its specificity between complementary and no template samples. (Samples lacking enzyme are sandwich hybridization assays—SHA's).

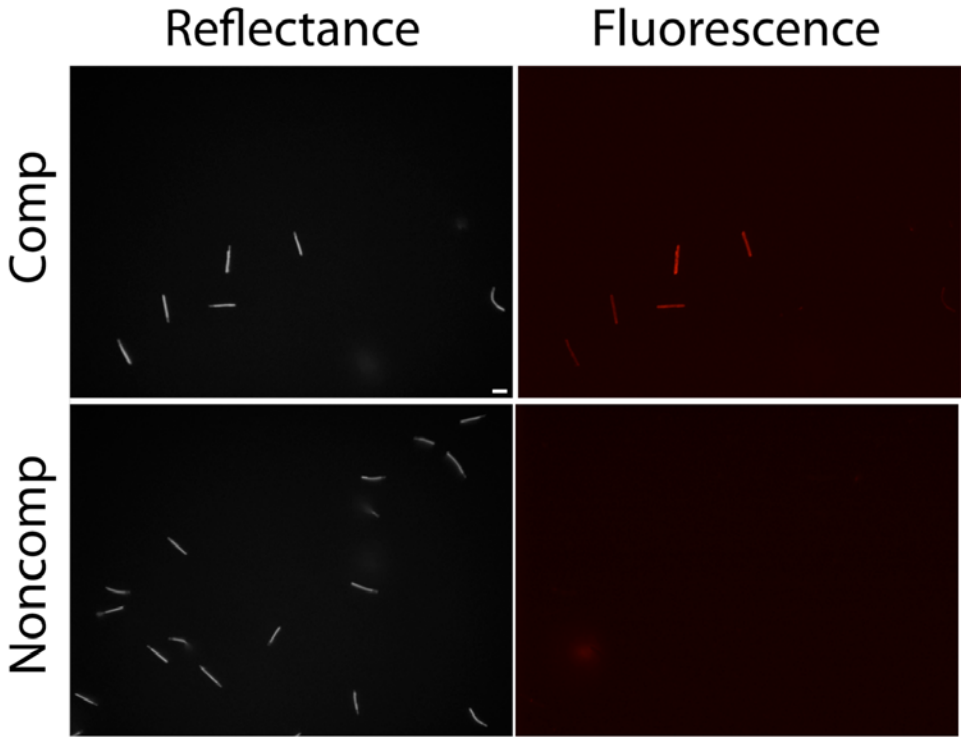

Figure 3-7. Contrast adjusted reflectance and fluorescence microscope images for complementary and noncomplementary single-plexed SARS LCR assay. Scale bar indicates 5 μm. Data is quantified in the next figure.

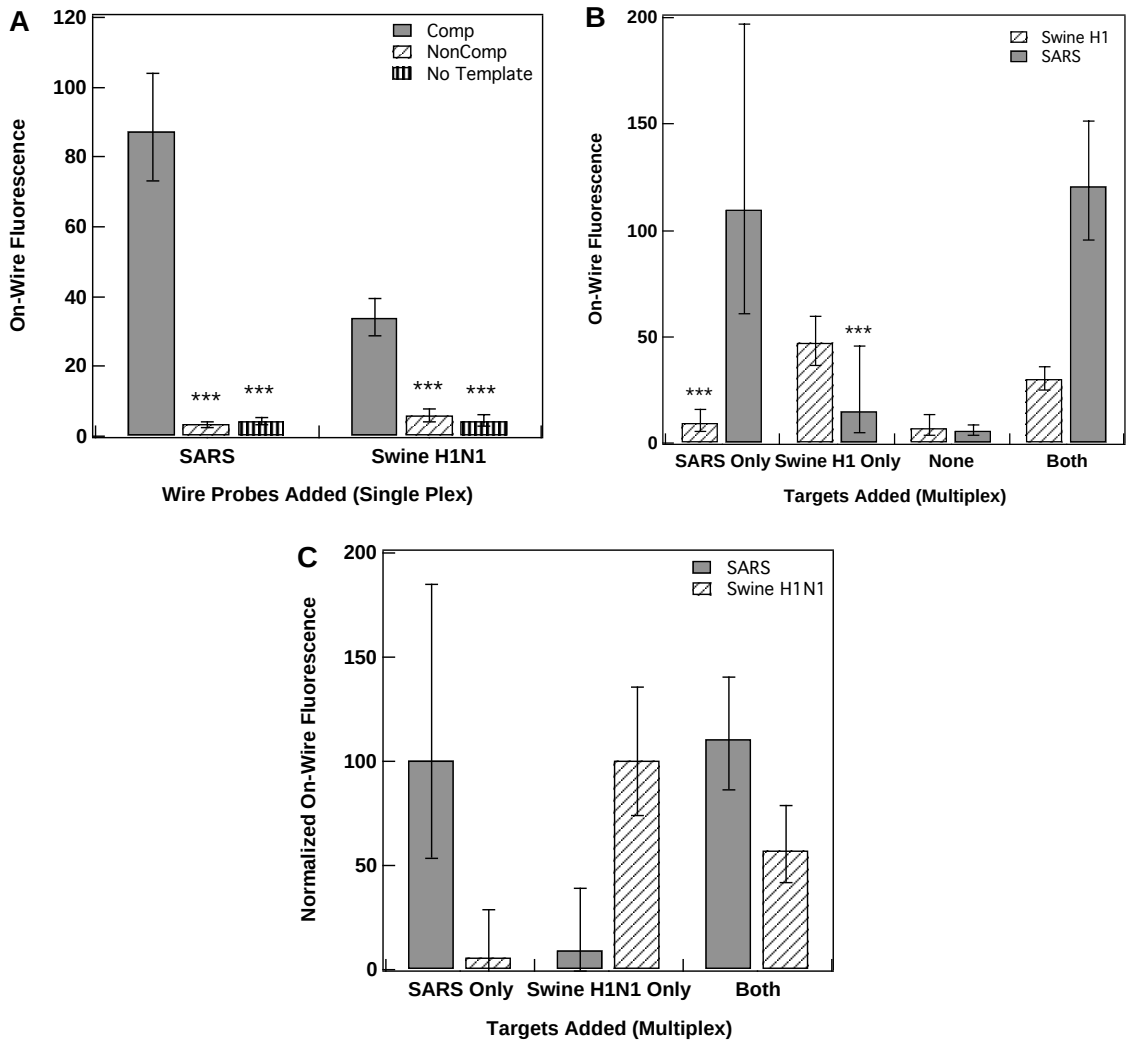

Figure 3-8. Quantification of microscope images for single- (A) and multiplexed (B) on-wire LCR samples using oligonucleotide templates. (C) Multiplexed samples background subtracted and normalized. *** p value < 0.001 versus signal from complementary template.

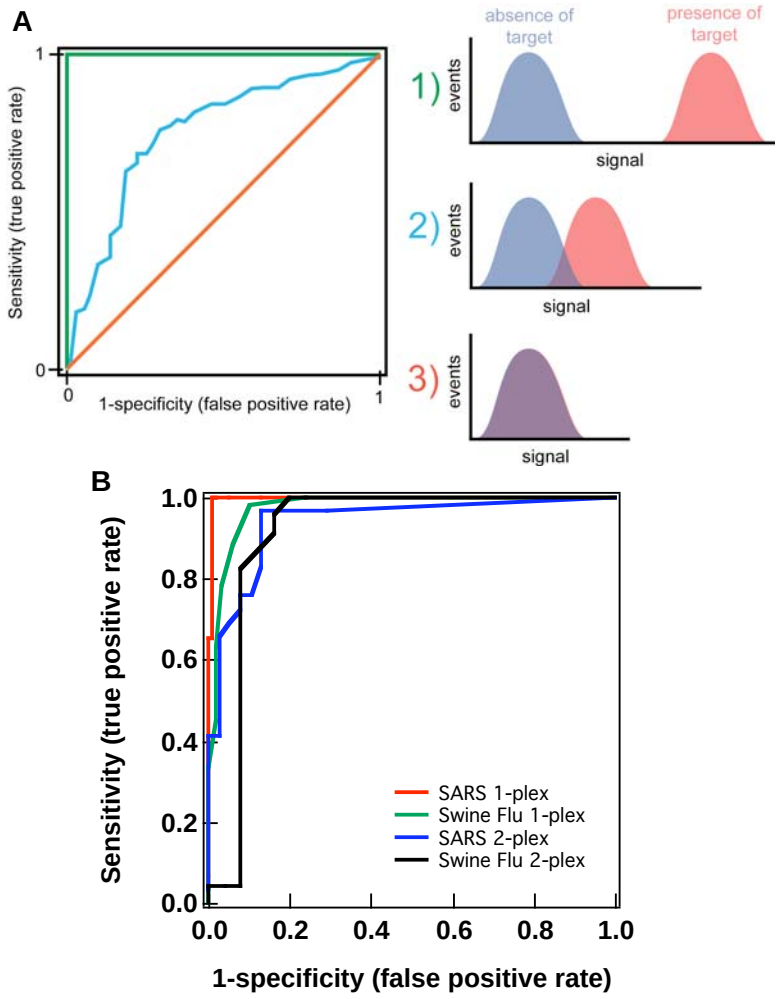

Figure 3-9. (A) Diagram of a Receiving Operating Characteristic curve illustrating examples of three different levels of discrimination between signal generated in the presence vs. absence of the target, where the first case of complete discrimination is represented by the green line in the ROC curve, the moderate level of discrimination the blue line, and the lack of discrimination the red line. A ROC curve showing complete discrimination between correct and false results will be composed of two straight lines, the first vertical along the y axis and the second horizontal along the value of 1 on the x axis, indicating a perfectly specific assay. (B) A ROC curve for the single- and multiplexed on-wire LCR fluorescence data shown previously in Figure E. The ROC curve shown here demonstrates the high specificity of the on-wire LCR assay. Figures plotted by Kristin Cederquist.

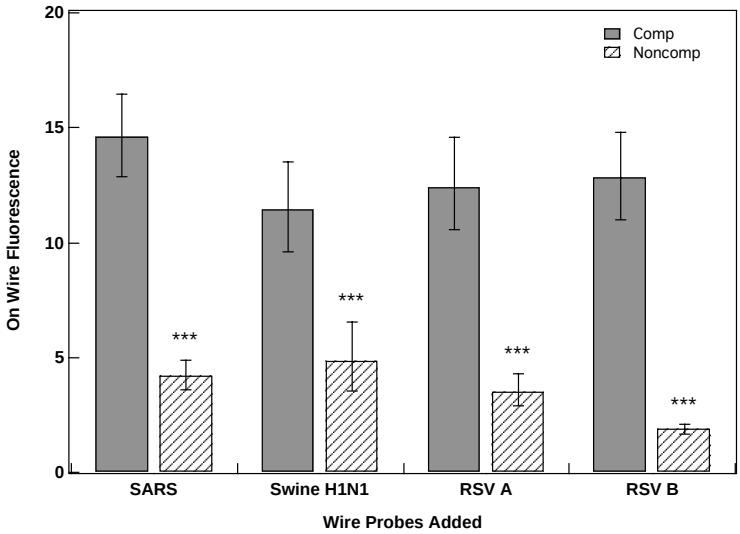

Figure 3-10. Quantification of microscope images for single-plexed on-wire LCR samples using ultramer templates. *** p value < 0.001 versus signal from complementary templates.

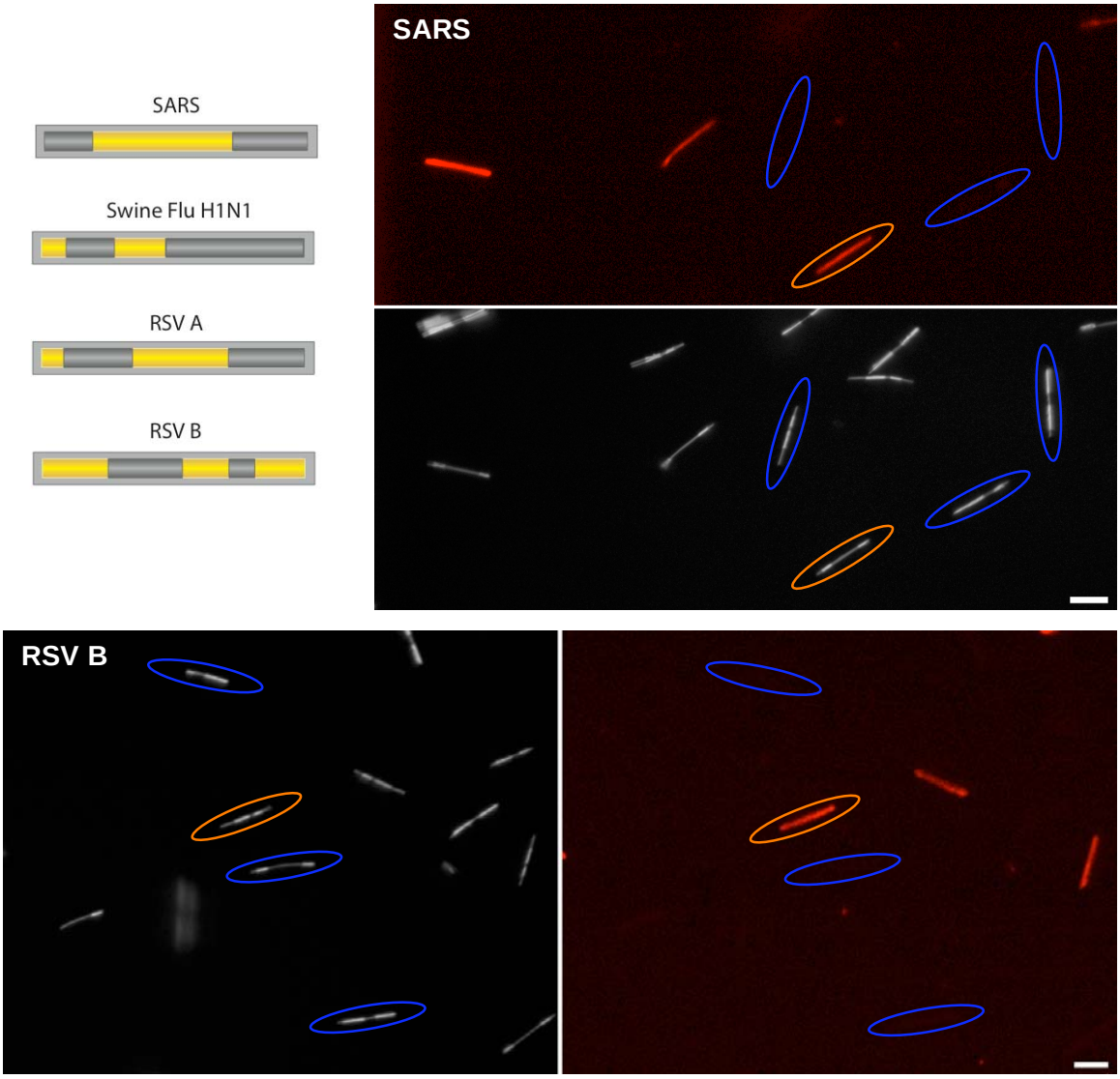

Figure 3-11. Contrast adjusted reflectance and fluorescence microscope images for multiplexed SARS & RSV B LCR assay. Scale bar indicates 5 μm. Data is quantified in the next figure. The respiratory virus sequence that the wire-bound probe captures and its corresponding nanowire barcode pattern are also indicated. Orange ovals indicate complementary nanowire:probes, blue ovals indicate noncomplementary nanowire:probes.

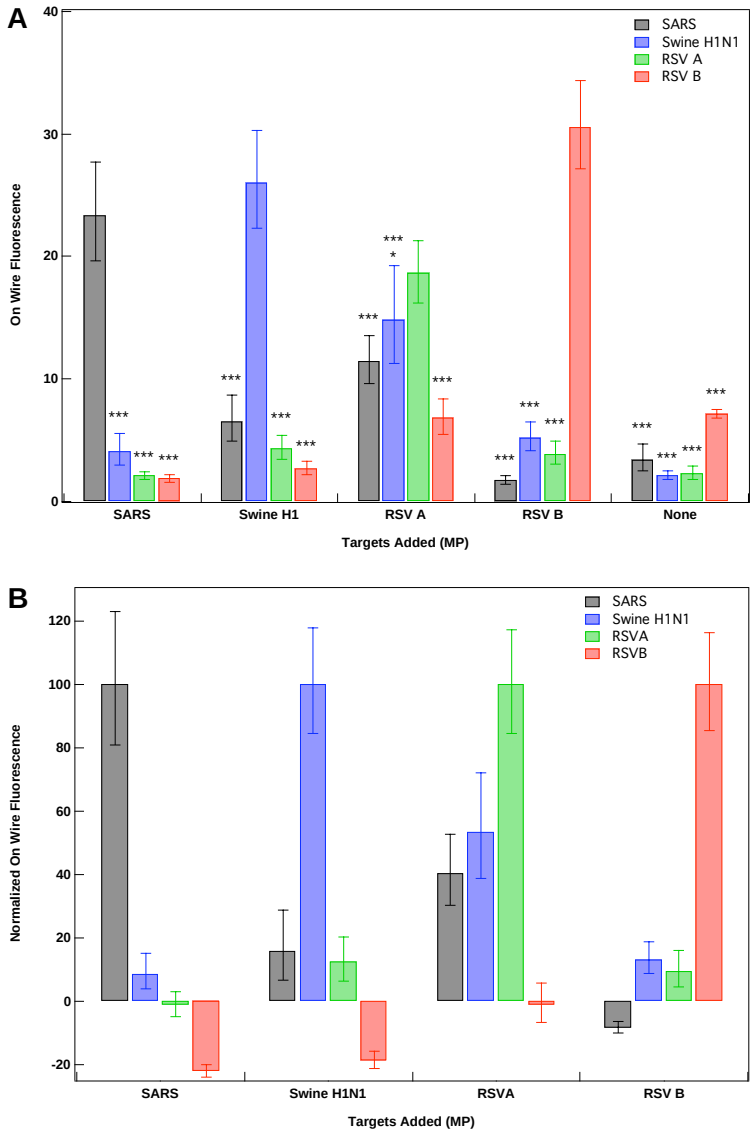

Figure 3-12. Quantification of microscope images for multiplexed (A) on-wire LCR samples using ultramer templates. Multiplexed samples are background subtracted and normalized in (B). *** p value < 0.001 versus signal from complementary wire:probes within the same multiplexed sample, versus signal from the same wire:probes within other multiplexed samples, and versus signal from no template samples with the same wire:probes. * p value < 0.05 versus the RSV A complementary wire:probes within the same multiplexed sample for only the Swine Flu H1N1 noncomplementary signal.

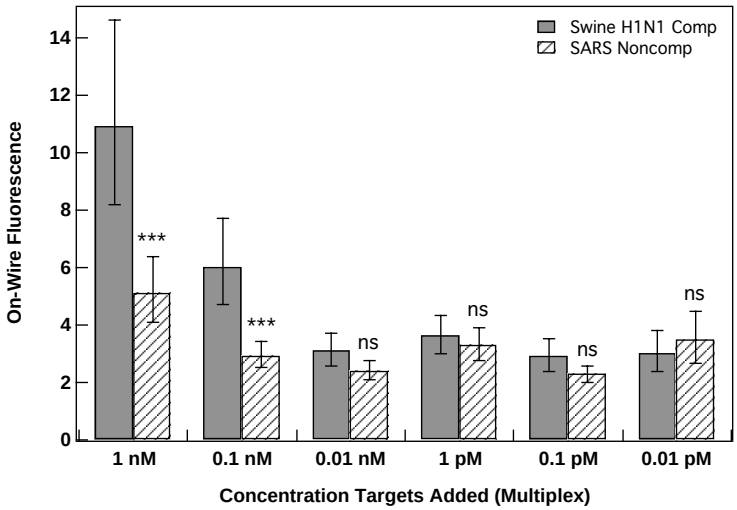

Figure 3-13. Multiplexed detection of serially diluted Swine Flu H1N1 template using the LCR assay. The noncomplementary signal was generated from SARS sequence probe:nanowires exposed to Swine Flu H1N1 strands in the multiplexed environment. *** p value < 0.001 when compared to signal from complementary nanowire:probes; ns indicates p value is not significant.

Chapter 4

DNA Patterning via Microcontact Printing

This work was collaborative with the lab of Dr. Paul Weiss. Daniel Dewey and T. J. Mullen both contributed microcontact printing expertise, and I contributed biomolecule expertise. Daniel Dewey also contributed to portions of writing.

Abstract

The work discussed here paves the way for patterning DNA using microcontact *insertion* printing, where DNA molecules are inserted into a preexisting self assembled monolayer, generating spatially encoded isolated DNA molecules; these surfaces could be used to perform single DNA molecule studies. Planar substrates were encoded using polydimethyl siloxane stamps to transfer DNA sequences onto gold (or glass) surfaces in a process called microcontact printing. Several parameters were tailored to generate specific substrate patterning, including stamp functionalization and signal transduction methodologies. DNA was shown to ink the stamp, to transfer from the stamp to the substrate, and to be available for complementary strand hybridization on the substrate.

Introduction

Soft lithography is a low-cost method of arraying that uses elastomeric materials to apply ink over an entire substrate at once by contact instead of spotting. In soft lithography, an even inking of the stamp should result in even deposition to the substrate, eliminating problems that occur when spotting without the use of surfactant additives in the spotting solution.[1] Also, the

flexible stamps used for soft lithography can print over a wider range of substrates and inks than those used in contact methods such as supramolecular nanostamping.[2, 3] Microcontact printing (μCP) is one patterning method that has been utilized in forming surfaces functionalized in certain spatial arrangements. Developed in the 1990's by the Whitesides lab,[4] μCP involves casting an elastomeric stamp in bas relief of a master, coating the stamp with ink, and bringing the stamp into conformal contact with a substrate to transfer the ink in the design of the raised sections of the stamp, as shown in Figure 4-1. This general method has been expanded into several alternative methods, such as microcontact insertion printing (μCIP) where the ink is inserted into a preexisting self assembled monolayer (or SAM) in order to isolate the transferred molecules. μCP has been used to configure metallic coatings or particles, epoxy, and small molecules such as alkanethiols.[5, 6] Microcontact displacement (μCDP) and insertion printing (μCIP) are two similar methods that apply the host matrix prior to printing.[5] In μCDP, the host layer is highly labile and rapidly exchanged by ink with higher intermolecular attraction.[7] In μCIP, the host layer is less labile, and only molecules at defect sites in the existing layer are exchanged.[8]

Printing methods have been applied to the patterning of biomolecules, as this is a gentle method, which does not detrimentally disrupt the structure of proteins.[6, 9] μCP has been used to print proteins such as bovine serum albumin (BSA) and proteins that promote cell adhesion and growth.[10-14] Printing capture proteins or molecules, followed by adsorbing proteins or cells from solution has been performed by several different research groups.[11, 15, 16] These techniques are often used to elucidate the mechanisms for the ways in which cells interact with synthetic surfaces and how this affects their subsequent competency and growth. DNA has also been patterned using μCP techniques;[14, 17] it can be patterned from one surface to another by hybridizing complementary DNA to the strands bound to the stamp surface, bringing this DNA

into contact with the substrate, and dehybridizing the complementary DNA so that it may remain bound to the substrate through its thiolated functionality.[3] When using stamps coated in DNA ink to transfer the macromolecules, increased hybridization efficiency was found as compared to traditional microarray patterning using robotics, due to increased accessibility.[9]

Biomolecules such as DNA[18] or serotonin[19] attached to a surface can be used as scaffolds; these scaffolds can specifically incorporate particles[18] or macromolecules such as antibodies[20]. Some possible functions for these ordered scaffolds include, but are not limited to, increasing efficiency of catalysis by placing certain moieties near each other, biosensing applications in microfluidic devices or microarrays, and nanomaterial design, where nanoparticles or other functional moieties can be oriented in a certain way.[5, 18] In addition to being able to pattern and sense for biomolecules, stamping molecules onto a surface also has use in altering film properties, in providing a reversible chemical modification, and in controlling the spacing of deposited molecules.[10, 20, 21]

Contact printing can be used to pattern pre-synthesized probes.[19] Fabricating patterns of fully synthesized probes is performed with three general surface attachment types: ionic interactions, affinity interactions, and covalent bonding. Ionic interactions use a positively charged surface (typically amine terminated) to bind the negative phosphate groups present on nucleic acid structures.[4, 22] Affinity interactions are typically used for protein and antibody binding, and use oligohistidine and nickel-chelate or biotin and streptavidin interactions, but have also been used for nucleic acids.[22-24] Surfaces functionalized with ketones, epoxys, and N-hydroxysuccinimidylesters are used for attachment to glass slides.[22, 25, 26] Another surface chemistry that is well studied for application in this area is the gold-thiol bond. Self-assembled monolayers (SAMs) created by gold-thiol chemistry can also reduce steric hindrances via dilution of the probe molecule in a matrix layer. The matrix layer can be formed by backfilling, insertion, and coadsorption (diagrams of backfilling and insertion are shown in Figure 4-1);[5] and a variety

of molecules can be used depending on the application. Designing functional arrays requires control over the coverage, wetting properties, and other aspects of molecules at the surface and their surrounding environment.[19, 21] The versatility of the gold-thiol system enables application-motivated adjustments to be made more readily.

Another method for the creation of microarrays, which does not utilize soft lithography, is the spotting of pre-synthesized sequences. Microarray spotting equipment can vary in quality and price, ranging from $20,000 to $200,000. While microarray spotters are capable of rapidly producing arrays at up to 200 spots per second, a common problem observed is uneven drying. Due to transport at the air/water interface, a ring forms as the sample dries with a thick layer of ink on the edges, and low coverage in the center.[1] This has been observed to reduce sensitivity, likely from steric hindrance.[17] The addition of surfactants to the ink solution is one method for controlling drying defects.[1] Microarrays of nucleic acids are used for high throughput parallel sample analysis. Microarrays may be fabricated by attaching fully synthesized probes or by synthesizing the probes on a reactive surface.[22] Nucleic acids are synthesized on the surface by activating select portions of the surface with UV light using either a mask or an array of mirrors.[22] The activated portions are then subjected to solutions of nucleotides in sequence. Photolabile protecting groups are used on each nucleotide to so that only activated areas react with the nucleotides. This technology has reached product level and is employed by companies such as Affymetrix and NimbleGen.

Soft lithography was combined here with gold-thiol chemistry as a potential low-overhead method of microarray fabrication.[9, 19, 27] An overview of the methods considered in this project is found in Figure 4-1. With the backfilling method used here, a pattern is initially created by contact printing, and then a different molecule is applied to the whole surface that fills the unpatterned areas.[7] This technique has been used extensively for small molecules, and 1-octane thiol (C8-SH) and mercaptodecanoic acid (MHDA) were used in earlier experiments as a control.

When Au surfaces functionalized with DNA are backfilled, DNA that has non-specifically adsorbed or is laying flat on the surface, is pushed off the surface, increasing its hybridization efficiency.[28, 29] In the preliminary investigations described here, the backfilling method was used in order to maximize DNA transfer so that visualization and optimization would be more straightforward.

Polydimethyl siloxane (PDMS) is predominantly used for soft lithographic stamps because of its mechanical properties (Young's Modulus = 1 MPa) and low reactivity.[6] As PDMS is authofluorescent at lower wavelengths, mostly due to the crosslinking moiety,[30, 31] detection of transferred DNA using fluorescence must be at higher wavelengths, such as 650 nm, shown in Figure 4-2. Stamp surface functionalization is often necessary to ink PDMS with polar compounds, because the native surface is incompatible with polar solvents. Oxidation and reaction with silanes was used to functionalize the surface.[13, 32, 33] Primarily, 2-[methoxy-(polyethyleneoxy)propyl] trimethoxy silane (MPPTS) (Figure 4-3) was used in functionalization, but aminopropyl trimethoxy silane (APTMS) has also been considered. MPPTS contains an oligo ethylene glycol (OEG) moiety, which predisposes the surface to be extremely hydrophilic. The stamp surface was characterized by contact angle measurements and confocal microscopy.

With these methods work has been done in a stepwise progression toward a system where DNA may be patterned to a surface by soft lithography and exist in a tailored environment that promotes binding and is characterized via fluorescence microscopy. Using these findings in the future, progress can be made in patterning DNA molecules by μCIP into a preexisting SAM for single molecule studies, which to our knowledge would be the first case of μCIP of DNA molecules.

Materials and Methods

Chemicals

Silanes used for this experiments were MPPTS and APTMS and were obtained from Gelest, Inc. DNA sequences were obtained already functionalized from IDT, Inc. Thiols, including 1-octane (C8) and mercaptodecanoic acid (MHDA), and were obtained from Sigma-Aldrich. Ultra pure water and 200 proof ethanol were used. Water was purified to 18.2 MΩ using a Barnstead nanopure system and all water and buffer solutions were autoclaved prior to use. 200 proof ethanol was purchased from Pharmo-Aaper. CentriSpin 10 columns were purchased from Princeton Scientific. Dithiothereitol (DTT) and buffer salts for phosphate buffered saline (PBS) were purchased from Sigma Aldrich. Phosphate buffered saline: 0.3 M sodium chloride, 10 mM phosphate, was made in house. The thiolated OEG backfill molecule used was 2-(2-(2-(11-mercaptoundecyloxy)ethoxy)ethoxy)ethanol (SPT-0011) was purchased from Sensopath Technologies Inc.

Substrates

The Au substrates were prepared by electron beam evaporation (Kurt J. Lesker) on Si{100} wafers with a 100 Å Chrome adhesion layer and 1000 Å of Au. The Au substrates were cleaned by hydrogen flame annealing prior to use. Glass slides used as stamping substrates were immersed in a 10 % sodium hydroxide solution overnight and then washed with water, a 1 % hydrochloric acid solution, water, and ethanol. They were then immersed in a 3 % APTMS solution for 30 minutes while on an orbital shaker. Then they were rinsed with ethanol and water, dried under N_2, and baked at 110 ^{o}C for 15 minutes. Positively charged gold substrates were

formed by exposure of Au on Si substrates to a 1 mM mercaptoethylamine solution for one hour at 80 ^{o}C. The substrate was then rinsed with ethanol and water, dried with Nitrogen, and baked for another 15 minutes at 80 ^{o}C. Stamping on charged surfaces was performed immediately after baking.

Stamp Fabrication

Stamps were formed over a functionalized Si wafer master to create 25 μm posts. A ratio of 9:1 base to curing agent of PDMS was cured at 70 °C for 1 week. After curing, stamps were removed and cut into ~1 cm squares, then rinsed in hexanes 4 times for 1 hour with shaking and dried at 70 °C for 1 week. Stamps were then hydrophilized by exposing them to O_2 plasma at 10 W for 10 seconds and subsequent ~1 minute exposure to 1 mM MPPTS, followed by ethanol rinse and N_2 drying. Before any treatment or experiment, stamps are rinsed with 50:50 DI water and ethanol and mild sonication, and dried with ethanol and N_2.

Stamping Press

Two home-made stamping presses were assembled to give more reproducible stamping results with long stamping times. The base was a machined L-shaped platform (aluminum or Delrin). A miniature laboratory jack was attached to the bottom platform. A hinge, locally obtained, was used to lower a machined ~55 g weight with a stamp attached at the bottom via adhesives.

Cleaving Thiolated DNA

A CentriSpin 10 column (Princeton Scientific) was vortexed for 15 seconds to remove air bubbles, then left to sit for 30 minutes after the addition of 650 μL H_2O. A 100 mM DTT solution was made and 50 μL of this was added to 50 μL of a 100 μM thiolated DNA solution. The mix was left to sit for at least 30 minutes. The spin column (with caps removed) was placed in a flat bottom wash tube and centrifuged at 750 *g* for 2 minutes. The bottom wash tube with the water was thrown away and the spin column was placed in a centrifuge tube. The DNA/DTT solution was placed on the column and the column was spun at 750 *g* for 2 minutes. The cleaved DNA was in the centrifuge tube and its concentration was determined by measuring its absorbance at 260 nm using a Hewlett-Packard 8453 diode-array UV Visible spectrophotometer.

Inking

All DNA sequences are presented in Table 4-1. The stamp was cleaned by sonication in an ethanol/water solution for 5 minutes. Inking by submersion was accomplished by placing the entire patterned surface of the stamp into the ink in a small vial overnight (Figures 4-5, 4-6, and 4-8) or for one hour (Figures 4-9 and 4-10). The stamp was inked with 7 μM Alexa647 conjugated DNA. The 1 mM SAM was made in one minute after stamping and rinsing with water.

Stamping

Before the inked stamp was used, the stamping press was aligned using a stamp from the same batch, and a waste substrate. Two aspects must be aligned. First, the z-direction is aligned

by adjusting the laboratory jack height to account for changes in substrate and stamp thickness. Second, markings on the weight and laboratory jack surface can be made to ensure contact in the X-Y plane. After alignment, inked stamps where placed on the weight of the stamping press using weak adhesives, and the stamp was brought to the substrate. The stamp was placed into contact with the substrate for a designated amount of time (overnight for Figures 4-6 & 4-7, and 10 minutes for Figures 4-5, 4-8, & 4-10) and the surfaces were then rinsed with DI water or PBS and dried with a gentle N_2 stream. When DNA was hybridized to the stamped probe sequences (Figure 4-10), 2 μL of each the target (either complementary or noncomplementary to the probe) and the complementary tag strands were added to 198 μL of PBS and deposited onto the substrate surface. The substrates were then rotated on an orbital shaker overnight.

Imaging

Samples were attached to glass slides using double stick tape, facing downwards on inverted microscopes. A Carl Zeiss, Inc. (Oberkochen, Germany) LSM-5 Pascal Laser Scanning confocal microscope was used to generate all images, except those shown in Figure 4-7, which was generated using an Olympus (Center Valley PA) Fluoview 1000 confocal microscope. TAMRA was excited with a 543 nm laser, and Alexa 647 with a 633 nm laser, and Plan-Apochromat air objectives were used. Pascal, Fluoview, and Axiovision software were used. Imaging by scanning electron microscopy (SEM) was performed on a Hitachi S-3000H SEM at 20 kV with 5.1 mm WD for Au colloid.

Colloidal Detection

To make tag DNA:colloidal particle conjugates, 50 μL 100 μM DNA was added to 1 mL of 50 nm colloid and put on a heat block for one hour at 37 ^{o}C. PBS buffer, 25 μL, was then added. After 30 more minutes on the heat block, 25 μL of PBS buffer was added. After 30 more minutes, 100 μL buffer were added and it was heated for an additional 30 minutes. PBS buffer, 150 μL, was then added, the tubes were allowed to sit on the heat block for 30 more minutes, and the last 128 μL buffer were then added. The tubes were heated at 37 ^{o}C overnight, and then rinsed by centrifuging at 8100 *g* for 15 minutes and resuspending in 100 μL PBS. The colloidal particles were rinsed two more times by centrifuging at 8100 *g* for 5 minutes. After the final rinse, the particles were resuspended in 1 mL PBS and 20 μL 20 μM target DNA was added to the solution. The tubes were put on a heat block at 47 ^{o}C for one hour, and then rinsed again following the procedure above. After rinsing the particles were resuspended in 200 μL PBS. The stamp was inked with 7 μM probe DNA by the submersion method for one hour. The substrate was stamped for 10 minutes using a slightly recovered stamp (discussed later). After backfilling to make the SAM for 10 minutes, the substrate was rinsed with water and dried. The substrate was placed on an orbital shaker and 100 μL of the colloid:target strand conjugate solution was placed onto the substrate; the substrate was shaken overnight in the presence (within a closed Petri dish) of a damp kimwipe to avoid evaporation. The substrates were rinsed with PBS and imaged with SEM.

Results and Discussion

Initial work described here aimed to deconvolute the signal generated from the stamping of fluorescently tagged DNA and that of the autofluorescence from transferred PDMS. Once

overcoming the obstacle of PDMS interference, other parameters were investigated, specifically the surface functionalization of the stamp. Control experiments were performed to confirm the transfer of DNA from the stamp to the substrate, and to ensure signal transduction from stamped oligonucleotides; hybridization assays were also performed. Progress made in microcontact printing of DNA described here will help to make μCIP of isolated DNA molecules, and subsequent single molecule studies, more feasible.

In order to confirm DNA printing, PDMS stamps were coated in DNA and brought into contact with substrates, which were gold-coated Si {100} slides. DNA patterning on the substrates was then visualized using optical microscopy to detect fluorescently tagged oligonucleotides. When stamping was performed in duplicate with two different labeled sequences, one with a TAMRA fluorophore and one with an Alexa 647 fluorophore, there was pattern seen using the first, but not the second sequence, which may be due not to the selective stamping of different DNA sequences, but rather due to the presence of PDMS and its autofluorescence at lower wavelengths. Substrate patterning was seen when the substrate was imaged using scanning electron microscopy (SEM) after the substrate was patterned with a stamp not exposed to DNA (shown in Figure 4-4), indicating the transfer of PDMS itself. It has been shown that the crosslinking moiety used in generating PDMS stamps is fluorescent across a range of wavelengths.[30] Because of the wavelength at which PDMS autofluoresces, (Figure 4-2)[31] the pattern observed was most likely due to the transfer of PDMS instead of the transfer of fluorescently tagged DNA strands. This PDMS layer may also have been preventing DNA from attaching to the gold surface. In order to prevent spectral overlap of the fluorophore (in this case TAMRA) with that of PDMS, Alexa 647 (which emits at a higher wavelength) was used instead; and in order to prevent PDMS transfer onto the substrate, stamping times were limited to 10 minutes.[34, 35] Several other parameters were varied, including DNA concentration, inking time, DNA submersion inking techniques, and rinsing techniques. To maximize the probability that if

DNA were present it would be easily visualized, bifunctional strands were used, where both a thiol and a fluorophore were present on each DNA strand, eliminating the decrease in efficiency introduced when the fluorescently tagged sequences need to hybridize to the patterned DNA. Substrates were also stamped with DNA and then backfilled with a SAM (instead of stamping into a previously deposited SAM) in order to achieve a maximum possible concentration of DNA.

There were three possible steps where DNA may be lost during the stamping procedure: 1) after inking the stamp may not have retained DNA 2) the DNA ink was not transferred to the substrate, 3) the DNA was present on the substrate, but the fluorescence signal was being quenched by the surface. The success of DNA transfer was directly investigated after each of these steps; while μCP of DNA molecules has been reported in the literature,[14, 17] the optimization of these procedures during μCP is applicable to microcontact insertion printing for possible future studies of isolated DNA molecules, which to the best of our knowledge has not yet bee accomplished. Controls such as imaging the inked stamps with confocal microscopy, stamping onto positively charged glass substrates, and using colloidal particles as reporters instead of fluorescent tags helped to confirm DNA inking and transfer, and led to changes in parameters such as using stamps that have undergone O_2 plasma oxidation and subsequent silanization and then been allowed to recover some hydrophobic character. It has been observed (in our lab as well as mentioned in the literature) that after oxidation and silanization the stamp slowly begins go through a process of hydrophobic recovery as unfunctionalized, uncrosslinked PDMS migrates to the surface of the stamp;[13, 36-38] which can be observed by contact angle measurements.

DNA Inking Confirmation

To confirm that the stamp was being successfully inked with DNA tagged with Alexa 647, the parameters were changed to maximize the probability of the stamp retaining the DNA,

this included increasing the DNA concentration, submersing the surface of the stamp in the solution of DNA in water, and increasing the inking time to overnight. Native, hydrophobic PDMS was forced into contact with the DNA solution by submersion and confocal microscopy of the stamp surface was performed. (Figure 4-5). The surface was covered only partially with DNA and both aggregates and halos were observed, indicating poor surface compatibility between the hydrophobic PDMS and the hydrophilic aqueous DNA solution. Freshly functionalized stamps were then exposed to DNA and imaged after contact with the substrate. These stamps were oxidized with O_2 plasma and silanized with a one minute exposure to 1 mM MPPTS (2-[methoxy-(polyethyleneoxy)propyl] trimethoxy silane—shown in Figure 4-3), a silane containing an oligo ethylene glycol (OEG) moiety, and were therefore maximally hydrophilic. This process created a glass-like layer containing OEG functionality at the surface of the stamp. Imaging the stamp surface showed that while DNA was present, it was not uniform across the surface (Figure 4-6). This may have been due to the generation of a shell of water molecules on the surface of the stamp when it had the highest percentage of oligo ethylene glycol (OEG) silane present.[39] The stamps were resubmerged in the DNA solution for three days and imaged again on the confocal microscope (Figure 4-7). The DNA solution was then uniform across the surface of the stamps. Compared with the native PDMS stamps and the initially functionalized stamps, the slightly recovered stamps gave a more uniform coating after inking. This indicated that successful inking resulted from accurate timing after functionalization; the inking was uniform when performed approximately 3 days after the O_2 plasma and silanization of the stamp. This stamp recovery resulted from native PDMS migrating to the stamp surface and most likely disrupting the water shell around the OEG SAM, enabling increased DNA adsorption to the stamp surface.

DNA Transferring Confirmation

After confirming the DNA was inking the stamp, further control experiments were performed to determine if the DNA ink was being transferred to the substrate from the stamp, the first of which was to stamp DNA onto positively charged silanized glass slides using nonfunctionalized (no O_2 plasma or silanization), or partly recovered functionalized stamps. The lack of a metallic surface eliminated the possible problem of quenching; the slide was positively charged with a silane to encourage DNA transfer in spite of the absence of gold. DNA pattern of 25 μm squares was seen on the substrates stamped with the nonfunctionalized and the substrates stamped with the partly recovered stamps. The fluorescence images of the sample where DNA was transferred to the slide using the unfunctionalized stamp contained a bright dot in every square, indicating a higher concentration of fluorescently labeled DNA in that area (as compared to where the rest of the stamp post contacted the substrate), while there was no bright dot present in the images of the sample where DNA was transferred to the slide using a slightly recovered stamp (Figure 4-8). Transmitted images taken on the confocal of unfunctionalized stamps show a raised dot present on each post; it is possible that the functionalization process also smoothes out the top surface of the stamp posts, removing stamp defects and creating a more even ink distribution.

As the DNA did transfer from the stamp to a positively charged glass slide, the stamping was tested to see if it would transfer DNA to a positively charged gold substrate. The substrate had some fluorescent spots present, but there was no pattern present, which may have been due to quenching of the fluorophore by the gold substrate (not shown). In order to visualize the DNA without using a fluorophore, the DNA was labeled with colloidal particles in a sandwich hybridization, where the probe was stamped onto the substrate and exposed to a solution containing hybridized target and tag DNA strands (tag sequences were already bound to a

colloidal particle). A thiolated backfilling molecule containing an OEG segment was used to reduce solution drying and nonspecific adsorption during the overnight exposure to the colloidal solution. Pattern of 10 μm square posts were seen in both duplicates exposed to complementary target DNA. Patterning was confirmed to be due to colloidal particles by taking images at higher magnification (shown in Figure 4-9). No pattern was seen in one of the two duplicates exposed to noncomplementary target DNA; the other duplicate did present some faint pattern, indicating less gold nanoparticles per square area. The presence of patterned nanoparticles proved that the DNA was being transferred from the stamp to the substrate and that the sandwich hybridization between the DNA strands had occurred.

Using the optimized parameters discussed above, such as using a slightly recovered stamp, decreasing stamping time, generating a SAM with an OEG moiety, and increasing the fluorophore excitation wavelength, the stamping procedure was repeated using a sandwich hybridization method with a fluorescently tagged strand on gold substrates (see Figure 4-10). There was no pattern seen in samples that were exposed to noncomplementary target. Those samples that were exposed to complementary target DNA did have patterned areas, but were not over as large an area of the substrate as when using particles for tags instead of fluorophores. The pattern itself was more a series of dots instead of squares; this may be due to a lack of sufficient conformal contact between the stamp and substrate in delivering the DNA to the surface. This may also be due to the quenching of any diluted fluorescently tagged DNA strand that may have folded closer to the surface in spite of the use of a spacer within the strand between the thiol and the hybridizing bases. Future work may be done to elucidate the cause of this stamping of dots rather than squares.

Conclusions and Future Directions

Initial work has been performed in optimizing successful stamping of DNA patterns onto substrates. It was determined that functionalized PDMS stamps can be inked with DNA, and that DNA can be transferred to a positively charged glass surface as well as a gold surface. Slightly recovered functionalized stamps work better than unfunctionalized or freshly functionalized stamps for DNA inking and transfer, which is due to the optimization of the surface interactions between the PDMS and MPPTS stamp surface with the DNA and water molecules present in the inking solution. DNA on the surface was shown to be available for subsequent hybridization events. The higher wavelength emitting fluorophore Alexa 647 is the better match with PDMS than TAMRA to avoid autofluorescence of residual PDMS, and shorter stamping times (around 10 minutes) may be used to better avoid PDMS transfer from stamps.

The DNA's fluorescent signal can be quenched by the gold substrate, and because of this the optimal DNA concentration may change once optimization of its visualization on the gold surface has occurred. This possible quenching problem could be addressed by increasing the length of the host SAM, or using an alternative stamp silanizing molecule, to force the fluorophore further from the quenching gold surface. Because of its positive charge, APTMS could promote DNA multilayers on the stamp surface. Multiple layers of DNA would more easily allow for DNA transfer without PDMS transfer from the stamp to the substrate. After optimizing fluorescence signal visualization, further hybridization and capture experiments could be performed. The findings described here pave the way for using microcontact insertion printing to pattern isolated DNA molecules, which could be useful in single molecule DNA studies.

References

1. Deng, Y.; Zhu, X. Y.; Kienlen, T.; Guo, A. Transport at the air/water interface is the reason for rings in protein microarrays. *J. Am. Chem. Soc.* **2006**, *128* (9), 2768-2769.

2. Yu, A. A.; Savas, T. A.; Taylor, G. S.; Guiseppe-Elie, A.; Smith, H. I.; Stellacci, F. Supramolecular nanostamping: Using DNA as movable type. *Nano Lett.* **2005**, *5*, 1061-1064.

3. Akbulut, O.; Jung, J. M.; Bennett, R. D.; Hu, Y.; Jung, H. T.; Cohen, R. E.; Mayes, A. M.; Stellacci, F. Application of supramolecular nanostamping to the replication of DNA nanoarrays. *Nano Lett.* **2007**, *7*, 3493-3498.

4. Kumar, A.; Whitesides, G. M. Features of gold having micrometer to centimeter dimensions can be formed through a combination of stamping with an elastomeric stamp and an alkanethiol ink followed by chemical etching. *Appl. Phys. Lett.* **1993**, *63*, 2002-2004.

5. Saavedra, H. M.; Mullen, T. J.; Zhang, P.; Dewey, D. C.; Claridge, S. A.; Weiss, P. S. Hybrid strategies in nanolithography. *Rep. Prog. Phys.* **2010**, *73*, 036501.

6. Whitesides, G. M.; Ostuni, E.; Takayama, S.; Jiang, X. Y.; Ingber, D. E. Soft lithography in biology and biochemistry. *Ann. Rev. Biomed. Eng.* **2001**, *3*, 335-373.

7. Dameron, A. A.; Hampton, J. R.; Gillmor, S. D.; Hohman, J. N.; Weiss, P. S. Enhanced molecular patterning via microdisplacement printing. *J. Vac. Sci. Technol., B* **2005**, *23*, 2929-2932.

8. Mullen, T. J.; Srinivasan, C.; Hohman, J. N.; Gillmor, S. D.; Shuster, M. J.; Horn, M. W.; Andrews, A. M.; Weiss, P. S. Microcontact insertion printing. *Appl. Phys. Lett.* **2007**, *90*, 063114.

9. Ruiz, S. A.; Chen, C. S. Microcontact printing: A tool to pattern. *Soft Matter* **2007**, *3*, 168-177.

10. Salim, A.; Ding, Z.; Ziaie, B. Micromachined hydrogel stamper for soft printing of biomolecules with adjustable feature dimensions. *Anal. Chem.* **2009**, *81* (11), 4551-4554.

11. Bernard, A.; Renault, J. P.; Michel, B.; Bosshard, H. R.; Delamarche, E. Microcontact printing of proteins. *Adv. Mater.* **2000**, *12* (14), 1067-1070.

12. Renault, J. P.; Bernard, A.; Bietsch, A.; Michel, B.; Bosshard, H. R.; Delamarche, E.; Kreiter, M.; Hecht, B.; Wild, U. P. Fabricating arrays of single protein molecules on glass using microcontact printing. *J. Phys. Chem. B* **2003**, *107* (3), 703-711.

13. Delamarche, E.; Donzel, C.; Kamounah, F. S.; Wolf, H.; Geissler, M.; Stutz, R.; Schmidt-Winkel, P.; Michel, B.; Mathieu, H. J.; Schaumburg, K. Microcontact printing using

poly(dimethylsiloxane) stamps hydrophilized by poly(ethylene oxide) silanes. *Langmuir* **2003**, *19*, 8749-8758.

14. Chlmeau, J.; Thibault, C.; Carcenac, F.; Vieu, C. Self-aligned patterns of multiple biomolecules printed in one step. *Appl. Phys. Lett.* **2008**, *93*, 133901.

15. Feng, C. L.; Embrechts, A.; Bredebusch, I.; Schnekburger, J.; Domschke, W.; Vancso, G. J.; Schönherr, H. Reactive microcontact printing on block copolymer films: Exploiting chemistry in microcontacts for sub-micrometer patterning of biomolecules. *Adv. Mater.* **2007**, *19*, 286-290.

16. Offenhäusser, A.; Böcker-Meffert, S.; Decker, T.; Helpenstein, R.; Gasteier, P.; Groll, J.; Möller, M.; Reska, A.; Schäfer, S.; Schulte, P.; Vogt-Eisele, A. Microcontact printing of proteins for neuronal cell guidance. *Soft Matter* **2007**, *3*, 290-298.

17. Lange, S. A.; Benes, V.; Kern, D. P.; Horber, J. K. H.; Bernard, A. Microcontact printing of DNA molecules. *Anal. Chem.* **2004**, *76* (6), 1641-1647.

18. Weizmann, Y.; Braunschweig, A. B.; Wilner, O. I.; Cheglakov, Z.; Willner, I. A polycatenated DNA scaffold for the one-step assembly of hierarchical nanostructures. *Proc. Nat. Acad. Sci. USA* **2008**, *105* (14), 5289-5294.

19. Shuster, M. J.; Vaish, A.; Szapacs, M. E.; Anderson, M. E.; Weiss, P. S.; Andrews, A. M. Biospecific recognition of tethered small molecules diluted in self-assembled monolayers. *Adv. Mater.* **2008**, *20* (1), 164-167.

20. Mullen, T. J.; Dameron, A. A.; Andrews, A. M.; Weiss, P. S. Selecting and driving monolayer structures through tailored intermolecular interactions. *Aldrichimica Acta* **2007**, *40* (1), 21-31.

21. Weiss, P. S. Functional molecules and assemblies in controlled environments: formation and measurements. *Acc. Chem. Res.* **2008**, *41* (12), 1772-1781.

22. Venkatasubbarao, S. Microarrays - status and prospects. *Trends in Biotechnol.* **2004**, *22* (12), 630-637.

23. Collett, J. R.; Cho, E. J.; Ellington, A. D. Production and processing of aptamer microarrays. *Methods* **2005**, *37* (1), 4-15.

24. Park, J. U.; Lee, J. H.; Paik, U.; Lu, Y.; Rogers, J. A. Nanoscale patterns of oligonucleotides formed by electrohydrodynamic jet printing with applications in biosensing and nanomaterials assembly. *Nano Lett.* **2008**, *8* (12), 4210-4216.

25. Chrisey, L. A.; Lee, G. U.; Oferrall, C. E. Covalent attachment of synthetic DNA to self-assembled monolayer films. *Nucleic Acids Res.* **1996**, *24* (15), 3031-3039.

26. Chrisey, L. A.; Oferrall, C. E.; Spargo, B. J.; Dulcey, C. S.; Calvert, J. M. Fabrication of patterned DNA surfaces. *Nucleic Acids Res.* **1996**, *24* (15), 3040-3047.

27. Chakra, E. B.; Hannes, B.; Dilosquer, G.; Mansfield, C. D.; Cabrera, M. A new instrument for automated microcontact printing with stamp load adjustment. *Rev. Sci. Instrum.* **2008**, *79*, 064102.

28. Herne, T. M.; Tarlov, M. J. Characterization of DNA probes immobilized on gold surfaces. *J. Am. Chem. Soc*. **1997**, *119*, 8916-8920.

29. Peterlinz, K. A.; Georgiadis, R. M.; Herne, T. M.; Tarlov, M. J. Observation of hybridization and dehybridization of thiol-tethered DNA using two-color surface plasmon resonance spectroscopy. *J. Am. Chem. Soc*. **1997**, *119*, 3401-3402.

30. Cesaro-Tadic, S.; Dernick, G.; Juncker, D.; Buurman, G.; Kropshofer, H.; Michel, B.; Fattinger, C.; Delamarche, E. High-sensitivity miniaturized immunoassays for tumor necrosis factor a using microfluidic systems. *Lab on a Chip* **2004**, *4*, 563-569.

31. Yokokawa, R.; Tamaoki, S.; Sakamoto, T.; Murakami, A.; Sugiyama, S. Transcriptome analysis device based on liquid phase detection by fluorescently labeled nucleic acid probes. *Biomed. Microdevices* **2007**, *9*, 869-875.

32. Owen, M. J.; Smith, P. J. Plasma treatment of polydimethylsiloxane. *J. Adhes. Sci. Technol.* **1994**, *8*, 1063-1075.

33. Duan, X. X.; Sadhu, V. B.; Perl, A.; Peter, M.; Reinhoudt, D. N.; Huskens, J. Bifunctional, chemically patterned flat stamps for microcontact printing of polar inks. *Langmuir* **2008**, *24*, 3621-3627.

34. Thibault, C.; Séverac, C.; Mingotaud, A.-F.; Vieu, C.; Mauzac, M. Poly(dimethylsiloxane) contamination in microcontact printing and its influence on patterning oligonucleotides. *Langmuir* **2007**, *23* (21), 10706-10714.

35. Åsberg, P.; Nilsson, K. P. R.; Inganäs, O. Surface energy modified chips for detection of conformational states and enzymatic activity in biomolecules. *Langmuir* **2006**, *22*, 2205-2211.

36. Hillborg, H.; Geede, U. W. Hydrophobicity Recovery of polydimethylsiloxane after exposure to corona discharges. *Polymer* **1998**, *39*, 1991-1998.

37. Fritz, J. L.; Owen, M. J. Hydrophobic recovery of plasma-treated polydimethylsiloxane *J. Adhesion* **1995**, *54*, 33-45.

38. Kim, J.; Chaudhury, M. K.; Owen, M. J. Hydrophobicity loss and recovery of silicone HV insulation. *IEEE Trans. Dielectr. Electron. Insul.* **1999**, *6*, 695-702.

39. Feldman, K.; Hähner, G.; Spencer, N. D.; Harder, P.; Grunze, M. Probing resistance to protein adsorption of oligo(ethylene glycol)-terminated self-assembled monolayers by scanning force microscopy. *J. Am. Chem. Soc.* **1999**, *121* (43), 10134-10141.

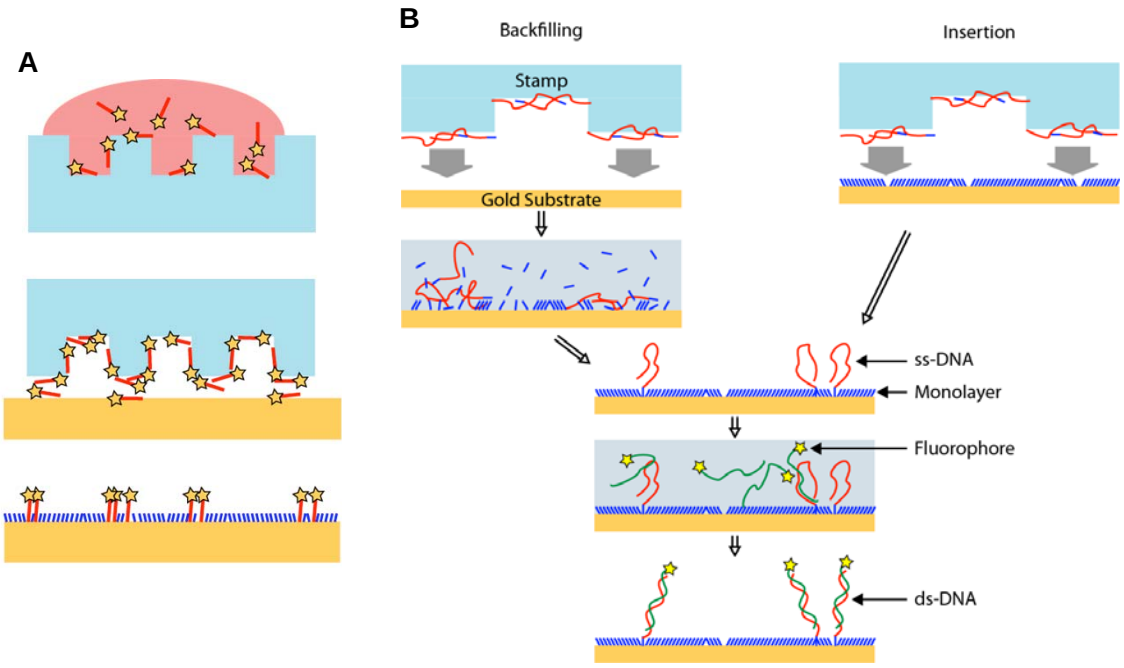

Figure 4-1. (A) Method of inking stamp with bifunctional, thiolated, fluorescent DNA, and subsequent transferring and backfilling onto substrate. The stamp is flipped after inking. (B) General method of fabrication for backfilling and insertion methods to create surfaces with DNA probes diluted in a tailored host matrix layer. Figure made by Daniel Dewey.

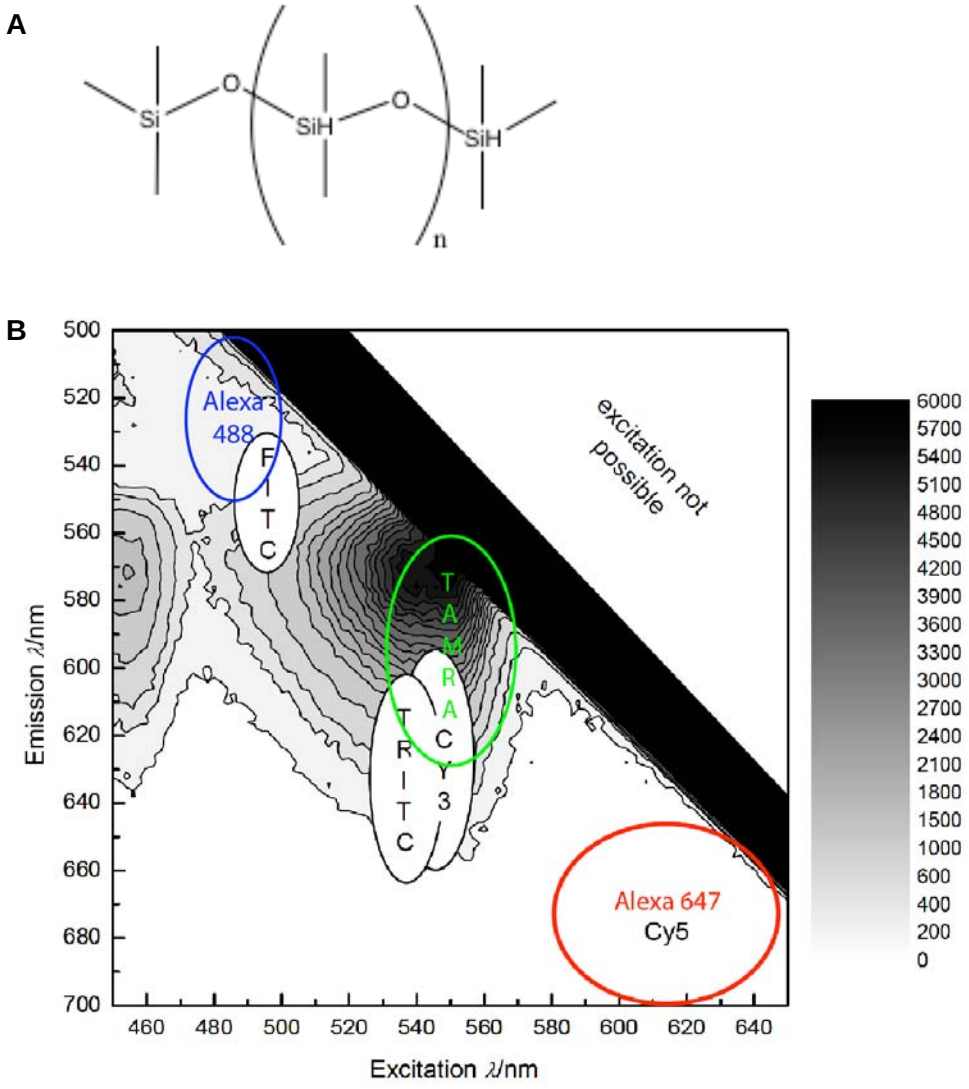

Figure 4-2. (A) Structure of polydimethyl siloxane. (B) Graph displaying the fluorescence intensity of a PDMS sample resulting from scanning through excitation and emission wavelengths on a fluorimeter. The absorbance and emission spectra of several organic dyes in relation to that of the autofluorescence of PDMS. TAMRA (green), and Alexa 647 (red) were used in experiments discussed within the chapter. The z scale represents the fluorescence intensity recorded at the combination of excitation and emission wavelengths intersecting at that point. Modified from Cesaro-Tadic, S.; Dernick, G.; Juncker, D.; Buurman, G.; Kropshofer, H.; Michel, B.; Fattinger, C.; Delamarche, E. High-Sensitivity Miniaturized Immunoassays for Tumor Necrosis Factor a Using Microfluidic Systems. *Lab on a Chip* **2004**, *4*, 563-569 – Reproduced by permission of The Royal Society of Chemistry.[30] http://dx.doi.org/10.1039/b408964b

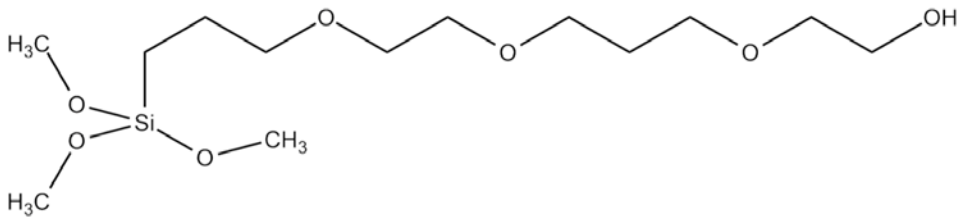

Figure 4-3. 2-[methoxy(polyethyleneoxy)propyl] trimethoxysilane (MPPTS) used to silanize the stamp surface. Silanizing the oxidized stamp slows down the recovery of the stamp back to its initial hydrophobic state, and replaces the native hydrophobic properties with those of the silane.

Table 4-1: DNA sequences used in stamping work

Name	Sequence (5' to 3')	Comments[A]
HIVSBiThiolTag647	Thiol – TGT CAC TTC CCC TT – Alexa 647	Bifunctional strand
Flu A Probe	Thiol – ttt ttt ttt tGA CCA ATC CTG TCA C	
Flu A Target	TTC CCT TAG TCA GAG GTG ACA GGA TTG GTC	Sandwich hybridization assay target for Flu A
Flu A Tag	CTC TGA CTA AGG GAA ttt ttt ttt t – Thiol	For conjugation to gold nanoparticle
Flu B Target	AGG AAT GGG AAC AAC AGC AAC AAA AAA GAA	Noncomplementary target to Flu A
RSV A Probe	Thiol – taa cat tTT CTG CAC ATC ATA ATT AGG AGT ATC AAT ACT ATC	
RSV A Target	CAT CCA ACG GAG CAC AGG AGA TAG TAT TGA TAC TCC TAA TTA TGA TGT GCA GAA	
RSV A Tag	TCC TGT GCT CCG TTG GAT G – Alexa 647	
Swine Flu H1N1 Target	CCA GTC ACA ATT GGA AAA TAG AGT TTA AAC AGA TGC CAC AGG ATT AAG GAA TAT CCC G	Noncomplementary target to RSV A

[A] lower case letters indicate spacer bases not participating in hybridization

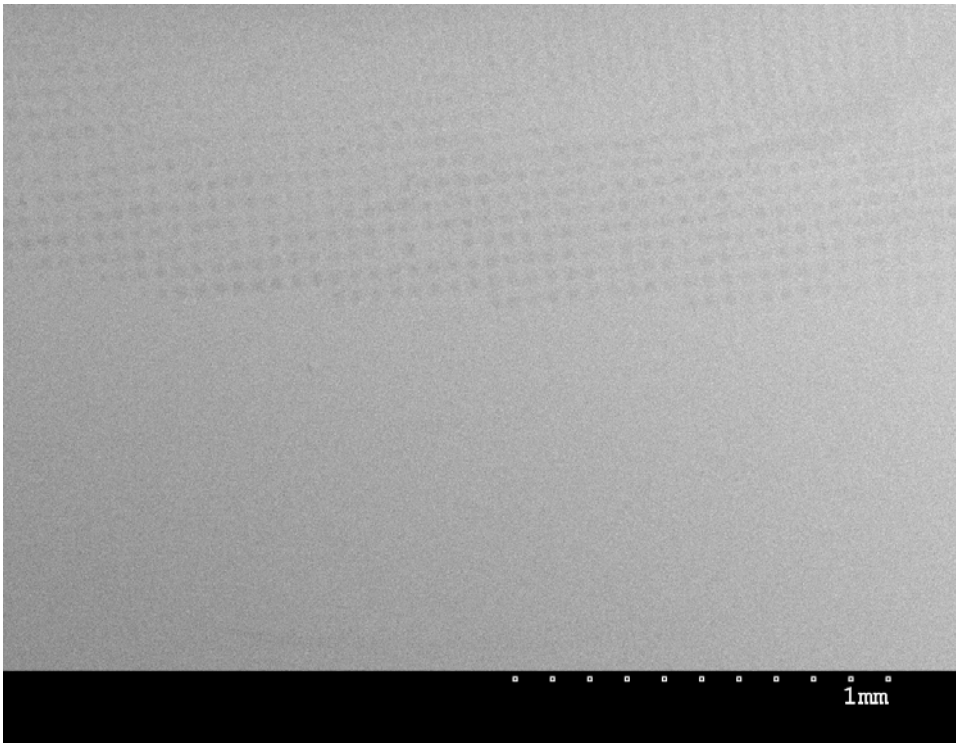

Figure 4-4. SEM image of substrate exposed to an uninked stamp, but still patterned with 25 μm square posts, most likely due to PDMS transfer.

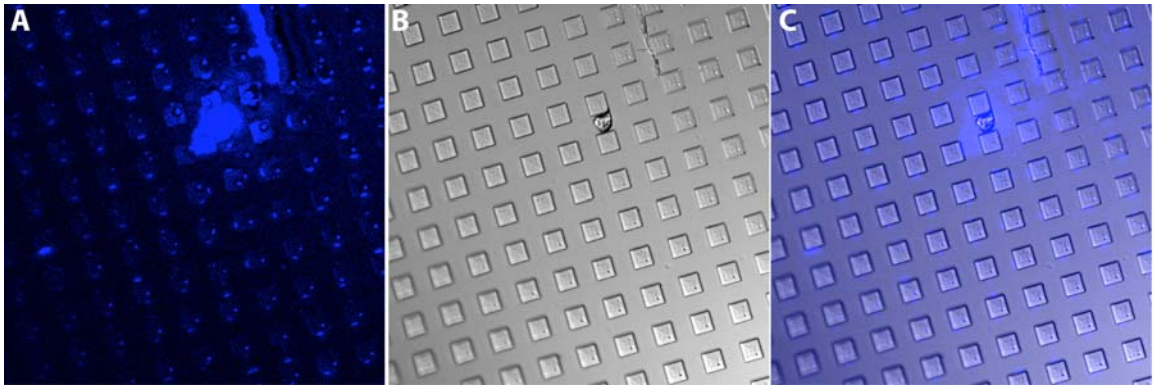

Figure 4-5. Confocal microscope image of unfunctionalized stamp with 25 μm square posts after inking by submersion with bifunctional HIV DNA (with 5' thiol and 3' Alexa 647). Contrast adjusted fluorescence (A), differential interference contrast (DIC) (B), and overlain (C) images are shown.

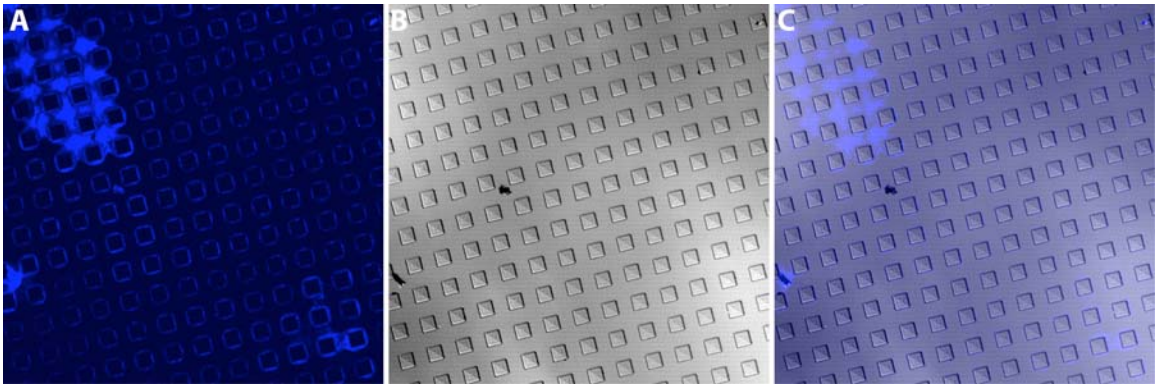

Figure 4-6. Freshly functionalized stamps with 25 μm square posts inked with bifunctional HIV DNA with 3' Alexa 647. Contrast adjusted fluorescence (A), DIC (B), and overlain (C) images are shown. The ink is not uniform and is present in halos, indicating poor compatibility between the DNA solution and the stamp surface properties.

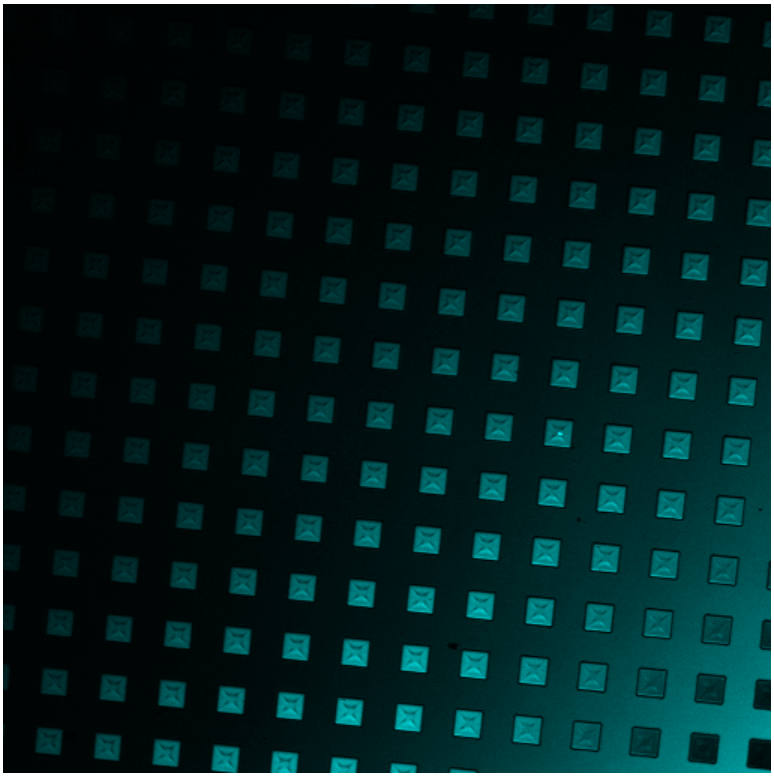

Figure 4-7. Overlain confocal image of stamps with 25 μm square posts exposed to bifunctional HIV DNA with 5' thiol and 3' Alexa 647. These stamps were exposed to the DNA and imaged several days after functionalization, partial recovery of the surface resulted in more uniform inking.

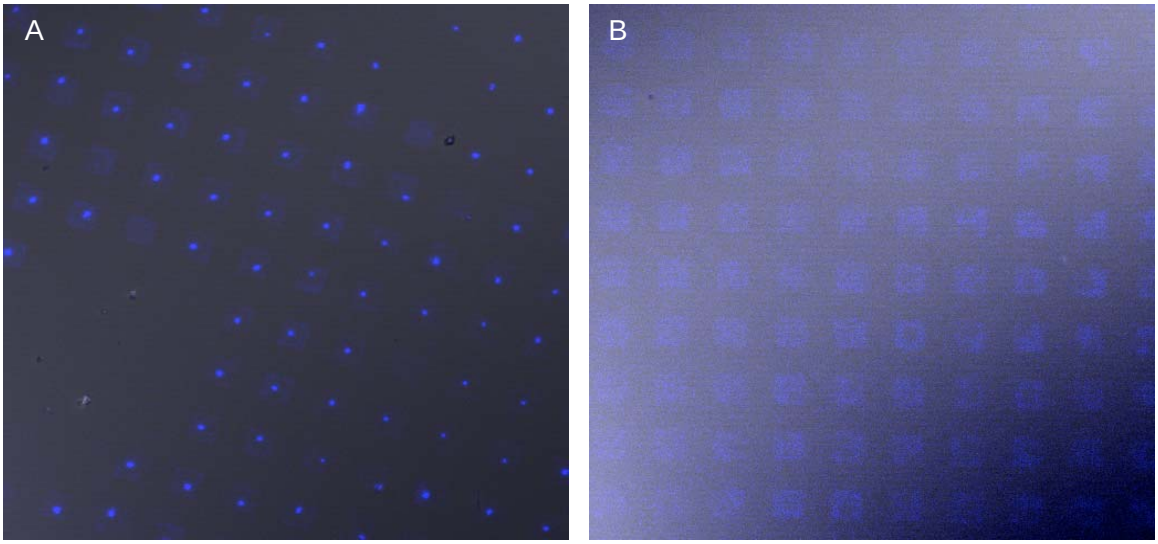

Figure 4-8. Images of glass slides stamped with bifunctional DNA coding for HIV (containing 5' thiol and 3' Alexa 647 fluorophore) inked using unfunctionalized (A) and slightly recovered (B) stamps. Scale: 25 μm square posts.

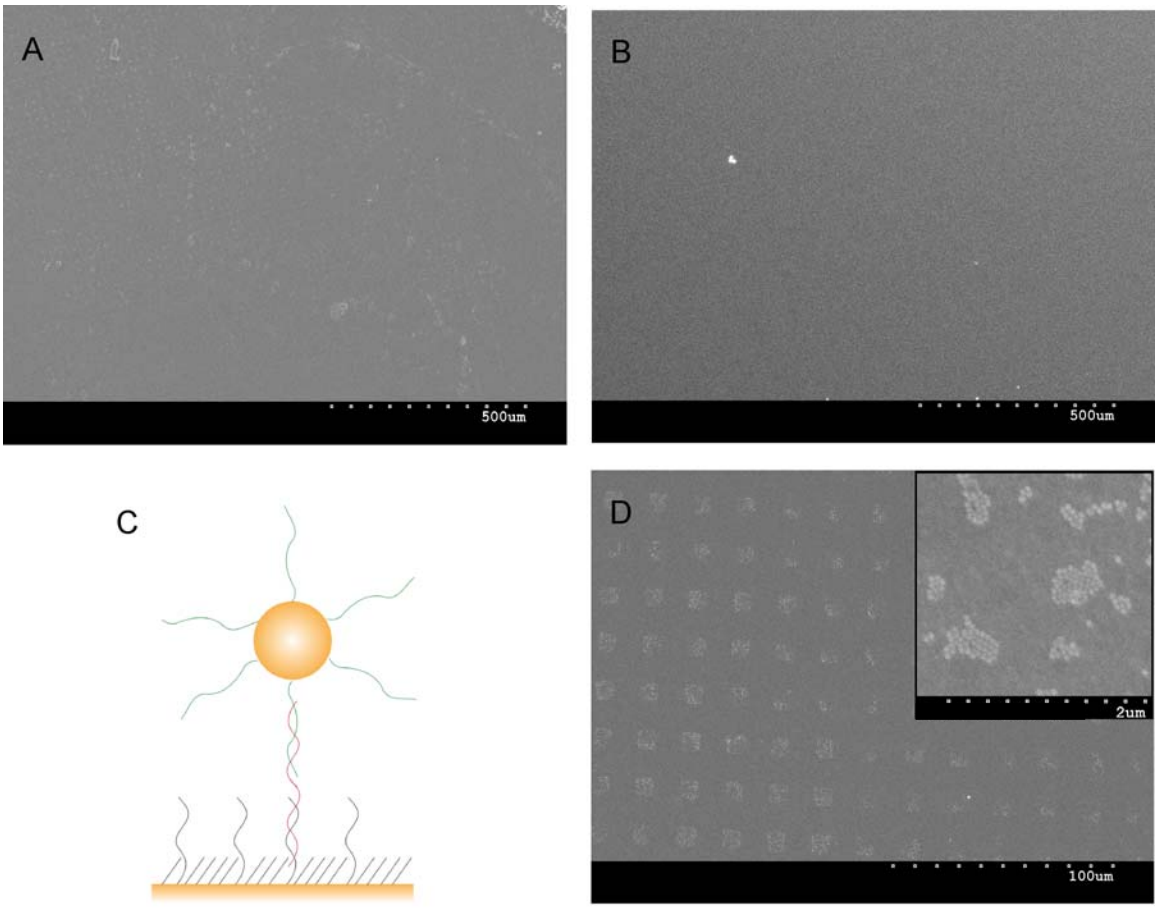

Figure 4-9. SEM images of DNA detection with 50 nm gold nanoparticles, using Flu A sandwich hybridization assay (Flu B noncomplementary template). Square 10 μm pattern is shown in the sample exposed to complementary template (A), but not in the sample exposed to noncomplementary template (B). (C) Representation of sandwich hybridization with nanoparticle tag for detection. (D) Magnified view of sample in (A); inset shows image taken at increased magnification showing that pattern is due to colloidal particles.

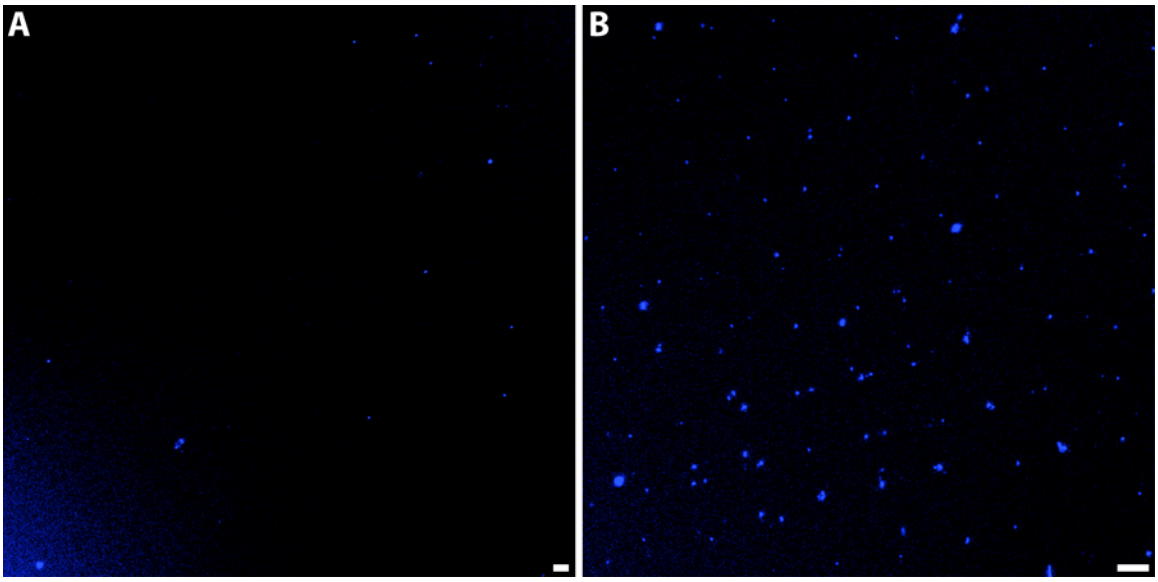

Figure 4-10. Confocal images of fluorescence of Alexa 647 on gold substrates stamped with DNA complementary (A) and noncomplementary (Swine Flu H1N1) (B) to RSV A target strand in sandwich hybridization assay. Stamp posts were 10 μm across; scale bars also represent 10 μm. Images were contrast enhanced equally.

Chapter 5

Conclusions and Future Directions

Conclusions

This thesis described progress made in understanding and controlling the functionalization of surfaces (particulate and planar) with DNA and using these surfaces as substrates in bioassays for sensing applications. Four projects related to this goal were covered. The first was the use of barcoded nanowires as encoded substrates in immobilized Polymerase Chain Reaction (PCR) for the detection of sequences of pathogens. Several parameters were investigated and adjusted in order to increase the reproducibility of specific on-wire PCR reactions. Sulfo-SMCC used with thiolated DNA and an aminated glass surface was shown to be the most thermostable attachment chemistry. The need of a secondary labeling step used in most PCR performed on surface bound nucleic acids in the literature negates the benefit of using intercalating dye, as the assay can no longer be closed tube, which introduces the possibility of contamination between samples, a great detriment in the clinical setting. Those assays performed in the literature using secondary tags, however, seem as though they may be more specific than the assays described in this thesis using intercalating dye as the reporter. This is most likely due not to the specificity of one assay over another, but rather due to the intercalating dye fluorescing in the presence of all amplification products in a non-sequence specific way. One example of an assay that was performed with either an intercalating dye or a secondary tag hybridization step showed that the intercalating dye did not give as satisfying a signal to noise ratio as did the secondary tag.[1] Unfortunately, no controls were performed in this report to confirm the cause of this discrepancy, which may have been due to intercalating dye itself. It is likely that if on-wire

PCR were performed without intercalating dye and then subjected to a secondary sequence-specific tagging step, that the specificity would more closely match that reported in the literature using the same labeling method. Most likely due to the differing systems of each study, many different factors have been identified as the key issue in obtaining quality surface bound amplification. These range from reagent concentration to thermocycling protocol to volume of reaction chamber.[2-5] In order to maintain applicability to other systems performing surface bound amplification reactions, several control experiments were run in this work. Control experiments indicated that the background fluorescence was generated from the interaction of the intercalating dye with the DNA and was specifically dependent on the sequence of the primers. The lack of reproducibility and specificity was most likely due to the generation of a mat of DNA on the wire, which would provide both a competing enzymatic substrate and an environment for the intercalating dye to fluoresce. The second project used Ligase Chain Reaction (LCR) in template detection, which provided for a more reproducible, specific assay, and bypassed the generation of a mat of DNA on the wire surface. This increase in reproducibility of the ligase may have been due to the need for only one enzymatic linkage reaction per amplicon (perhaps limiting DNA mat generation), as opposed to polymerases, which need to perform an enzymatic linkage for every base added. The increase in specificity of the reaction may have been due to the need for three strands of DNA to hybridize, as opposed to only two strands in PCR, to generate an amplicon. On-wire LCR shows a promising exponential amplification reaction alternative to on-wire PCR. The next chapter of this dissertation covered surface functionalization and the stamping of patterned DNA sequences onto a planar substrate as the first step in either multiplexed target detection based on spatial encoding or further nanoarchitecture generation. It was determined that PDMS stamps can be inked with DNA, and that DNA can be transferred from a PDMS stamp to a positively charged glass surface as well as a gold substrate, and that slightly recovered functionalized stamps work better than unfunctionalized or freshly functionalized stamps for

DNA inking and transfer. The DNA's fluorescent signal was most likely being quenched by the gold substrate, or may have been attenuated due to poor conformal contact between the stamp and the substrate. Further investigations into limiting substrate quenching of the fluorophore, such as altering the spacer moiety between the thiol end of the DNA and the span of sequence used to hybridize to the target, as well as altering the backfilling molecule to increase the distance between the substrate and the fluorophore, may be investigated in the future. This methodology may be applied to microcontact insertion printing for the generation of spatially encoded, isolated DNA strands for use in single molecule studies. Lastly, a general chemistry experiment discussing properties on the nanoscale was developed, where students synthesized nanoparticles, performed flocculation experiments, and observed slides with multilayers of colloid, which is covered in the Appendix. This laboratory exercise was originally developed as a makeup lab for use in the first two semesters of general chemistry and has since been incorporated into the experiment schedule for the Materials emphasis laboratory class. Its purpose is to differentiate between properties of the bulk material and nano-scale materials, as well as illustrate basic concepts such as the light spectrum and physical vs. chemical changes.

This thesis described understanding gained in evaluating attachment chemistries, nucleic acid interactions, and alternate enzymatic product permutations affecting immobilized amplification efficiency. Different enzymes were optimized for nucleic acid manipulation and multiplexed sequence detection was accomplished. Surface modification and stamping of patterned DNA sequences was performed. A general chemistry exercise covering nanomaterial properties was also developed.

Future Directions

In the future, on-wire LCR would ideally be used to analyze clinical samples for the presence of respiratory pathogens. Clinical isolate samples have been sent to our lab after being sampled from patients, cultured on Rhesus monkey kidney cells, and extracted, but preliminary LCR experiments utilizing them as templates have not produced detectable signal. Quantified microscopy data for single- and multi-plexed LCR using cDNA (or complementary DNA generated during reverse transcription) produced from clinical isolate samples of Swine Flu H1N1 and RSV B are shown in Figure 5-1. Fluorescence intensity resulting from the presence of complementary clinical cDNA was extremely small and further investigation was done to elucidate the cause. The results of these experiments guide the direction of the future work.

A sandwich hybridization assay was performed using sequences to detect for Swine Flu H1N1 and RSV A, which was much the same format as LCR, but did not include any enzyme, ligation, or amplification. The targets included oligonucleotide, ultramer, or post-PCR product of the aforementioned clinical isolate samples (all sequences used are listed in DNA tables in Chapters 2 and 3). The quantified fluorescence intensity on-wire is shown in Figure 5-2, and while the Swine Flu H1N1 signal for both oligonucleotide and ultramer targets was significantly larger than the RSV A signal, they were both orders of magnitude more intense than the signal generated from the captured clinical isolate samples post-PCR product in this sandwich hybridization assay, and in on-wire LCR using clinical isolate samples. This is partly due to the increased steric hindrance in longer genomic strands (Swine Flu H1N1 oligonucleotide is 58 bases, the ultramer and PCR product are 135 bases, RSV A oligonucleotide is 54 bases, the ultramer and PCR product are 84 bases), as longer ultramers produced less fluorescence signal than their respective shorter oligonucleotides, but is also due to the significantly lower concentration of the clinical isolate samples when compared to synthetic strands. Ultramer and

oligonucleotide templates were added to make a final concentration of 1 μM in the sandwich hybridization assay, and a final concentration of 1 nM in the LCR assays. The Swine Flu H1N1 and RSV B clinical post-PCR products used in the LCR assay were analyzed in real time to monitor amplification and then melting temperature, which are shown in Figure 5-3, and can be used to approximate clinical template concentration. By comparing with known ultramer standards, the concentration was found to be approximately 0.08 pM; this is the same concentration of the clinical template that was used in LCR experiments. In light of the current 0.1 nM limit of detection for the LCR assay, the clinical isolate samples used previously will not be able to generate discernable signal with this procedure.

Clinical samples meeting different criteria may be able to produce specific signal in the future. These criteria include ensuring a ratio of 1.5 or higher for a 260/230 nm measurement, indicating a high ratio of RNA to protein remaining after extraction (the samples in this work generated a 260/230 nm ratio of approximately 0.8), as remaining protein may inhibit the on-wire amplification. RNA should be of a consistent, known concentration (preferably higher than pico molar) and in good condition, *i.e.* not degraded. Once these conditions are met, on-wire LCR can be optimized for detection of RNA template from clinical samples and work can be done to lower the limit of detection.

Because the ligase does not generate the same lack of reproducible specificity that the polymerase does, which seems to be due to the lack of the development of a nucleic acid mat on the nanowire surface, parameters that did not help the optimization of the on-wire PCR may still help the optimization of the on-wire LCR. In order to increase the specificity of the reaction, the association of the enzyme onto the nanowire-bound probe needs to be made more favorable than it currently is; this could be accomplished by making changes in parameters such as varying the surface coverage of the bound probes or altering the linker used between the thiol and the section of sequence on the probe that hybridizes to the template strand. These alterations may not only

provide less steric inhibition to the association of the enzyme onto the hybridized DNA strands bound to the nanowire, but may also decrease the sterics inhibiting the template from hybridizing to the bound probe, especially if that strand is a longer ultramer or PCR amplicon.

By optimizing the interaction of the enzyme with the immobilized DNA strands, the on-wire LCR sensitivity could be increased and the detection of clinical isolate template samples could be achieved. As each on-wire amplification for different pathogen specific sequences will have a differing efficiency, parameters such as probe concentration could be modified to generate comparable signal across multiple detection sequences. Once on-wire LCR was optimized for the detection of clinical isolates, other clinical samples could be used, such as RNA that has been extracted from patients' clinical specimens, but that has not been cultured. This process could then be transferred to being performed solely in the diagnostic lab; wires with bound probes and on-wire LCR reaction mix could be pre-made in a kit format so that laboratory technicians could complete the assay without need for materials generation or optimization. If this kit could successfully identify multiple possible pathogens present in clinical samples, then additional experimentation to generate specific signal in the presence of possible contamination from the sampling process could also be explored. On-wire LCR shows promise as a method for pathogen detection in clinical settings and could streamline the currently labor intensive and time consuming diagnostic process.

References

1. von Nickish-Rosenegk, M.; Marschan, X.; Andresen, D.; Abraham, A.; Heise, C.; Bier, F. F. On-chip PCR amplification of very long templates using immobilized primers on glassy surfaces. *Biosens. Bioelectron.* **2005**, *20* (8), 1491-1498.

2. Tiemann-Boege, I.; Curtis, C.; Shinde, D. N.; Goodman, D. B.; Tavaré, S.; Arnheim, N. Product length, dye choice, and detection chemistry in the bead-emulsion amplification of millions of single DNA molecules in parallel. *Anal. Chem.* **2009**, *81* (14), 5770-5776.

3. Carmon, A.; Vision, T. J.; Mitchell, S. E.; Thannhauser, T. W.; Müller, U.; Kresovich, S. Solid-phase PCR in microwells: Effects of linker length and composition on tethering, hybridization, and extension. *Biotechniques* **2002**, *32* (2), 410-420.

4. Palanisamy, R.; Connolly, A. R.; Trau, M. Considerations of solid-phase DNA amplification. *Bioconjugate Chem.* **2010**, *21* (4), 690-695.

5. Drobyshev, A. L.; Nasedkina, T. V.; Zakharova, N. V. The role of DNA diffusion in solid phase polymerase chain reaction with gel-immobilized primers in planar and capillary microarray format. *Biomicrofluidics* **2009**, *3* (4), 0441122.

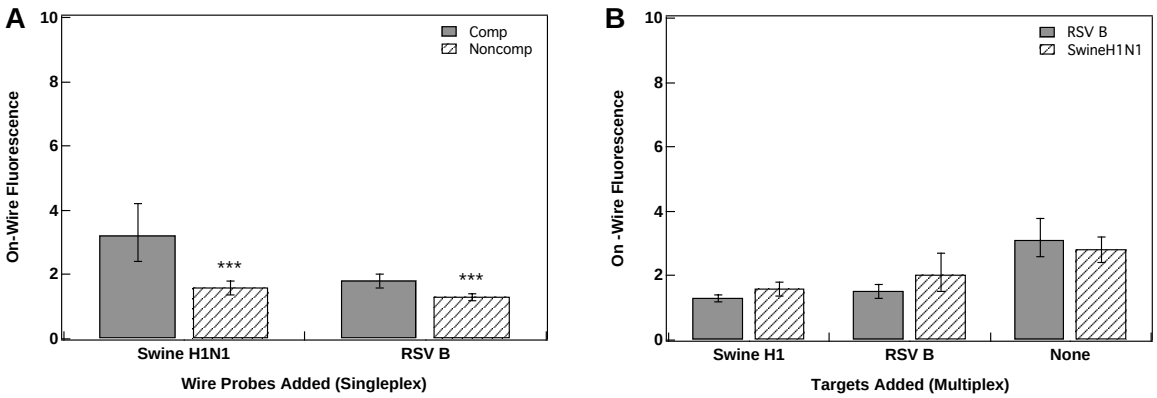

Figure 5-1. Quantified on-wire fluorescence for single- (A) and multi-plexed (B) LCR assay using Swine Flu H1N1 and RSV B cDNA from clinical samples as the template. *** p value < 0.001 versus signal in the presence of complementary template.

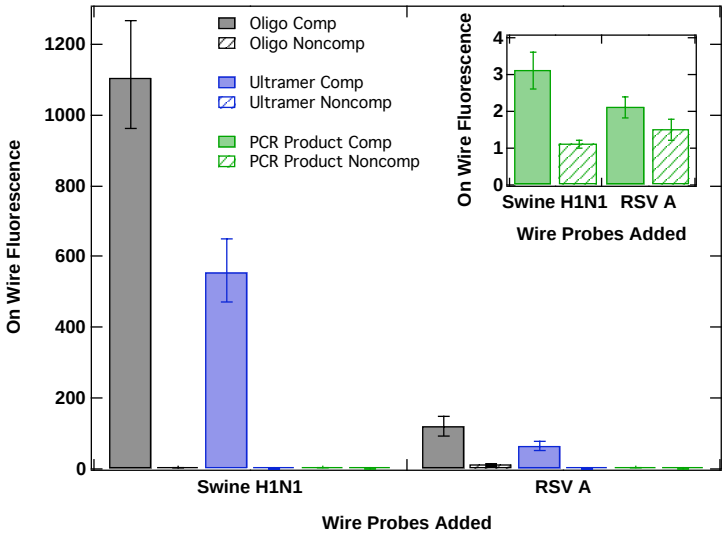

Figure 5-2. Single-plexed sandwich hybridization assay using oligonucleotide, ultramer, and post-PCR products of clinical isolate samples as the templates, respectively, for both Swine Flu H1N1 and RSV A sequences. Inset shows post-PCR product hybridization in more detail. The ultramer and PCR amplicons share the same sequence hybridized to the wire-bound probe as the oligonucleotides, however they have tens more bases protruding into solution.

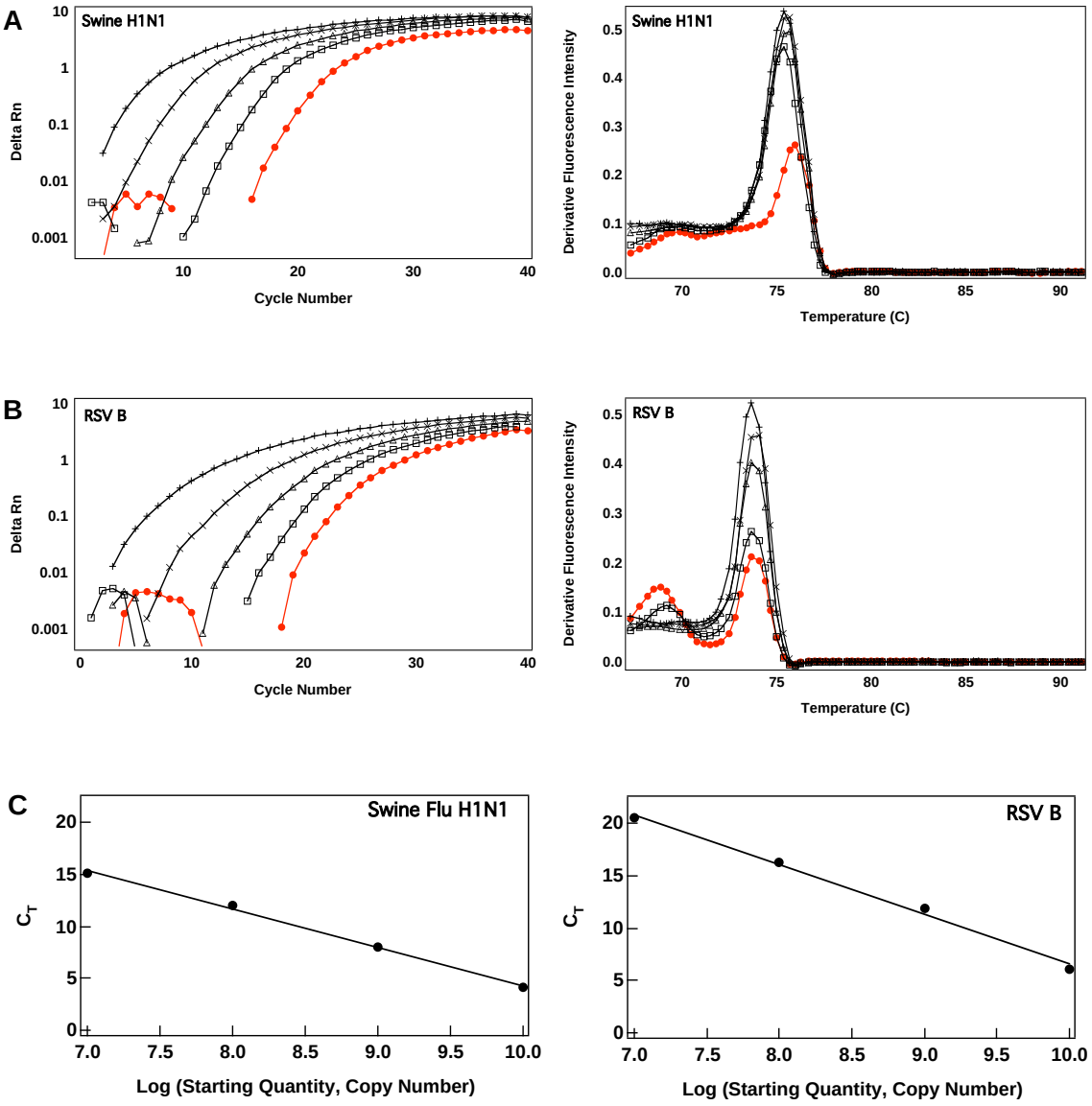

Figure 5-3. Real time PCR amplification plots and dissociation curves for ultramer and clinical sample Swine Flu H1N1 (A) and RSV B (B) templates. Each line in black shows ultramer control amplification at different concentrations; hash marks represent 0.83 nM template, x's 0.08 nM, triangles 8.3 pM, and squares 0.83 pM. The clinical samples are shown in red filled circles, and are approximately 0.08 pM (found using the standard curve in C), which is the same concentration used in LCR experiments.

Appendix

Introductory Chemistry Laboratory Experiment: Gold Nanoparticles – Synthesis and Multilayering

High school teacher Seth Dougherty developed a laboratory exercise on multilayering gold nanoparticles onto slides, which included movies on nanoscale concepts; this work is complementary to that.

Abstract

This laboratory exercise was originally developed as a makeup lab for use in the first two semesters of general chemistry and has since been incorporated into the experiment schedule for the Materials emphasis laboratory class. Its purpose is to differentiate between properties of the bulk material and nano-scale materials, as well as illustrate basic concepts such as the light spectrum and physical vs. chemical changes.

Included here are all the files necessary to run this exercise, including:

The lab manual, complete with introduction and practice quiz

The pre-lab quiz

All necessary answer keys and the grade sheet

The pre-lab talk overhead and TA notes

The list of materials needed

The lab overview of concepts to study for the final

A post-lab quiz to evaluate the exercise's success

This exercise has been revised several times after multiple trial runs with students. In the future, this lab may be submitted to the Journal of Chemical Education.

Gold Nanoparticles –

Synthesis and Multilayering

Name: _____

Partner's Name: _____

TA: _____

Chemistry 14 - 106

Gold Nanoparticles: Synthesis and Multilayering

Sarah Brunker

Background

Nanoparticles have been used over a long period of time for a wide variety of applications. They are believed to have been in use as far back in time as Ancient Rome and are still in use today. Gold colloid was used both as a pigment to make stained glass windows as well as a cure-all, and today can be used to stain tissue samples when bound to proteins. In this lab you will be making gold colloid as well as observing its properties as its environment is changed.

Colloidal solutions are comprised of tiny particles (usually between 1 and 150 nm) that are suspended throughout another medium, which do not fall out of solution due to Brownian motion, or collisions with solvent molecules. Gold colloid can be made by adding sodium citrate to a gold salt solution. The gold ions are reduced by the sodium citrate and begin to "stick" to other gold atoms to form nanoparticles. By stirring the colloidal solution, an even distribution of nanoparticle size results. The sodium citrate is absorbed into these particles and gives them a negative charge, which results in the particles repelling each other, preventing aggregation. Aggregation is the further clumping together of the nanoparticles, until they are so large that they crash out of solution.

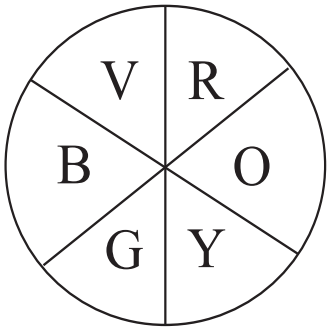

Color wheel demonstrating complementary colors.[9]

Colloidal solutions scatter light, but also absorb certain wavelengths, which depend on the size of the particle. Gold colloid will absorb green light and thus looks red, since that is the color transmitted. See the color wheel to visualize this "opposing" color relationship. If the

colloidal solution is forced to aggregate, as the number of particles in the aggregates and the diameter of the aggregates increases, the distance between the aggregates decreases. The wavelength absorbed shifts and the aggregates look blue. This aggregation can be initiated by adding charged particles to the solution (dissolved salt, for example). These charges "screen" the particles' charges from one another; their negative charges no longer repel each other, and they begin to clump together and fall out of solution, or aggregate. The distance at which charge can influence other charges is called the Debye length; by increasing the salt concentration of the surrounding solution, the Debye length of the charged particles decreases and the charged particles fail to repel each other, enabling particle interaction and eventual aggregation. Particles interact due to van der Waals forces, or attractions that are not covalent or electrostatic, such as those between dipoles, which are oppositely charged poles of a molecule or particle.

Included in this packet is a picture of a gold colloid solution that was prepared in the same manner that you will prepare it in this lab. This image was acquired using a transmission electron microscope, or TEM, which (instead of shining light on the sample) illuminates the sample with electrons, allowing for much better resolution, or the ability to see very small dimensions. The increased resolution of electron microscopy over optical microscopy is due to the fact that photons, or light particles, oscillate with a certain wavelength, which produces different colors of light. This oscillation limits the resolution of light microscopy to several hundred nanometers (or nm); electron microscopy enables three orders of magnitude better resolution. The particles shown in the TEM image are spherical and uniform, and approximately 13 nm in diameter. This small size is could not be distinguished with light microscopy, but by observing the decreased transmission of electrons through the particles, which results in the dark contrast of the particles, electron microscopy can provide an image of these tiny particles.

A flocculation assay will be performed on these nanoparticles, which means that a substance will be added to purposefully aggregate the colloids. Aggregation depends on the

substance added to the colloidal solution, as well as how much of it is added. The aggregation is indicated with a color change, which can be observed using an UV/Vis Spectrophotometer, or by your eyes. Two substances will be added to the colloid solution, which may or may not aggregate the nanoparticles; they are sodium chloride and sucrose.

TEM Image of Gold Nanoparticles

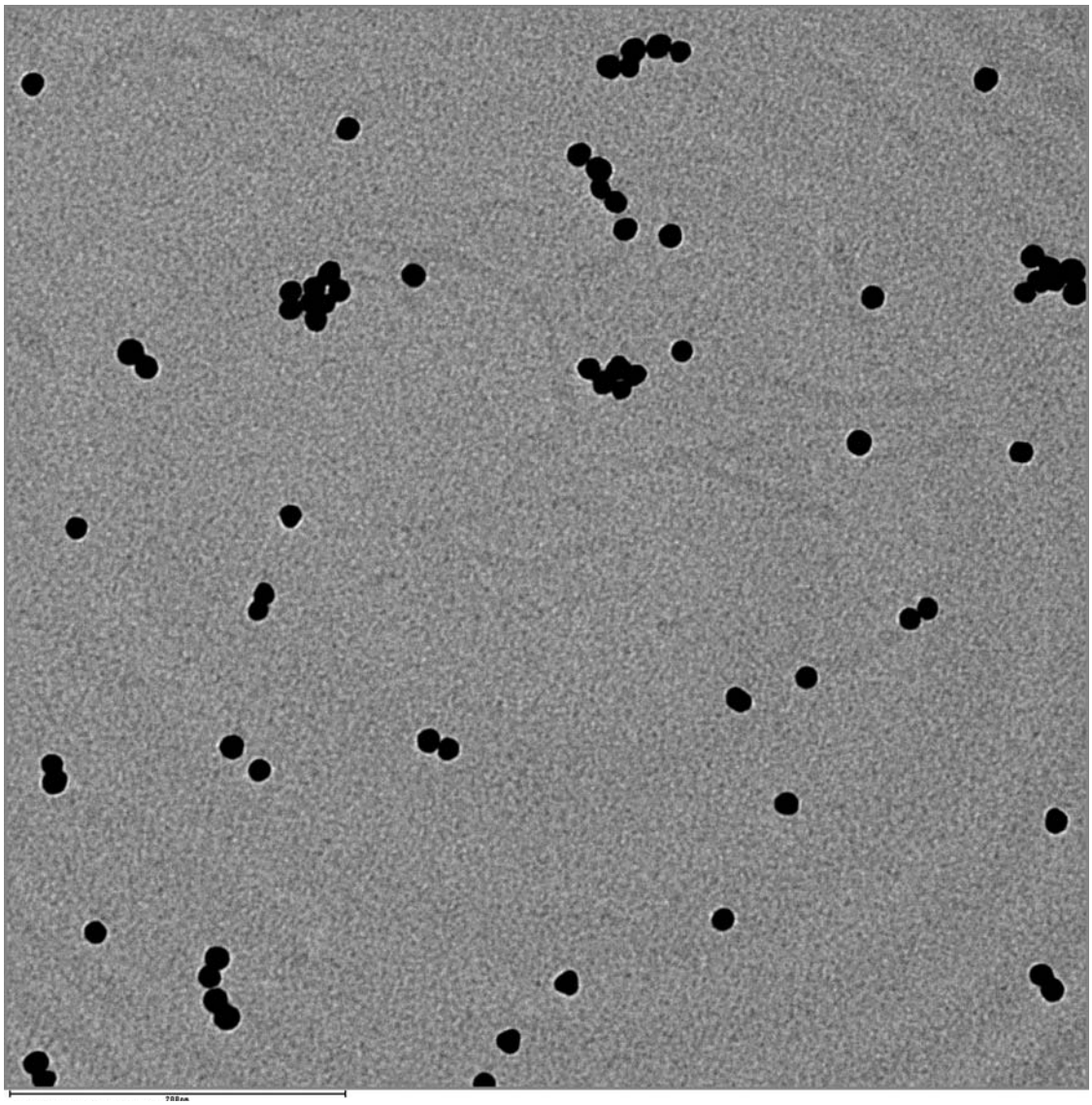

200 nm

It is possible to protect the nanoparticles from aggregating by coating them in compounds such as enzymes, proteins, or small molecules, as well as other substances. In this experiment, you will be coating your nanoparticles with a layer of surfactant, or a molecule with a hydrophilic head group and a hydrophobic tail, which decreases surface tension. Surfactant molecules (a.k.a. detergent molecules) can group together to form layers (known as monolayers) or spheres, which are known as micelles. When a nanoparticle is exposed to a surfactant solution, van der Waals forces physisorb (a type of adsorption—or sticking to the surface) the surfactant to the particle surface, see the figure below. When a nanoparticle is coated with a surfactant, steric (or physical) interactions prevent the gold nanoparticles from touching each other, therefore protecting them from aggregating with one another. This is a physical interaction, there is no charge repulsion between the Tween 20 molecules. Even when ions are introduced to the system, and the nanoparticles are screened from one another, they will not aggregate because the surfactant molecules are in between them, preventing them from touching each other and crashing out of solution.[10]

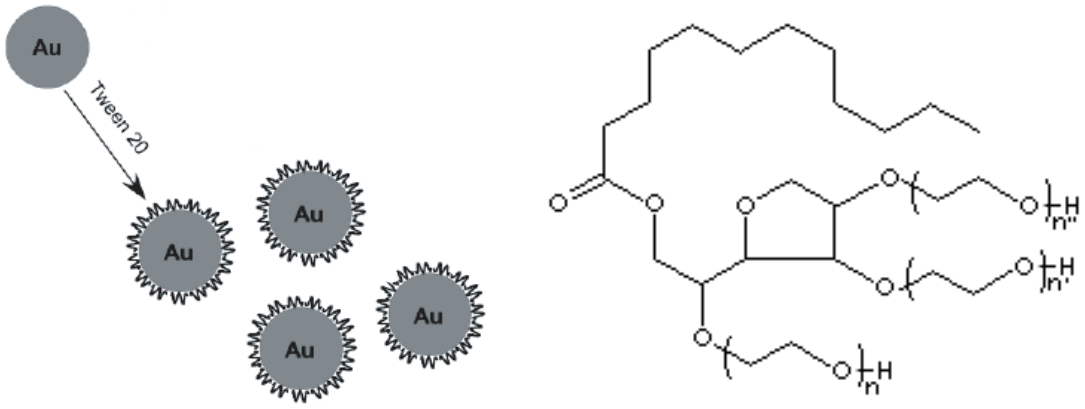

Left: Gold nanoparticles being coated with Tween 20 (symbolized by kinked lines).[10] Despite being screened from each other, the nanoparticles do not aggregate due to steric interference. **Right:** Schematic of Tween 20.

You will also compare bulk properties, those of a material that has enough atoms to act as a larger piece of the material, to nanoscale properties, where the size of the material is on the nanometer scale. Although they may seem as though they should be the same, as you increase the amount of substance present, often the properties change. This can be illustrated by slides that have been made to each have a different number of layers of gold colloid. Eventually the properties, such as reflectivity, resistance, and color will approach the properties of the bulk material.

These slides started out as plain glass slides. These glass slides were derivatized with APTMS (3-aminopropyltrimethoxysilane), which acts like glue between the glass and the gold nanoparticles. The OH group on the glass reacts with the OCH_3 group on the APTMS, and the APTMS is bound to the slide. The slide is rinsed off with distilled water and methanol to make sure there are no other particles or substances present, and then the colloid is exposed to the slide, creating a layer of gold. The slide is again rinsed with water, and then dipped in mercaptoethylamine (MEA), which binds to the colloid at both the SH and the NH_2 end, as well as screens the colloid's repulsive charges between layers. These rinses and dips in MEA result in multiple layers of gold nanoparticles on a surface. The structures drawn below should help to visualize this process, there will also be a short movie shown during the prelab discussion demonstrating this process.

APTMS

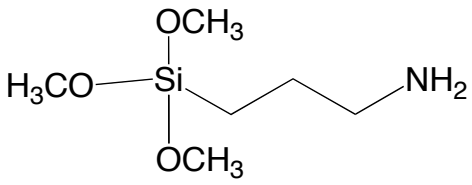

MEA

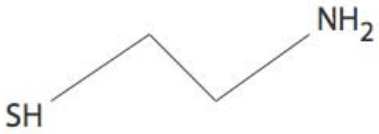

Sucrose

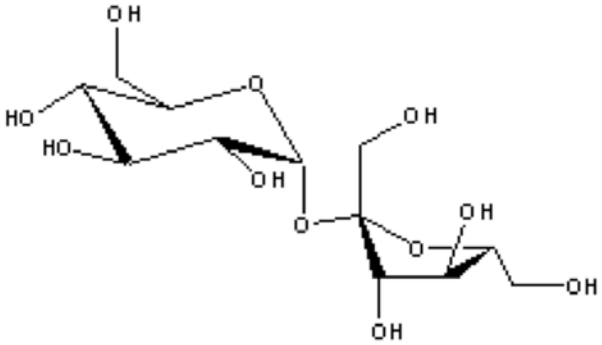

Sodium Citrate

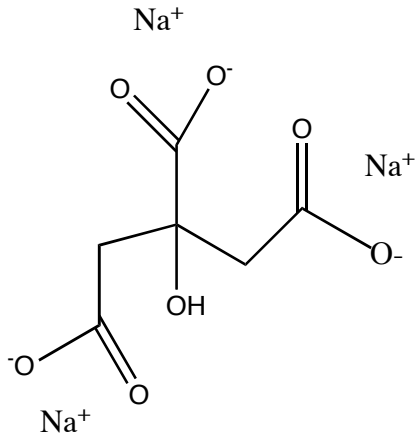

Silanization of Slide[1]

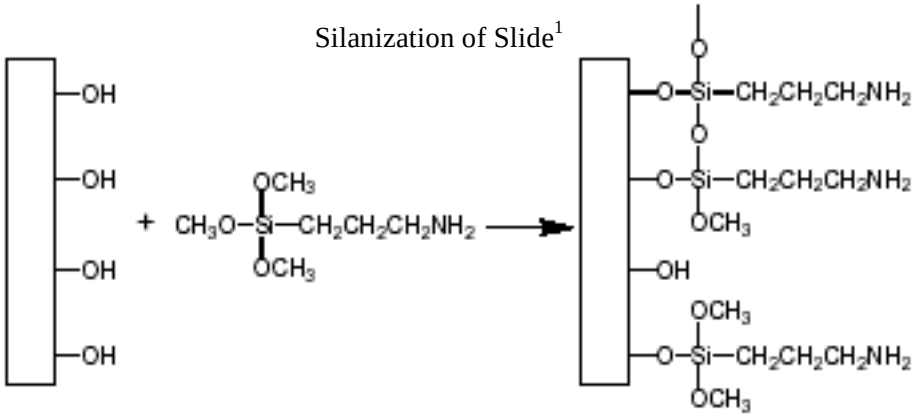

Slide Reaction Diagram[8]

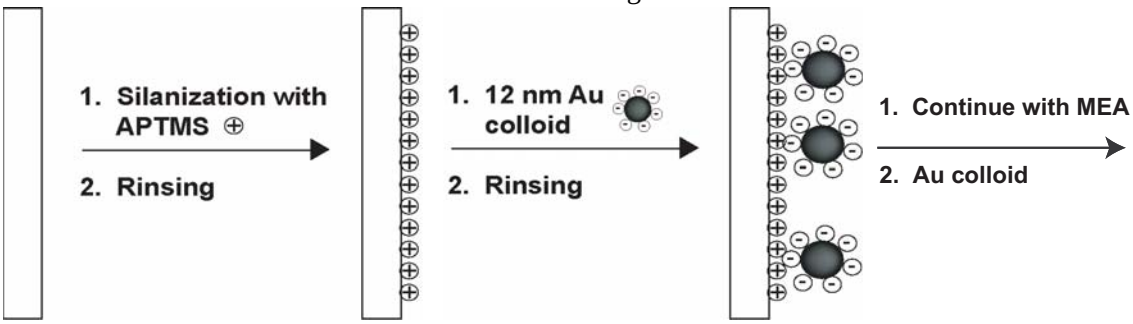

References

1. Keating, C. D.; Musick, M. D.; Keefe, M. H.; Natan, M. J. Kinetics and thermodynamics of Au colloid monolayer self-assembly: Undergraduate experiments in surface and nanomaterials chemistry. *J. Chem. Educ.* **1999**, *76*, 949–955.

2. McFarland, A. D.; Haynes, C. L.; Mirkin, C. A.; Van Duyne, R. P.; Godwin, H. A. Color my nanoworld. *J. Chem. Educ.* **2004**, *81*, 544A.

3. Musick, M. D.; Keating, C. D.; Keefe, M.; Natan, M. J. Stepwise construction of conductive Au colloid multilayers from solution. *Chem. Mater.* **1997**, *9*, 1499-1501.

4. Musick, M. D.; Keating, C. D.; Lyon, L. A.; Botsko, S. L.; Peña, D. J.; Holliway, W. D.; McEnvoy, T. M.; Richardson, J. N.; Natan, M. J. Metal films prepared by stepwise assembly. 2. Construction and characterization of colloidal Au and Ag. *Chem. Mater.* **2000**, *12*, 2869-2881.

5. Musick M.; Pena D.; Botsko S.; McEvoy T. Electrochemical properties of colloidal Au-based surfaces: Multilayer assemblies and seeded colloid films. *Langmuir* **1999**, *15*, 844-850.

6. Grabar, K. C.; Allison, K. J.; Baker, B. E.; Bright, R. M.; Brown, K. R.; Freeman, R. G.; Fox, A. P.; Keating, C. D.; Musick, M. D.; Natan, M. J. Two-dimensional arrays of colloidal gold particles: A flexible approach to macroscopic metal surfaces. *Langmuir* **1996**, *12*, 2353-2361.

7. Dougherty, S. *Nanoparticles*. Personal Communication.

8. Brennan, J. Personal Communication.

9. Thompson, S. *PSU Chemtrek*, Hayden-McNeil Publishing, Inc., Plymouth, MI, **2004-2005** Version, pg. 3-4.

10. Aslan, K.; Pérez-Luna, V. H. Surface modification of colloidal gold by chemisorption of alkanethiols in the presence of a nonionic surfactant. *Langmuir* **2002**, *18*, 6059-6065.

Quiz Outline

Name 2 applications for gold nanoparticles in the past.

What is a colloidal solution?

Explain why gold colloid looks red.

What is a flocculation assay? What is aggregation?

What are some properties that may be different between nanoparticles and a bulk sample of the same composition?

Draw a picture of how the multiple layers were placed on the glass slide (you may use chemical abbreviations.)

What are the four types of reactions that were described in Experiment 7 in your Chemtrek?

How many grams of NaCl will you need to make up 15 mL of a 0.25 M NaCl solution? (Na = 22.99 g/mol, Cl = 35.45 g/mol)

What is a physical change? What is a chemical change?

What compounds can be used to protect a colloid solution from aggregation?

What is a surfactant? What is physisorption?

Sample Quiz

1. How many grams of sucrose ($C_{12}H_{22}O_{11}$, or table sugar) would you need to make up 10 mL of 1.5 M sucrose solution? (C = 12.01 g/mol, H = 1.008 g/mol, O = 16.00 g/mol)

2. List the four types of reaction that were outlined in Experiment 7 of your Chemtrek.

3. Define colloidal solution.

4. What was the chemical used to bind a layer of gold nanoparticles on top of another layer, and how did it work?

5. What does a flocculation assay do to the sample?

Section A: Making Colloid Solution

You should work with your lab partner. You will also need **eye protection** and **nitrile gloves** due to the caustic nature of $HAuCl_4$.

1. Clean the following glassware once with soap and rinse well with distilled water: two 10 mL graduated cylinders, 2 small beakers, two 8 mL vials, two 20 mL vials, and a small Erlenmeyer flask. Make sure you rinse your glassware with distilled water and not tap water.

2. Obtain 2 mL of 0.038 M $Na_3C_6H_5O_7$ (sodium citrate) solution. Pour some solution into a small beaker, and measure out 2 mL into the second beaker using the 1 mL pipetor. Take only the second beaker back to your station. The excess sodium citrate solution may be dumped down the drain with running water.

3. Place a magnetic stir bar (that has been rinsed with distilled water) into your flask. Measure out 20 mL of the 0.001 M $HAuCl_4$ solution into a graduated cylinder; you may use a plastic pipet to achieve exactly the correct volume. Pour the 0.001 M $HAuCl_4$ (gold salt) solution into the flask. Take only this flask back to your station. Place the hot plate in front of the fume hood. Bring the gold salt solution to a rolling boil on a hot plate while vigorously stirring the solution.

4. After the solution has begun to boil, add the 2 mLs of the $Na_3C_6H_5O_7$ solution. The solution should continue to boil and be stirred. Watch carefully, several changes will occur.

Q1: a) What did the solution look like before you added the sodium citrate solution to your gold salt solution?

b) Record your observations of what happened immediately after you added the sodium citrate solution.

5. As the water boils off, add distilled water to keep the volume at about 20 mLs. Heat on the hot plate, and **remove after 10 minutes**. Then, remove the solution from the hot plate with tongs or heat resistant gloves, and allow it to cool.

Q2: What other color changes occurred as you heated your solution?

Q3: a) Of the four types of reactions described in Experiment 7, what type of reaction just occurred to create these nanoparticles?

b) Why was stirring the solution necessary?

Q4: What is a colloidal solution?

Q5: a) Evaluate the quality of your colloid solution.

b) Is it the color and consistency it should be?

c) Do you think the particles are uniform? (You may want to look at the TEM image of a colloid solution prepared in this manner.)

Section B: Flocculation Assay

You will observe the effects of adding different substances to your colloid solution, including whether or not the nanoparticles aggregate and fall out of solution. You will also protect your colloid solution using a surfactant.

1. Make up a 10 mL solution of 1.0 M sodium chloride in one of your 20 mL vials. Be sure to wash your graduated cylinder thoroughly between solutions with distilled water and soap. (Na = 22.99 g/mol, Cl = 35.45 g/mol)

Q6: How many grams of NaCl will you need to make this solution? Make sure to show your calculation in your notebook.

2. Make up a 10 mL solution of 1.0 M sucrose ($C_{12}H_{22}O_{11}$, or table sugar) in your other 20 mL vial. (C = 12.01 g/mol, H = 1.008 g/mol, O = 16.00 g/mol)

Q7: How many grams of sucrose will you need to make this solution? Make sure to show your calculation in your notebook.

3. You will need your two 8 mL vials for this step. Place 3 mLs of your colloid solution into each of the two vials. Also, place 3 mLs of distilled water into the two vials. You should now have a diluted colloid solution in each vial.

4. With a pipet, drop 5-10 drops of the NaCl solution into the first vial of diluted colloid. Be sure to observe the effects from above as well as from the side.

Q8: a) Record your observations.

b) How is the solution different from what it looked like before you added the salt?

c) Is this a physical or a chemical change, and why?

d) Draw a picture of what you think is going on at the microscopic level.

5. With a pipet, drop 5-10 drops of the sucrose solution into the second vial of diluted colloid.

Q9: a) Record your observations.

b) How is the solution different from what it looked like before you added the sugar?

c) Can you add enough sugar to achieve the same results as you did with the salt solution?

Q10: a) Why does adding the salt solution have a different effect than adding the sugar solution? (Hint: think about dissociation and its effects.)

b) Why do the particles in solution not aggregate (come together to form larger particles) before you add anything else to the solution? (Hint: don't forget about the negatively charged absorbed citrate ions).

6. Dump out your sucrose solution and wash the vial. Keep your other three vials of solution. Place 3 mLs of your colloid solution, and 3 mLs of distilled water in the vial. Add three drops of the surfactant Tween 20 directly from the dropper bottle to your vial. Shake the solution gently and then let it sit for 20 minutes.

Q11: a) What is a surfactant?

b) What is physisorption?

Q12: a) What is the purpose of adding the Tween 20 to your colloid solution?

b) What do you think will happen if you add your salt solution to the mixture?

c) Draw, on a microscopic scale, your prediction.

Q13: What are steric interactions and how do they prevent aggregation of gold nanoparticles?

7. Draw up some sodium chloride solution into a pipet and place the pipet into the solution *below* the level of bubbles. Dispel some of the NaCl solution into the colloid/Tween 20 solution.

Q14: a) Record your observations.

b) Compare the colloid/Tween 20 solution (after NaCl has been added) to the two other colloid solutions without Tween 20. How were the results of the three solutions similar and different after the NaCl was added?

c) Draw, on a microscopic scale, what actually happened to your colloid/Tween 20 solution after you added the NaCl.

8. When you dump your colloid solutions in the waste container, make sure to remove the stir bar first.

Section C: Observing Multilayered Gold-Covered Slides

At the front of the room there are glass slides that have been coated with gold outside of class. The questions in this section pertain to these slides.

Q15: Before you begin, explain how the slides were made (including chemical names), you may want to include a diagram.

1. Do not take the slides out of their containers. Look at the slide marked "1" straight on.

Q16: What does the slide look like? Draw a picture of the slide and label its colors.

2. Now, look at all the slides, 1-10.

Q17: a) Draw a picture of slide #10 and label its colors.

b) What are the differences between the slides?

c) What accounts for these differences?

3. Pick up the container holding slide #10. Angle the vial so that the light shines off the slide. Now, pick up slide #1, and angle it so that the light hits it.

Q18: How do the two slides look different when light is shone on them?

4. In the eleventh container there is a piece of bulk gold. Look at this piece of metal both straight on and from an angle.

Q19: a) What does the piece of bulk gold look like, what color is it?

b) How does the piece of bulk gold look different from the glass slide that has 10 coatings of gold on it?

c) Which do you think conducts electricity better, and why?

d) Why are the properties of these two substances so different?

Q20: a) If the slides were continued to be covered in layers of gold, what would they eventually resemble?

b) How is it possible to put multiple layers of gold nanoparticles (which has a negative charge) on the surface of the glass slides? (Do not just restate the procedure – explain how/why the procedure works.)

5. Surface coverage is a property that describes how many small particles can fit on a larger particle or material. We will calculate the maximum possible surface coverage (or number of gold particles) for our 2.5 cm × 0.9 cm slides. Assume that the diameter of one nanoparticle sphere is 12 nm. Also assume that there is no empty space (don't worry about how the particles pack or that they may repel each other). You may imagine the edge of the colloid to be flexible, where its shape may be altered to fit the available space, so long as the area taken up does not change.

Q21: Calculate the "footprint" area of the nanoparticle sphere. (If you were looking down on one colloid, what would you see, and how big would it be?)

Q22: Calculate the maximum surface coverage the slides will have when covered with these particles. Be sure to explain whether this answer is for one side or both sides of the slide.

Name:_____

TA:_____

Date: _____

Pre Lab Quiz for Nanoparticle Makeup Lab

1. How many grams of NaCl will you need to make up 5 mL of a 0.75 M NaCl solution? (Na = 22.99 g/mol, Cl = 35.45 g/mol)

2. What is a colloidal solution?

3. Explain what aggregation is.

4. If I made a nanoparticle that was blue, what color would it be absorbing? What color would be passed through it?

5. Give one example of each: a physical change and a chemical change. (They do not need to be examples from today's lab).

Nanoparticle Makeup Lab Answer Key

Q1: a) What did the solution look like before you added the sodium citrate solution to your gold salt solution? b) Record your observations of what happened immediately after you added the sodium citrate solution.

(3 pts) A: a) Before the sodium citrate was added, the solution was boiling and yellow. b) Immediately after the sodium citrate was added, the solution went clear, and then gray.

Q2: What other color changes occurred as you heated your solution?

(2 pts) A: As the solution was heated it turned purple; it finally became wine red.

Q3: a) Of the four types of reactions described in Experiment 7, what type of reaction just occurred to create these nanoparticles? b) Why was stirring the solution necessary?

(2 pts) A: a) A redox reaction occurred. Gold colloid can be made by adding sodium citrate to a gold salt solution. The gold is reduced by the sodium citrate and begins to "stick" to other gold particles to form nanoparticles. The sodium citrate is absorbed into these particles and gives them a negative charge, which results in the particles repelling each other, preventing aggregation, or further clumping together and crashing out of solution. b) By stirring the colloidal solution, an even distribution of nanoparticles size results.

Q4: What is a colloidal solution?

(3 pts) A: Colloid solutions are comprised of tiny particles (usually between 1 and 150 nm) that are suspended throughout another medium, which do not fall out of solution due to Brownian motion, or collisions with solvent molecules. Colloidal solutions scatter light, but also absorb certain wavelengths, which depend on the size of the particle.

Q5: a) Evaluate the quality of your colloid solution. b) Is it the color and consistency it should be? c) Do you think the particles are uniform? (You may want to look at the TEM image of a colloid solution prepared in this manner.)

(3 pts) A: a/b) The colloid solution will be of good quality if it is wine red and not clumpy. c) Yes, the particles are spherical (approximately 12-13 nm wide) and uniform as demonstrated in the TEM image.

Q6: How many grams of NaCl will you need to make this solution? Make sure to show your calculation in your notebook.

(4 pts) A: Want 10 mL of 1.0 M NaCl solution

M = mol/L so: (M)(L) = mol

10 mL / (1000mL/L) = 0.01 L

(1.0 M)(0.01 L) = 0.01 mol NaCl

23 g/mol + 35g/mol = 58 g/mol NaCl

(0.01 mol)(58 g/mol) = 0.58 g NaCl needed

Q7: How many grams of sucrose will you need to make this solution? Make sure to show your calculation in your notebook.

(4 pts) A: Sucrose = $C_{12}H_{22}O_{11}$

Need 10 mL of 1.0 M sucrose

Need 0.01 M sucrose (same calc. as Q6)

(12 g/mol)(12 C) + (1 g/mol)(22 H) + (16 g/mol)(11 O) = 342 g/mol sucrose

(0.01 mol)(342 g/mol) = 3.42 g sucrose needed

Q8: a) Record your observations. b) How is the solution different from what it looked like before you added the salt? c) Is this a physical or a chemical change, and why? d) Draw a picture of what you think is going on at the microscopic level.

(7 pts) A: a/b) The solution turned from reddish to bluish. It looked wispy, and the blue solution fell to the bottom of the vial (should be seen when observing the vial from the side). c) This is a physical change because the particles are simply coming together, or aggregating. There is no chemical reaction occurring.

d) The picture should show groups of particles coming together to form larger groups of particles in the presence of ions. (Like diagram from video).

Q9: a) Record your observations. b) How is the solution different from what it looked like before you added the sugar? c) Can you add enough sugar to achieve the same results as you did with the salt solution?

(3 pts) A: a/b) The solution is still red, although there were some clear wispy currents in the solution. c) No, with 60 drops of sugar solution added, the colloid solution is still red.

Q10: a) Why does adding the salt solution have a different effect than adding the sugar solution? (Hint: think about dissociation and its effects.) b) Why do the particles in solution not aggregate (come together to form larger particles) before you add anything else to the solution? (Hint: don't forget about the negatively charged absorbed citrate ions).

(6 pts) A: a) The salt solution completely dissociates into ions in solution, these ions screen the particles from one another so that they don't repel each other. The colloid then aggregates. The sugar solution does not dissociate, and so does not create ions. The colloid continues to repel itself. b) The particles in the solution don't aggregate because they have negatively charged citrate ions absorbed into them, which repel each other. The colloids never come close enough to each other to aggregate.

Q11: a) What is a surfactant? b) What is physisorption?

(4 pts) A: a) A molecule with a hydrophilic head group and a hydrophobic tail, which decreases surface tension, a.k.a. detergent. b) A type of adsorption—or sticking to the surface, due to Vander Waals forces.

Q12: a) What is the purpose of adding the Tween 20 to your colloid solution? b) What do you think will happen if you add your salt solution to the mixture? c) Draw, on a microscopic scale, your prediction.

(6 pts) A: a) Tween 20 is added to act as a protecting agent for the colloid against aggregation. It coats the surface in a monolayer and keeps the particles apart by steric interference. b) If salt is added to the mixture, it will dissociate into ions, but they will not aggregate the particles because, although they screen them from each other, the surfactant will protect the colloid. c) The picture should look like the picture in the background section, but there should also be Na^+ and Cl^- ions in the solution. There should be no aggregation.

Q13: What are steric interactions and how do they prevent aggregation of gold nanoparticles?

(2 pts) A: Steric (or physical) interactions prevent the gold nanoparticles from touching each other, therefore protecting them from aggregating with one another. This is a physical interaction, there is no charge repulsion between the Tween 20 molecules. Even when ions are introduced to the system, and the particles are screened from one another, they will not aggregate because the surfactant molecules are in between them, preventing them from touching each other and crashing out of solution.

Q14: a) Draw up some sodium chloride solution into a pipet and place the pipet into the solution *below* the level of bubbles. Dispel some of the NaCl solution into the colloid/Tween 20 solution. Record your observations. b) Compare the colloid/Tween 20 solution (after NaCl has been added) to the two other colloid solutions without Tween 20. How were the results of the three solutions similar and different after the NaCl was added? c) Draw, on a microscopic scale, what actually happened to your colloid/Tween 20 solution after you added the NaCl.

(4 pts) A: a) After the NaCl is added to the colloid/Tween 20 solution, nothing should happen. b) The results were the same as after the sucrose was added to the colloid solution. There was no aggregation. The results were different from adding the salt solution to the colloid solution without Tween 20 because there solution did not turn blue, there was no aggregation.

c) This picture should look like the answer to Q12 c's answer.

Q15: Before you begin, explain how the slides were made (including chemical names), you may want to include a diagram.

(6 pts) A: These slides started out as plain glass slides. These glass slides were derivatized with APTMS (3-aminopropyltrimethoxysilane), which acts like glue between the glass and the gold colloid. The OH group on the glass reacts with the CH_3 group on the APTMS, and the APTMS is bound to the slide. The slide is rinsed off with distilled water and methanol to make sure there are no other particles or substances present, and then the colloid is exposed to the slide, creating a layer of gold. The slide is again rinsed with water, and then dipped in mercaptoethylamine (MEA), which binds to the colloid at both the SH and the NH_2 end, as well as screens the colloid's repulsive charges between layers

See also: slide reaction diagrams in background chemistry.

Q16: What does the slide look like? Draw a picture of the slide and label its colors.

(2 pts) A: The first slide should be rectangular, relatively transparent, not very reflective, and pink. As the slides progress they get blue/gray/purple, sometimes a little splotchy, and more reflective.

Q17: a) Draw a picture of slide #10 and label its colors. b) What are the differences between the slides? c) What accounts for these differences?

(3 pts) A: a) Slide #10 should be reflective, opaque, and bluish purple. b) The color from slide to slide is different. The color darkens as the number of layers of gold colloid increases. c) The increasing amount of gold accounts the changing properties.

Q18: How do the two slides look different when light is shone on them?

(2 pts) A: The reflectivity increases as the number of layers of gold colloid increases.

Q19: a) What does the piece of bulk gold look like, what color is it? b) How does the piece of bulk gold look different from the glass slide that has 10 coatings of gold on it? c) Which do you think conducts electricity better, and why? d) Why are the properties of these two substances so different?

(5 pts) A: a) Bulk gold is gold in color, and very reflective. b) The bulk gold is more yellow in color, the slide with 10 coatings of colloid is bluish in color. The bulk gold is also more reflective than the slide. c) The bulk gold conducts electricity better; it is more reflective and has a sea of electrons available to conduct electricity. The slide does not have as much gold present, so it will not conduct electricity as well. d) The properties are so different because bulk properties are not the same as nano-scale properties, the difference is between the amount of the gold present.

Q20: a) If the slides were continued to be covered in layers of gold, what would they eventually resemble? b) How is it possible to put multiple layers of gold nanoparticles (which has a negative charge) on the surface of the glass slides? (Do not just restate the procedure – explain how/why the procedure works.)

(3 pts) A: a) Eventually, the glass slide covered in gold colloid would resemble the bulk gold in color and reflectivity, as well as conductivity. b) The mercaptoethylamine (MEA) used to stick the layers of gold nanoparticles to each other screens the nanoparticles' repulsive charges between layers, allowing for them to get close enough that they bind to the MEA and form multilayers.

Q21: Calculate the "footprint" area of the nanoparticle sphere. (If you were looking down on one colloid, what would you see, and how big would it be?)

(3 pts) A: Footprint area = surface area of a circle = πr^2

Diameter = 12 nm, radius = 6 nm = 6E-9 m

SA: π(6E-9 m)^2 = 1.13E-16 m^2 (OR: 1.13E-12 cm^2, OR: 113 nm^2)

Q22: Calculate the maximum surface coverage the slides will have when covered with these particles. Be sure to explain whether this answer is for one side or both sides of the slide.

(3 pts) A: SA slide = 2.5 by 0.9 cm = 2.5E-2 m by 0.9E-2 m

l times w = (2.5E-2 m)(0.9E-2 m) = 2.25E-4 m^2

slide/footprint area: (2.25E-4 m^2) / (1.13E-16 m^2) = 1.989E12

approx. 2E12 particles for each side of the slide

Chem 14 – 106 Makeup Lab

Gold Nanoparticles: Synthesis and Multilayering

Grade Sheet

Section A	Q1	3 points	_____
	Q2	2 points	_____
	Q3	2 points	_____
	Q4	3 points	_____
	Q5	3 points	_____
Section B	Q6	4 points	_____
	Q7	4 points	_____
	Q8	7 points	_____
	Q9	3 points	_____
	Q10	6 points	_____
	Q11	4 points	_____
	Q12	6 points	_____
	Q13	2 points	_____
	Q14	4 points	_____
Section C	Q15	6 points	_____
	Q16	2 points	_____
	Q17	3 points	_____
	Q18	2 points	_____
	Q19	5 points	_____
	Q20	3 points	_____
	Q21	3 points	_____
	Q22	3 points	_____
Notebook Pages		15 points	_____
Title, Date, TA Name, Sloppy			
Miscellaneous		5 points	_____
Lab Practice, Time Management			
		Total 100 points	_____/100

Pre Lab Quiz for Nanoparticle Makeup Lab – ANSWER KEY

1. How many grams of NaCl will you need to make up 5 mL of a 0.75 M NaCl solution? (Na = 22.99 g/mol, Cl = 35.45 g/mol)

(2 pts) A: Want 5 mL of 0.75 M NaCl solution

M = mol/L so: (M)(L) = mol

5 mL / (1000mL/L) = 0.005 L

(0.75 M)(0.005 L) = 0.00375 mol NaCl

23 g/mol + 35g/mol = 58 g/mol NaCl

(0.00375 mol)(58 g/mol) = 0.2175 g NaCl needed

2. What is a colloidal solution?

(2 pts) A: Colloidal solutions are comprised of tiny particles (usually between 1 and 150 nm) that are suspended throughout another medium, which do not fall out of solution due to Brownian motion, or collisions with solvent molecules. Colloidal solutions scatter light, but also absorb certain wavelengths, which depend on the size of the particle.

3. Explain what aggregation is.

(2 pts) A: Aggregation is further clumping together of gold nanoparticles and crashing out of solution. If the colloid is forced to aggregate, as the distance between the particles decreases, and the diameter of the particles increases, the wavelength absorbed shifts and the particles look blue. This aggregation can be initiated by adding charged particles to the solution (dissolved salt, for example). These charges "screen" the particles from one another, their negative charges no longer repel each other, and they begin to clump together, or aggregate.

The picture should show groups of particles coming together to form larger groups of particles in the presence of ions. (Like diagram from video).

4. If I made a nanoparticle that was blue, what color would it be absorbing? What color would be passed through it?

(2 pts) A: If a nanoparticle were blue it would be absorbing the color red or orange. The blue color would be transmitted, or pass through it. This is illustrated in the color wheel, with "opposing colors."

5. Give one example of each: a physical change and a chemical change. (They do not need to be examples from today's lab.)

(2 pts) A: Physical Change: melting water

Chemical Change: burning a log in a fireplace

(Other examples are just fine).

Prelab Talk Overhead

Gold Nanoparticles: Synthesis and Multilayering

Work in Pairs, be sure to answer the questions in your own words.

Wear gloves and safety glasses. $HAuCl_4$ is very caustic.

Half the lab should start with Section A; half the lab should start with Section C.

Section A:

Make sure you clean your glassware between solutions.

Use distilled water, NOT tap water and Rinse Well.

The gold salt and sodium citrate solutions are up front.

Use the 1 mL pipetor to measure the sodium citrate solution.

Take only your measured solutions back to your seat.

Boil your gold salt solution in front of the fume hood.

Do not pick up the hot flask with your hands.

Section B:

When you're done, the sugar and salt solutions can go down the drain.

Any solution with colloid or $HAuCl_4$ must be put in the waste container up front, be sure to remove the stir bar.

Tween 20 is a soap, it will drip from the pipets.

Section C:

Do NOT move the slides from their station.

Do NOT open the containers the slides are in.

We will watch 2 short movies. There will be questions on them in the lab.

Leave your packet with me at the end of lab.

Materials and Equipment/group (working in pairs):

Bolded items not in students' C drawers

2 10 mL grad. cylinders

1 sm beaker

1 sm Erlenmeyer flask—not in C drawer

1 magnetic stir bar

1 heating/stir plate

neoprene or nitrile gloves

1 1-2 mL pipetor with tips

2 20 mL vials

2 8 mL vials

plastic pipets

Chem 15 M: brown, or foil-wrapped bottles

Solutions/Reagents:

2 mL sodium citrate solution

20 mL gold salt solution

Gold colloid

0.5 g NaCl with a scupula

3.5 g table sugar with a scupula

3 drops of Tween 20

Whole class needs:

1 piece of bulk metal (prefer. Gold, cu ok)

Heat resistant gloves or tongs

Magnet to remove stir bars from solutions

TV/DVD player with remote

TA Notes

Nanoparticles Chem 15 M Lab

Sarah Brunker 2/06

The purple Kimberly Clark nitrile gloves are the safest for this lab.

The TA will need to demonstrate how to use the pipetor, and that pipet tips are necessary and disposable.

The $HAuCl_4$ solid will eat through metal spatulas, plastic is recommended when working with this.

Make sure to distinguish between the colloidal solution, and the actual particles, which are gold nanoparticles.

It is more important that the students rinse their glassware well than use a lot of soap.

Make sure the students remove the magnetic stir bar before dumping their colloid solution into the waste container.

The $HAuCl_4$ solution should be heated at about 300^oC and stirred enough that a small funnel can be seen in the solution. When there are large bubbles in the solution, then the sodium citrate can be added.

Do not add too much distilled water all at once or the solution with stop boiling.

The colloid solution is a good solution if it is wine red, is not cloudy, and has nothing settled at the bottom of the flask.

While the students are waiting for the Tween 20 to coat the nanoparticles for 20 minutes, they can move on to Section C. It doesn't matter if the Tween 20 sits for more than 20 minutes, but it must sit for at least 20 minutes before the NaCl is added.

Gold Nanoparticles Lab Review

1) Be able to define aggregation and explain what you observed when the colloidal solution aggregated.

2) Know how the Tween 20 protected the colloid from aggregation, and be able to draw a picture of what happened on the microscopic scale.

3) Be able to explain the difference between nanoscale and bulk properties, and list examples.

4) Explain how gold particles with negative sodium citrate ions on them can be layered on top of each other to form multilayered slides.

5) Describe how you made the gold colloid solution, and what observations you made during that process.

Gold Nanoparticles Post Lab Quiz and Evaluation

1) Please rate your overall understanding of the topics covered in this lab (types of reactions, materials chemistry, etc.) after completing the lab, as compared to your understanding before completing the lab.

Much Improved Slightly Improved No Change Slightly Confused Greatly Confused

2) Please evaluate the quality of the lab (how it was written, the questions asked, etc.).

Enjoyable All Right No Opinion Slightly Disliked Greatly Disappointed

3) Is there anything you would like to see changed, added, or deleted from this lab? Please write any suggestions for improvement here.

4) Define aggregation and explain what you observed when the colloidal solution aggregated.

5) Give one example of each: a physical change and a chemical change.

6) Explain how gold particles with negative sodium citrate ions on them can be layered on top of each other to form multilayered slides.

VITA

Sarah Elizabeth Brunker

Education

2010 The Pennsylvania State University – University Park, PA
Ph.D. in Chemistry: Advisor Dr. Christine Keating

2004 Coe College – Cedar Rapids, IA
B.A. in Chemistry: Advisor Dr. Martin St. Clair
Secondary Education Certification
Minor in Writing

Publications

Brunker, S. E.; Keating, C. D. Barcoded nanowires coupled with enzymatic amplification reactions for pathogen detection. *Manuscript in preparation.*

Brunker, S. E.; Cederquist, K. B.; Keating, C. D. Metallic barcodes for multiplexed bioassays. *Nanomedicine* **2007**, *2*, 711-724.

Presentations

Barcoded nanowire surfaces and enzymatic amplification reactions of nucleic acids for pathogen detection, Poster, **S. E. Brunker**, C. D. Keating, Bioanalytical Sensors Gordon Research Conference, New London, NH (June 2010).

Detecting pathogens using enzymatic amplification reactions and barcoded surfaces, Poster, **S. E. Brunker**, C. D. Keating, The Pennsylvania State Graduate Exhibition, University Park, PA (March 2010).

Enzymatic amplification reactions performed on barcoded nanowire surfaces for pathogen detection, Poster, **S. E. Brunker**, C. D. Keating, American Association for the Advancement of Science Annual Conference, San Diego, CA (February 2010).

Pathogen detection using barcoded nanowires and on-wire polymerase chain reaction, Talk, **S. E. Brunker**, B. He, C. D. Keating, Pittsburgh Conference, Chicago, IL (March 2009).

Pathogen detection using barcoded nanowires and on-wire polymerase chain reaction, Talk, **S. E. Brunker**, B. He, C. D. Keating, Bioanalytical Sensors Gordon-Kennan Graduate Research Seminar and Gordon Research Conference, Smithfield, RI (June-July 2008).

Pathogen detection using barcoded nanowires and on-wire polymerase chain reaction, Poster, **S. E. Brunker**, B. He, C. D. Keating, Bioanalytical Sensors Gordon-Kennan Graduate Research Seminar and Gordon Research Conference, Smithfield, RI (June-July 2008).

Barcoded nanowires: Surface chemistry for pathogen detection, Poster, **S. E. Brunker**, C. D. Keating, American Chemical Society National Meeting, Chicago, IL (March 2007).

Towards single base extension on barcoded nanowires for multiplexed single nucleotide polymorphism detection, Poster, **S. E. Brunker**, R. L. Stoermer, C. D. Keating, Middle Atlantic Regional American Chemical Society Meeting (MARM), Hershey, PA (June 2006).

A general chemistry lab experiment involving gold nanoparticles, Poster, **S. E. Brunker**, S. Dougherty, C. D. Keating, J. T. Keiser, Middle Atlantic Regional American Chemical Society Meeting (MARM), Hershey, PA (June 2006).